İSTANBUL TECHNICAL UNIVERSITY ★ INSTITUTE OF SCIENCE AND TECHNOLOGY

STRESS DISTRIBUTION AND ELASTO PLASTIC SETTLEMENTS UNDER SHALLOW FOUNDATIONS

Master Thesis by
Civil Eng. Bora OKUMUŞOĞLU
(501041303)

Date of submission : **24 April 2006**
Date of defence examination : **15 June 2006**

Supervisor (Chairman): **Prof.Dr. Ahmet SAĞLAMER**
Members of the Examining Committee: **Prof.Dr. Mete İNCECİK**
Prof.Dr. Sönmez YILDIRIM (Y.T.Ü.)

JUNE 2006

İSTANBUL TEKNİK ÜNİVERSİTESİ ★ FEN BİLİMLERİ ENSTİTÜSÜ

YÜZEYSEL TEMELLER ALTINDA GERİLME DAĞILIMI VE ELASTO PLASTİK OTURMALAR

YÜKSEK LİSANS TEZİ

İnş.Müh. Bora OKUMUŞOĞLU
(501041303)

Tezin Enstitüye Verildiği Tarih : 24 Nisan 2006
Tezin Savunulduğu Tarih : 15 Haziran 2006

Tez Danışmanı: Prof.Dr. Ahmet SAĞLAMER
Diğer Jüri Üyeleri: Prof.Dr. M. Mete İNCECİK
Prof.Dr. Sönmez YILDIRIM (Y.T.Ü.)

HAZİRAN 2006

PREFACE

I would like to express my deepest gratitude to Prof. Dr. Ahmet SAĞLAMER for his supervision throughout my studies for the elaboration of this master thesis. His guidance and inspiration have provided an invaluable experience that will help me in my career.

My special thanks to Mustafa Hatipoğlu for helping me with my thesis and to Assist.Prof.Dr. Aykut Şenol and Tolga Yılmaz Özüdoğru for their support. I also thank the Professors at the Soil Mechanics and Geotechnical Engineering Department.

Last but not the least, I would like to thank my family for their unconditional love and support.

May 2006 Bora OKUMUŞOĞLU

TABLE OF CONTENTS

LIST OF TABLES

LIST OF FIGURES

LIST OF SYMBOLS

$\boldsymbol{a}$	: Radius of a circular load
$\boldsymbol{B}$	: Width or diameter of a foundation
$\boldsymbol{c}$	: Cohesion
$\boldsymbol{D}$	: Diameter
$\boldsymbol{D_f}$	: Depth of embedment for foundations
$\boldsymbol{D_r}$	: Relative density
$\boldsymbol{D_{10}}$	: Soil particle size corresponding to 10% of grain size distribution
$\boldsymbol{D_{60}}$	: Soil particle size corresponding to 60% of grain size distribution
$\boldsymbol{e}$	: Void ratio
$\boldsymbol{E}$	: Young's modulus
$\boldsymbol{E_f}$	: Young's modulus of foundation
$\boldsymbol{E_s}$	: Young's modulus of soil
$\boldsymbol{I_c}$	: Consistency index
$\boldsymbol{I_{i,}}$	: Influence factors for elastic settlement
$\boldsymbol{I_f}$	: Influence factor for stress increment
$\boldsymbol{I_p}$	: Plasticity index
$\boldsymbol{OCR}$	: Overconsolidation ratio
$\boldsymbol{k_s}$	: Modulus of subgrade reaction
$\boldsymbol{K_0}$	: Coefficient of lateral pressure at rest
$\boldsymbol{K_0'}$	: Coefficient of effective lateral pressure at rest
$\boldsymbol{K_{spring}}$	: Spring coefficient
$\boldsymbol{L}$	: Length of a foundation
$\boldsymbol{M}$	: Moment for beam on elastic foundation
$\boldsymbol{N}$	: Blow count in SPT
$\boldsymbol{P}$	: Surcharge
$\boldsymbol{q}$	: Magnitude of the distributed load
$\boldsymbol{q_c}$	: Tip resistance in CPT
$\boldsymbol{Q}$	: Shear for beam on elastic foundation
$\boldsymbol{r}$	: $\sqrt{(x^2 + y^2)}$ in rectangular coordinates
$\boldsymbol{R}$	: Radius

S	: Degree of saturation
S_e	: Elastic settlement
S_{ep}	: Elasto plastic settlement
u	: Pore water pressure or neutral stress
V_P	: Compressive (or primary) wave velocity
V_S	: Shear (or secondary) wave velocity
x, y, z	: Rectangular coordinates
y	: Deflection for beam on elastic foundation
z	: Depth
$\varepsilon_x, \varepsilon_y, \varepsilon_z$	: Principle strains
δ	: Settlement at ground surface
γ_0	: Unit weight of soil
γ_w	: Unit weight of water = 9.81 kN/m^3
ρ	: Bulb density
μ	: Poisson's ratio
ϕ	: Angle of internal friction of the soil
θ	: Rotation for beam on elastic foundation
σ	: Total stress
σ'	: Effective stress
σ_1 , σ_3	: Principles stresses
σ_x , σ_y	: Horizontal normal stresses
σ_z	: Vertical normal stress
$\Delta\sigma$	: Stress increment
τ_{ij}	: Shear stresses in stress tensor

YÜZEYSEL TEMELLER ALTINDA GERİLME DAĞILIMI VE ELASTO PLASTİK OTURMALAR

ÖZET

Bu çalışmada, yüzeysel temel inşaatının sonucunda zeminde meydana gelen gerilme artımları ve elasto plastik oturmalar ele alınmıştır. Klasik ve modern yöntemler kullanılarak zemindeki ani oturmaların hesaplanması mevzusu incelenmiş ve bu yöntemlerin sonuçları kendi aralarında ve ayrıca saha ölçümleri ile karşılaştırılmıştır.

Elastisite teorisinin sağladığı denklemler ile oturmalar, hesabın doğruluk oranının düşük olmasına rağmen kolay ve hızlıca hesaplanabilir. Winkler yayları ise özellikle mütemadi kiriş veya radye temel olarak teşkil edilmiş yapı elemanlarında oluşan moment ve kesit kuvvetlerinin hesaplanabilmesini sağlar, fakat zemine dair sadece bir parametrenin yeraldığı bu yöntem ile hesaplanan oturmalar pek güvenilir olmayabilir.

Ticari olarak paket halinde satılan ve özellikle mühendisler arasındaki kullanımı oldukça yaygın olan sonlu elemanlar programları, üretici firma ya da mühendisin tecrübe ve uzmanlığını sunarak karmaşık problemleri, herkes tarafından çözülebilir bir konuma getirmektedir. Lakin bu programları kullanırken dikkatli davranmak gerekir, çünkü herhangi bir bilgi veya kullanım yetersizliği yanlış bir tasarımın ortaya çıkmasına kolaylıkla neden olabilir.

Zeminin elasto plastik davranışını, yani gerilme ile sertleşmesi sürecini dikkate alan hiperbolik modeli kullanan bir sayısal yöntemin verildiği bu çalışmada, bu yöntem ile elde edilen düşey oturma sonuçlarının, hem sonlu elemanlar programı ile elde edilen değerlere hem de iki farklı vaka analizine dair saha ölçümleriyle iyi bir şekilde uyuştuğu gösterilmiştir.

STRESS DISTRIBUTION AND ELASTO PLASTIC SETTLEMENTS UNDER SHALLOW FOUNDATIONS

SUMMARY

In this study, the calculation of stress increments and elasto plastic settlements due to the construction of a shallow foundation has been discussed. Conventional and contemporary methods of estimating the deformation of soil in short term, has been inspected and compared both between themselves and actual measurements from case studies.

The theory of elasticity gives simple equations where it is possible to estimate the settlements quickly though in expense of accuracy. Winkler springs enables the calculation of moments and forces acting on the structural elements designed as foundations such as beams and rafts, while it is not a trustworthy method for the computation of the settlement since it only depends on one parameter for the consideration of the soil.

The finite element programs, which are commercial available and very common amongst the professionals today, present the expertise of programming firm/engineer for the solution of complex problems by anyone. Yet they should be approach with caution since the misunderstanding of the procedure leading to an invalid application may result in a design error.

The numerical procedure given in this study, which incorporates the well established hyperbolic model to mimic the hardening behavior of the soil, is shown to produce close results in vertical settlement to the analysis with finite element method and to the field measurements of two different case studies.

1. INTRODUCTION

All manmade structures are inevitably supported by the earth: let them be a skyscraper, a dam or a highway pavement, or even retaining elements for cuts, embankments and tunnels where the major load is the earth itself. The engineering concerns are the situation just and long before the act of building and the response after. Through this perspective, soil mechanics is defined by Harr (1966) as the phase of the physical sciences which deals with the state of rest or motion of soil bodies induced by forces.

Two major concepts of soil mechanics are of interest for this study: stress and strain. “Stresses” are the internal forces acting within the soil body, occurring upon the application of acceleration – persistent such as the gravity, temporary and cyclic as in an earthquake – or a force system – via foundations – from the boundary of the body. Induced by these facts, “strains” are the changes in the relative position of soil particles.

The soil, being a complex conglomeration of discrete particles, behaves in a unique way which differs that of a homogeneous continuous media. Despite this fact, engineers and scientists involving in soil mechanics have benefited the continuum mechanics by altering the old accordingly while defining new terms, yet resulting in a better understanding of this material, which is originally fabricated by the nature.

This study aims to supply an up-to-date and consolidated summary of the accumulated information regarding geotechnical engineering for the stress distribution and the estimation of short-term settlements under shallow foundations. Other engineering processes which are required for the design such as the bearing capacity, the consolidation settlement and the liquefaction are not examined here, because of their distinctive mechanics.

2. GEOSTATIC AND INCREMENTS OF STRESS IN SOIL

Geostatic stresses are the stresses in the soil body before any structural load is appended to the geological stresses, which can be illustrated by a stress tensor at each point inside the strata. The vertical normal stress can be easily calculated by multiplying the depth with the unit weight of the soil. Therefore, in order to determine the horizontal stress, a ratio of these two – namely the coefficient of lateral pressure at rest, K_0 – is utilized.

The pore water pressure inside the voids of the soil does not affect volume changes and the shear strength. Consequently the part of the total stress that is responsible for such events, defined as the effective stress, is to be investigated while dealing with the ground deformations.

The external load to the soil boundary, which happens to be the civil influence to the nature, initiates the problems for engineering. Firstly the characteristics of this influence have to be defined: the intensity and the dynamics of the external load, the geometry and the rigidity of the foundation. Then the effect – the stress distribution – can be quantified by a mathematical model of a halfspace which approximates the real soil or by the means of numerical models such as the finite element method.

After all stresses are determined, the stress tensor and related equilibriums can be established to obtain the principles stresses, which play the major roles for the estimation of strains.

2.1. Geostatic Stress

The overburden weight of the soil at any depth, defines the geostatic stresses at that point. The state of stresses for a profile with a horizontal surface, is axi-symmetrical, where the normal vertical stress is σ_z and the normal horizontal stresses are $\sigma_x = \sigma_y$.

The representation of all normal and shear stress with their defined positive direction is shown in Figure 2.1 below for an elemental cube. Due to the fact that the mostly interested loadings are compressive in soil mechanics, the positive normal stresses are directed into the surface of the cube.

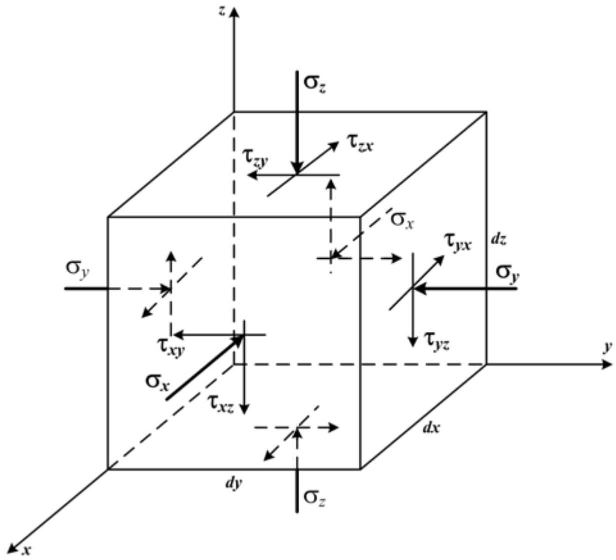

Figure 2.1 : Stress tensor components (Harr, 1966)

The expression of stress components in the matrix form is as follows:

$$\begin{bmatrix} \sigma_x & \tau_{xy} & \tau_{xz} \\ \tau_{xy} & \sigma_z & \tau_{yz} \\ \tau_{xz} & \tau_{yz} & \sigma_z \end{bmatrix} \quad \textbf{(2.1)}$$

2.1.1. Vertical Geostatic Stress

In the natural case of the stress state, in which the soil's own weight produces normal stresses, for a horizontal surface with a constant unit weight ratio, the vertical geostatic stress is calculated as below.

$$\sigma_z = \gamma_0 z \quad \textbf{(2.2)}$$

Under these conditions, the normal stresses are the principles stresses and all the shear stresses τ_{ij} in the stress tensor are zero, satisfying that:

$$\sigma_x = \sigma_y \quad \textbf{(2.3)}$$

For an inclined surface, as shown in Figure 2.2 the stress parallel (p_l) to the slope of infinite length, has a symmetrical distribution and the vertical stress (p_z) is defined as:

$$p_z = \gamma_0 z \cos\beta \qquad \textbf{(2.4)}$$

If we substitute $z \cos\beta = z'$ then it can be simplified as an analogy to (2.2) as:

$$p_z = \gamma_0 z' \qquad \textbf{(2.5)}$$

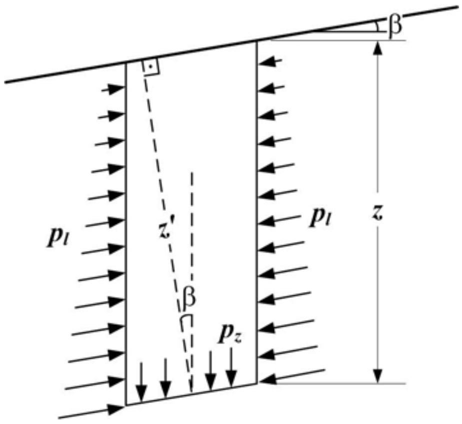

Figure 2.2 : Geostatic stresses in an inclined surface (Feda, 1978)

For any point inside the soil, Mohr's circle can be utilized in order to derive the principles stresses, where as in Figure 2.3 $|OA| = p_z$ and $|OP|=|OB| = p_l$. Deriving the principles stresses with the help of Mohr's circle, will be covered in the last section of this chapter.

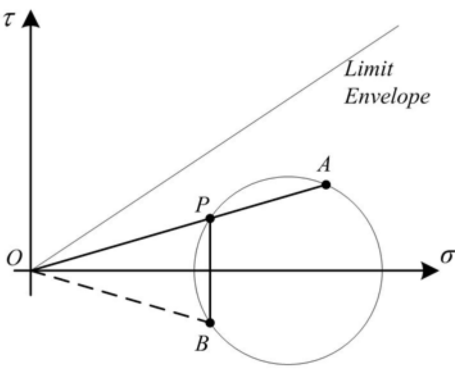

Figure 2.3 : The state of stress for a slope in Mohr's circle (Feda, 1978)

2.1.2. Horizontal Geostatic Stress

As easily as the vertical geostatic stress is defined, the horizontal geostatic stress is rather a controversial topic to discuss. Yet the research that has been going on for over half a century enables the engineers to design safe and feasible structures with sufficient precision.

There are two fundamental ways to determine the horizontal geostatic stress: One is where the media is investigated as statically indeterminate, thus the constitutive equations are employed; and the other and more common practice is to assume the condition of failure to create a statically determine condition and use Mohr's circle to derive the coefficient of lateral pressure at rest, K_0, which is:

$$\sigma_x = K_0 \sigma_z \quad \textbf{(2.6)}$$

Investigating via a simple constitutive equation, say using the Hooke's law for homogeneous, isotropic and elastic materials,

$$\begin{aligned} \varepsilon_x &= 1/E\left[\sigma_x - \mu(\sigma_y + \sigma_z)\right] \\ \varepsilon_y &= 1/E\left[\sigma_y - \mu(\sigma_z + \sigma_x)\right] \\ \varepsilon_z &= 1/E\left[\sigma_z - \mu(\sigma_x + \sigma_y)\right] \end{aligned} \quad \textbf{(2.7)}$$

where ε_x, ε_y, ε_z are the principle strains, E is Young's modulus (modulus of elasticity) and μ is the Poisson's ratio ($0 \leq \mu \leq 0.5$), if $\varepsilon_x = \varepsilon_y = 0$ (zero or very small lateral displacement) and $\sigma_x = \sigma_y$, then:

$$\sigma_x = \frac{\mu}{1-\mu} \sigma_z \quad \textbf{(2.8)}$$

Common values for the Poisson's ratio for soils, is given below:

Table 2.1: Value ranges for Poisson's ratio (Bowles, 1996)

μ	**Soil type**
0.40 – 0.50	Most clay soils
0.45 – 0.50	Saturated clay soils
0.30 – 0.40	Cohesionless, medium and dense
0.20 – 0.35	Cohesionless, loose and medium
0.20 – 0.30	Sandy clay
0.30 – 0.35	Silt
0.10 – 0.40	Rock (depends on type of rock)
0.10 – 0.30	Loess

As a more generalized exercise, the Mohr's circle can be established to estimate the coefficient of lateral pressure at the case of failure – when the circle touches the limit envelope – in order to find K_0. There are two principles stress during failure: minor (a) It could be either that $a = \sigma_{x,min} < \sigma_z = b$ or $a = \sigma_z < \sigma_{x,max} = b$ for failure and major (b).

The stress state of a failure is illustrated in Figure 2.4 for a cohesionless soil, where ϕ is the angle of internal friction of the soil – the strength parameter for Mohr-Coulomb failure criteria –.

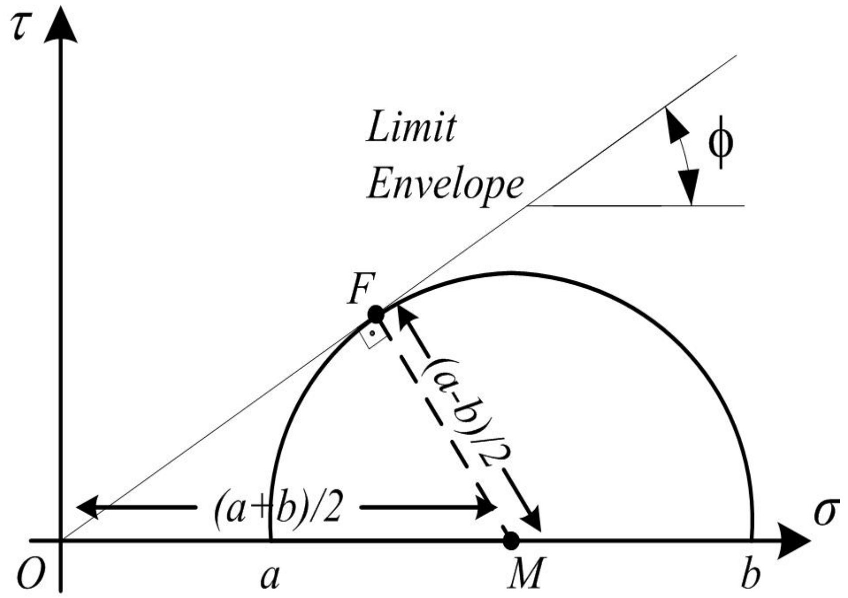

Figure 2.4 : Mohr circle for deriving K_0

The trigonometry of the triangle *MFO* and its further solution give,

$$\begin{aligned}
&\sin\phi = (a-b)/2 \big/ (a+b)/2 \\
&(a+b)\sin\phi = (a-b) \\
&a(\sin\phi - 1) = b(-1-\sin\phi) \\
&\frac{a}{b} = \frac{-1-\sin\phi}{\sin\phi - 1} = \frac{1+\sin\phi}{1-\sin\phi}
\end{aligned} \tag{2.9}$$

combining with the principles stresses,

$$\frac{\sigma_{x,\min}}{\sigma_z} = \frac{\sigma_z}{\sigma_{x,\max}} = \frac{1-\sin\phi}{1+\sin\phi} \tag{2.10}$$

and finally rewriting it with K_0 of (2.6),

$$(1-\sin\phi)/(1+\sin\phi) \le K_0 \le (1+\sin\phi)/(1-\sin\phi) \qquad \textbf{(2.11)}$$

For cohesive soils Florin (1959) formulated this relationship as:

$$\sigma_z \tan^2\left(\frac{\pi}{4}-\frac{\phi}{2}\right)-2c\tan\left(\frac{\pi}{4}-\frac{\phi}{2}\right) \le \begin{matrix}\sigma_x \\ \text{or} \\ \sigma_y\end{matrix} \le \sigma_z \tan^2\left(\frac{\pi}{4}+\frac{\phi}{2}\right)+2c\tan\left(\frac{\pi}{4}+\frac{\phi}{2}\right) \qquad \textbf{(2.12)}$$

Despite these theoretical definitions of K_0, the following simplified equation is still the most universally accepted expression, while having an accuracy of ±15% to ±20% according to Feda (1978).

$$K_0 = a - \sin\phi \qquad \textbf{(2.13)}$$

where a=1 for cohesionless soils and a=0.95 for cohesive soils.

Saglamer (1973) has obtained a similar expression in his study, where he also stated that for granular soils K_0 depends on the relative density with looser soils having a higher value:

$$K_0 = 0.97 - 0.94\sin\phi' \qquad \textbf{(2.14)}$$

The overconsolidation feature of the soil, also affects K_0. Below are the results of laboratory measurements on undisturbed samples of overconsolidated London clay, which have eroded overburden heights of 150 meters and 440 meters, respectively.

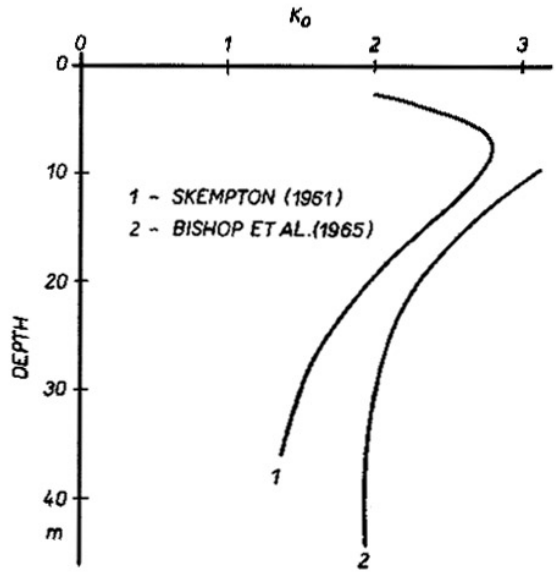

Figure 2.5 : Depth vs. K_0 for London clays of relevant case histories (Feda, 1978)

Another experimental result is in Figure 2.6, giving the relationship between K_0, *OCR* and the effective angle of internal friction.

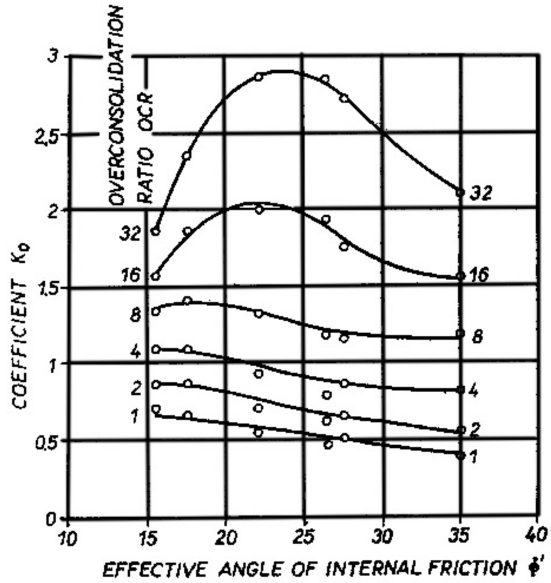

Figure 2.6 : K_0 based on *OCR* and shear resistance (Brooker and Ireland, 1965)

Similar effects K_0 on can be observed due to construction operations such as compaction and pile driving.

2.2. Effective Stress

A glance at Figure 2.7 of a saturated soil portion indicates that there are two parts of the stress acting among the cross-section "a-a": one is the pore water pressure within the voids between solid particles, which happens to be isotropic – equal magnitude in all directions –, and the other is the sum of vertical forces concentrated at the contact points of solid particles divided by the cross-sectional area of the portion. Second one called the effective stress.

In the presence of the groundwater, the effective stress is the factor dominating the mechanical process in which the settlement occurs. As defined above, the effective stress can be formulated by:

$$\sigma' = \frac{P_{1(v)} + P_{1(v)} + P_{1(v)} + \cdots + P_{n(v)}}{\bar{A}} \qquad \textbf{(2.15)}$$

If the total cross-sectional area occupied by only the soil contacts is $a_s = a_1 + a_2 + a_3 + \ldots + a_n$, then the pore pressure can also be written as:

$$\sigma = \sigma' + \frac{u(\bar{A} - a_s)}{\bar{A}} = \sigma' + u(1 - a_s / \bar{A}) \qquad \textbf{(2.16)}$$

where u = H_A γ_w according to Figure 2.7. Since $a_s / \bar{A}$ is extremely small and therefore negligible for practical reasons:

$$\sigma = \sigma' + u \qquad \textbf{(2.17)}$$

is the ultimate equation of total pressure as a sum of the effective stress and the pore water pressure (or neutral stress).

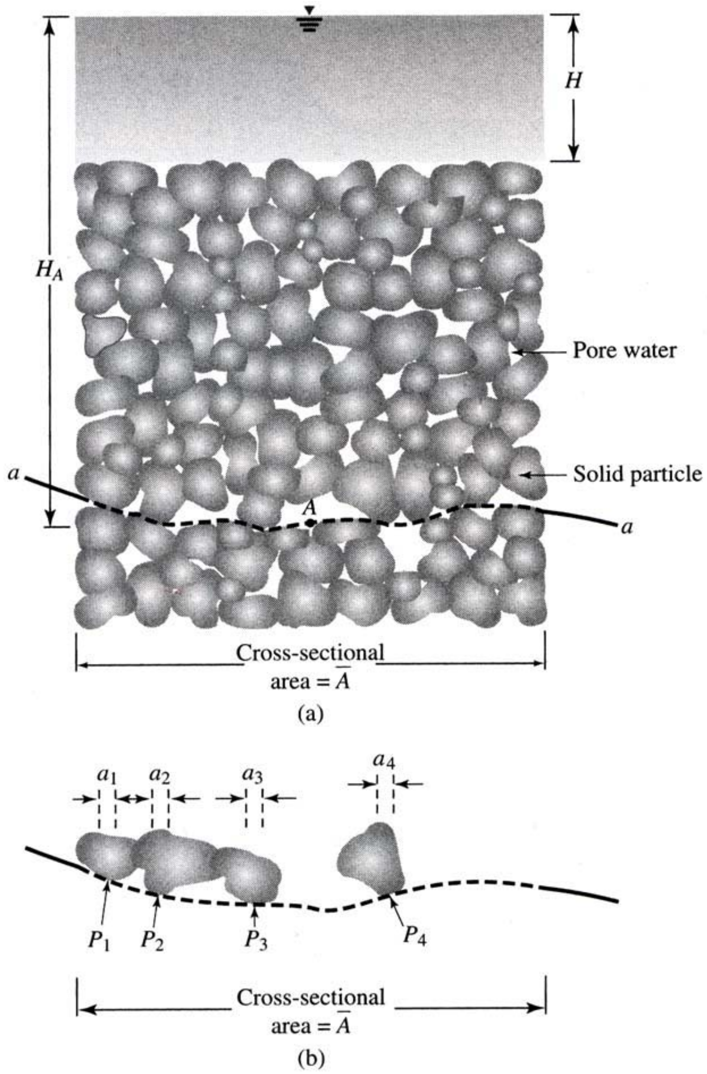

Figure 2.7 : Saturated soil portion (Das, 2001)

A partially saturated portion of the soil exists just above the groundwater level, which is the natural outcome of the phenomenon called the capillarity. As illustrated in Figure 2.8, there are two regions above the static groundwater level, which does not greatly influenced for a temperate climate (not too humid or hot, dry, cold etc.): fully saturated area due to capillarity and partially saturated area, which tends to be unsaturated as it gets closer the surface.

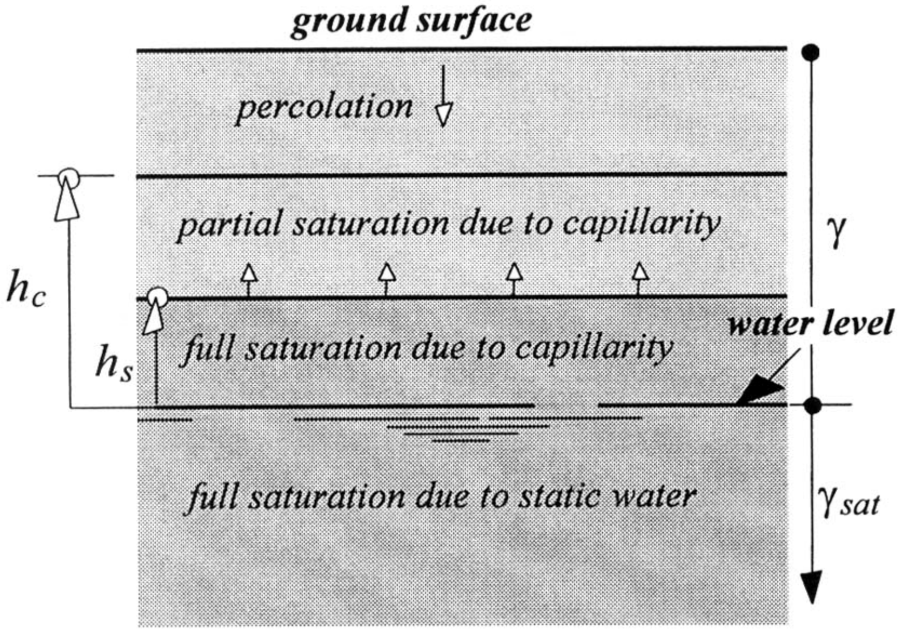

Figure 2.8 : Capillarity rise in soil (Azizi, 2000)

Terzaghi and Peck (1967) suggested the below relations for the calculation of capillarity rise:

$$h_c \approx \frac{C}{eD_{10}} \text{ and } h_s \approx h_c \frac{D_{10}}{D_{60}} \quad \textbf{(2.18)}$$

where C is a constant with a range of 10 to 50 mm^2.

The neutral stress at the zone of capillarity rise can easily be calculated according to the degree of saturation at that point:

$$u = -(S/100)\gamma_w h \quad \textbf{(2.19)}$$

where h is the height of the calculation point from the ground water level. Note that it has a negative magnitude, which is why it is rather related as the water suction.

The drainage condition of the soil profile is another issue affecting the distribution of the effective stress. This phenomenon is investigated in Figure 2.9: firstly sand underlied by impermeable clay is shown, where the effective stress is simply reduced by the water (neutral) pressure acting inside the sand layer; a decrease in the neutral pressure is confronted in case of low permeable strata as illustrated secondly; and finally the effect of the water suction due to capillary rise is clarified again.

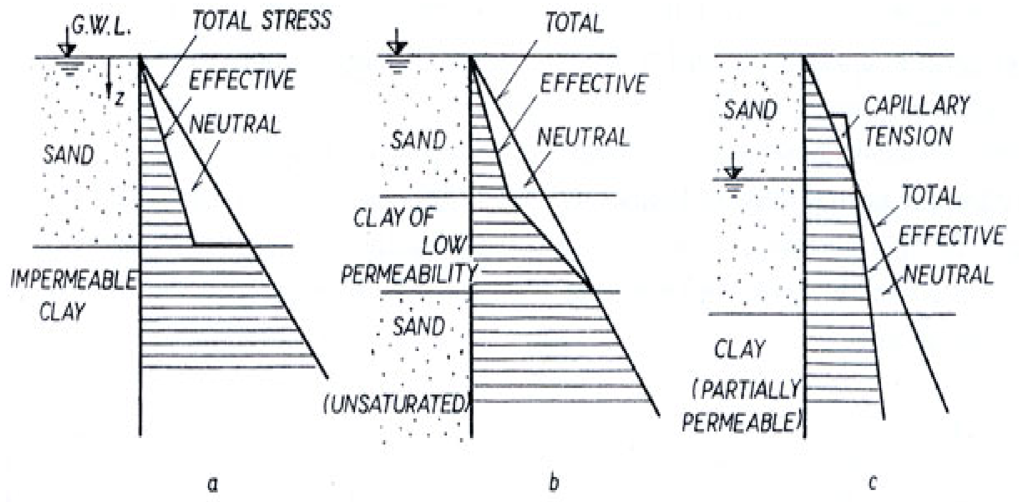

Figure 2.9 : Effective stress under different drainage conditions (Feda, 1978)

The existence of an artesian pressure created by a flow may also bring a downfall in the effective stress in overlying permeable layers, which may yet result in heaving of soil as presented in AAA where AB is the pressure of the flow inside the bottom sand layer.

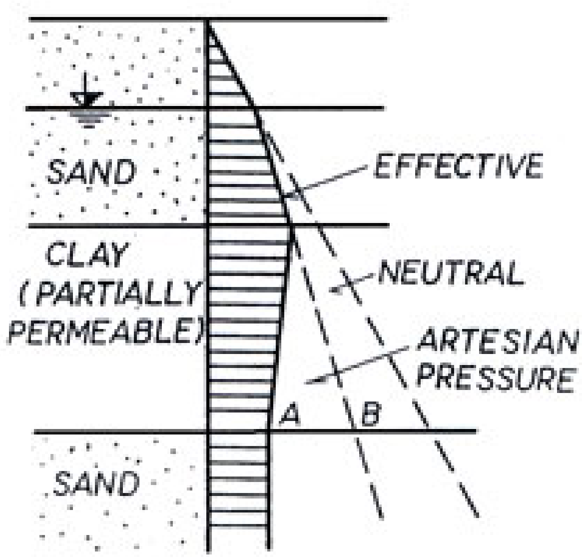

Figure 2.10 : Effective stress under artesian pressure (Feda, 1978)

It is more convenient to define the coefficient of lateral pressure at rest in terms of effective stresses, for the relevant cases mentioned above. Therefore according to the definition in (2.6):

$$K_0' = \sigma_x' / \sigma_z' \quad \textbf{(2.20)}$$

This coefficient of effective lateral pressure at rest may also be utilized to estimate the total horizontal pressure:

$$\sigma_x = K_0' \sigma_z' + u \quad \textbf{(2.21)}$$

2.3. Stress Increments via External Loads

Constructing any type of civil engineering structure on a soil mass is bound to generate changes in the stress, which will further cause the settlement of underlying strata. Solutions for the calculation of this change in the stress, namely the stress increment, are based on the mathematical models of an infinite halfspace which may have some mechanical properties for better simulations according to the fact that natural soils are likely to be anisotropic and heterogeneous, yet requiring complex constitutive models with many parameters. Accurate nevertheless complicated analysis could be unfeasible for regular geotechnical problems and time-consuming for engineering judgment process. Therefore the geotechnical literature for this problem has been benefiting from the theory of elasticity, where the soil is assumed to be isotropic and homogeneous. Yet it is also pointed by Burland et al. (1977) that elastic solutions correlate well with the solution of sophisticated methods.

A great variety of the solution exists depending on the geometry and the rigidity of foundations as well as the stiffness of underlying soils. Firstly, it is sensible to define the cases for the stress analysis on different types of shallow foundations. Then the selected solutions of the theory of elasticity are to be given accordingly. The stress distribution in the occasion of soil stratification with contrasting elasticity will be summarized lastly.

2.3.1. Structures and Contact Pressures

The contact pressure is the reaction of the soil to the load transmitted via the foundation of the relevant structure. In case of uniformly distributed load acting on the foundation, there are two major factors affecting the contact pressure: the rigidity of the foundation, the confinement of foundation soil. For flexible foundations, the contact pressure is uniform with the same magnitude of the structural load as shown in Figure 2.11-a. The profile of the contact pressure for rigid foundations depends on the confinement of foundation soil. In contrast to flexible foundations, a rigid foundation tends to settle uniformly as illustrated in Figure 2.11-b, which leads to an inverted parabolic distribution in the contact pressure. Yet if the foundation is not embedded, the cohesionless soils lack the confinement to resist the high pressures acting on the edges, which results in a parabolic distribution as indicated in Figure 2.11-c. The mathematical approximations for the contact pressure beneath rigid foundations will be given later in this chapter.

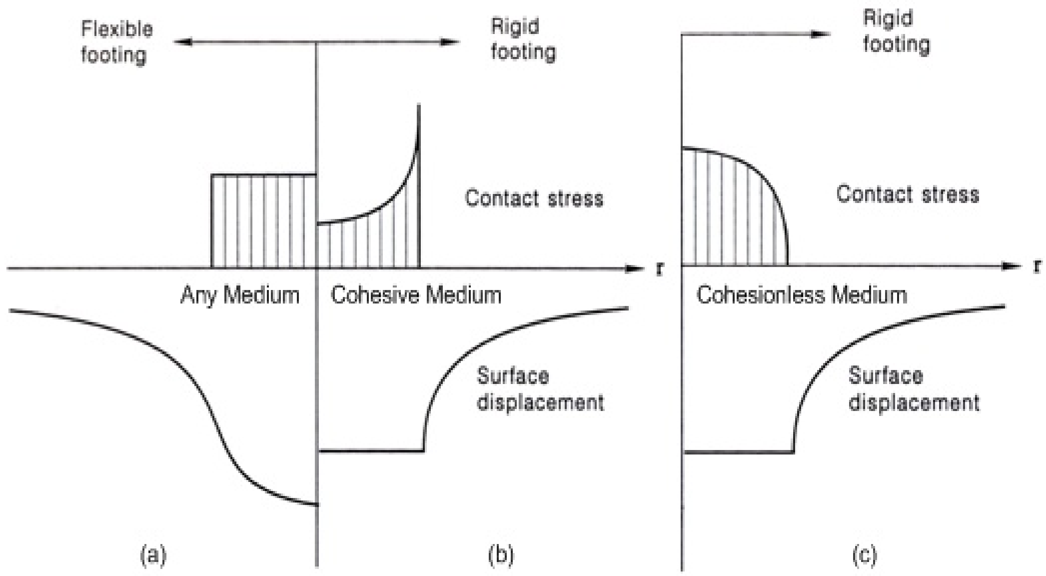

Figure 2.11 : Contact pressures based on rigidity of foundation and the type of the underlying soil (Davis and Selvadurai, 1996)

In Figure 2.12, some real world examples for both flexible and rigid foundations have been shown. Note that for embankments, which naturally have a flexible foundation, the load deceases linearly beneath the slopes.

Under some specific type of structures, the problem of contact pressure may be developed to be a more complicated matter. For retaining structures such as abutments of a bridge or a dam, which support the lateral pressure of the approach fill or the water reservoir as well as the structural load, the foundation load will linearly vary for both vertical and horizontal components as revealed in Figure 2.13.

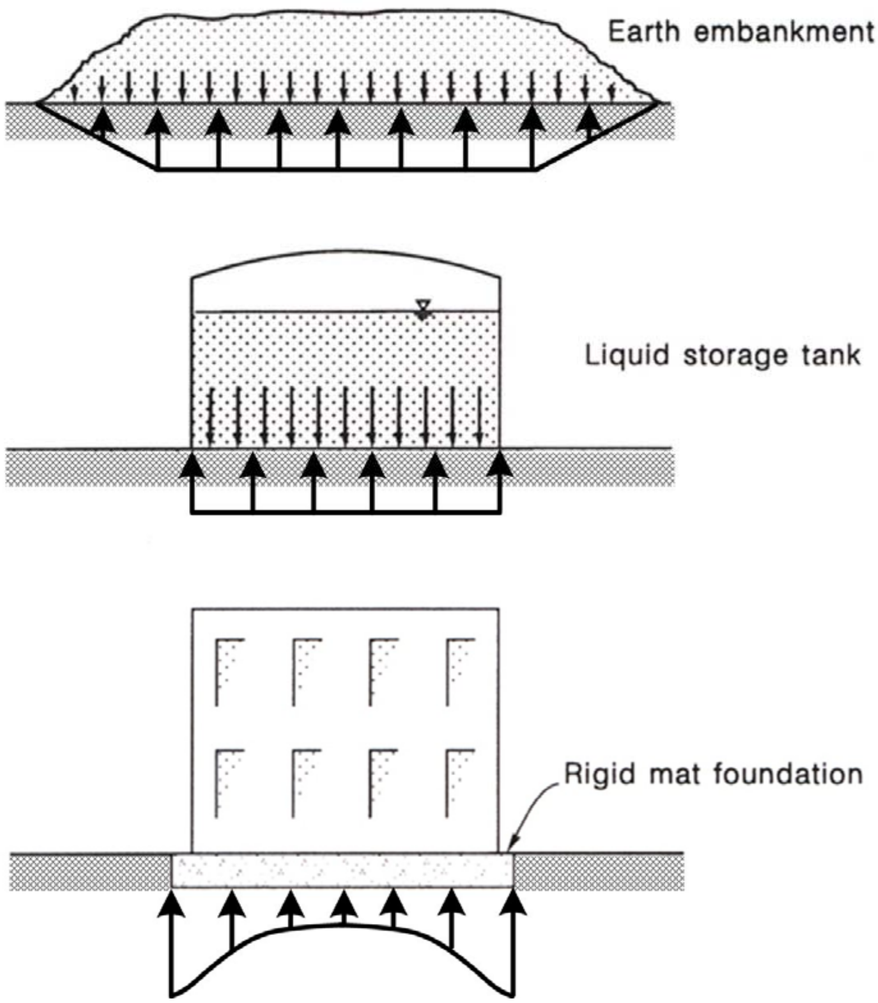

Figure 2.12 : Contact pressures for some regular structures with different kinds of foundations (Davis and Selvadurai, 1996)

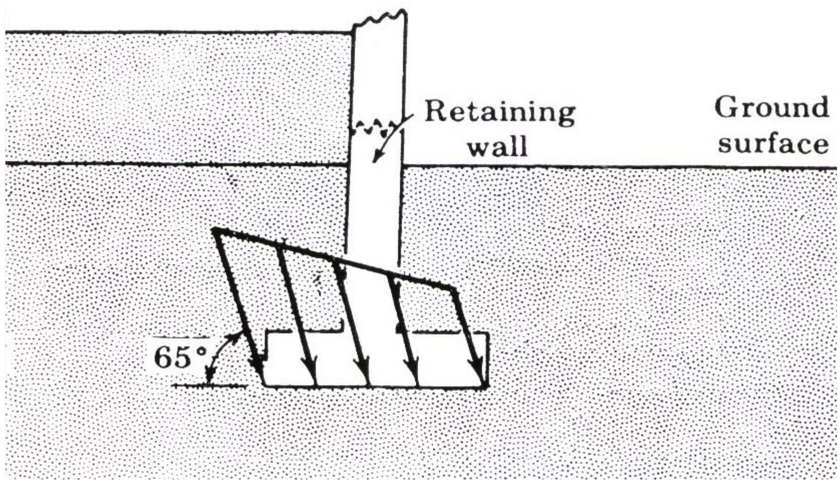

Figure 2.13 : The foundation load in case of an abutment (Harr, 1966)

A raft of a multistory structure as seen in Figure 2.14, with some degree of flexible, is another unique problem where the foundation-soil interaction is of greater importance considering the equilibrium in structural load and contact pressure, together with the geometrical compatibility between the displacement of the raft and the settlement of the soil. This type of problems might require coupled analysis with the help of special methods such as Winkler springs or by means of more advanced numerical analysis.

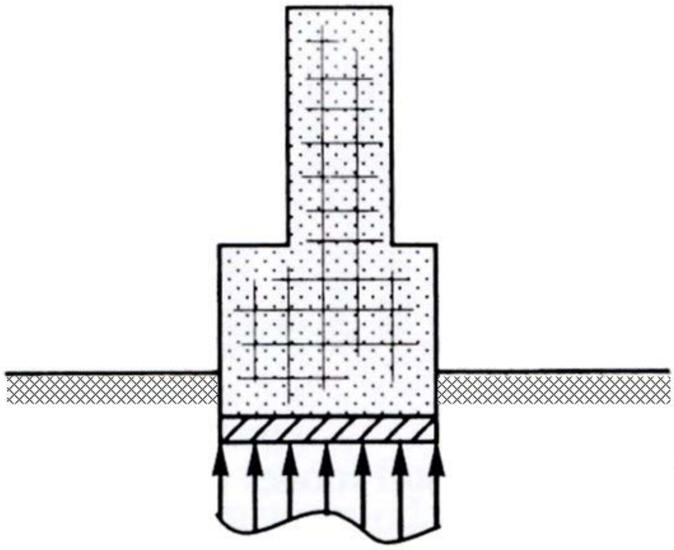

Figure 2.14 : The interactive problem of contact pressure for the flexible raft foundation of a multistory structure (Davis and Selvadurai, 1996)

2.3.2. Functions for Stress Increments

The contact pressures illustrated above are approximated by uniformly loaded rectangular or circular areas based on the plan view of foundations. Before going through the functions of stress increments for these specific shapes, it is convenient to give the functions for a singular load, which is indeed used for the integrals to derive them. Note that, the soil is considered to be weightless during these analyses.

2.3.2.1. Single Vertical and Horizontal Load

The problem of a point (single) load acting normal to the surface of an elastic half-space, as shown in Figure 2.15, was solved by Joseph Boussinesq in 1878, and yet this solution is still the most useful portion of elasticity in geotechnics.

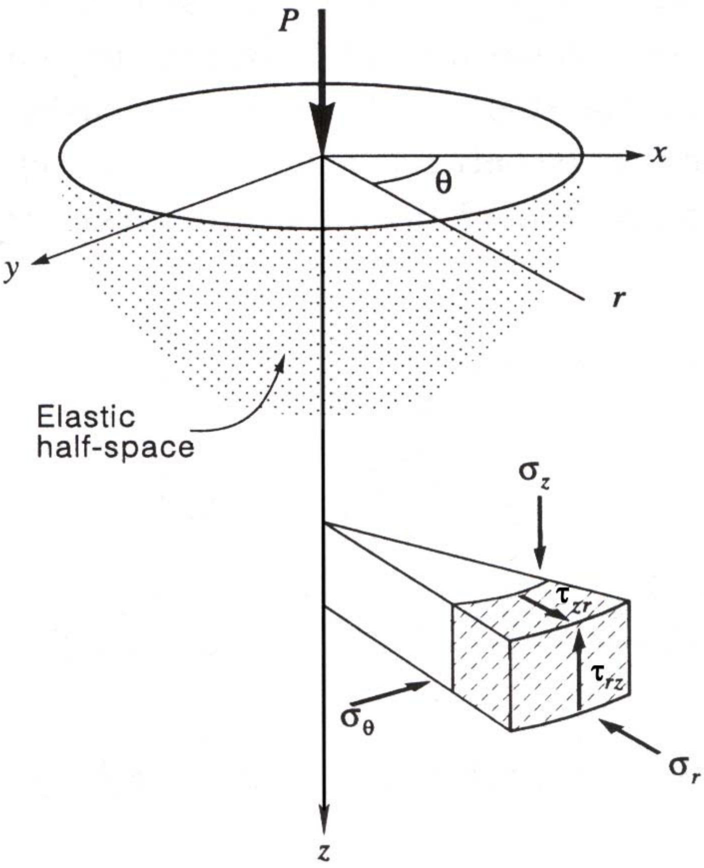

Figure 2.15 : Boussinesq's problem (Davis and Selvadurai, 1996)

The functions of stress increments with respect to Figure 2.15 are given below:

$$\sigma_r = -\frac{P}{2\pi}\left[\frac{(1-2\mu)}{R(R+z)} - \frac{3r^2 z}{R^5}\right] \tag{2.22}$$

$$\sigma_\theta = -\frac{P(1-2\mu)}{2\pi}\left[\frac{z}{R^3} - \frac{1}{R(R+z)}\right] \tag{2.23}$$

$$\sigma_z = \frac{P}{2\pi}\left[\frac{3z^3}{R^5}\right] \tag{2.24}$$

$$\tau_{rz} = \tau_{zr} = \frac{P}{2\pi}\left[\frac{3rz^2}{R^5}\right] \tag{2.25}$$

$$\tau_{r\theta} = \tau_{\theta r} = \tau_{\theta z} = \tau_{z\theta} = 0 \tag{2.26}$$

all in where $R^2 = r^2 + z^2$.

For horizontal point (single) load acting at the surface of an elastic half-space (Figure 2.16), the solution for the stress increments is given by Cerrutti in 1882.

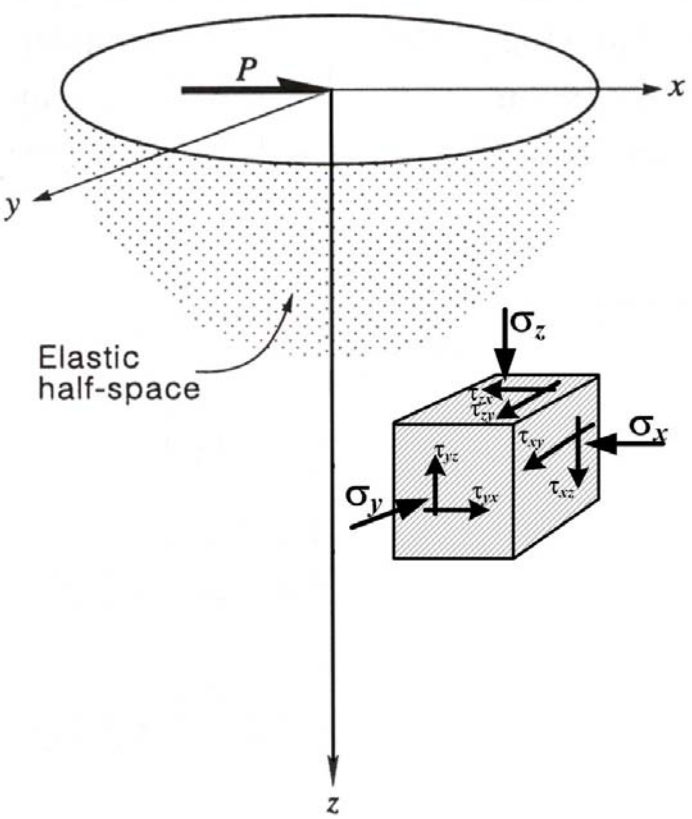

Figure 2.16 : Cerruttis problem (Davis and Selvadurai, 1996)

The functions of stress increments with respect to Figure 2.16 are given below. Note that this problem does not have the radial symmetry as established in Boussinesq's, so that rectangular coordinate system is used instead of the cartesian coordinates.

$$\sigma_x = -\frac{Px}{2\pi R^3}\left\{-\frac{3x^2}{R^2} + \frac{1-2\mu}{(R+z)^2}\left[R^2 - y^2 - \frac{2Ry^2}{R+z}\right]\right\} \quad \textbf{(2.27)}$$

$$\sigma_y = -\frac{Px}{2\pi R^3}\left\{-\frac{3y^2}{R^2} + \frac{1-2\mu}{(R+z)^2}\left[R^2 - x^2 - \frac{2Rx^2}{R+z}\right]\right\} \quad \textbf{(2.28)}$$

$$\sigma_z = \frac{3Pxz^2}{2\pi R^5} \quad \textbf{(2.29)}$$

$$\tau_{xy} = \tau_{yx} = -\frac{Py}{2\pi R^3}\left\{-\frac{3x^2}{R^2} + \frac{1-2\mu}{(R+z)^2}\left[-R^2 + x^2 + \frac{2Rx^2}{R+z}\right]\right\} \quad \textbf{(2.30)}$$

$$\tau_{yz} = \tau_{zy} = \frac{3Pxyz}{2\pi R^5} \quad \textbf{(2.31)}$$

$$\tau_{zx} = \tau_{xz} = \frac{3Px^2 z}{2\pi R^5} \quad \textbf{(2.32)}$$

all in where $R^2 = x^2 + y^2 + z^2$.

2.3.2.2. Distributed Loads

As stated above, the stress increments for distributed loadings of certain shapes are derived via taking the integral of single loads; either vertical or horizontal.

Apart from the mathematical expressions, the results of integration may also be given in the form of charts, where the influence factors for the stress increment at a specific point inside the soil strata is given in terms of some ratios depending on the geometry of the shape of loading and the location of the relevant point such as:

$$\Delta\sigma = I_f \cdot q \quad \textbf{(2.33)}$$

where I_f is the influence factor, q is the magnitude of the distributed load and $\Delta\sigma$ is the stress increment, generally the vertical one in the direction of z axis.

Yet for some shapes, it is mathematically difficult to conduct the integration – e.g. circles, arcs – in which the solution can be produced via numerical integration techniques, and illustrated only via charts.

2.2.3.2.1. Uniformly Loaded Rectangular Area

The stress increment function, which produces the stress beneath the corner of a rectangular area of a uniform vertical load (Figure 2.17), is produced via following integral using (2.24) (Newmark, 1935):

knowing that $R = [x^2 + y^2 + z^2]^{1/2} \Rightarrow R^5 = [x^2 + y^2 + z^2]^{5/2}$

$$\Delta\sigma_z = \int_0^L \int_0^B \frac{3z^3 q dx dy}{2\pi (x^2 + y^2 + z^2)^{5/2}}$$

$$= \frac{q}{4\pi}\left[\frac{2mn(m^2+n^2+2)\sqrt{m^2+n^2+1}}{(m^2+n^2+m^2n^2+1)(m^2+n^2+1)} + \tan^{-1}\left(\frac{2mn\sqrt{m^2+n^2+1}}{m^2+n^2+m^2n^2-1}\right)\right] \quad \textbf{(2.34)}$$

where $m = L / z$ and n $= B / z$.

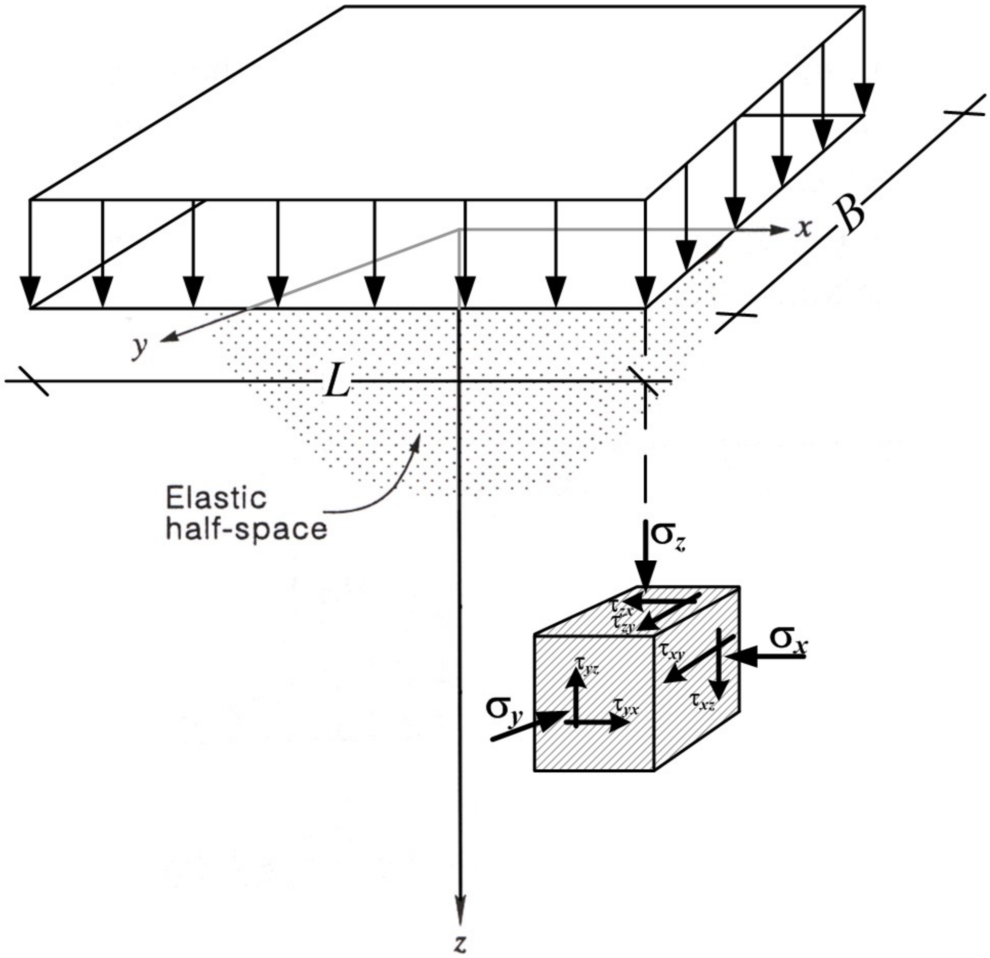

Figure 2.17 : Uniformly loaded rectangular area, vertical load. (produced from Davis and Selvadurai, 1996)

Finally for the uniform vertical loading of rectangular area, Holl (1940) gives following expressions for stresses beneath the corner of the rectangle, in which the result for vertical stress is identical to Newmark's integration:

$$\sigma_x = \frac{q}{2\pi}\left[\tan^{-1}\frac{lb}{zR_3} - \frac{lbz}{R_1^{\,2}R_3}\right] \qquad \textbf{(2.35)}$$

$$\sigma_y = \frac{q}{2\pi}\left[\tan^{-1}\frac{lb}{zR_3} - \frac{lbz}{R_2^{\,2}R_3}\right] \qquad \textbf{(2.36)}$$

$$\sigma_z = \frac{q}{2\pi}\left[\tan^{-1}\frac{lb}{zR_3} + \frac{lbz}{R_3}\left(\frac{1}{R_1^{\,2}} + \frac{1}{R_2^{\,2}}\right)\right] \qquad \textbf{(2.37)}$$

$$\tau_{xz} = \frac{q}{2\pi}\left[\frac{b}{R_2} - \frac{z^2 b}{R_1^{\,2}R_3}\right] \qquad \textbf{(2.38)}$$

$$\tau_{yz} = \frac{q}{2\pi}\left[\frac{l}{R_1} - \frac{z^2 l}{R_2{}^2 R_3}\right] \quad \textbf{(2.39)}$$

$$\tau_{xy} = \frac{q}{2\pi}\left[1 + \frac{z}{R_3} - z\left(\frac{1}{R_1} - \frac{1}{R_2}\right)\right] \quad \textbf{(2.40)}$$

where $R_1 = (l^2 + z^2)^{1/2}$, $R_2 = (b^2 + z^2)^{1/2}$ and $R_3 = (l^2 + b^2 + z^2)^{1/2}$.

Fadum (1948) has also produced the following chart for the sake of ease during calculation.

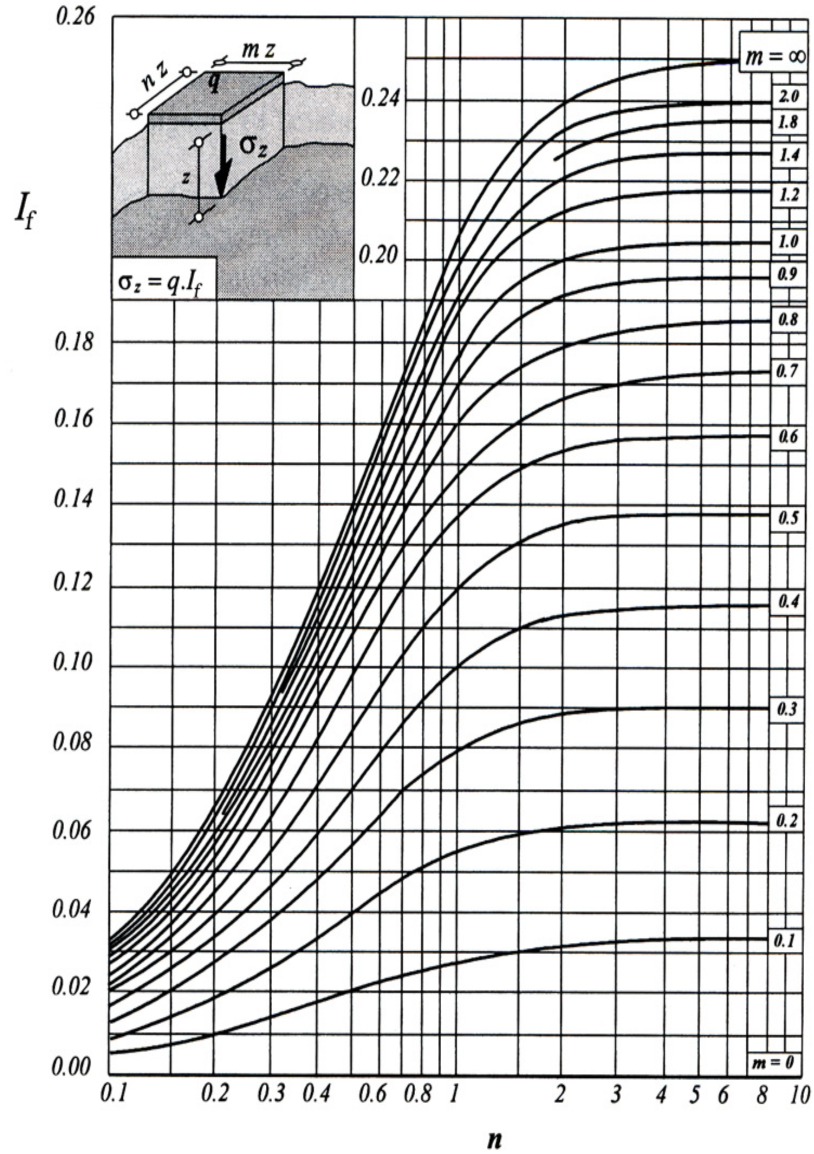

Figure 2.18 : Influence factors for the vertical stress increment of uniformly loaded rectangular area (Azizi, 2000)

For the uniform horizontal load, Holl (1940) has established the following expressions which are valid under the corners *A* and *B* of a rectangular area shown in Figure 2.20.

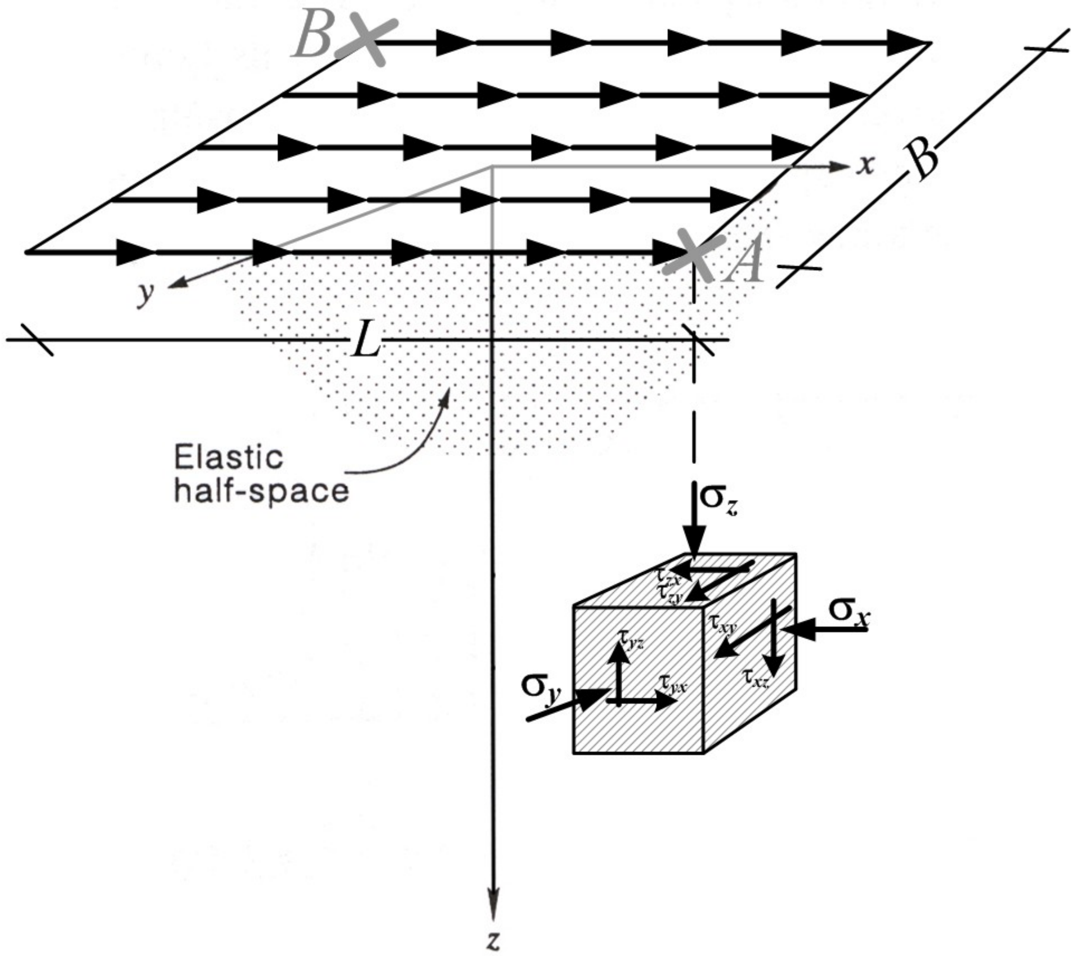

Figure 2.19 : Uniformly loaded rectangular area, horizontal load. (produced from Davis and Selvadurai, 1996)

$$\sigma_x = \frac{q}{\pi}\left[\ln\frac{R_1(b+R_2)}{z(b+R_3)} - \frac{l^2 b}{2R_1^2 R_3}\right] \quad \textbf{(2.41)}$$

$$\sigma_y = \frac{q}{2\pi}\left[\ln\frac{R_1(b+R_2)}{z(b+R_3)} - b\left(\frac{1}{R_2} - \frac{1}{R_3}\right)\right] \quad \textbf{(2.42)}$$

$$\sigma_z = \frac{q}{2\pi}\left[\frac{b}{R_2} - \frac{z^2 b}{R_1^2 R_3}\right] \quad \textbf{(2.43)}$$

$$\tau_{xz} = \frac{q}{2\pi}\left[\tan^{-1}\frac{lb}{zR_3} - \frac{lbz}{R_1{}^2 R_3}\right] \quad \textbf{(2.44)}$$

$$\tau_{yz} = \frac{q}{2\pi}\left[1 + \frac{z}{R_3} - z\left(\frac{1}{R_1} + \frac{1}{R_2}\right)\right] \quad \textbf{(2.45)}$$

$$\tau_{xy} = \frac{q}{2\pi}\left[\ln\frac{(R_1 + l)(R_3 - l)}{zb} + l\left(\frac{1}{R_3} - \frac{1}{R_1}\right)\right] \quad \textbf{(2.46)}$$

where $R_1 = (l^2 + z^2)^{1/2}$, $R_2 = (b^2 + z^2)^{1/2}$ and $R_3 = (l^2 + b^2 + z^2)^{1/2}$. It should be noted that the values of τ_{xz}, τ_{yz} and σ_z for uniform horizontal loading correspond to the values of σ_x, τ_{xy}, τ_{xz} and σ_z for uniform vertical loading (from reciprocal theorem as stated by Poulos and Davis (1974).

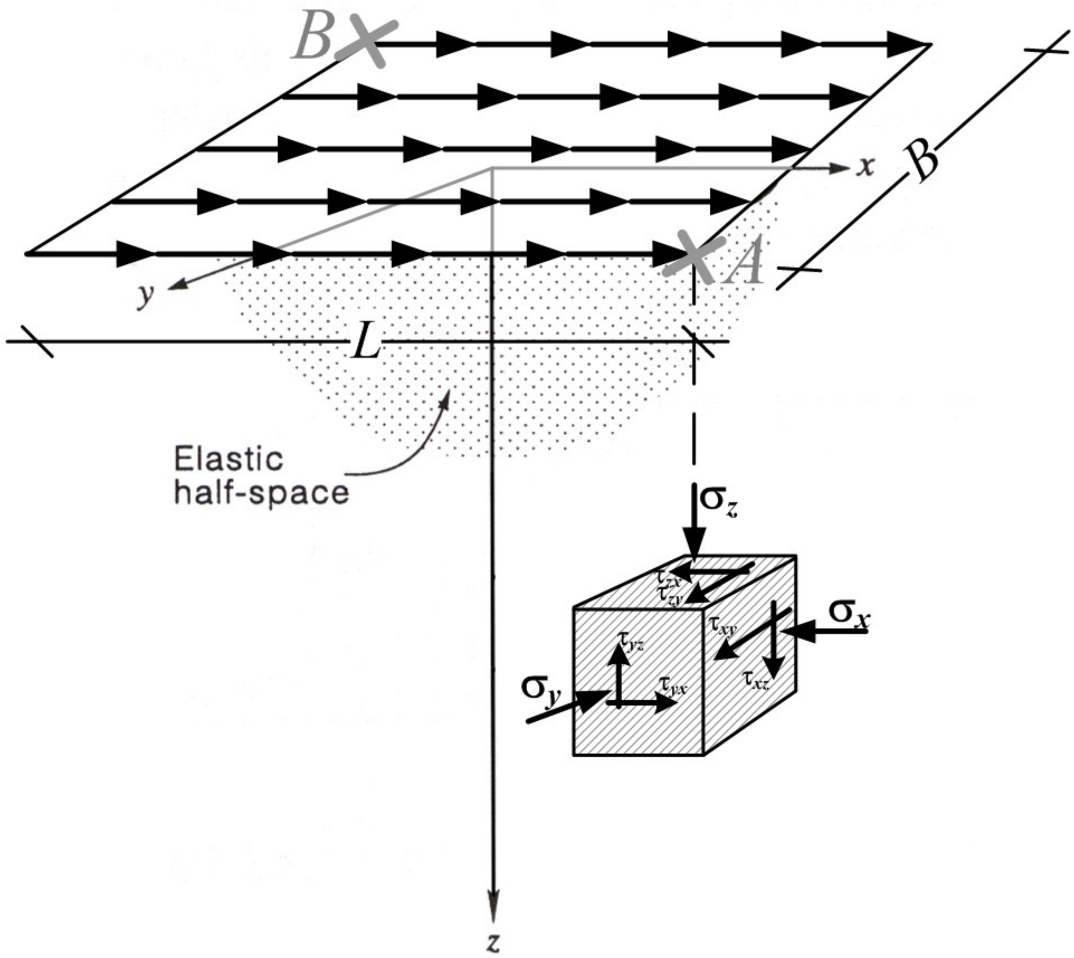

Figure 2.20 : Uniformly loaded rectangular area, horizontal load. (produced from Davis and Selvadurai, 1996)

There exists a solution for the linear contact load distributed over a rectangular area, which relates to the real world problem of abutment foundations (Figure 2.13) by Giroud (1970).

The solution gives the stress increments for three normal stress components, where the distributed load is composed of four elements as illustrated in Figure 2.21: *q*, the uniform load; *p*, antisymmetric normal load; *s*, uniform shear load; *t*, antisymmetric shear load.

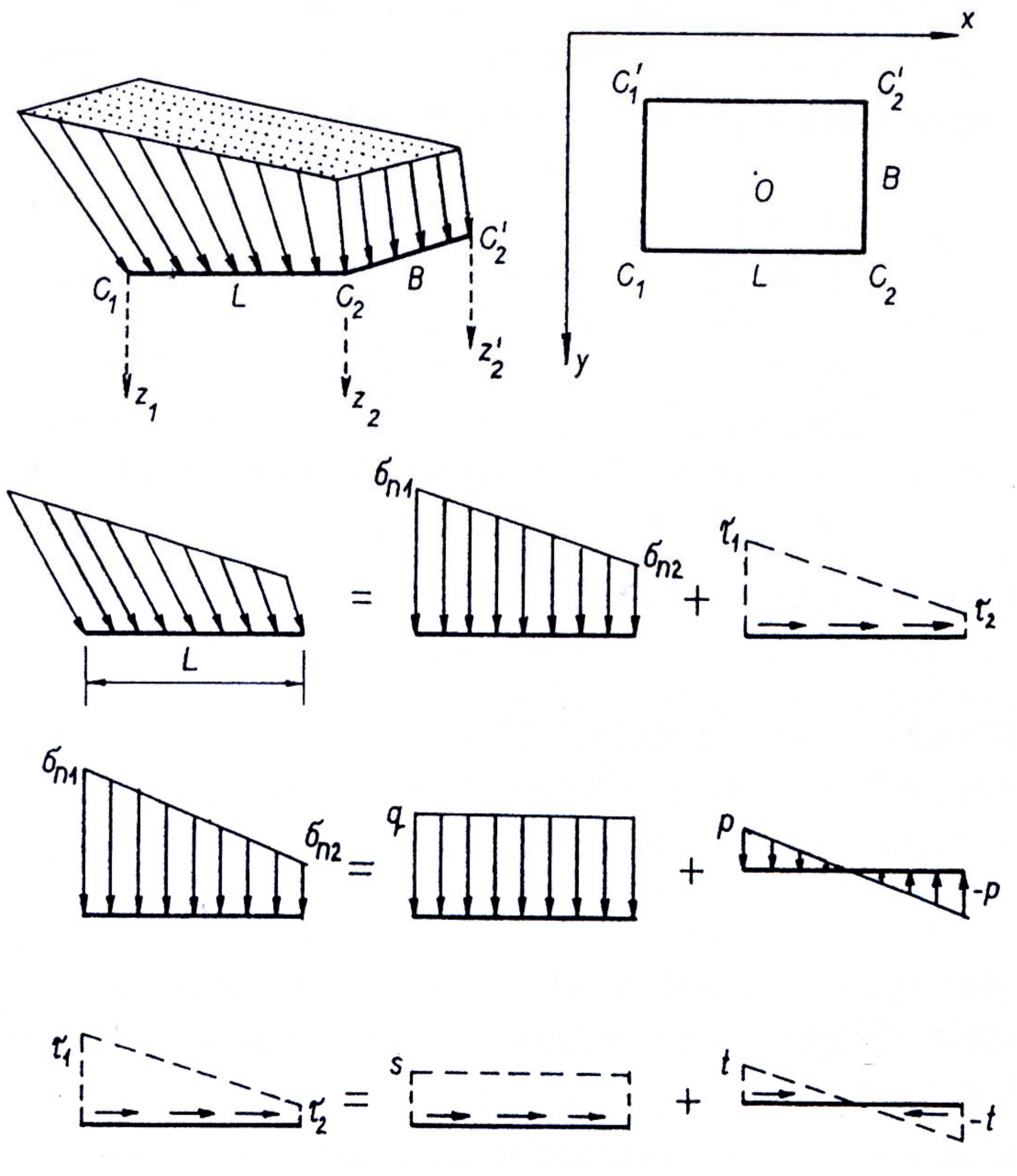

Figure 2.21 : Linear distribution of contact pressure on a rectangular area and its composition (Giroud, 1970)

The expressions for the stress beneath corners are:

$$\sigma_x = q[K_2 - (1-2\mu)K_2'] + \zeta p[M_2 - (1-2\mu)M_2'] \\ -\zeta s[K_3 - (1-2\mu)K_3'] - t[M_3 - (1-2\mu)M_3'] \quad \textbf{(2.47)}$$

$$\sigma_y = q[L_2 - (1-2\mu)L_2'] + \zeta p[N_2 - (1-2\mu)N_2'] \\ -\zeta s[K_5 - (1-2\mu)K_5'] - t[M_5 - (1-2\mu)M_5'] \quad \textbf{(2.48)}$$

$$\sigma_z = qK_0 + \zeta pM_0 - \zeta sK_1 - tM_1 \quad \textbf{(2.49)}$$

The expressions for the stress beneath center are:

$$\sigma_x = 4q[K_2 - (1-2\mu)K_2'] + 2t[K_3 - M_3 - (1-2\mu)(K_3' - M_3')] \quad \textbf{(2.50)}$$

$$\sigma_y = 4q[L_2 - (1-2\mu)L_2'] + 2t[K_5 - M_5 - (1-2\mu)(K_5' - M_5')] \quad \textbf{(2.51)}$$

$$\sigma_z = 4qK_0 + 2t(K_1 - M_1) \quad \textbf{(2.52)}$$

where $\zeta = +1$ under the corners C_1 and C'_1 and $\zeta = -1$ under the corners C_2 and C'_2. The tables for the coefficients of *K*, *L*, *M*, *N* are given in Appendix A. Note that the ratio of depth and length should be taken as z / L for the corners and $2z / L$ for the center, and z / L in both for the load *p*, that is for the coefficients M_2, M'_2, N_2, N'_2 and M_0.

2.2.3.2.2. Uniformly loaded Circles and Arcs

The integration for a circular area is more complex than rectangle. Egorov (1958) conducted the following integral in a manner depicted in Figure 2.22:

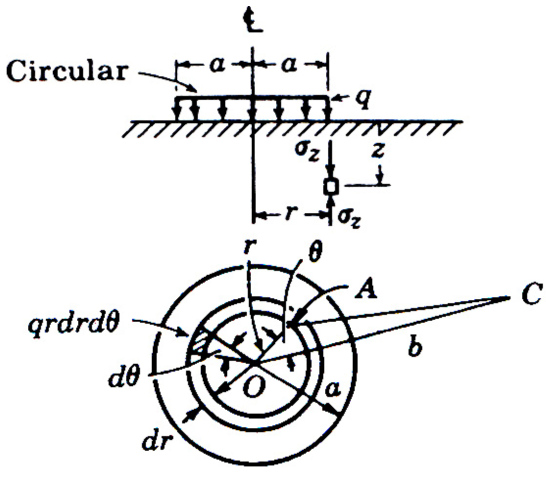

Figure 2.22 : Integration for circular area (Harr, 1966)

substituting $P = qdrd\theta$ and $R = [r^2 + b^2 + z^2 - 2br\cos\theta]^{1/2}$
for the vertical stress under point C,

$$\Delta\sigma_z = \int_0^a \int_0^{2\pi} \frac{3z^3 qdrd\theta}{2\pi(r^2 + b^2 + z^2 - 2br\cos\theta)^{5/2}}$$

$$= q\left\{A - \frac{n}{\pi\sqrt{n^2 + (1+t)^2}}\left[\frac{n^2 - 1 + t^2}{n^2 + (1-t)^2}E(k) + \frac{1-t}{1+t}\Pi_0(k,P)\right]\right\} \quad \textbf{(2.53)}$$

where $E(k)$ and $\Pi_0(k, p)$ are complete elliptic integrals of the second and third kind respectively, depending on modulus k and parameter p (detailed information can be found in the appendix of Harr, 1962), $t = r / a$, $n = z \ /a$, $k^2 = 4t / (n^2 + (t + 1)^2)$, $p = -4t / (t+1)^2$, and $A=1$ *if* $r < a$, $A=1/2$ *if* $r = a$, $A=0$ *if* $r > a$.

The expression for the vertical stress under the center is rather simple:

$$\Delta\sigma_z = q\left\{1 - \frac{1}{\left[(a/z)^2 + 1\right]^{3/2}}\right\} \quad \textbf{(2.54)}$$

Foster and Ahlvin (1954) have also produced the following chart for the sake of ease during calculation.

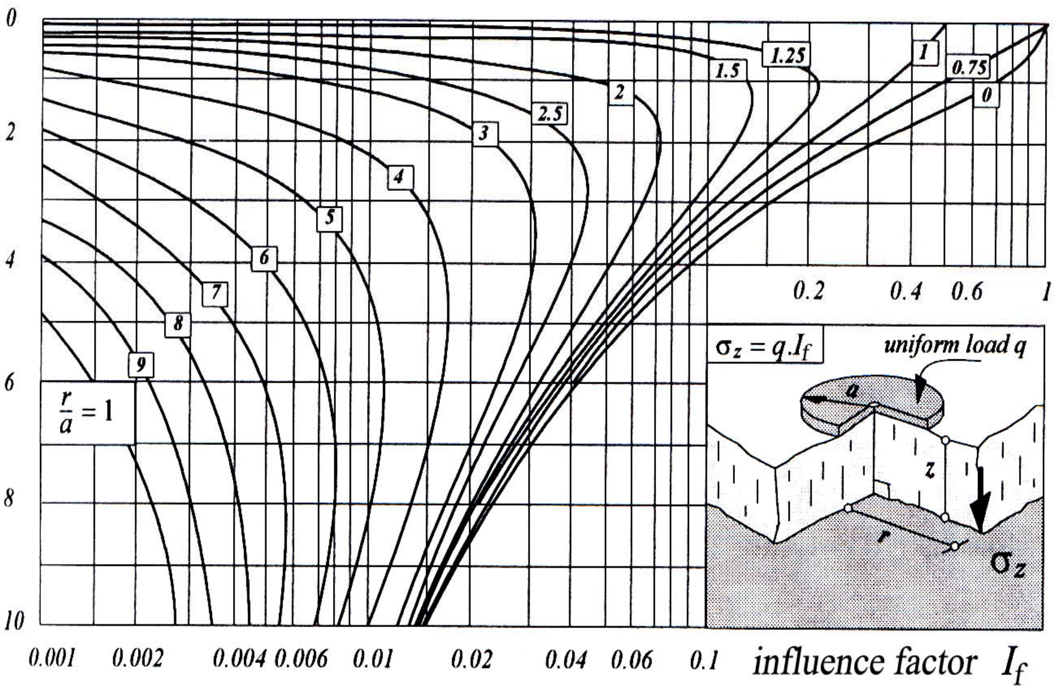

Figure 2.23 : Influence factors for the vertical stress increment of uniformly loaded circular area (Azizi, 2000)

The stress increment functions of the rectangular area – say for the vertical stress (2.34) – can be used to generate the stresses for circular or even arc-shaped areas via numerical integration techniques where a circular portion is divided into rectangular areas as illustrated in Figure 2.24.

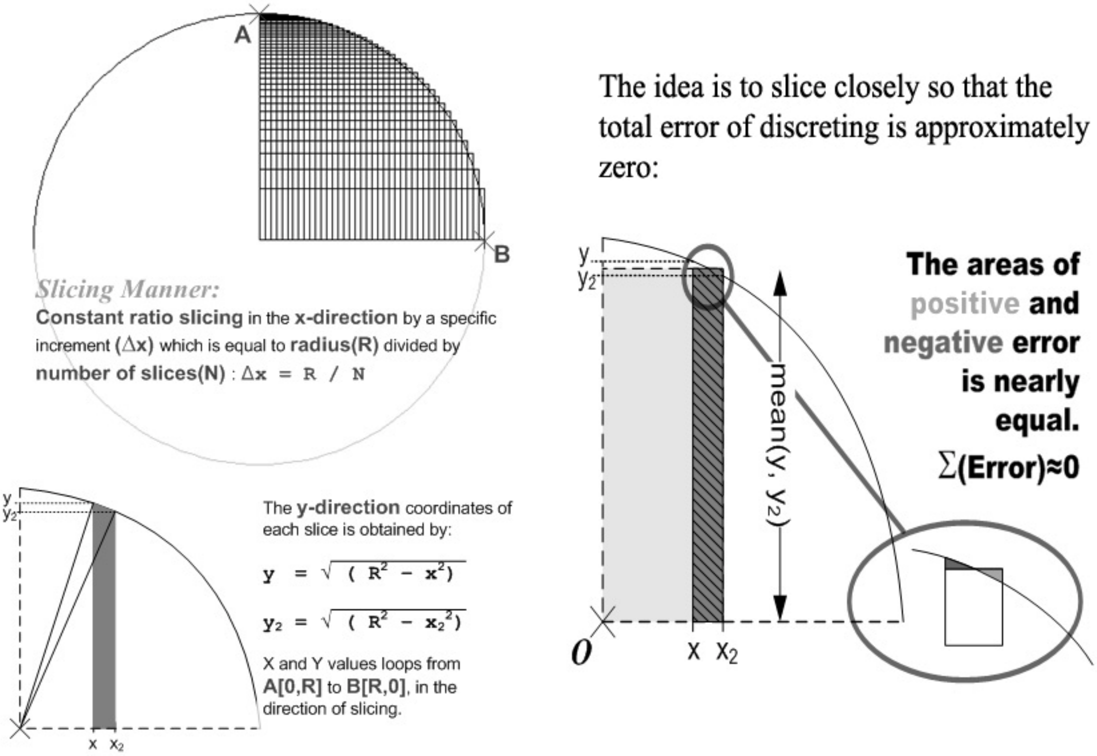

Figure 2.24 : The fashion of numerical integration for circular areas

The stress increment problem of a uniform arc-shaped load can be defined by four parameters (Figure 2.25): the angle of arch, α; the angle for point, β which is the angle from the starting corner of the arc to the line *OP* passing through the center to the projection of the stress point on ground surface; ratio of depth z / R where R is the radius of the arc and z is the depth of stress point; ratio of radius where r is the length of the line *OP*.

The summation or the extraction of these areas based on the principle of superposition – valid since the theory of elasticity is considered – can produce the desired geometry as depicted for the arc-shaped areas in Figure 2.26.

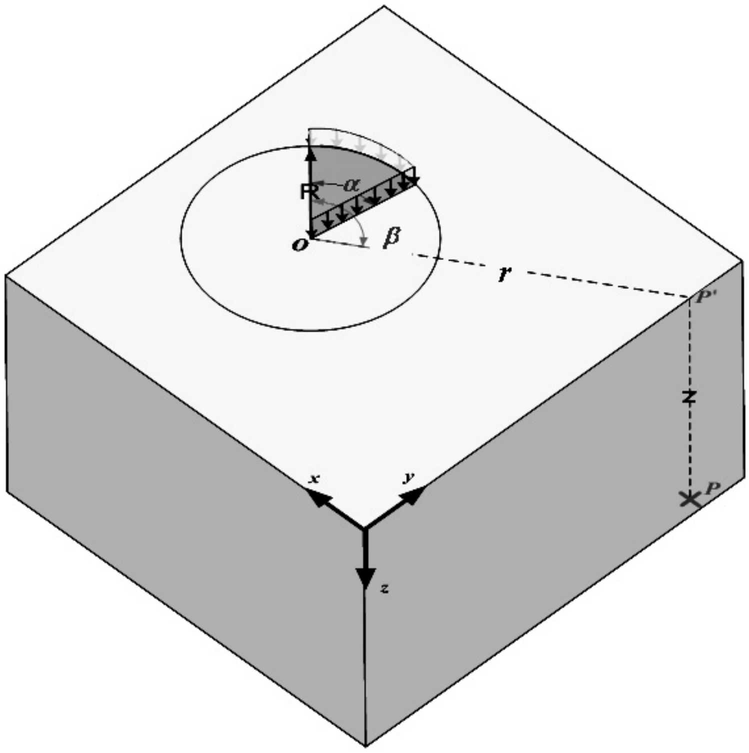

Figure 2.25 : Definition of a uniform arc-shaped load

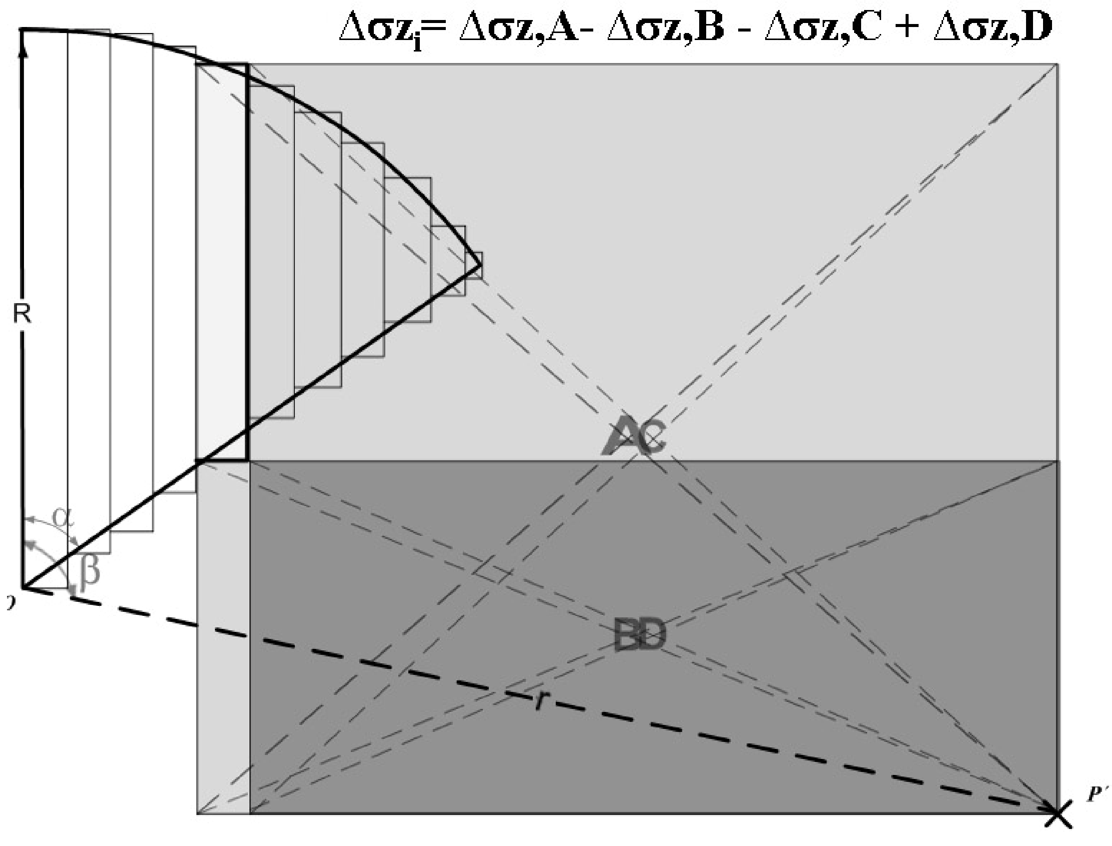

Figure 2.26 : Superposition for an arc

The result of the numerical integration is given below in Figure 2.27 for certain range of ratios, where every slice of the circle gives the influence factor for an arc of 10 degrees in plan view. The chart only has one *z* / *R* ratio, and five different *r* / *R* ratios designated with distinctive colors. Note that for *r* / *R* = 0, which corresponds to the center of the circular shape, the influence factor is the same for every slice.

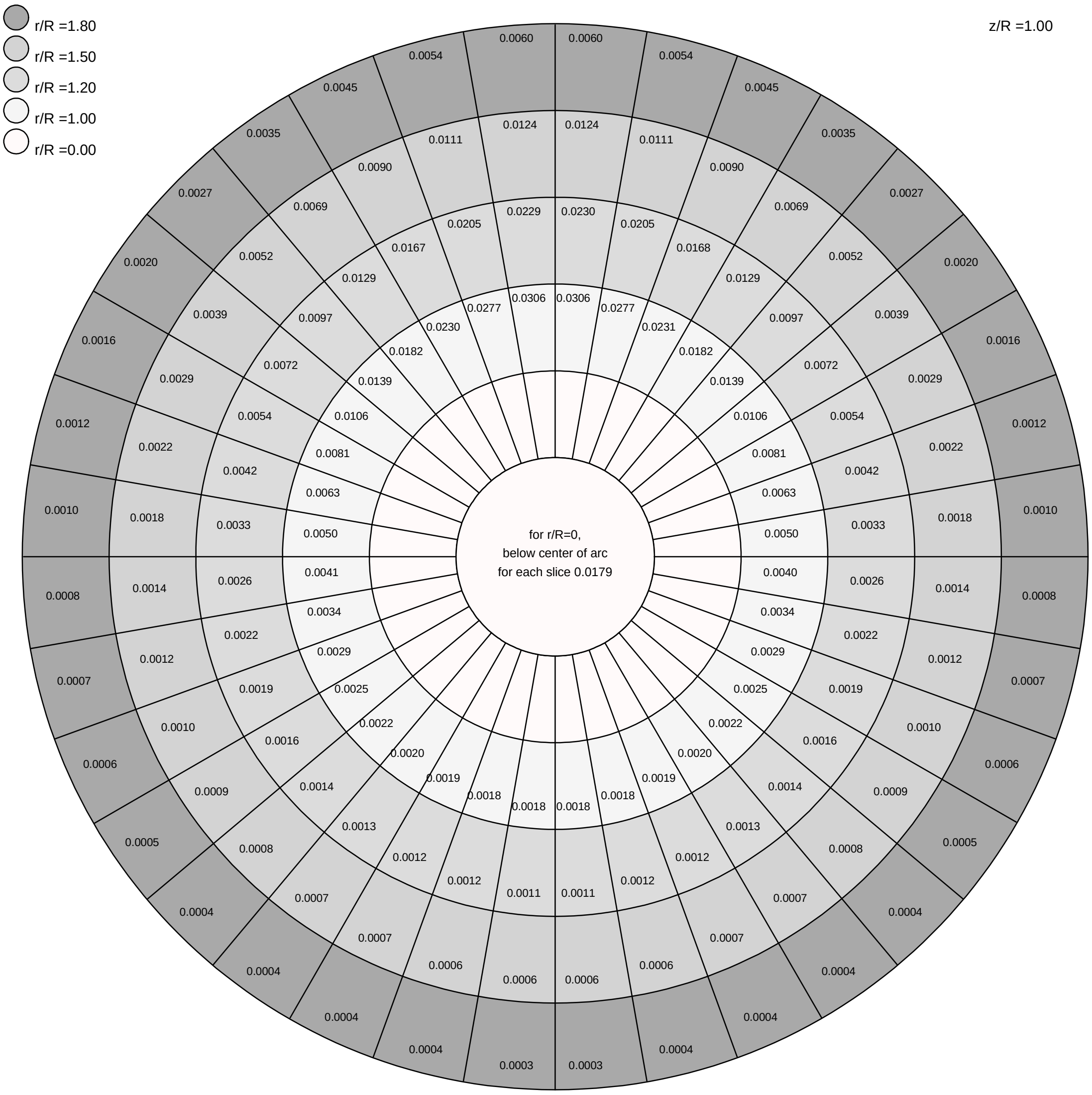

Figure 2.27 : Influence factors for the vertical stress increment of uniformly loaded arc-shaped area

To illustrate the usage of this chart consider the case where α=40°, β=60°, *r* / *R* = 1.5 and *z* / *R* = 1.0. The influence factors, which are to be summed, are selected by using the angles for related ratios as shown in Figure 2.28.

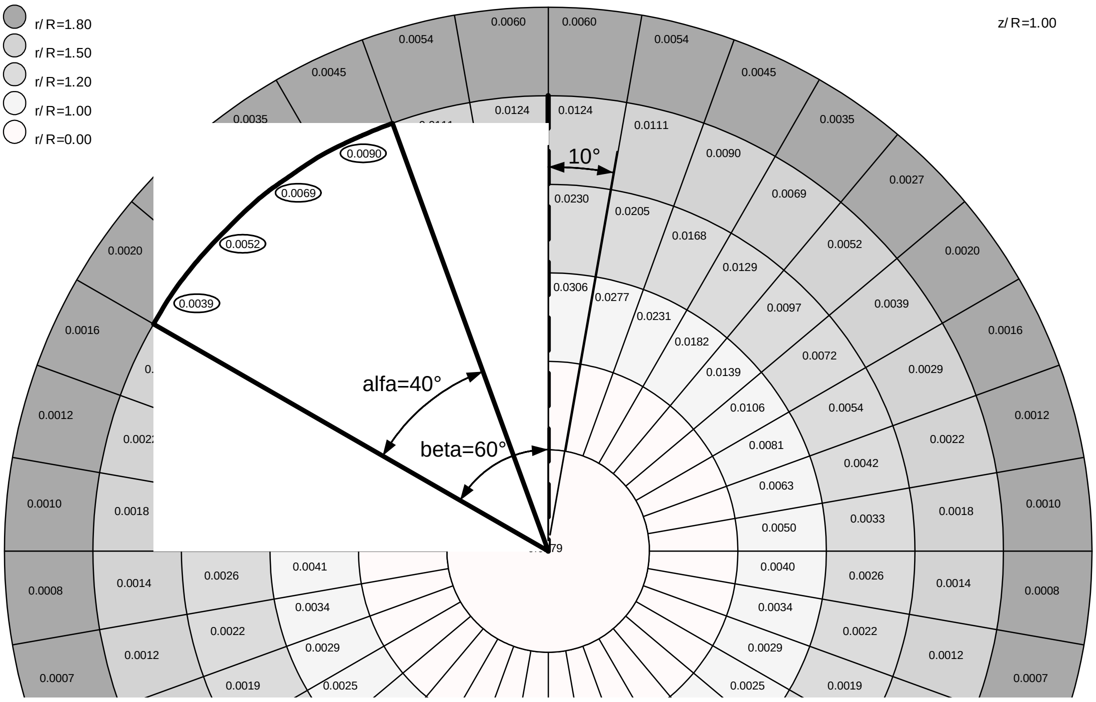

Figure 2.28 : Example for using the charts for arc-shaped areas

Thus $I_f = 0.0039 + 0.0052 + 0.0069 + 0.0090 = 0.025$, yet (2.33) can be used simply for calculation the vertical stress increment for any uniform load on the arc-shaped area.

More charts with different geometrical ratios are given in Appendix B. The program producing similar charts based on user input can be downloaded from *http://www.boraokumusoglu.net/zg.zip*.

2.2.3.2.3. Any Uniformly Loaded Shape

Newmark (1942) has devised graphical solutions for the stress increments of any uniformly loaded shape where the shape is drawn on a chart – namely a Newmark's chart – with a given scale based on the depth which the stress increment is to be calculated. The idea is based on drawing circles with respect to a constant rate growth in the influence factor – ratio of surcharge to stress increment as previously stated in (2.33) – and arranging these circles on the ratio of their diameter vs. the depth. (2.54) can be rewritten in terms of these ratios as:

$$D/z = 2\left\{\left[1/\left(1-\Delta\sigma_z/q\right)\right]^{2/3}-1\right\}^{1/2} \quad \textbf{(2.55)}$$

The ratios can be tabulated on the basis of constant rate growth in the influence factor:

Table 2.2 : Ratios for constructing a Newmark's chart (Azizi, 2000)

$\Delta\sigma_z/q$	**0.1**	**0.2**	**0.3**	**0.4**	**0.5**	**0.6**	**0.7**	**0.8**	**0.9**	**1.0**
D/z	0.54	0.80	1.04	1.27	1.53	1.84	2.22	2.77	3.82	∞

If circles drawn according to the ratios in Table 2.2, are subdivided radially into 20 equal elements, each element will have a influence factor value of 0.1 / 20 = 0.005. Thus the relevant Newmark's chart can be illustrated as follows:

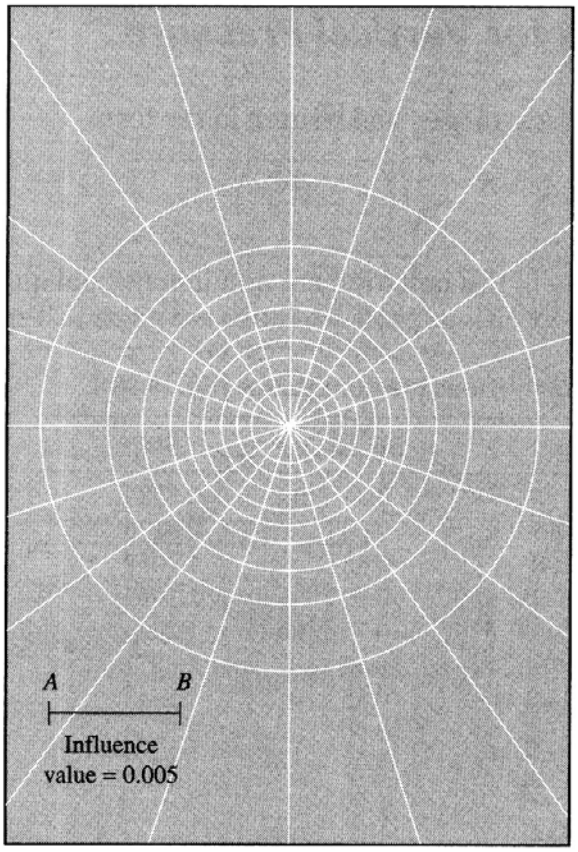

Figure 2.29 : Newmark's Chart for vertical stress increment (Das, 2001)

The following expression is used to estimate the vertical stress increment from the chart:

$$\Delta\sigma_z = (IV)qM \qquad \textbf{(2.56)}$$

where *IV* is influence value of the chart and *M* is the count of elements covered by the shape which is to be drawn according the scale *AB*. The magnitude of the line *AB* is equal to the depth of the investigated point.

As an example, consider a 3x3 meters square footing with a uniform load of 660 kN. If the vertical stress increment at 3 meters depth is to be estimated using the Newmark's chart, the footing is drawn on the chart with one edge equal to the scale on the chart, since the depth and the footing length is equal:

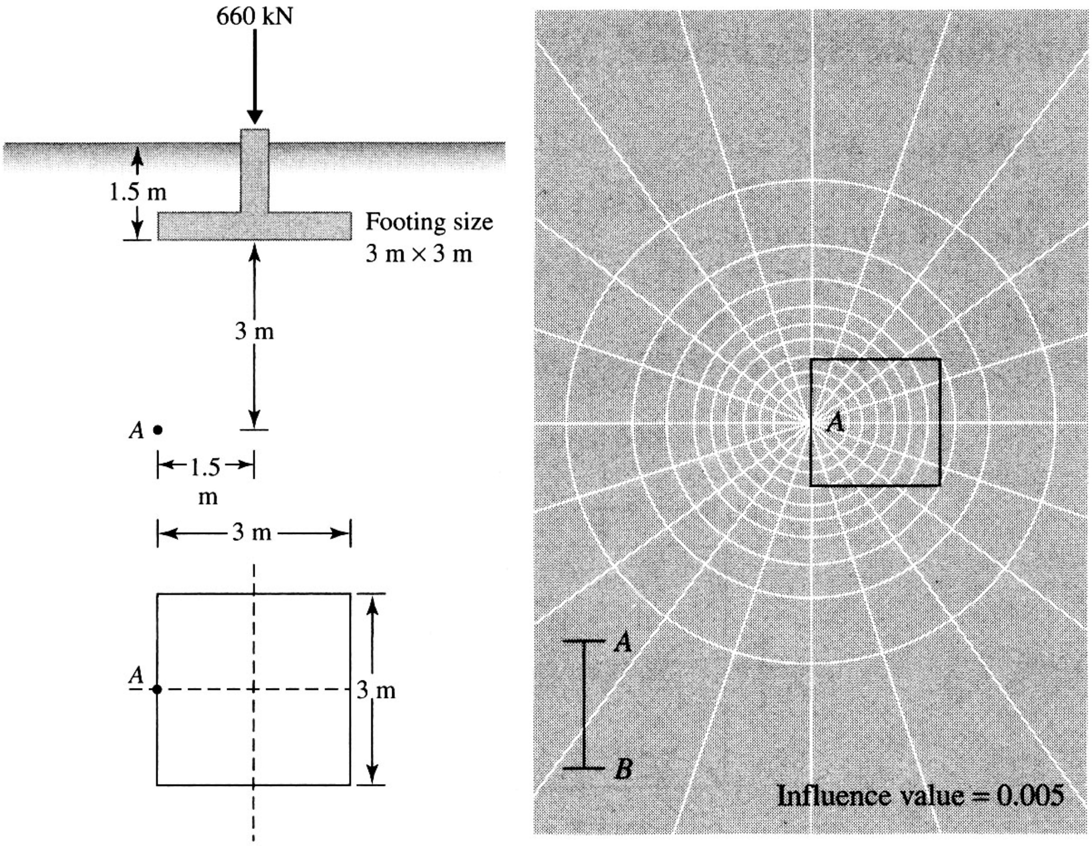

Figure 2.30 : An example for the utilization of Newmark's Chart (Das, 2001)

The count of elements within the area of the footing from Figure 2.30, is about 48.5. Using (2.56) the stress increment is 0.005 * (660 / [3*3]) * 48.5 = 17.78 kN/m2.

More Newmark's charts for other stress increments are given in Appendix C.

2.3.2.3. Stress Increments for Embankments

Since being another regular design in geotechnical engineering, it is also necessary to determine the increase of vertical stress in a soil mass caused by embankments. The expression, which is based on geometrical parameters given in Figure 2.31, is stated below:

$$\Delta\sigma_z = \frac{q}{\pi}\left[\left(\frac{B_1 + B_2}{B_1}\right)(\alpha_1 + \alpha_2) - \frac{B_1}{B_2}(\alpha_2)\right] \qquad \textbf{(2.57)}$$

where, $\alpha_1 = \tan^{-1}\left(\left[B_1 + B_2\right]/z\right) - \tan^{-1}\left(B_1/z\right)$ and $\alpha_2 = \tan^{-1}\left(B_1/z\right)$. Note that α_1 and α_2 are in radians.

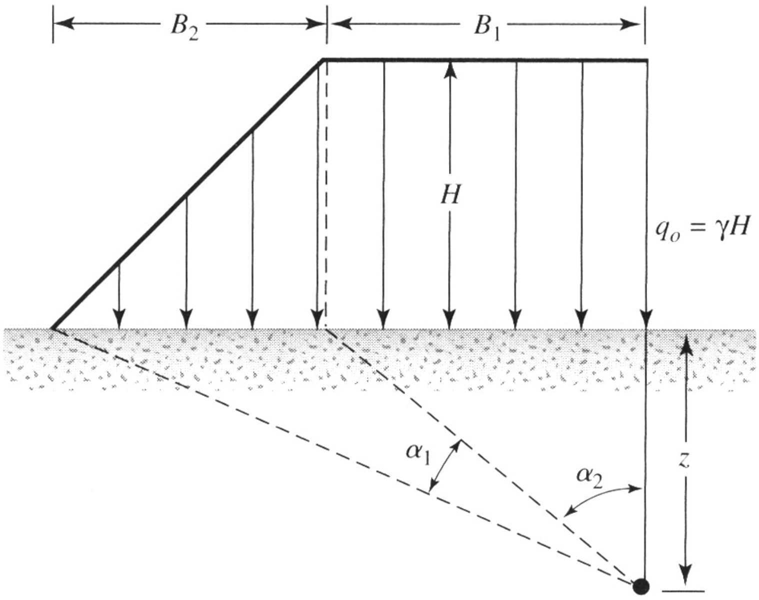

Figure 2.31 : Stress increment for embankments (Das, 2001)

The increase in vertical stress for points other than the one assigned in Figure 2.31, can be found by a superposition of three different embankment geometries as illustrated below in Figure 2.32.

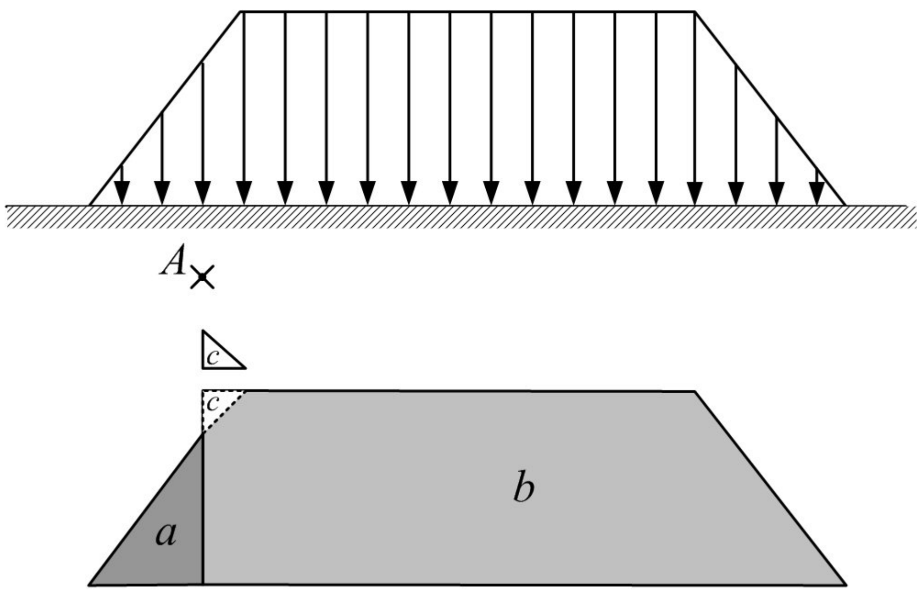

$$\Delta\sigma_z(\text{for point A}) = \left(I_{f,a} + I_{f,b} - I_{f,c}\right) \times q$$

Figure 2.32 : Superposition for embankments

Osterberg (1957) has produced the following chart for the sake of ease during calculation, which gives the influence factor used in conjunction with (2.33).

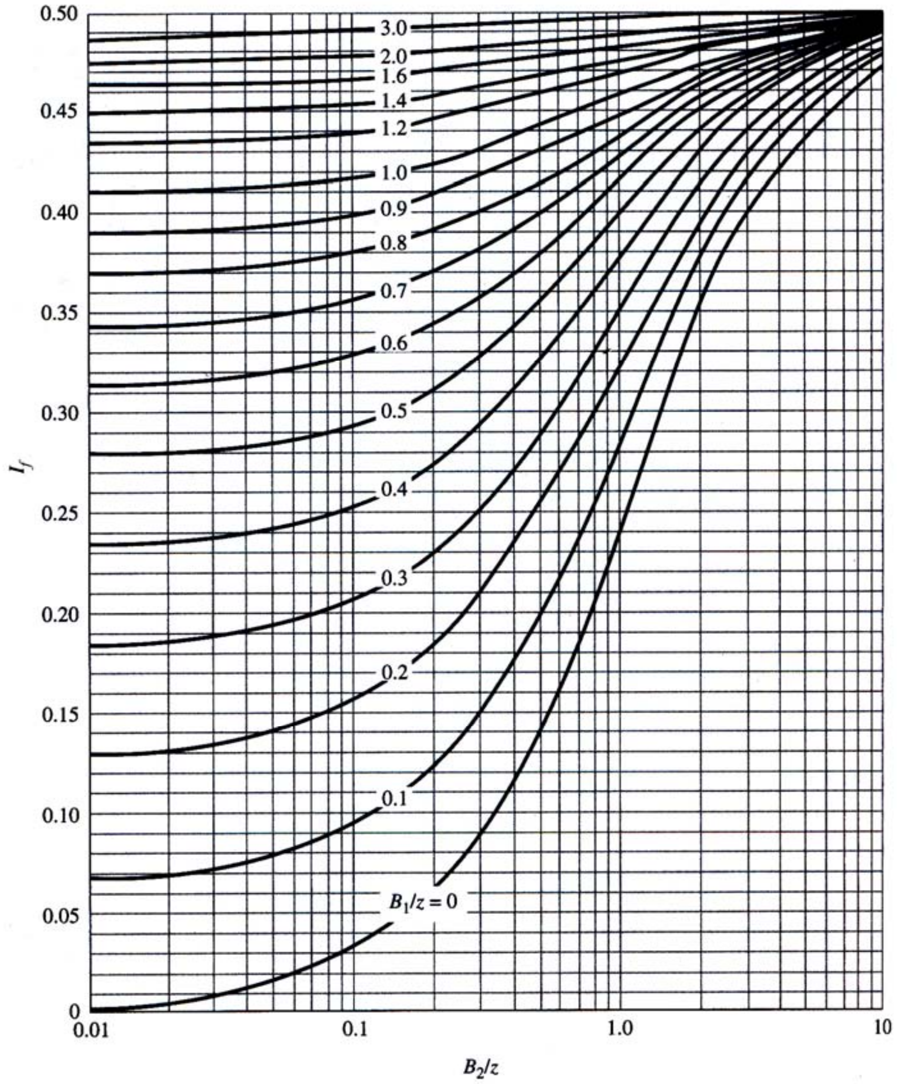

Figure 2.33 : Influence factors for the vertical stress increment of embankment (Das, 2001)

2.3.3. Special Cases of Soil Stratification

In the preceding sections, the soil is assumed to be homogeneous semi-infinitely. In the field, it is possible to encounter with soils with different elasticity e.g. soft soil underlied by rock or a stiff soil over a softer one.

Fox (1948) has given a comparison of vertical stress bulbs due to a uniformly loaded circular area between a homogeneous soil (the solution of Boussinesq) and in a case where the underlying soil has a remarkable low modulus of elasticity in contrast to the top layer:

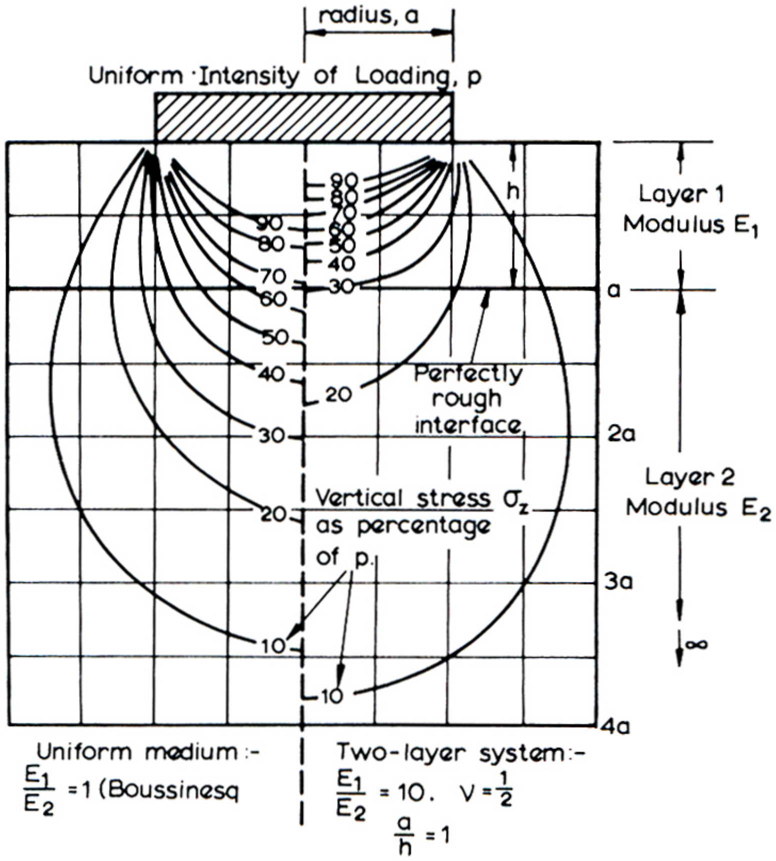

Figure 2.34 : Stress bulbs for different stratification (Poulos and Davis, 1974)

In addition, there is a chart by Fox (1948) which gives the vertical stress increase at the interface of two layers according to the ratios of elasticity modulus and the depth of the top layer:

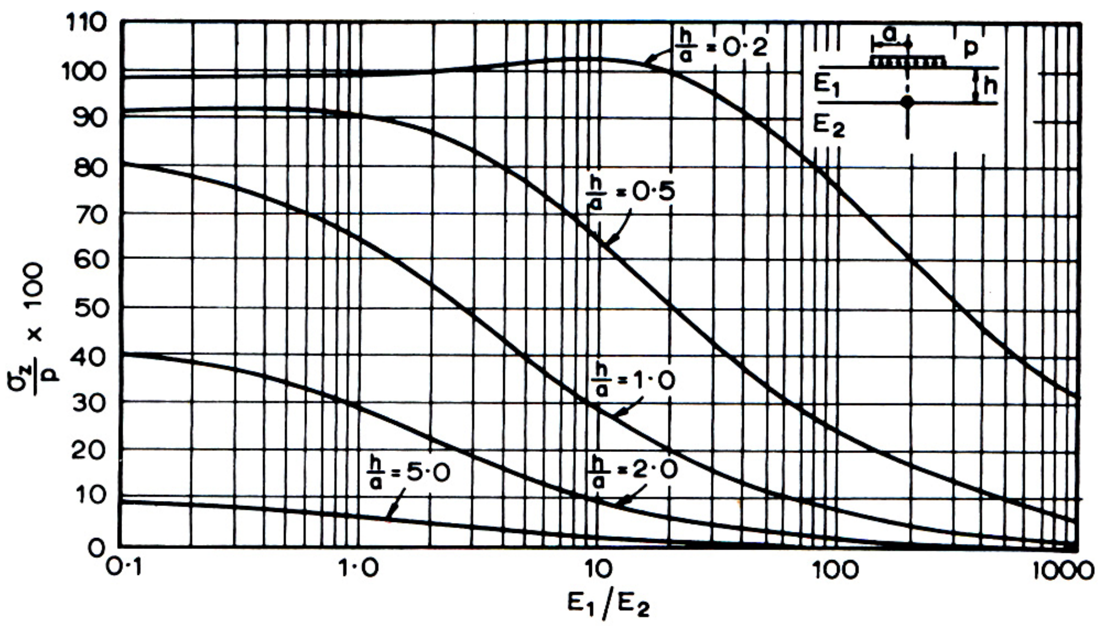

Figure 2.35 : Influence factors at interface of two layers (Poulos and Davis, 1974)

A chart for the influence factors for other ratios of elasticity modulus are developed by Burmister (1958):

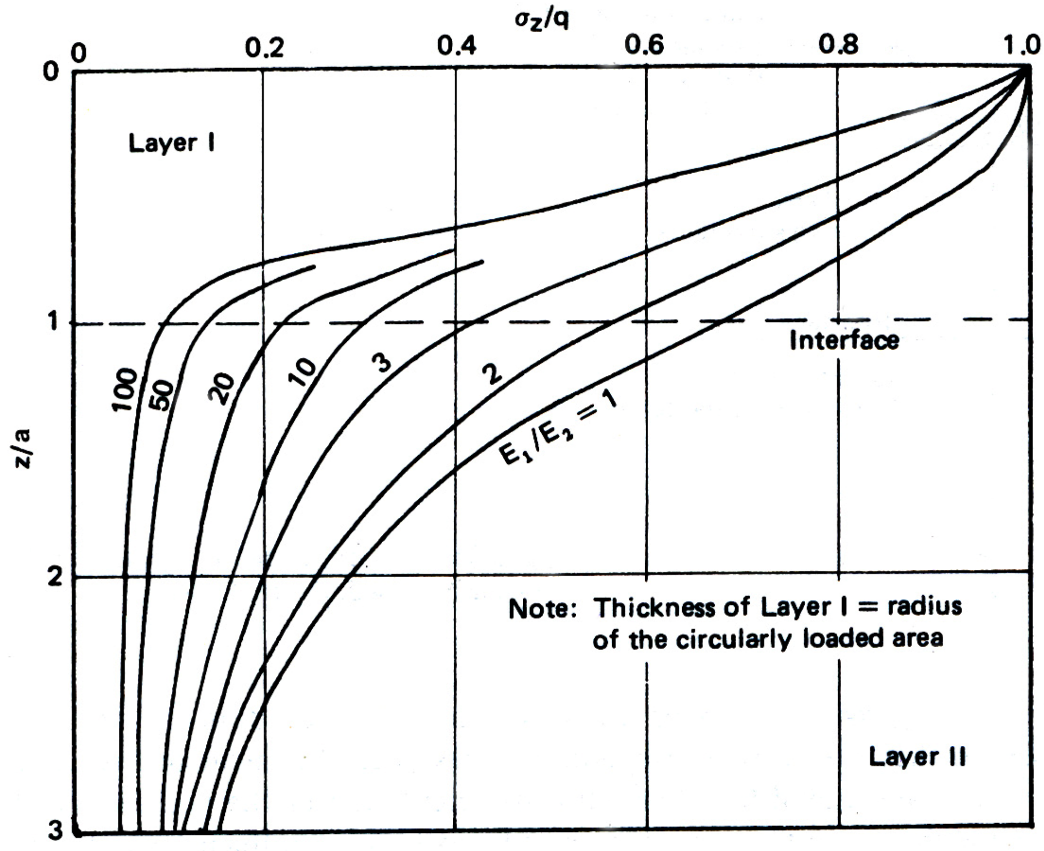

Figure 2.36 : Influence factors for two layered profile (Das, 1985)

There are many other charts (Poulos and Davis, 1974) in geotechnical literature related with this topic – namely stress in multi-layer systems –, though it is clarified by Das (1985) they are more related with highway pavement design.

2.3.4. Approach for Rigidity

It was stated before in 2.3.1 that the contact pressure under rigid foundations varies according to the elastic properties of both the foundation and the underlying soil, and the geometry of the foundation. It is in the shape of an inverted parabola for a soil supplying enough confinement at the edges (Figure 2.37-a) – for cohesive soils or also valid for granular soil in case of an embedded foundation –, or either has a parabolic distribution (Figure 2.37-b) – for granular soils without insufficient confinement –. The basic mathematical expressions are given below on the figure:

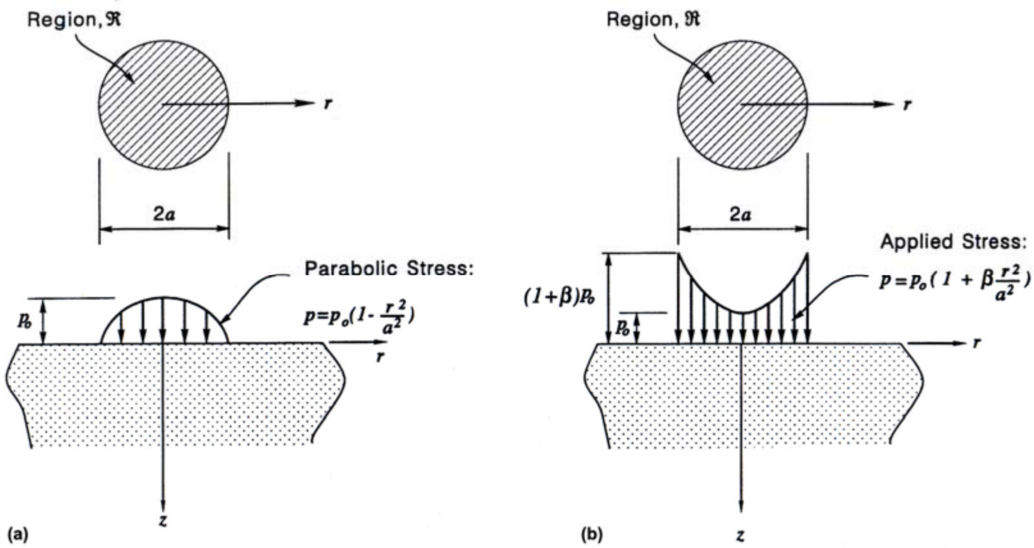

Figure 2.37 : Functions for contact pressure (Davis and Selvadurai, 1996)

Borowicka (1936) has analyzed the problem for uniformly loaded strip and circular rigid foundations underlied by an elastic medium and have given the contact pressures (Figure 2.38) according to the dimensionless coefficient K_r:

$$K_r = \frac{1}{6}\left(\frac{1-\mu_S^{\,2}}{1-\mu_F^{\,2}}\right)\left(\frac{E_F}{E_S}\right)\left(\frac{T}{b}\right)^3 \tag{2.58}$$

where S, F indexes indicate the properties for soil and foundation respectively, T is the thickness and b is the half of the width of foundations.

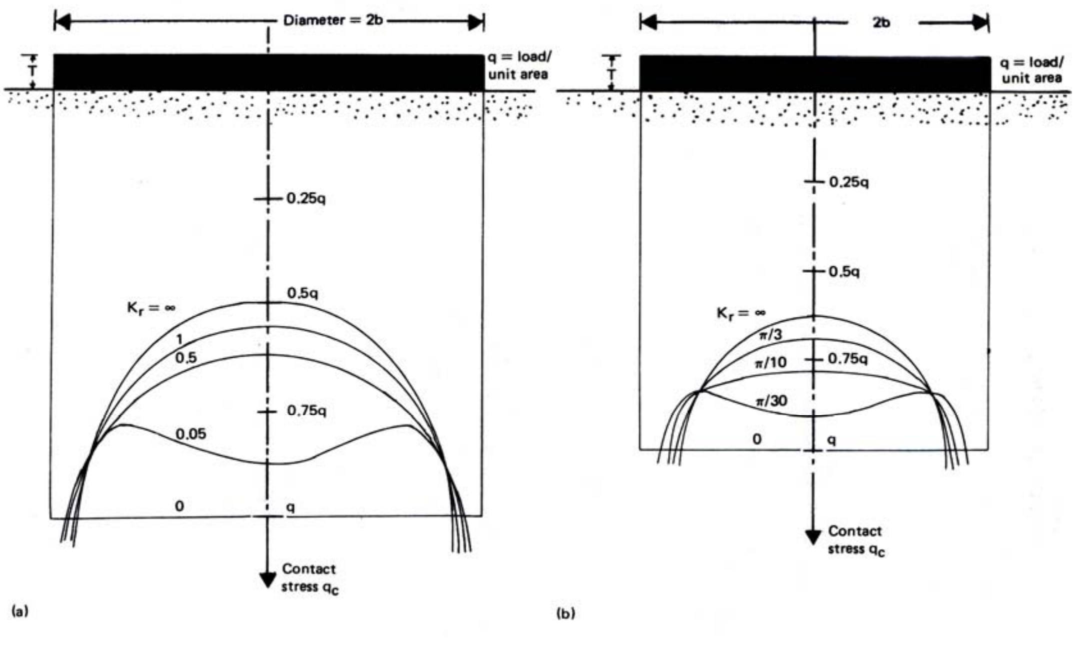

Figure 2.38 : Distribution of contact pressure under an elastic medium (Das, 1985)

Indeed the soil is not an infinitely elastic material, since it has a finite strength beyond which the plastic flow will occur. Thus the actual contact pressure will be truncated as indicated in Figure 2.39.

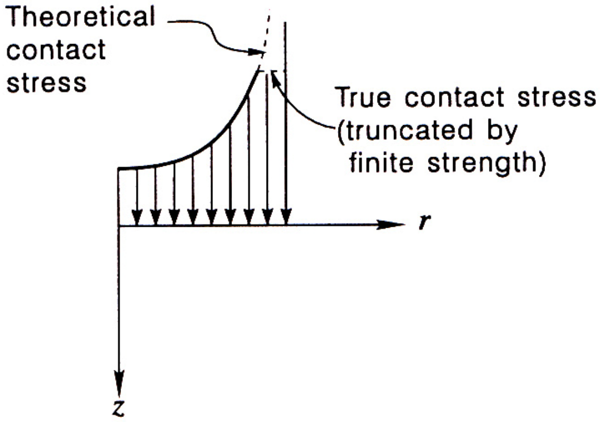

Figure 2.39 : Limitation for theoretical distribution of contact pressure in practice (Davis and Selvadurai, 1996)

A more recent study (Figure 2.40) by Dempsey and Li (1989) gives the contact pressure and vertical stress (Figure 2.41) within the underlying layer for a rigid rectangular footing, as a result of a numerical analysis of soil-structure interaction.

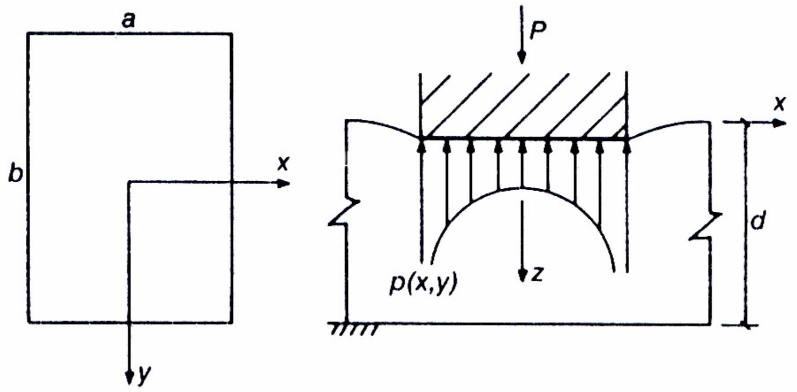

Figure 2.40 : An interactive numerical model for investigating contact pressure (Dempsey and Li, 1989)

Note that, results are dimensionless as being normalized to average contact pressure.

Despite the intricacy for stresses in soil under rigid foundations, there are many practical methods to estimate the resultant uniform settlement, which will be covered in the following chapter.

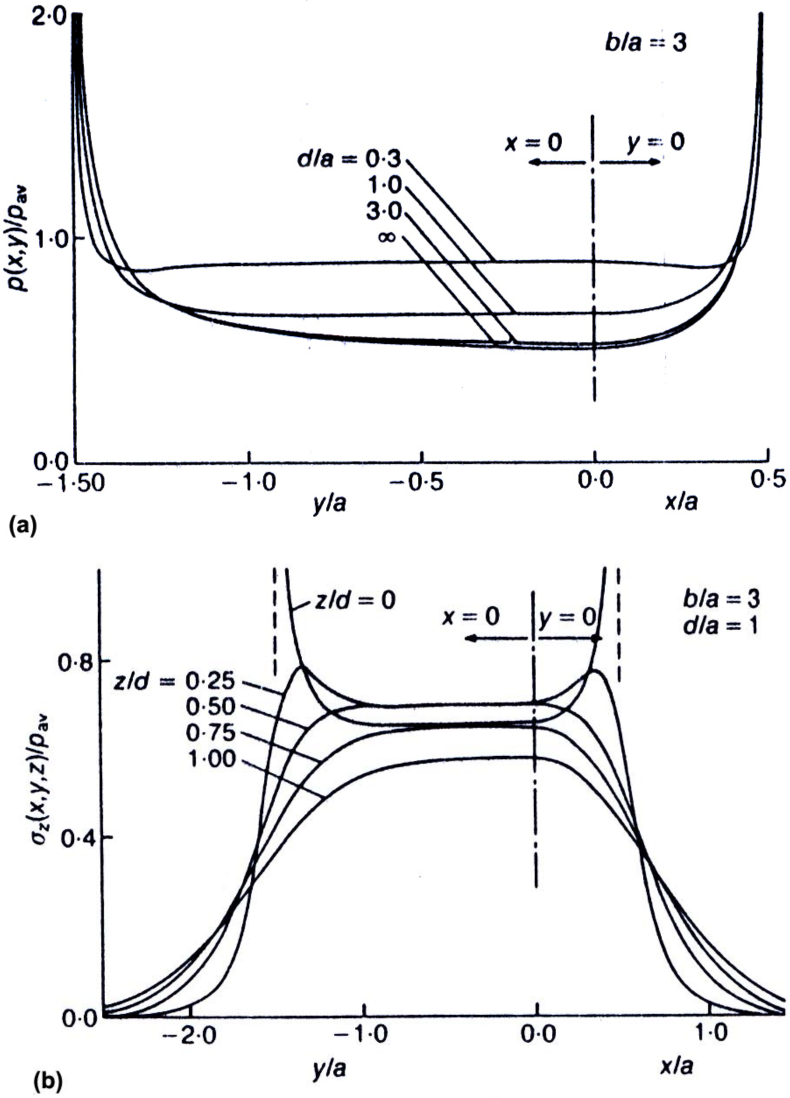

Figure 2.41 : Distribution of contact pressure (a) and vertical stress increment (b), both normalized to average contact pressure (Dempsey and Li, 1989)

3. ELASTO PLASTIC STRESS-STRAIN RELATIONSHIPS FOR SOILS

The displacements at the soil boundaries, are driven by the strains – occurring within the soil body – which are produced by additional loading by a construction or even by some exceptional events such as cyclic loading from machinery, effects of an earthquake, lowering of the groundwater level for the requirement of a dry construction or as a result of an irrigation, industrial mining etc., which are reported by Terzaghi and Peck, 1967. Thus, simply the engineering structures settle in a diverse number of ways differing in magnitude, time and mechanism.

The separation of the most common incidents of this phenomenon is based on the reaction of the volume change during loading for the granular soils and the clayey soils. As an aggregation of macroscopic particles, saturated granular soils tend to settle immediately, showing little resistance to the flow of water with a ready drainage. For saturated clayey soils, which are composed of microscopic particles, the drainage takes a significant amount of time resulting in the development of the excess pore pressure. As this pressures dissipates, in other words as the pressure caused by the structure is gradually transmitted to the soil skeleton – as first recognized by Terzaghi, 1924 – the consolidation settlement occurs. It is necessary to state that Terzaghi has assumed that the immediate settlement of clay is zero, while Skempton and Bjerrum (1957) favored to include the immediate settlement of clay obtained from elastic theory in their calculations.

Other interesting and relatively fresh topics in this area, are the tertiary consolidation and the creep settlement, where soil continues to settle for a longer period of time under constant load, respectively for clays – with organic content as investigated by Yilmaz and Saglamer, 2001 – and for sands – under excessive loading as studied by Briaud and Gibbens, 1999 –.

In this chapter, the calculation methods for immediate settlement caused by the construction of shallow foundations are presented. Other types of settlement (e.g. consolidation), requiring distinctive engineering analyses, are kept outside the scope of this study.

Nevertheless, before going further into the methods for the calculation of immediate settlement, it is crucial to notify that for any design, the check for the safety against the bearing capacity failure of the foundation is required to be conducted in the first place. An analysis of settlement will be pointless, unless the stability of the soil is assured. For convenience, the calculation of the bearing capacity for shallow foundations is given in Appendix D.

3.1. Theory of Elasticity

The fastest yet simplest way to calculate ground settlements in geotechnical problems is to use the governing equations from theory of elasticity. This methodology only requires two soil parameters: the Poisson's ratio, which has been defined and given the range of values in Table 2.1; and the modulus of elasticity or the Young Modulus.

The most representative values for the modulus of elasticity are obtained from triaxial tests as depicted in Figure 3.1.

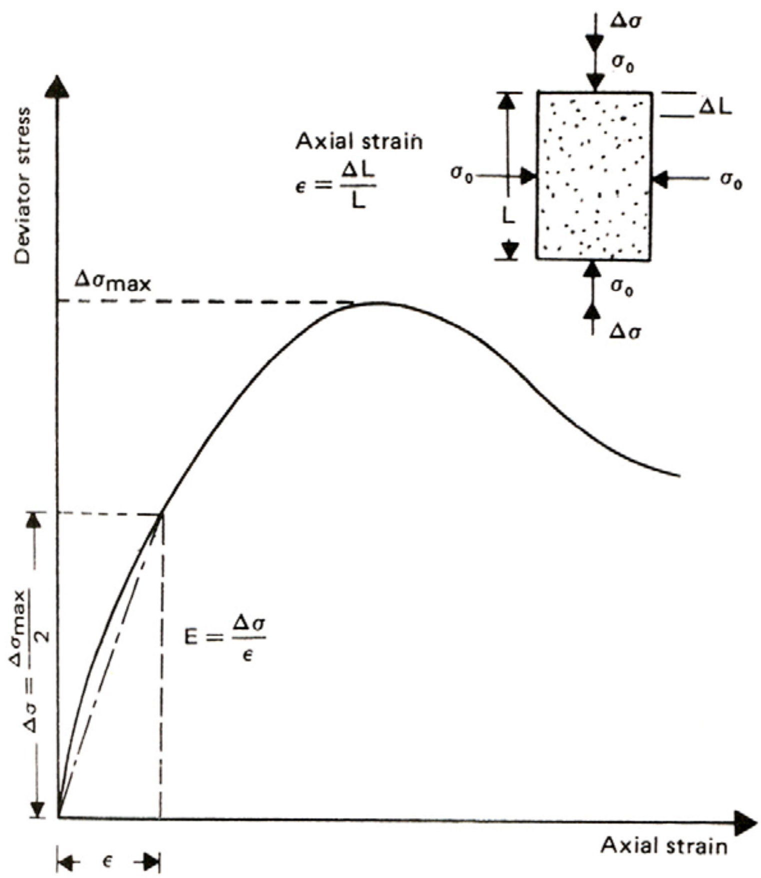

Figure 3.1 : Stress-strain curve from a triaxial test (Das, 1985)

The results of in-situ tests, such as the Standard Penetration Test – a.k.a SPT – or the Cone Penetration Test – a.k.a CPT – can be correlated to the modulus of elasticity via empirical, yet verified and standardized expressions given in Table 3.1.

Table 3.1 : Elasticity Modulus derived from in-situ tests (Bowles, 1996)

Soil	SPT	CPT
Sand (normally consolidated)	$E_s = 500\ (N + 15)$ $= 7\ 000\ N^{1/2}$ $= 6\ 000\ N$ $= (15\ 000 \text{to} 20\ 000)\ \ln N$	$E_s = (2 \text{ to } 4)\ q_u$ $= 8\ 000\ N^{1/2}$ $= 1.2\ (3D_R^{\ 2} + 2)\ q_c$ $= (1 + D_R^{\ 2})\ q_c$
Sand (saturated)	$E_s = 250\ (N + 15)$	$E_s = F\ q_c$ $e = 1.0 \quad F = 3.5$ $e = 0.6 \quad F = 7.0$
Sands, all (normally consolidated)	$E_s = (2600 \text{ to } 2900)\ N$	
Sand (over consolidated)	$E_s = 40\ 000 + 1050\ N$ $E_{s(OCR)} = E_{s\ (NC)}\ \text{OCR}^{1/2}$	$E_s = (6 \text{ to } 30)\ q_u$
Gravelly sand	$E_s = 1200\ (N + 6)$ $= 1200\ (N + 6)$ $= 1200\ (N + 6) + 2\ 000$	 $N \leq 15$ $N > 15$
Clayey sand	$E_s = 320\ (N + 15)$	$E_s = (3 \text{ to } 6)\ q_c$
Silts, sandy silt or	$E_s = 300\ (N + 6)$	$E_s = (1 \text{ to } 2)\ q_c$
Clayey silt	If $q_c < 2500$ kPa use $2500 < q_c < 5000$ kPa where E'_s (constrained modulus) = =	 $E'_s = 2.5\ q_c$ $E'_s = 4\ q_c + 5\ 000$ $E_s\ (1 - \mu) / \{ (1 + \mu)\ (1 - 2\mu) \}$ $1 / m_v$
Soft clay or clayey silt		$E_s = (3 \text{ to } 8)\ q_c$

Note that the modulus of elasticity is in kPa for SPT and units of q_c for CPT. For SPT, the blow count N should be corrected for an efficiency of 55%, thus the value of N_{55} is to be used in this correlations. Constrained modulus E_s’ is the modulus of elasticity when only one dimensional compression occurs, where as under a loading of wide area.

For clayey soils it is more preferable to use the undrained shear strength calculated from in-situ tests, to estimate the modulus of elasticity as summarized in Table 3.2, where Atterberg limits are required for a more precise estimation.

Table 3.2 : Elasticity Modulus via undrained shear strength (Bowles, 1996)

Clay and silt	$I_P > 30$ or organic	$E_s = (100 \text{ to } 500)\, s_u$
Silty or sand clay	$I_P < 30$ or stiff	$E_s = (500 \text{ to } 1500)\, s_u$
	again	$E_{s(OCR)} = E_{s\,(NC)}\, OCR^{1/2}$
		use smaller s_u -coefficient for highly plastic clay

Of general application in clays is

$$E_s = K\, s_u \text{ (units of } s_u \text{)}$$

where K is defined as

$$K = 4200 - 142.54\, I_P + 1.73\, I_P^2 - 0.007\, I_P^3$$

and I_P = plasticity index in percent. Use $20\% \leq I_P \leq 100\%$ and round K to the nearest multiplier of 10.

Another equation of general application is

$$E_s = 9400 - 8900\, I_P + 11\,600\, I_C - 8800\, S \text{ (kPa)}$$

Other field tests are also available for this purpose such as the Plate Loading Test, in which the determination of the settlement by recording the load and corresponding vertical movement when a rigid plate is loading the ground. The resulting load-settlement values can be used as follows to obtain the elasticity modulus:

$$E_{PLT} = \frac{\Delta p}{\Delta s} \cdot \frac{\pi b}{4}\left(1 - \mu^2\right) \tag{3.1}$$

where b is the diameter of the plate, Δp and Δs are the increments in load and settlement respectively. Yet it should be realized that due to the smaller dimensions of the test plate in contrast to the actual foundation, the stress bulb does not develop much further into depths of soil, thus resulting in a poor characterization of the modulus of elasticity. This is the reason why the elasticity modulus calculated above, is symbolized by E_{PLT}. All respective field tests – together with the Pressuremeter Test, the Flat Dilatometer Test etc. – which are suitable for achieving the modulus of elasticity, are covered with great detail in equipment, procedure and evaluation in Eurocode 7, 2000.

The seismic tests – such as Cross-hole and Down-hole methods – are used widely to determine the elastic properties throughout a construction field; great detail on this subject can be found in Ishihara, 1996 and an example of practical investigations has been conducted by Iyisan, 1994. Following relationships can be utilized to obtain elastic properties of soil from the shear (or secondary) wave velocity – V_S in meters/sec. – and the compressive (or primary) wave velocity - V_P in meters/sec:

$$\mu = 0.5\left(1-2[V_S/V_P]^2\right)\Big/\left(1-[V_S/V_P]^2\right) \tag{3.2}$$

$$E = \rho \cdot V_P^{\,2}\left(3V_S^{\,2}-4V_P^{\,2}\right)\Big/\left(V_S^{\,2}-V_P^{\,2}\right) \tag{3.3}$$

where ρ is the bulb density in kg/m^3 and E is in Pa = N/m^2. For convenience typical values of the modulus of elasticity are listed below in Table 3.3:

Table 3.3 : Ranges of elasticity modulus (Bowles, 1996)

Soil	***E*, MPa**
Clay	
Very soft	2-15
Soft	5-25
Medium	15-50
Hard	50-100
Sandy	25-250
Glacial till	
Loose	10-150
Dense	150-720
Very dense	500-1440
Loess	15-60
Sand	
Silty	5-20
Loose	10-25
Dense	50-81
Sand and gravel	
Loose	50-150
Dense	100-200
Shale	150-5000
Silt	2-20

3.1.1. Settlement under a Point Load

For a vertical point load depicted in Figure 2.15, using the Hooke's Law stated in (2.7) and the stress increments given in (2.22) to (2.24), the strain at a depth of z is:

$$\varepsilon_z = \frac{P}{2\pi E}\left[\frac{3(1+\mu)r^2 z}{(r^2+z^2)^{5/2}} - \frac{3+\mu(1-2\mu)z}{(r^2+z^2)^{3/2}}\right] \tag{3.4}$$

The total settlement at a depth of z can be calculated by integrating (3.4) as:

$$S_e = \int \varepsilon_z dz = \frac{P}{2\pi E}\left[\frac{(1+\mu)z^2}{(r^2+z^2)^{3/2}} + \frac{2(1-\mu^2)}{(r^2+z^2)^{1/2}}\right] \tag{3.5}$$

If we set $z = 0$, the resultant equation will give the surface settlement:

$$S_e(\text{surface}) = \frac{P}{\pi E r}(1-\mu^2) \qquad \textbf{(3.6)}$$

where $r = \sqrt{x^2 + y^2}$.

3.1.2. Settlement under Uniformly Loaded Areas

Using the same procedure, expressions for the settlement of uniformly loaded areas can be found from the theory of elasticity, for which of the stress increment are given in the preceding chapter.

For a uniformly loaded circular area (Figure 2.22), the surface settlement can be estimated by:

$$S_e(\text{surface}) = qa\frac{1-\mu^2}{E} I_2 \qquad \textbf{(3.7)}$$

where the influence factor I_2, which is a function of z / a and r / a, is tabulated in Table 3.4 and Table 3.5.

Table 3.4 : Influence factor I_2 for settlement of circular areas (Das, 1985)

	r/a								
z/a	0	0.2	0.4	0.6	0.8	1	1.2	1.5	2
0	2.0	1.97987	1.91751	1.80575	1.62553	1.27319	.93676	.71185	.51671
0.1	1.80998	1.79018	1.72886	1.61961	1.44711	1.18107	.92670	.70888	.51627
0.2	1.63961	1.62068	1.56242	1.46001	1.30614	1.09996	.90098	.70074	.51382
0.3	1.48806	1.47044	1.40979	1.32442	1.19210	1.02740	.86726	.68823	.50966
0.4	1.35407	1.33802	1.28963	1.20822	1.09555	.96202	.83042	.67238	.50412
0.5	1.23607	1.22176	1.17894	1.10830	1.01312	.90298	.79308	.65429	.49728
0.6	1.13238	1.11998	1.08350	1.02154	.94120	.84917	.75653	.63469	
0.7	1.04131	1.03037	.99794	.91049	.87742	.80030	.72143	.61442	.48061
0.8	.96125	.95175	.92386	.87928	.82136	.75571	.68809	.59398	
0.9	.89072	.88251	.85856	.82616	.77950	.71495	.65677	.57361	
1	.82843	.85005	.80465	.76809	.72587	.67769	.62701	.55364	.45122
1.2	.72410	.71882	.70370	.67937	.64814	.61187	.57329	.51552	.43013
1.5	.60555	.60233	.57246	.57633	.55559	.53138	.50496	.46379	.39872
2	.47214	.47022	.44512	.45656	.44502	.43202	.41702	.39242	.35054
2.5	.38518	.38403	.38098	.37608	.36940	.36155	.35243	.33698	.30913
3	.32457	.32403	.32184	.31887	.31464	.30969	.30381	.29364	.27453
4	.24620	.24588	.24820	.25128	.24168	.23932	.23668	.23164	.22188
5	.19805	.19785				.19455			.18450
6	.16554					.16326			.15750
7	.14217					.14077			.13699
8	.12448					.12352			.12112
9	.11079					.10989			.10854
10								.09900	.09820

Table 3.5 : Influence factor I_2 for settlement of circular areas, *continued* (Das, 1985)

z/a	r/a = 3	4	5	6	7	8	10	12	14
0	.33815	.25200	.20045	.16626	.14315	.12576	.09918	.08346	.07023
0.1	.33794	.25184	.20081						
0.2	.33726	.25162	.20072	.16688	.14288	.12512			
0.3	.33638	.25124							
0.4									
0.5	.33293	.24996	.19982	.16668	.14273	.12493	.09996	.08295	.07123
0.6									
0.7									
0.8									
0.9									
1	.31877	.24386	.19673	.16516	.14182	.12394	.09952	.08292	.07104
1.2	.31162	.24070	.19520	.16369	.14099	.12350			
1.5	.29945	.23495	.19053	.16199	.14058	.12281	.09876	.08270	.07064
2	.27740	.22418	.18618	.15846	.13762	.12124	.09792	.08196	.07026
2.5	.25550	.21208	.17898	.15395	.13463	.11928	.09700	.08115	.06980
3	.23487	.19977	.17154	.14919	.13119	.11694	.09558	.08061	.06897
4	.19908	.17640	.15596	.13864	.12396	.11172	.09300	.07864	.06848
5	.17080	.15575	.14130	.12785	.11615	.10585	.08915	.07675	.06695
6	.14868	.13842	.12792	.11778	.10836	.09990	.08562	.07452	.06522
7	.13097	.12404	.11620	.10843	.10101	.09387	.08197	.07210	.06377
8	.11680	.11176	.10600	.09976	.09400	.08848	.07800	.06928	.06200
9	.10548	.10161	.09702	.09234	.08784	.08298	.07407	.06678	.05976
10	.09510	.09290	.08980	.08300	.08180	.07710			

For a uniformly loaded rectangular area (Figure 2.17), the surface settlement beneath the corner can be estimated by:

$$S_e(\text{corner}) = \frac{qB}{2E}\left(1-\mu^2\right)\left[I_3 - \left(\frac{1-2\mu}{1-\mu}\right)I_4\right] \quad \textbf{(3.8)}$$

where

$$I_3 = \frac{1}{\pi}\left[\ln\left(\frac{\sqrt{1+m'^2+n'^2}+m'}{\sqrt{1+m'^2+n'^2}-m'}\right)+m'\ln\left(\frac{\sqrt{1+m'^2+n'^2}+1}{\sqrt{1+m'^2+n'^2}-1}\right)\right] \quad \textbf{(3.9)}$$

$$I_4 = \frac{n'}{\pi}\tan^{-1}\left(\frac{m'}{n'\sqrt{1+m'^2+n'^2}}\right) \quad \textbf{(3.10)}$$

in which $m' = \dfrac{L}{B}$ and $n' = \dfrac{z}{B}$.

For the sake of ease during calculation, values of I_3 and I_4 have been tabulated in Table 3.6 and Table 3.7.

Table 3.6 : Influence factor I_3 for settlement of rectangular areas (Das, 1999)

	m'									
n'	1	2	3	4	5	6	7	8	9	10
0.00	1.122	1.532	1.783	1.964	2.105	2.220	2.318	2.403	2.477	2.544
0.25	1.095	1.510	1.763	1.944	2.085	2.200	2.298	2.383	2.458	2.525
0.50	1.025	1.452	1.708	1.89	2.032	2.148	2.246	2.331	2.406	2.473
0.75	0.933	1.371	1.632	1.816	1.959	2.076	2.174	2.259	2.334	2.401
1.00	0.838	1.282	1.547	1.734	1.878	1.995	2.094	2.179	2.255	2.322
1.25	0.751	1.192	1.461	1.650	1.796	1.914	2.013	2.099	2.175	2.242
1.50	0.674	1.106	1.378	1.570	1.717	1.836	1.936	2.022	2.098	2.166
1.75	0.608	1.026	1.299	1.493	1.641	1.762	1.862	1.949	2.025	2.093
2.00	0.552	0.954	1.226	1.421	1.571	1.692	1.794	1.881	1.958	2.026
2.25	0.504	0.888	1.158	1.354	1.505	1.627	1.730	1.817	1.894	1.963
2.50	0.463	0.829	1.095	1.291	1.444	1.567	1.670	1.758	1.836	1.904
2.75	0.427	0.776	1.037	1.233	1.386	1.510	1.613	1.702	1.780	1.850
3.00	0.396	0.728	0.984	1.179	1.332	1.457	1.561	1.650	1.729	1.798
3.25	0.369	0.686	0.935	1.128	1.281	1.406	1.511	1.601	1.680	1.750
3.50	0.346	0.647	0.889	1.081	1.234	1.359	1.465	1.555	1.634	1.705
3.75	0.325	0.612	0.848	1.037	1.189	1.315	1.421	1.511	1.591	1.662
4.00	0.306	0.580	0.809	0.995	1.147	1.273	1.379	1.470	1.550	1.621
4.25	0.289	0.551	0.774	0.957	1.107	1.233	1.339	1.431	1.511	1.582
4.50	0.274	0.525	0.741	0.921	1.070	1.195	1.301	1.393	1.476	1.545
4.75	0.260	0.501	0.710	0.887	1.034	1.159	1.265	1.358	1.438	1.510
5.00	0.248	0.479	0.682	0.855	1.001	1.125	1.231	1.323	1.404	1.477
5.25	0.237	0.458	0.655	0.825	0.969	1.093	1.199	1.291	1.372	1.444
5.50	0.227	0.440	0.631	0.797	0.939	1.062	1.167	1.260	1.341	1.413
5.75	0.217	0.422	0.608	0.770	0.911	1.032	1.137	1.230	1.311	1.384
6.00	0.208	0.406	0.586	0.745	0.884	1.004	1.109	1.201	1.282	1.355
6.25	0.200	0.391	0.566	0.722	0.858	0.977	1.082	1.173	1.255	1.328
6.50	0.193	0.377	0.547	0.699	0.834	0.952	1.055	1.147	1.228	1.301
6.75	0.186	0.364	0.529	0.678	0.810	0.927	1.030	1.121	1.203	1.275
7.00	0.179	0.352	0.513	0.658	0.788	0.904	1.006	1.097	1.178	1.251
7.25	0.173	0.341	0.497	0.639	0.767	0.881	0.983	1.073	1.154	1.227
7.50	0.168	0.330	0.482	0.621	0.747	0.860	0.960	1.050	1.131	1.204
7.75	0.162	0.320	0.468	0.604	0.728	0.839	0.939	1.028	1.109	1.811
8.00	0.158	0.310	0.455	0.588	0.710	0.820	0.918	1.007	1.087	1.160
8.25	0.153	0.301	0.442	0.573	0.692	0.801	0.899	0.987	1.066	1.139
8.50	0.148	0.293	0.430	0.558	0.676	0.783	0.879	0.967	1.046	1.118
8.75	0.144	0.285	0.419	0.544	0.660	0.765	0.761	0.948	1.027	1.099
9.00	0.140	0.277	0.408	0.531	0.644	0.748	0.843	0.930	1.008	1.080
9.25	0.137	0.270	0.398	0.518	0.630	0.732	0.826	0.912	0.990	1.061
9.50	0.133	0.263	0.388	0.506	0.616	0.717	0.810	0.895	0.972	1.043
9.75	0.130	0.257	0.379	0.494	0.602	0.702	0.794	0.878	0.955	1.026
10.00	0.126	0.251	0.370	0.483	0.589	0.688	0.778	0.862	0.938	1.009

Table 3.7 : Influence factor I_4 for settlement of rectangular areas (Das, 1999)

	m'									
n'	1	2	3	4	5	6	7	8	9	10
0.25	0.098	0.103	0.104	0.105	0.105	0.105	0.105	0.105	0.105	0.105
0.50	0.248	0.167	0.172	0.174	0.175	0.175	0.175	0.176	0.176	0.176
0.75	0.166	0.202	0.212	0.216	0.218	0.219	0.220	0.220	0.220	0.220
1.00	0.167	0.218	0.234	0.241	0.244	0.246	0.247	0.248	0.248	0.248
1.25	0.160	0.222	0.245	0.254	0.259	0.262	0.264	0.265	0.265	0.266
1.50	0.149	0.220	0.248	0.261	0.267	0.271	0.274	0.275	0.276	0.277
1.75	0.139	0.213	0.247	0.263	0.271	0.277	0.280	0.282	0.283	0.284
2.00	0.128	0.205	0.243	0.262	0.273	0.279	0.283	0.286	0.288	0.289
2.25	0.119	0.196	0.237	0.259	0.272	0.279	0.284	0.288	0.290	0.292
2.50	0.110	0.186	0.230	0.255	0.269	0.278	0.284	0.288	0.291	0.293
2.75	0.102	0.177	0.223	0.250	0.266	0.277	0.283	0.288	0.291	0.294
3.00	0.096	0.168	0.215	0.244	0.262	0.274	0.282	0.287	0.291	0.294
3.25	0.090	0.160	0.208	0.238	0.258	0271	0.279	0.285	0.290	0.293
3.50	0.084	0.152	0.200	0.232	0.253	0.267	0.277	0.283	0.288	0.292
3.75	0.079	0.145	0.193	0.226	0.248	0.263	0.273	0.281	0.287	0.291
4.00	0.075	0.138	0.186	0.219	0.243	0.259	0.270	0.278	0.285	0.289
4.25	0.071	0.132	0.179	0.213	0.237	0.254	0.267	0.276	0.282	0.287
4.50	0.067	0.126	0.173	0.207	0.232	0.250	0.623	0.272	0.280	0.285
4.75	0.064	0.121	0.167	0.201	0.227	0.245	0.259	0.269	0.277	0.283
5.00	0.061	0.116	0.161	0.195	0.221	0.241	0.255	0.266	0.274	0.281
5.25	0.059	0.111	0.155	0.190	0.216	0.236	0.251	0.263	0.271	0.278
5.50	0.056	0.107	0.150	0.185	0.211	0.232	0.247	0.259	0.268	0.276
5.75	0.054	0.103	0.145	0.179	0.206	0.227	0.243	0.255	0.265	0.273
6.00	0.052	0.099	0.141	0.174	0.201	0.223	0.239	0.252	0.262	0.270
6.25	0.050	0.096	0.136	0.170	0.197	0.218	0.235	0.248	0.259	0.267
6.50	0.048	0.093	0.132	0.165	0.192	0.214	0.231	0.245	0.256	0.265
6.75	0.046	0.089	0.128	0.161	0.188	0.210	0.227	0.241	0.252	0.262
7.00	0.045	0.087	0.124	0.156	0.183	0.205	0.223	0.238	0.249	0.259
7.25	0.043	0.084	0.121	0.152	0.179	0.201	0.219	0.234	0.246	0.256
7.50	0.042	0.081	0.117	0.149	0.175	0.197	0.216	0.231	0.243	0.253
7.75	0.040	0.079	0.114	0.145	0.171	0.193	0.212	0.227	0.240	0.250
8.00	0.039	0.077	0.111	0.141	0.168	0.190	0.208	0.224	0.236	0.247
8.25	0.038	0.074	0.108	0.138	0.164	0.186	0.205	0.220	0.233	0.244
8.50	0.037	0.072	0.105	0.135	0.160	0.182	0.201	0.217	0.230	0.241
8.75	0.036	0.070	0.103	0.132	0.157	0.179	0.198	0.214	0.227	0.238
9.00	0.035	0.069	0.100	0.129	0.154	0.176	0.194	0.210	0.224	0.235
9.25	0.034	0.067	0.098	0.126	0.151	0.172	0.191	0.207	0.221	0.233
9.50	0.033	0.065	0.095	0.123	0.147	0.169	0.188	0.204	0.218	0.230
9.75	0.032	0.064	0.093	0.120	0.145	0.166	0.185	0.201	0.215	0.227
10.00	0.032	0.062	0.091	0.118	0.142	0.163	0.182	0.198	0.212	0.224

Some points of interest for uniformly loaded areas – which again represent flexible foundations due to the contact pressure resemblance – are, for a uniformly loaded circular area:

$S_e = \left[qB \left(\frac{1-\mu^2}{2E} \right) \right] I_2$, where I_2 is equal to 2 at center, 1.27 at the edge and 1.7 as an average value of settlement. **(3.11)**

For a uniformly loaded rectangular area:

$S_e = \left[qB \left(\frac{1-\mu^2}{E} \right) \right] I_5$, where I_5 is equal to I_3 at center, $0.5I_3$ at the edge and $0.848I_3$ as an average value of settlement. **(3.12)**

Considering the rigidity of foundation, where a uniform settlement profile occurs as illustrated in Figure 2.11, for a circular area, the settlement is:

$$S_e = 0.79 \left[qB \left(\frac{1-\mu^2}{2E} \right) \right] \quad \textbf{(3.13)}$$

For a rectangular area, the settlement is:

$S_e = \left[qB \left(\frac{1-\mu^2}{2E} \right) \right] I_8$, and I_8 is tabulated in Table 3.8. **(3.14)**

Table 3.8 : Influence factor I_8 for settlement of rigid rectangular areas (Das, 1985)

L/B	I_8	L/B	I_8	L/B	I_8	L/B	I_8
1	0.884	3	1.406	10	2.006	50	2.814
2	1.208	5	1.660	20	2.353	100	3.162

In order to sum up all documented results, consider the below equation in conjunction with Table 3.9 for C_d, the shape and rigidity factor.

$$S_e = C_d qB\left(1-\mu^2\right)/E \quad \textbf{(3.15)}$$

Table 3.9 : Shape and rigidity factor C_d (Wyllie, 1992)

Shape	*Centre*	*Corner*	*Middle of short side*	*Middle of long side*	*Average*
Circle	1.00	0.64	0.64	0.64	0.85
Circle (rigid)	0.79	0.79	0.79	0.79	0.79
Square	1.12	0.56	0.76	0.76	0.95
Square (rigid)	0.99	0.99	0.99	0.99	0.99
Rectangle: length/width					
1.5	1.36	0.67	0.89	0.97	1.15
2	1.52	0.76	0.98	1.12	1.30
3	1.78	0.88	1.11	1.35	1.52
5	2.10	1.05	1.27	1.68	1.83
10	2.53	1.26	1.49	2.12	2.25
100	4.00	2.00	2.20	3.60	3.70
1000	5.47	2.75	2.94	5.03	5.15
10000	6.90	3.50	3.70	6.50	6.60

3.1.3. Effect of a Rock Base on Settlement

In the case of a rock base beneath the soil (Figure 3.2), the settlement tends to be less then that in the elastic half-space.

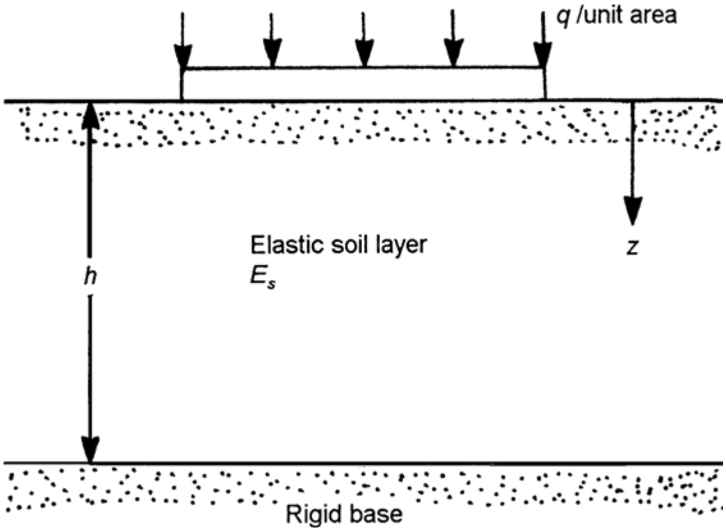

Figure 3.2 : Limited depth of elastic layer (Das, 1999)

For a circular area:

$$S_e(\text{center,flexible}) = aq\left(1-\mu^2\right)\alpha_1 \big/ E$$

$$S_e(\text{center,rigid}) = aq\left(1-\mu^2\right)\alpha_2 \big/ E$$

Values of relevant coefficients are tabulated below.

Table 3.10 : Coefficients for circular area on limited elastic layer (Das, 1999)

h/R	α_1	α_2
0	0	0
0.5	0.52	0.45
1.0	1.00	0.79
2.0	1.44	1.16
3.0	1.62	1.32
5.0	1.78	1.48
10.0	1.88	1.64

For a rectangular area:

$$S_e(\text{center,flexible}) = Bq\left(1-\mu^2\right)\alpha_3 \big/ E$$

$$S_e(\text{center,rigid}) = Bq\left(1-\mu^2\right)\alpha_4 \big/ E$$

Values of relevant coefficients are tabulated below.

Table 3.11 : Coefficients for rectangular area on limited elastic layer (Das, 1999)

H/B	L/B = 1		2		3		4		5	
	α_3	α_4	α_3	α_4	α_3	α_4	α_3	α_4	α_3	α_4
0	0	0	0	0	0	0	0	0	0	0
0.25	0.25	0.226	0.25	0.23	0.25	0.23	0.25	0.24	0.25	0.238
0.5	0.51	0.403	0.51	0.43	0.51	0.44	0.51	0.44	0.51	0.446
1	0.77	0.609	0.87	0.7	0.88	0.73	0.88	0.75	0.88	0.764
1.5	0.88	0.711	1.07	0.86	1.12	0.91	1.13	0.95	1.13	0.982
2.5	0.98	0.8	1.24	1.01	1.36	1.12	1.44	1.2	1.45	1.256
5	1.05	0.873	1.39	1.16	1.56	1.31	1.75	1.48	1.87	1.619

3.1.4. Effect of a Less Stiff Underlying Layer on Settlement

In the case of a stiff layer – with a modulus of elasticity, E_1 – overlying a more compressible formation – with a modulus of elasticity, E_2 which is less then E_1–, the settlement is first calculated as if the foundation is entirely composed of the less stiff soil, then a correction factor given in Table 3.12, is multiplied by this quantity to estimate the corresponding settlement for this condition.

$$S_e(\text{stiff over compressible}) = \zeta S_e(\text{compressible only}) \quad \textbf{(3.16)}$$

Table 3.12 : Correction factor ζ for stiff layer over compressible (Wyllie, 1992)

H/B	E_1/E_2 = 1	2	5	10	100
0	1.0	1.00	1.00	1.00	1.00
0.1	1.0	0.972	0.943	0.923	0.76
0.25	1.0	0.885	0.779	0.699	0.431
0.5	1.0	0.747	0.566	0.463	0.228
1.0	1.0	0.627	0.399	0.287	0.121
2.5	1.0	0.55	0.274	0.175	0.058
5.0	1.0	0.525	0.238	0.136	0.036
∞	1.0	0.500	0.200	0.100	0.010

3.1.5. Effect of Embedment on Settlement

For practical purposes such as to increase the bearing capacity, instead of built directly on the ground surface, foundations are embedded to a certain depth (D_f) as shown in Figure 3.3, which results in reduction of the settlement magnitude.

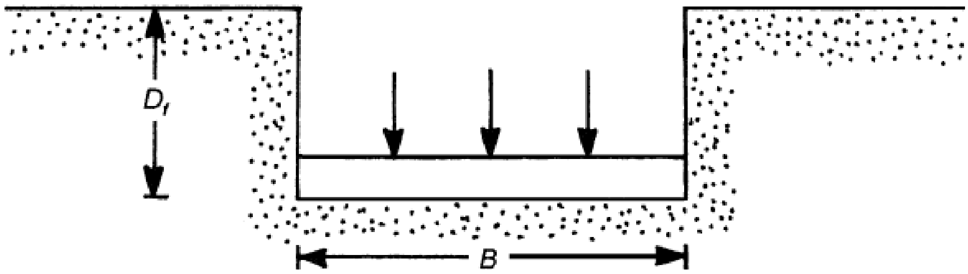

Figure 3.3 : Foundation with embedment (Das, 1999)

The following table gives the ratios of settlement of embedded foundations to foundations with no embedment as calculated up to here during this chapter.

Table 3.13 : Ratios of S_e(average, D_f)/ S_e(average, D_f=0) (Das, 1999)

$\frac{D_f}{\sqrt{LB}}$	L/B = 1	5	10
0	1	1	1
0.1	0.981	0.975	0.969
0.2	0.959	0.947	0.931
0.3	0.928	0.906	0.893
0.4	0.894	0.875	0.856
0.5	0.863	0.844	0.831
0.6	0.825	0.819	0.813
0.8	0.763	0.775	0.781
1.0	0.732	0.737	0.738

3.1.6. Undrained Settlement of Saturated Clays

Janbu et. al. (1956) has proposed a general method to estimate the undrained (immediate) settlement of uniformly loaded flexible rectangular foundation over saturated clays (Figure 3.4) as follows:

$$S_e = \mu_1 \mu_2 \frac{qB}{E} \qquad \textbf{(3.17)}$$

where μ_1 and μ_2 are function of depth of embedment, depth of clay layer and dimensions of the foundation, which can be obtained from Table 3.14 and Table 3.15, respectively.

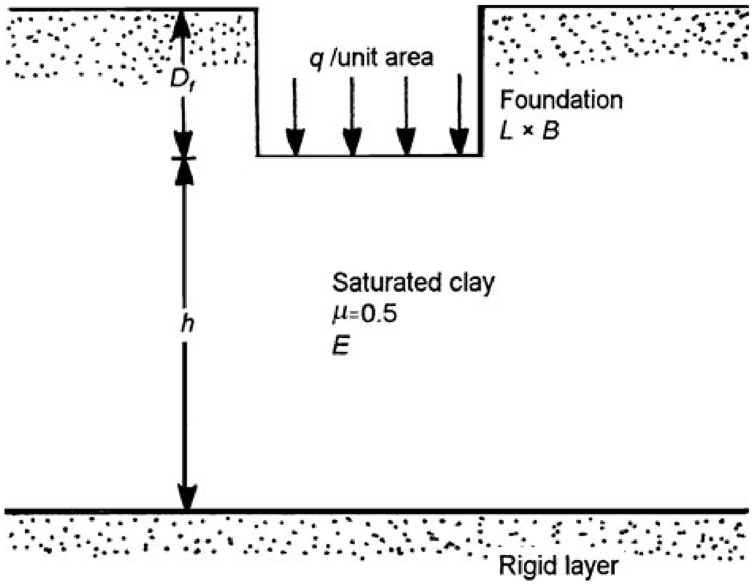

Figure 3.4 : Definitions for undrained settlement of saturated clay (Das,1999)

Table 3.14 : Coefficient μ_1 for undrained settlement of saturated clay (Das, 1999)

D_f/B	μ_1
0	1.0
2	0.9
4	0.88
6	0.875
8	0.87
10	0.865
12	0.863
14	0.860
16	0.856
18	0.854
20	0.850

Table 3.15 : Coefficient μ_2 for undrained settlement of saturated clay (Das, 1999)

		L/B				
h/B	Circle	1	2	5	10	∞
1	0.36	0.36	0.36	0.36	0.36	0.36
2	0.47	0.53	0.63	0.64	0.64	0.64
4	0.58	0.63	0.82	0.94	0.94	0.94
6	0.61	0.67	0.88	1.08	1.14	1.16
8	0.62	0.68	0.90	1.13	1.22	1.26
10	0.63	0.70	0.92	1.18	1.30	1.42
20	0.64	0.71	0.93	1.26	1.47	1.74
30	0.66	0.73	0.95	1.29	1.54	1.84

3.1.7. Improved Relationship for Immediate Settlement

Mayne and Poulos (1999) has recently improved and combined the governing equations of the theory of elasticity for the calculation of immediate settlement, for which the rigidity and the embedment of foundation and the depth of elastic layer are taken into account together with the thickness of the foundation and the increase in the elasticity modulus of soil with depth. The parameters for this solution are depicted in Figure 3.5. Note that this analysis is only valid for flexible foundations since the distribution of contact pressure is uniform.

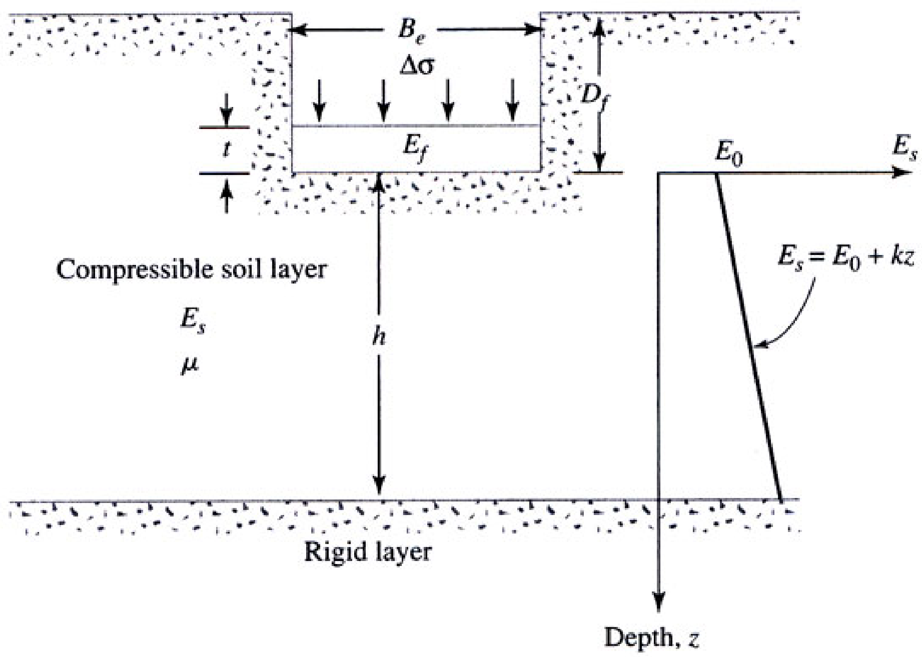

Figure 3.5 : Definitions for improved relation for immediate settlement (Das, 2001)

This new relationship is as follows:

$$S_e = \frac{qB_e I_G I_F I_E}{E_0}\left(1-\mu^2\right) \qquad \textbf{(3.18)}$$

where, B_e is the equivalent diameter of the foundation, which is $\sqrt{4BL/\pi}$ for rectangular foundations and is equal to B – the diameter – for circular foundation,

I_G is the influence factor for the variation of E with depth as given in Figure 3.6.

$$I_F = \frac{\pi}{4} + \left[4.6 + 10\left(\frac{E_F}{E_0 + 0.5B_e k}\right)\left(\frac{2t}{B_e}\right)^3\right]^{-1} \qquad \textbf{(3.19)}$$

is the influence factor for the foundation rigidity as given in Figure 3.7.

$$I_E = 1 - \left[3.5\exp\left(1.22\mu - 0.4\right)\left(B_e/D_f + 1.6\right)\right]^{-1} \qquad \textbf{(3.20)}$$

is the influence factor for the foundation embedment as given in Figure 3.8.

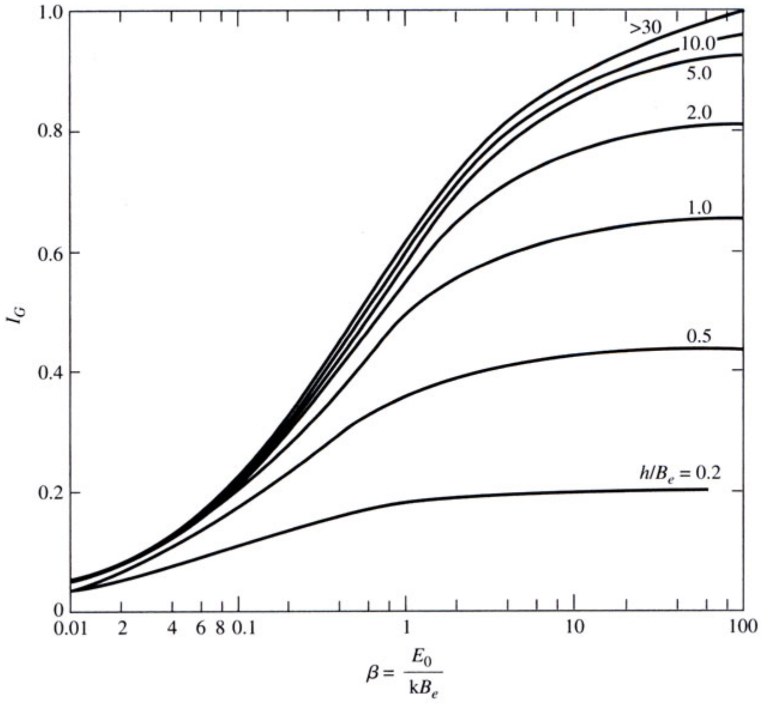

Figure 3.6 : Influence factor I_G for increase in the elasticity modulus (Das, 2001)

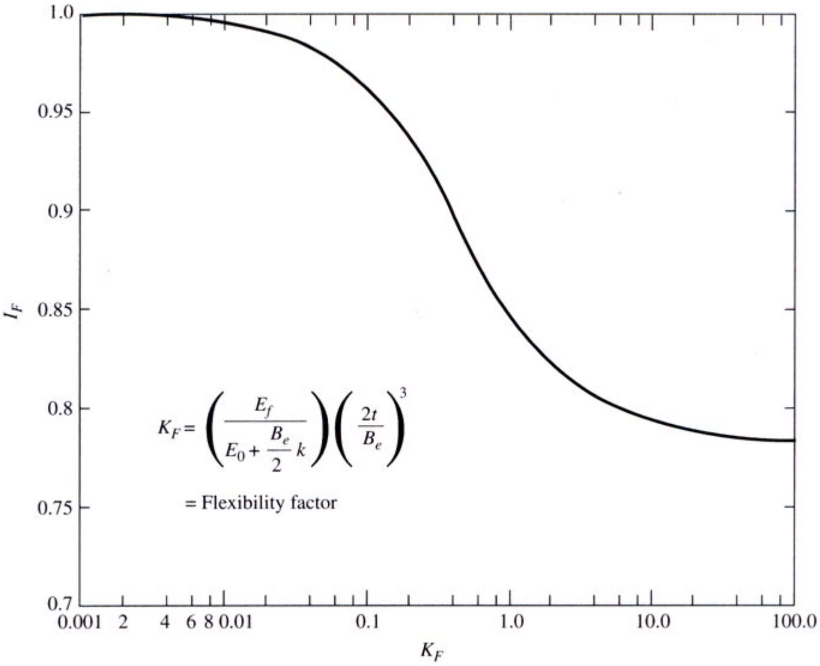

Figure 3.7 : Influence factor I_F for foundation rigidity (Das, 2001)

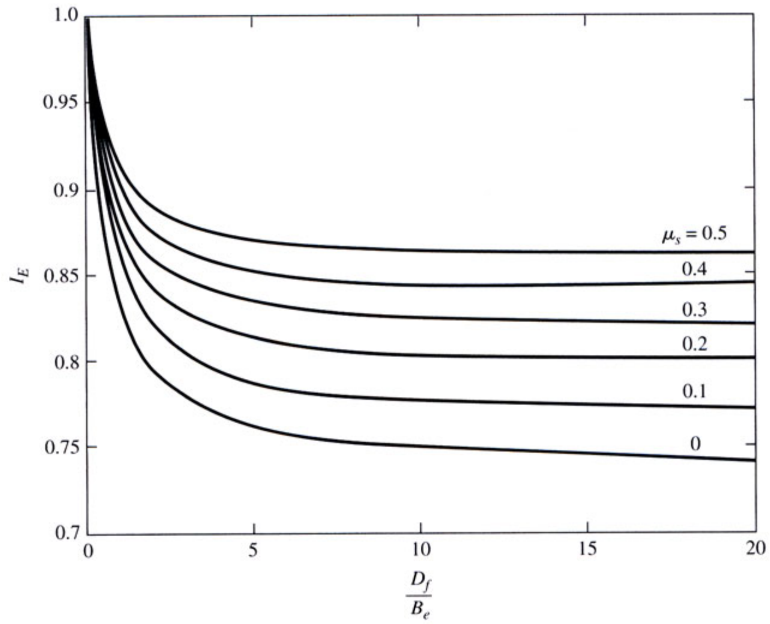

Figure 3.8 : Influence factor I_E for foundation embedment (Das, 2001)

3.2. Winkler Springs

A simple mathematical model derived by the German engineer Winkler (1867), which is called by its inventor's name as Winkler springs, enables engineers to predict settlement and contact pressures under shallow foundation. It has been extremely useful in the investigation of many soil-foundation interaction problems, yet it requires extensive understanding which in the absence of might result in a calculation of settlement at extreme large or small magnitudes leading to an over-design or worse to a structural damage due to extensive settlement afterwards. Considering this fact, Winkler springs are rather utilized to estimate moments and forces acting on structural elements (such as a beam as a strip foundation, or for a raft foundation) for the design and selection of reinforcements or sections. The design parameter in this method is the modulus of subgrade reaction, which is defined as:

$$k_s = q/\delta \qquad \textbf{(3.21)}$$

It is very crucial to produce this parameter correctly, since it is the only parameter affecting the calculations. Conventionally the Plate Loading Test (Eurocode 7, 2000) can be utilized to obtain a q vs δ curve and k_s could be derived with the help of following expressions given by Terzaghi (1955):

For footings on clay $k_s = k_1 \, B_1 / B$ **(3.22)**

For footings on sand, $k_s = k_1 \left(B + B_1 / 2B \right)^2$ **(3.23)**

where B_1 is the width or the diameter of the plate used during the test, which produces k_1 and B is the dimension of actual foundation. Note that these expression output valid values only if the ratio B/B_1 is smaller than 3, which means that the actual foundation dimensions should not be larger than three times the test plate.

A more refined procedure is defined by Vesic (1961) and improved by Bowles (1996), which incorporates the elasticity modulus of soil as follows:

$$k_s = \frac{E}{B(1-\mu^2)} \tag{3.24}$$

There is a great resemblance between the above equation and the expressions given before from the theory of elasticity as in (3.7) to (3.18). Therefore the correction factors given for elasticity – from Figure 3.6 to Figure 3.8 – can be applied on this equation for a better approximation of the modulus of subgrade reaction. They can even be utilized to switch from the modulus obtained from a test to the actual modulus of foundation with greater precision.

$$\frac{k_{s,1}}{k_{s,2}} = \frac{B_2 E_2 I_{G,2} I_{F,2} I_{B,2}}{B_1 E_1 I_{G,1} I_{F,1} I_{B,1}} \tag{3.25}$$

where the indices 1 and 2 represent the parameters defined in Figure 3.5 for the cases of testing procedure and actual foundation, respectively.

For guidance, the ranges of the modulus of subgrade reaction are listed below in Table 3.16.

Table 3.16 : Ranges for the modulus of subgrade reaction (Bowles, 1996)

Soil	**k_s, kN/m^3**
Loose sand	4800 – 16000
Medium dense sand	9600 – 80000
Dense sand	64000 – 128000
Clayey medium dense sand	32000 – 80000
Silty medium dense sand	24000 – 48000
Clayey soil $q_a \leq 200$ kPa	12000 – 24000
$200 < q_a \leq 800$ kPa	24000 – 48000
$q_a > 800$ kPa	> 48000

Lastly, it could be mentioned that the bearing capacity can be used to evaluate the modulus of subgrade reaction such that:

$$k_s = 40(\mathrm{SF})q_a \text{ in kN/m}^3 \text{ for } q_a \text{ in kPa} \qquad \textbf{(3.26)}$$

where SF is the safety factor for bearing capacity in which q_{ult} / SF = q_a. The factor 40 is based on the fact that the settlement at ultimate soil pressure is equal to one feet, that is approximately 25 mm. It could be adjusted as 160, 83 or 50 for a maximum settlement of 6, 12 and 20 mm respectively.

3.2.1. Beam on Elastic Foundation

Using the Winkler springs, the classical problem of infinite beam on elastic foundation is based on the following differential equation:

$$EI\frac{d^4y}{dx^4} = q = -Bk_s y \qquad \textbf{(3.27)}$$

Solutions of this equation for deflection, rotation, moment and shear of the beam are given in terms of the variable λ, in Figure 3.9.

$$\lambda = \sqrt[4]{Bk_s/4EI} \qquad \textbf{(3.28)}$$

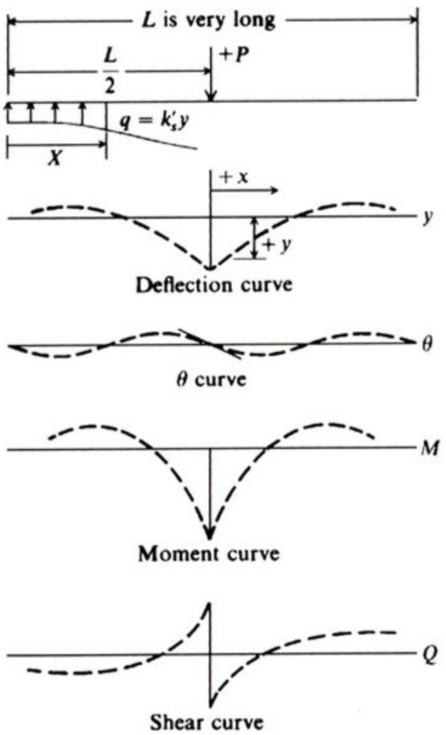

Concentrated load at end	Moment at end
$y = \dfrac{2V_1\lambda}{k_s'}D_{\lambda x}$	$y = \dfrac{-2M_1\lambda^2}{k_s'}C_{\lambda x}$
$\theta = \dfrac{-2V_1\lambda^2}{k_s'}A_{\lambda x}$	$\theta = \dfrac{4M_1\lambda^3}{k_s'}D_{\lambda x}$
$M = \dfrac{-V_1}{\lambda}B_{\lambda x}$	$M = M_1A_{\lambda x}$
$Q = -V_1C_{\lambda x}$	$Q = -2M_1\lambda B_{\lambda x}$
Concentrated load at center (+↓)	**Moment at center (+ ⌒)**
$y = \dfrac{P\lambda}{2k_s'}A_{\lambda x}$	$y = \dfrac{M_0\lambda^2}{k_s'}B_{\lambda x}$ deflection
$\theta = \dfrac{-P\lambda^2}{k_s'}B_{\lambda x}$	$\theta = \dfrac{M_0\lambda^3}{k_s'}C_{\lambda x}$ slope
$M = \dfrac{P}{4\lambda}C_{\lambda x}$	$M = \dfrac{M_0}{2}D_{\lambda x}$ moment
$Q = \dfrac{-P}{2}D_{\lambda x}$	$Q = \dfrac{-M_0\lambda}{2}A_{\lambda x}$ shear

The A, B, C, and D coefficients (use only $+x$) are as follows:

$$A_{\lambda x} = e^{-\lambda x}(\cos\lambda x + \sin\lambda x)$$
$$B_{\lambda x} = e^{-\lambda x}\sin\lambda x$$
$$C_{\lambda x} = e^{-\lambda x}(\cos\lambda x - \sin\lambda x)$$
$$D_{\lambda x} = e^{-\lambda x}\cos\lambda x$$

Figure 3.9 : Solutions for infinite beam on elastic foundation (Bowles, 1996)

A more useful case might be the solution of deflection, moment and shear along a finite beam stimulated by a point load applied at any distance from the left end as given in Figure 3.10.

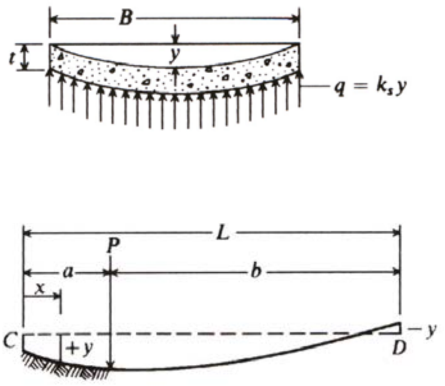

$$y = \frac{P\lambda}{k_s'(\sinh^2 \lambda L - \sin^2 \lambda L)}\{2\cosh \lambda x \cos \lambda x(\sinh \lambda L \cos \lambda a \cosh \lambda b - \sin \lambda L \cosh \lambda a \cos \lambda b) + (\cosh \lambda x \sin \lambda x + \sinh \lambda x \cos \lambda x)[\sinh \lambda L(\sin \lambda a \cosh \lambda b - \cos \lambda a \sinh \lambda b) + \sin \lambda L(\sinh \lambda a \cos \lambda b - \cosh \lambda a \sin \lambda b)]\}$$

$$M = \frac{P}{2\lambda(\sinh^2 \lambda L - \sin^2 \lambda L)}\{2\sinh \lambda x \sin \lambda x(\sinh \lambda L \cos \lambda a \cosh \lambda b - \sin \lambda L \cosh \lambda a \cos \lambda b) + (\cosh \lambda x \sin \lambda x - \sinh \lambda x \cos \lambda x) \times [\sinh \lambda L(\sin \lambda a \cosh \lambda b - \cos \lambda a \sinh \lambda b) + \sin \lambda L(\sinh \lambda a \cos \lambda b - \cosh \lambda a \sin \lambda b)]\}$$

$$Q = \frac{P}{\sinh^2 \lambda L - \sin^2 \lambda L}\{(\cosh \lambda x \sin \lambda x + \sinh \lambda x \cos \lambda x) \times (\sinh \lambda L \cos \lambda a \cosh \lambda b - \sin \lambda L \cosh \lambda a \cos \lambda b) + \sinh \lambda x \sin \lambda x[\sinh \lambda L(\sin \lambda a \cosh \lambda b - \cos \lambda a \sinh \lambda b) + \sin \lambda L(\sinh \lambda a \cos \lambda b - \cosh \lambda a \sin \lambda b)]\}$$

Figure 3.10 : Solutions for finite beam on elastic foundation (Bowles, 1996)

Note that, if *x* is larger than *a*, *a* is replaced with *b* in the equations and *x* is measured from the point *D*.

The solutions of both infinite and finite beams can be superposed. Therefore a beam with multiple loads – characterizing a strip foundation supporting several structural columns –, can be analyzed using above given expressions.

3.2.2. Finite Element Procedures with Winkler Springs

Other than solutions offered for strip foundations via differential equations, numerical methods such as a finite element procedure can be employed for the analysis of rafts – mat foundations –, where springs and loads are located on nodes, which divided the foundation into discrete elements, as illustrated in Figure 3.11.

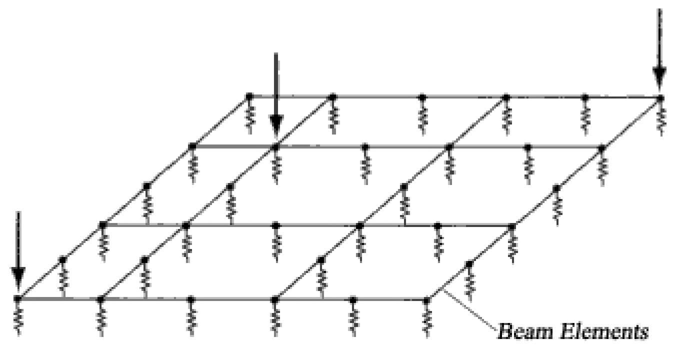

Figure 3.11 : Finite element method of modeling rafts (Hemsley, 2000)

The main concern in such an analysis is the placement of springs and the value of the spring coefficient. Consider the following finite element analysis by Bowles:

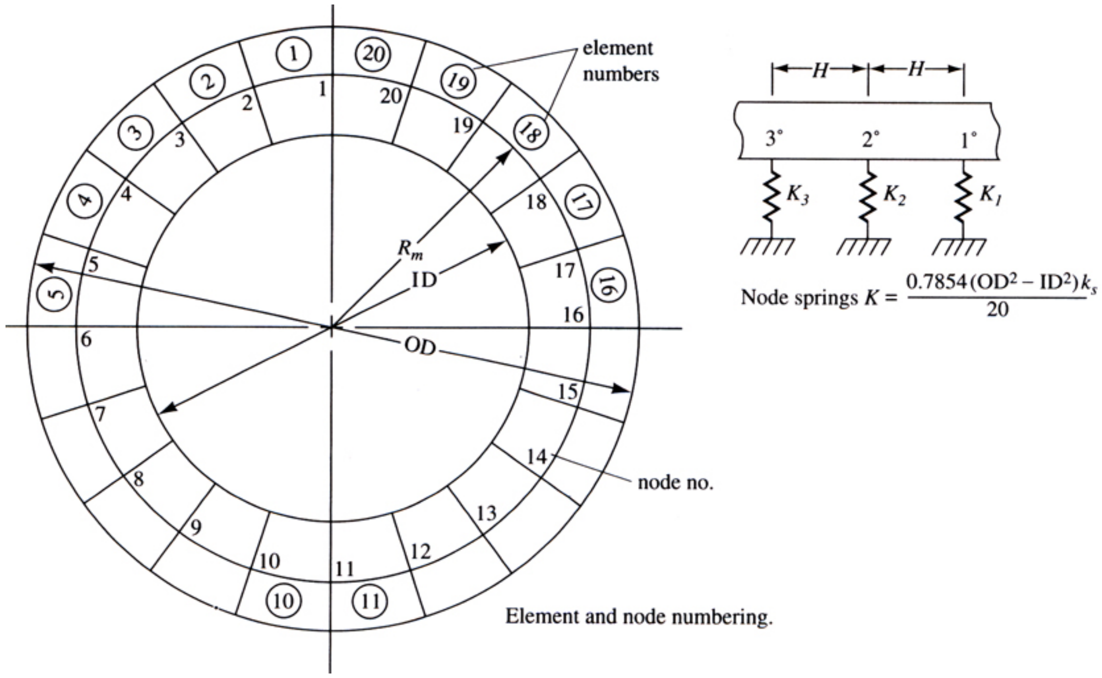

Figure 3.12 : Finite element analysis of ring foundation via springs (Bowles, 1996)

Since 0.7854 is the result of $\pi/4$, OD and ID is outer and inner diameter of ring respectively and 20 is the number of elements, it is apparent that for each element there is a spring at the node nearby, and the spring coefficient is calculated by multiplying the area of an element with the modulus of subgrade:

$$K_{spring} = \frac{\text{Total Area of Elements}}{\text{Number of Elements}} k_s \quad \textbf{(3.29)}$$

Better, that is more compatible results between nodes are obtained in solutions with more elements. Nevertheless, doing so will increase the computation time and the memory requirements, thus an optimal number of elements is adequate for a calculation with sufficient precision. Meanwhile, the result can be contrasted with the simple estimations of elasticity theory for verification.

If one lacks the experience in using Winkler springs, it is a better practice to obtain Winkler spring coefficient, after a settlement analysis is conducted, as a ratio of contact pressure and calculated settlement and use it only for purposes of structural design. Great detail in programming and analyzing of geotechnical structures is given in Bowles, 1974.

3.3. Finite Element Codes for the Estimation of Settlement

The finite element procedures (Figure 3.13) in commercial programs have powerful approximation techniques – either incremental or iterative which can be found in great detail at the scientific manual supported by relevant programs – to mimic the nonlinear behavior of soil in contrast to previously mentioned linear methods of elasticity theory and Winkler springs.

There are mainly two types of 2-dimensional analysis for geotechnical structures in finite element method: plane strain and axi-symmetric. Nevertheless three dimensional finite element packages also exist; currently rare in practice, though their application is spreading as they become more available and feasible both in means of cost and computational procedures.

The finite element mesh models the soil body basically like a truss, which is utilized to estimate the stresses and strains in each element with a calculation considering the equilibrium of the forces and the compatibility of displacements at nodes. The boundary conditions, such as restraints for vertical or horizontal displacements at the edges of the mesh or loads applied to nodes to define the foundational surcharge, the location of the ground water table and structural elements such as beams and anchors can defined as inputs in advanced finite element analysis programs, to check any design by means of stress, settlement and stability.

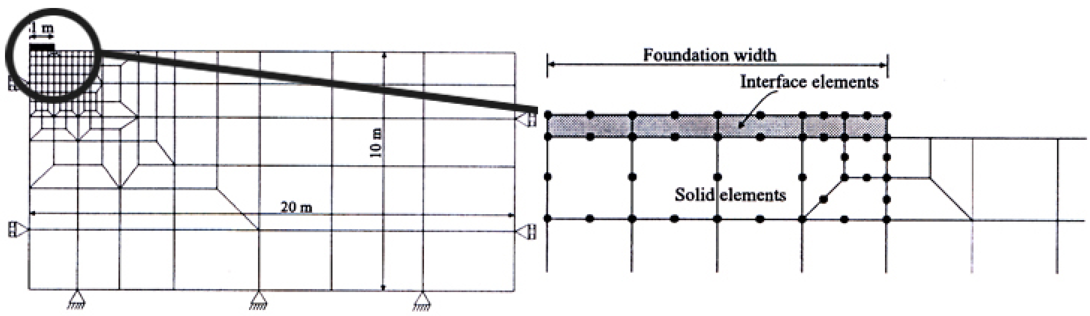

Figure 3.13 : Plane strain analysis of a strip foundation with Finite Element Method (Potts and Zdravkovic, 2001b)

The dimensions of a mesh are of importance since it defined the body in which the problem is handled numerically. Azizi (2000) has suggested the following dimension for the analysis of a shallow foundation resting on isotropic homogeneous soil:

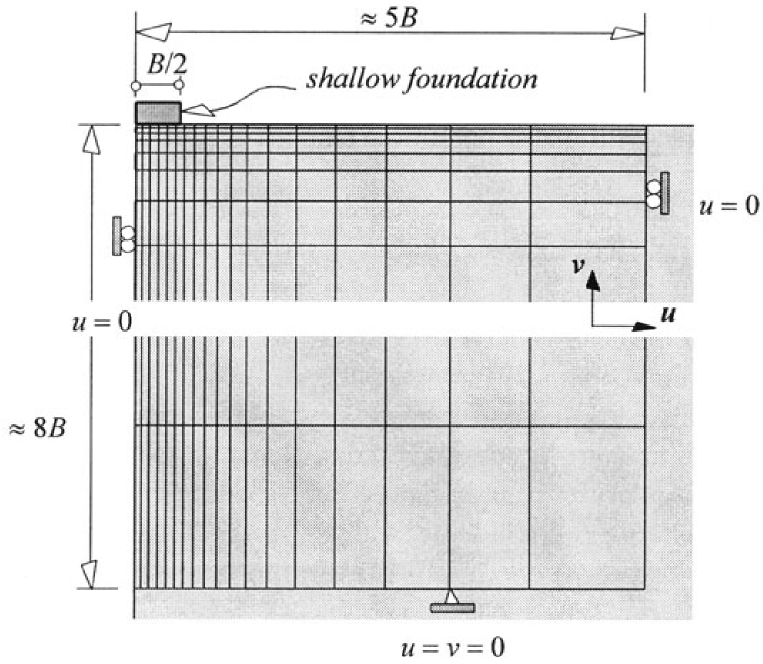

Figure 3.14 : Suggested mesh dimensions for axi-symmetric finite element analysis (Azizi, 2000)

Potts and Zdravkovic (2001a and 2001b) have written two dedicated books on the methodology and the application of finite element method for the analysis of geotechnical problems. To properly model the problem in a finite element program, the user should first basically understand the produce beneath the code and then consult its manual for the sake of accuracy in the analysis

3.4. A Final Note on Rigidity

As shown in the preceding sections that the settlement analysis of rigid foundations mostly requires complex analysis based on some what uncertain distribution of the contact stress involved, it is a common practice to estimate it from the settlement of a flexible foundation with same dimensions.

Poulos and Davis (1974) have given the following expression for the settlement of rigid foundations:

for a circle or strip foundation: $S_{rigid} = 0.5\left(S_{center} + S_{corner}\right)_{flexible}$ **(3.30)**

for a rectangular foundation: $S_{rigid} = 1/3 \times \left(2S_{center} + S_{corner}\right)_{flexible}$ **(3.31)**

Davis and Selvadurai (1996) have contrasted the settlements found by Dempsey and Li (1989) for a rigid footing with the findings of theory of elasticity for a flexible foundation. The results, which are also compared with (3.31), are given in Table 3.17.

Table 3.17 : Comparison of settlement between rigid and flexible footings

L / B	1	1.5	2	3	5	
rigid	0.4439	0.5268	0.5984	0.7061	0.8510	
fle. center	0.5611	0.6788	0.7659	0.8915	1.0523	
fle. corner	0.2806	0.3394	0.3829	0.4458	0.5262	
fle. to rigid	0.4676	0.5657	0.6382	0.7429	0.8769	: using (3.31)

It can be concluded that (3.30) and (3.31) are accurate expressions to estimate the settlement of rigid foundations from the calculations for the flexible ones.

Another way to handle the computation for rigid foundations is to calculate the settlement under the characteristic point of the foundation as it is flexible. The settlement at this point will be equal the amount of uniform settlement occurring in the case rigidity. For a rectangular foundation this point lies at a distance of $0.577B$ / 2 or $0.577L$ / 2 from the axis of symmetry. For a circular foundation it is at a distance of $0.707D$ / 2 from the center. These are the findings of Marivoet, 1948.

3.5. Limiting Values of Settlements

General inclination toward defining a settlement limit is to consider the type of movement related to the structure, which has a limiting factor based on its design. Such an approach is exemplified in Table 3.18.

Table 3.18 : Settlement limit based on movement type (Sower and Sower, 1970)

Type of Movement	**Limiting Factor**	**Maximum allowable settlement**
Total settlement	Drainage and access	15 to 60 cm
	Probability of differential settlement	
	Masony walls	2.5 to 5 cm
	Framed buildings	5 to 10 cm
Tilting	Towers, stacks	$0.004B$*
	Rolling of trucks, stacking of goods	$0.01S$*
	Crane rails	$0.003S$*
Curvature	Brick walls in buildings	$0.0005S$ to $0.002S$*
	Reinforced concrete building frame	$0.003S$*
	Steel building frame, continuous	$0.002S$*
	Steel building frame, simple	$0.005S$*

B is the base width; S is column spacing. * Differential settlement in distance B or S.

Another approach is based on the damage (which might be categorized as well) suffered by the building as shown in Table 3.19.

Table 3.19 : Settlement criteria for building damage (Koerner,1985)

Category	Description	Maximum radius of curvature
Architectural	Cracking	1/300
Structural	Strength reduction	1/150
Functional	Impaired use	1/50

Radius of curvature = ρ / s, where ρ = settlement and s = column spacing.

Based on numerous case histories by Skempton and MacDonald (1956) and Grant *et al*. (1974), the recommended values of limiting settlements for different foundation and soil conditions are given in Table 3.20.

Table 3.20 : Settlement limits for various foundation and soil types (Koerner,1985)

		Maximum allowable settlement	
Foundation type	**Soil type**	**Skempton and MacDonald**	**Grant *et al.***
Isolated footings	Granular	600 (ρ / s) max	600 (ρ / s) max
Isolated footings	Fine-grained	1000 (ρ / s) max	1200 (ρ / s) max
Mat foundations	Granular	750 (ρ / s) max	750 (ρ / s) max
Mat foundations	Fine-grained	1250 (ρ / s) max	1250 (ρ / s) max

ρ = settlement and s = column spacing.

According to Eurocode 1, 1994 (based on the limiting values for serviceability) and Eurocode 7, 1994 (based on maximum acceptable foundation movement), the maximum magnitudes of settlement, differential settlement and the angular distortion are as stated in Table 3.21.

Table 3.21 : Limiting values of Settlement according to Eurocode (Das, 1999)

Item	Parameter	Magnitude	Comments
Limiting values for serviceability	S_T	25 mm	Isolated shallow foundation
		50 mm	Raft foundation
	ΔS_T	5 mm	Frames with rigid cladding
		10 mm	Frames with flexible cladding
		20 mm	Open frames
	β	1/500	–
Maximum acceptable foundation movement	S_T	50 mm	Isolated shallow foundation
	ΔS_T	20 mm	Isolated shallow foundation
	β	=1/500	–

where, S_T is the total settlement at a point, ΔS_T is difference between total settlement between any two points and β is the angular distortion which is calculated as:

$$\beta = \frac{\Delta S_{T(i,j)}}{L_{(i,j)}} \qquad \textbf{(3.32)}$$

where $\Delta S_{T(i,j)}$ is the different in settlement between points i and j, which are located at a distance of $L_{(i,j)}$ according to each other.

4. NUMERICAL PROCEDURE USING HYPERBOLIC MODEL

Methods of the theory of elasticity and the Winkler springs are based on the assumption of linear elastic soil behavior, which tends to be valid until a certain degree of strain is reached as depicted in Figure 3.1. The fact, that the stress-strain curves are nonlinear, was simply omitted at the beginning to overcome the complexity in the process of design, yet resulting in a loss of accuracy in prediction of the behavior of soil. However it should be mentioned that with today's fast and feasible computer technology, nonlinear numerical analysis has become more cost and time efficient. There are a quite number of geotechnical analysis programs with affordable prices. Yet their solution mechanisms are only comprehensible by a minority of experts and academics. Therefore the question of liability rises as noted by the Committee on Modeling Techniques in Geomechanics of Transportation Research Board (2000): "…many practicing engineers lack a background in continuum mechanics, plasticity theory, and numerical techniques. Consequently, there may be a dependence on a "black box" approach in numerical modeling, an approach that understandably makes engineering companies uneasy."

4.1. Hyperbolic Model

The hyperbolic model, in which the required parameters of the soil profile for an analysis are as conventional as the Mohr-Coulomb strength parameters – cohesion, c and the angle of internal friction, ϕ –, the modulus of elasticity, the Poisson's ratio and the principle stresses – which are to be produced from geostatic and stress increments –, is widely used in today's finite element programs for the nonlinear analysis of geotechnical engineering problems.

The hyperbolic model defines a tangent modulus for the stress-strain curve of soil for immediate settlement, which can be accounted as elasto plastic since it happens as soon as the loading is commenced and can describe the deformation up to plastic flow. Yet as noted in the beginning of this chapter, if the soil tends to settle in a timedependent manner, other mechanisms involve and the settlement calculations given here are insufficient to predict such a behavior.

The original formulation of the tangent modulus for the hyperbolic model given by Duncan and Chang (1970) is as follows:

$$E_t = \left[1 - \frac{R_f(1-\sin\phi)(\sigma_1 - \sigma_3)}{2c\cos\phi + 2\sigma_3\sin\phi}\right]E_i \qquad \textbf{(4.1)}$$

where, c is cohesion and ϕ is the angle of internal friction as Mohr-Coulomb strength parameters, σ_1 and σ_3 are the principles stresses, R_f is failure ratio, and E_i is the initial value of the modulus of elasticity.

The failure ratio R_f, is simply the ratio between the finite value in the difference of principle stresses to the ultimate compressive strength of the soil, where the hyperbola of stress-strain curve remains below the ultimate strength as an asymptote as depicted in Figure 4.1. It takes values between 0.75 and 1.00 for different kind of soils, though the popular finite element programs take it as 0.90 unless it has been adjusted by the user otherwise.

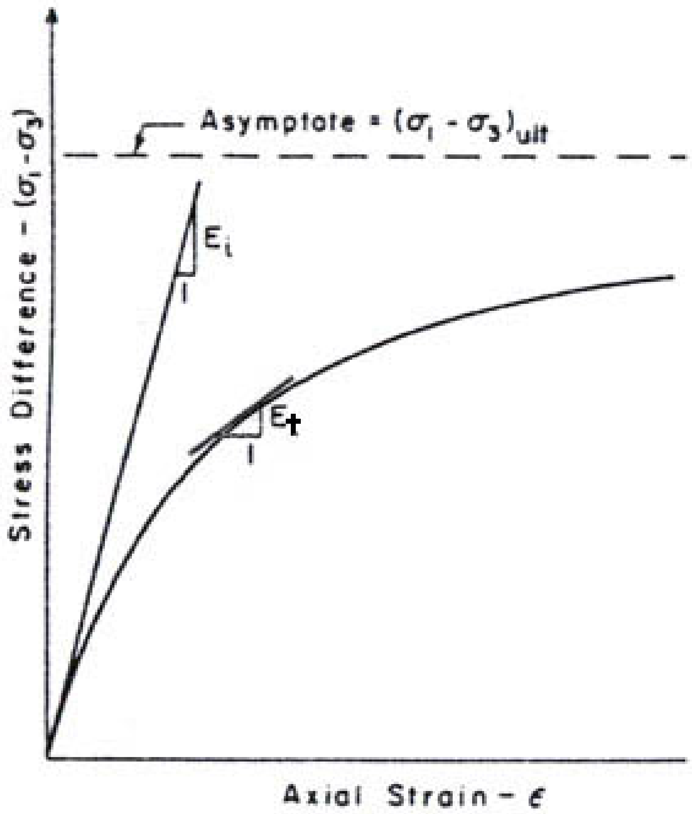

Figure 4.1 : Stress-strain curve examined as hyperbola (Duncan and Chang, 1970)

The initial modulus of elasticity is originally determined by using the below formulation via data from a series of triaxial tests by plotting the values of E_i against the confining pressure – that is the minor principle stress, σ_3 – on a log-log scale as exemplified in Figure 4.2.

$$E_i = KP_a\left(\sigma_3/P_a\right)^n \qquad \textbf{(4.2)}$$

where, K and n are regression parameters and P_a is the atmospheric pressure, which is equal to 1 atm = 101.325 kPa.

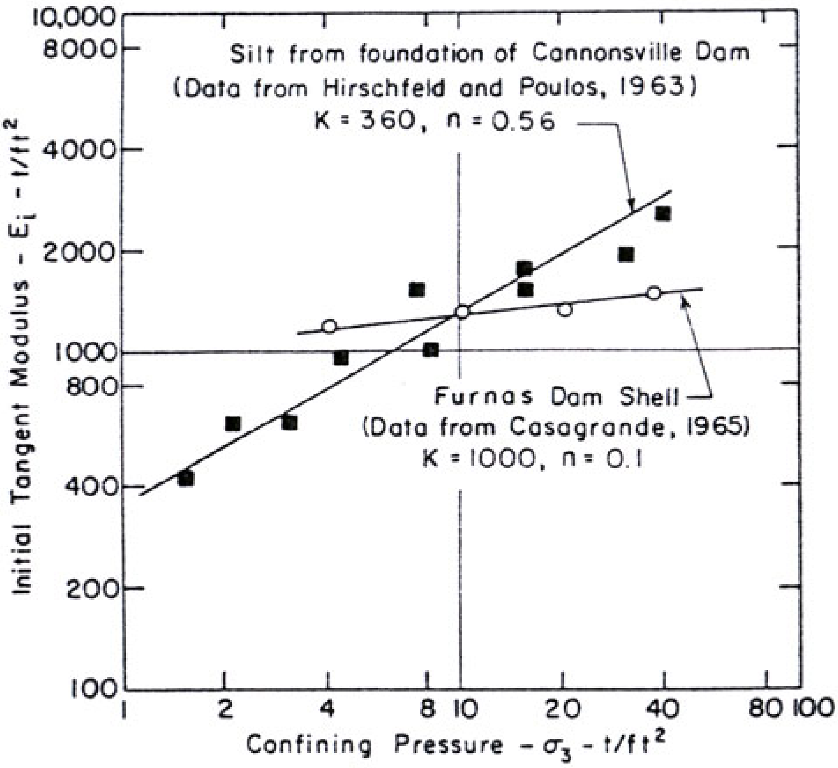

Figure 4.2 : Determination of initial elasticity (Duncan and Chang, 1970)

Yet for the requirement as an input of the numerical analysis, it has become a common practice to use the elasticity modulus of the soil determined via laboratory tests or in-situ investigation directly as the initial modulus of elasticity, E_i.

4.2. The Numerical Procedure

Once strength and the elasticity parameters are obtained for a soil, it is required to estimate the principle stresses of the in-situ condition relevant to the design, in order to calculate the strain at a point inside the soil body. If the strains – thus, the principles stresses – are calculated for points under the foundation at the x and y coordinates throughout a vertical direction (that is in the direction of z axis) then the settlement of the relevant point can be evaluated by summing up the strains multiplied by with the thickness of each discrete calculated portion. This manner is depicted at Figure 4.3 and related expression is given below:

$$S_{ep} = \sum \varepsilon_i \times \Delta z \tag{4.3}$$

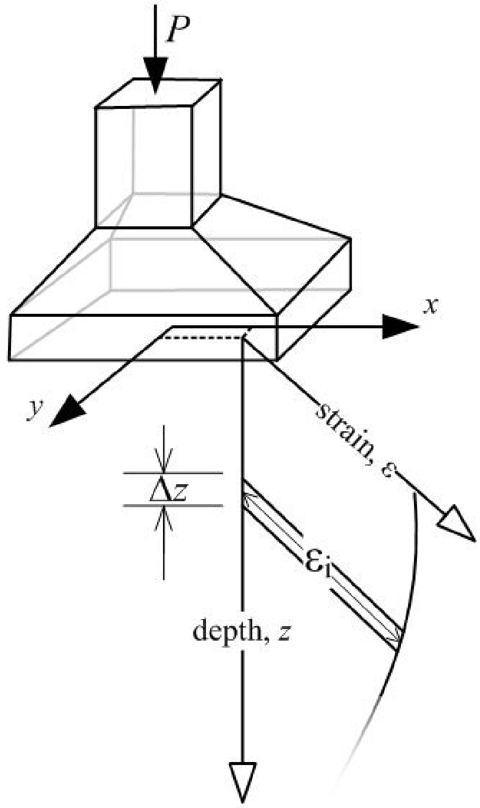

Figure 4.3 : Calculation of elasto plastic settlement under a footing

It is relevant that the calculation process has to be extended at depths where the strains become negligible. Nevertheless, the soil profile through these depths has to be known by means of borehole data. If there is an incompressible layer – e.g. a strong rock base – after a certain depth, then only the strains up to there is to be taken in account.

While using (4.3), the thickness Δz of which the soil profile is divided into is critical since taking it large might result in an inaccurate estimation (overestimated) of settlement and on the other hand using as small intervals as a millimeter requires a huge amount of computer memory and process power. For a calculation of 50 meters depth, different number of segmentation is worked out and the resultant settlement is normalized to the most accurate estimation, which is the analysis with most segments. The results are illustrated in Figure 4.4 as it can be concluded that segments which have a thickness of 50/1000 = 0.05 meters = 5 cm is sufficient to conduct precise estimations.

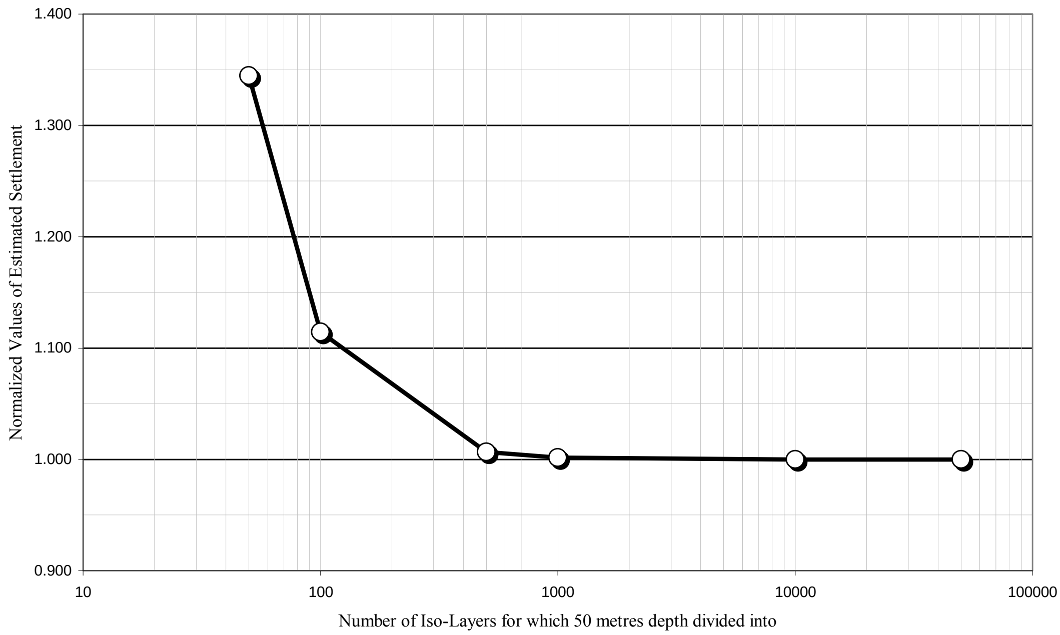

Figure 4.4 : Optimal number of segments for a settlement analysis

Principle stresses, for the use of hyperbolic model to produce the strains, are estimated by writing the nine component of stress tensor (Figure 2.1) into the matrix form and solving its characteristic function for its roots as explained in great detail at Harr, 1966. Consider uniformly loaded rectangular area acting on the soil surface as given the parameters in Figure 4.5.

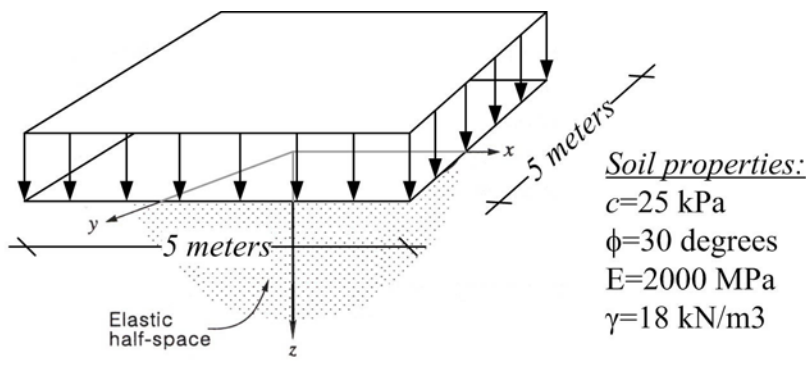

Figure 4.5 : A problem exampling the numerical analysis with hyperbolic model

By using the relationships of stress increments given from (2.35) to (2.40), the stresses at 10 meters depth from the corner of the rectangular is calculated together with the geostatic stresses are as follows:

$$\sigma_{z,geostatic} = \gamma z = 180 \text{ kPa}$$
$$\sigma_{x,geostatic} = \sigma_{y,geostatic} = K_0 \sigma_{z,geostatic} = (0.95 - \sin\phi) \times 180 = 81 \text{ kPa}$$

$$\begin{pmatrix} \Delta\sigma_z = 8.40 \text{ kPa} & \Delta\tau_{xy} = 28.91 \text{ kPa} \\ \Delta\sigma_x = 0.61 \text{ kPa} & \Delta\tau_{xz} = 1.92 \text{ kPa} \\ \Delta\sigma_y = 0.61 \text{ kPa} & \Delta\tau_{yz} = 1.92 \text{ kPa} \end{pmatrix} \text{are the stress increments}$$

$$\begin{pmatrix} \sigma_z = 188.40 \text{ kPa} & \tau_{xy} = 28.91 \text{ kPa} \\ \sigma_x = 81.61 \text{ kPa} & \tau_{xz} = 1.92 \text{ kPa} \\ \sigma_y = 81.61 \text{ kPa} & \tau_{yz} = 1.92 \text{ kPa} \end{pmatrix} \text{are the final stresses after loading}$$

which in this problem gives the characteristic function from the matrix form of stresses (2.1) as:

$$\begin{vmatrix} 188.40 - \sigma & 28.91 & 1.92 \\ 28.91 & 81.61 - \sigma & 1.92 \\ 1.92 & 1.92 & 81.61 - \sigma \end{vmatrix} = -1\sigma^3 + 351.61\sigma^2 - 36565.78\sigma + 1096808.64$$

Graphing this function as illustrated in Figure 4.6, the roots, thus the principles stresses are found as $\sigma_1 = 188.497$ kPa, $\sigma_2 = 110.422$ kPa and $\sigma_3 = 52.695$ kPa .

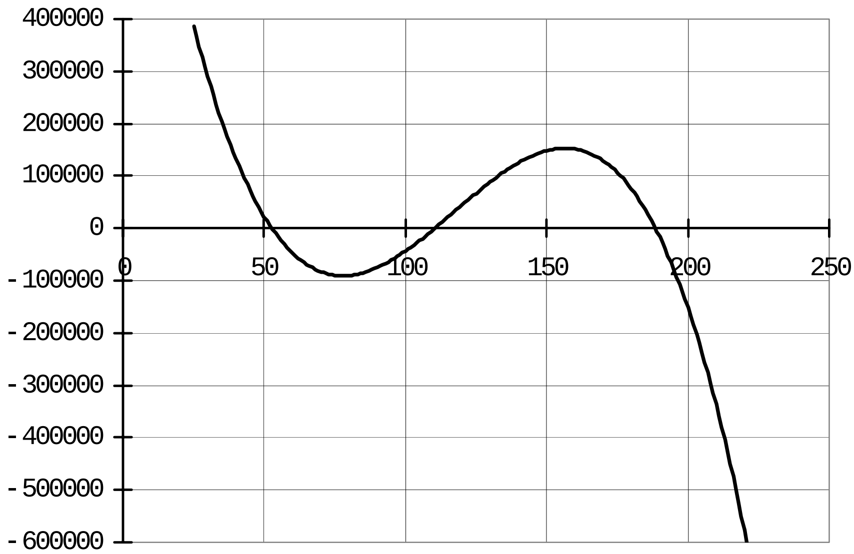

Figure 4.6 : The graph of characteristic function

Now the principles stresses are found, the hyperbolic relationship for stress-strain curve can be utilized to estimate the strain at 10 meters of depth. The following table gives the related calculations:

Table 4.1 : Calculations for hyperbolic stress-strain curve

Incremental. $\Delta\sigma$	E_t	**Incremental. ε**	$\Delta\sigma$	ε
kPA	**kPA**		**kPA**	
40.88	1.31E+06	3.128E-05	40.880	3.128E-05
23.91	9.70E+05	2.466E-05	64.794	5.594E-05
16.97	7.61E+05	2.230E-05	81.761	7.825E-05
13.16	6.16E+05	2.136E-05	94.921	9.961E-05
10.75	5.09E+05	2.111E-05	105.674	1.207E-04
9.09	4.27E+05	2.130E-05	114.766	1.420E-04
7.88	3.61E+05	2.179E-05	122.641	1.638E-04
6.95	3.08E+05	2.254E-05	129.588	1.863E-04
6.21	2.64E+05	2.353E-05	135.802	2.099E-04

Notice that the difference between the principles stresses ($\Delta\sigma$) is worked with a logarithmic function in nine steps to obtain the hyperbolic curve with a numerically feasible manner. The resultant stress-strain curve is as follows:

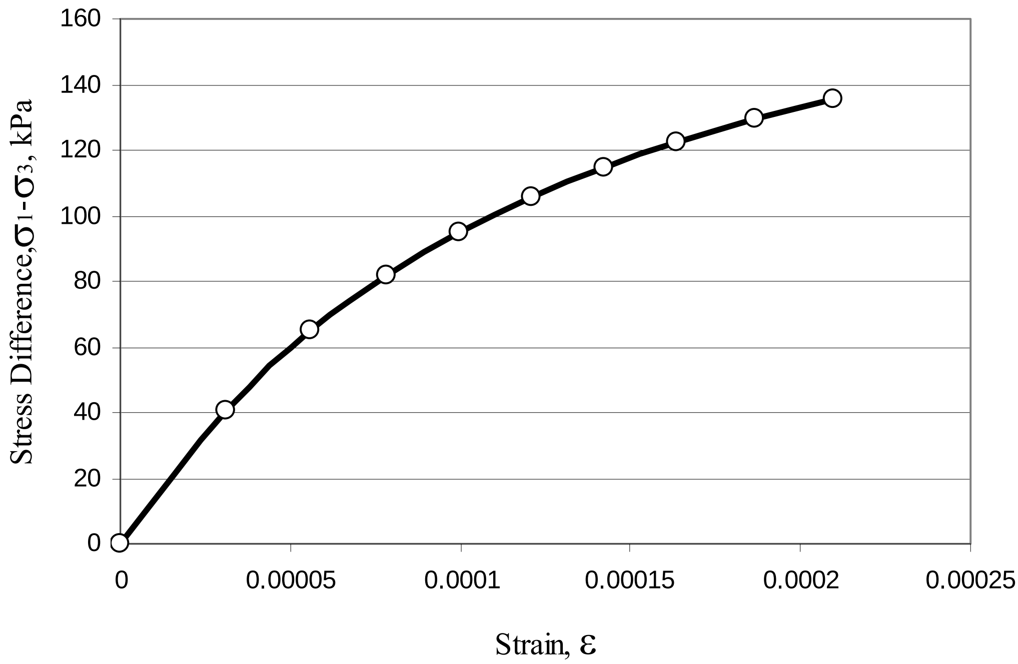

Figure 4.7 : Calculated hyperbola for stress and strain curve

This procedure combined with that of Figure 4.3, can be utilized to estimate the elasto plastic settlement of shallow foundations. Calculations accomplished with this methodology will be presented in the last chapter, with comparisons to other methods.

5. ILLUSTRATIVE EXAMPLES AND CASE STUDIES

The methods for estimating immediate settlement are pretty diverse in their way of comprehending the soil. The theory of elasticity mathematically handles it as a homogeneous halfspace holding a linear relationship between stress and strain. A similar manner is valid in Winkler springs, which is a preference for structural design. Still being very common in practice, these two methods have been used successfully to conduct the analysis of geotechnical problems since the calculations only require a simple calculator, a pen and a piece of paper.

As the civilization has further developed, new problems arise, requiring more realistic approaches, say like construction in highly urban areas for great infra and ultra structures – new metro lines or high rise buildings in already populated areas– or industrial complexes requiring stable foundations – machinery of high precise production or huge amount of storages or offshore platforms. These new challenges for engineers have been confronted with the consideration of the plastic settlement involving in the short term behavior of soil.

Solutions such as the finite element programmes is now popular amongst the practitioners, despite the fact that most of the users are lacking knowledge of what is going beneath the code, which tends to be the subject of academics. Meanwhile an engineer today has great opportunities and tools to conduct sophisticated analysis all by himself/herself using already known and verified elements of geotechnical literature, as one has given in the previous chapter for the calculation of immediate settlement as an elasto plastic behavior with the help of functions of stress increment and the hyperbolic model for the relevant phenomenon.

This chapter makes a comparison between the classic and relatively new methods of analysis for the elasto plastic settlement of soil with the settlement measurements of actual structures where possible.

5.1. Immediate Settlement of a Circular Footing

As a first example, a theoretical problem is considered where the immediate settlement of a uniformly loaded circular footing with the geometry and soil parameters given in Figure 5.1 is to be investigated.

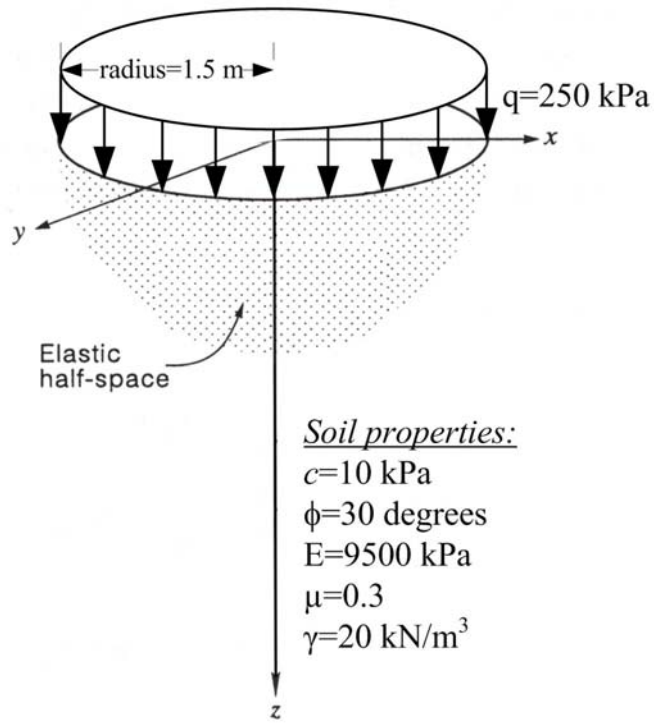

Figure 5.1 : Circular footing with subsoil properties

The settlement analysis will be conducted firstly for the center and corner (edge) points of the footing with the assumption of foundation being flexible. Rigidity will be considered as well by using (3.30) – the equation to obtain the settlement of a rigid circular foundation from the calculation those of a flexible one –, inserting a rigid beam into the finite element code – namely PLAXIS version 7– and finally by approximating the contact pressures given in Section 2.3.4.

Methods of theory of elasticity, finite element and the numerical procedure for hyperbolic model – which is referred shortly as HM from now on – will be used respectively.

5.1.1. Solutions of Theory of Elasticity

Table 3.9 and equation (3.15) are used to evaluate the settlement of circular footing at the center and at the corner as follows:

$$S_e(\text{center}) = \frac{qB(1-\mu)^2}{E} = \frac{250\times 2\times 1.5\times(1-0.3)^2}{9500} = 0.07184 \text{ m} = 71.84 \text{ mm}$$

$$S_e(\text{corner}) = \frac{0.64qB(1-\mu)^2}{E} = 0.64\times 0.07184 \ = 0.04598 \text{ m} = 45.98 \text{ mm}$$

Again referring to same equation the settlement in case of a rigid foundation is calculated as:

$$S_e = \frac{0.79qB(1-\mu^2)}{E} = 0.79\times 0.07184 \ = 0.05675 \text{ m} = 56.75 \text{ mm}$$

5.1.2. Solutions of Finite Element Method

The circular foundation is modeled as an axi-symmetric mesh as depicted in Figure 5.2. Note that the dimensioning of the mesh is done as suggested in Figure 3.14**,** since its width is 5*B*=5x2x1.5=15 meters and its length is 8*B*=8x2x1.5=24 meters.

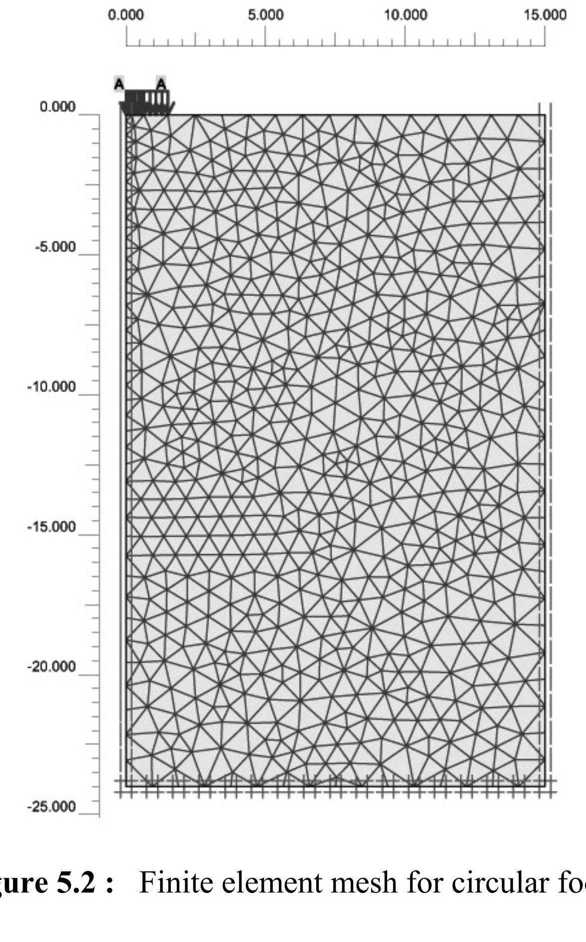

Figure 5.2 : Finite element mesh for circular footing

The deformed mesh and the magnitudes of vertical displacements for a flexible footing and for a rigid footing – modeled via a rigid beam element placed under the area of loading– with an identical mesh are given in Figure 5.3 and Figure 5.4.

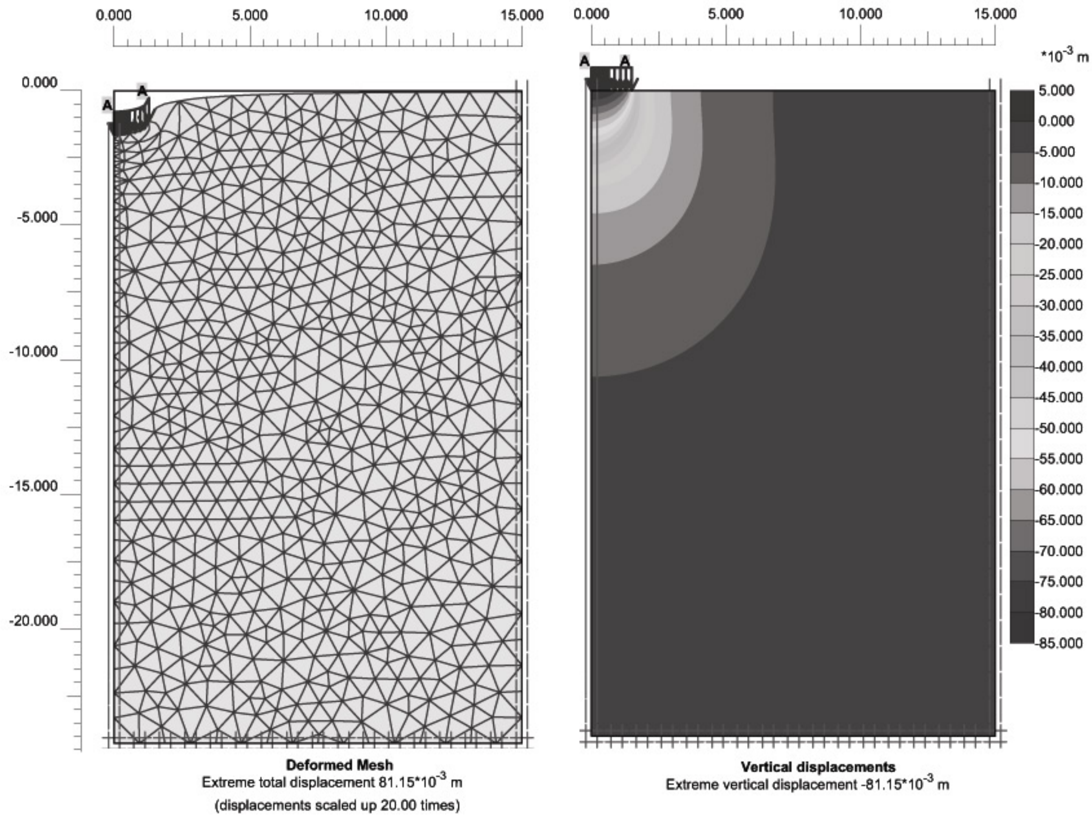

Figure 5.3 : Deformed mesh and vertical displacements for flexible footing

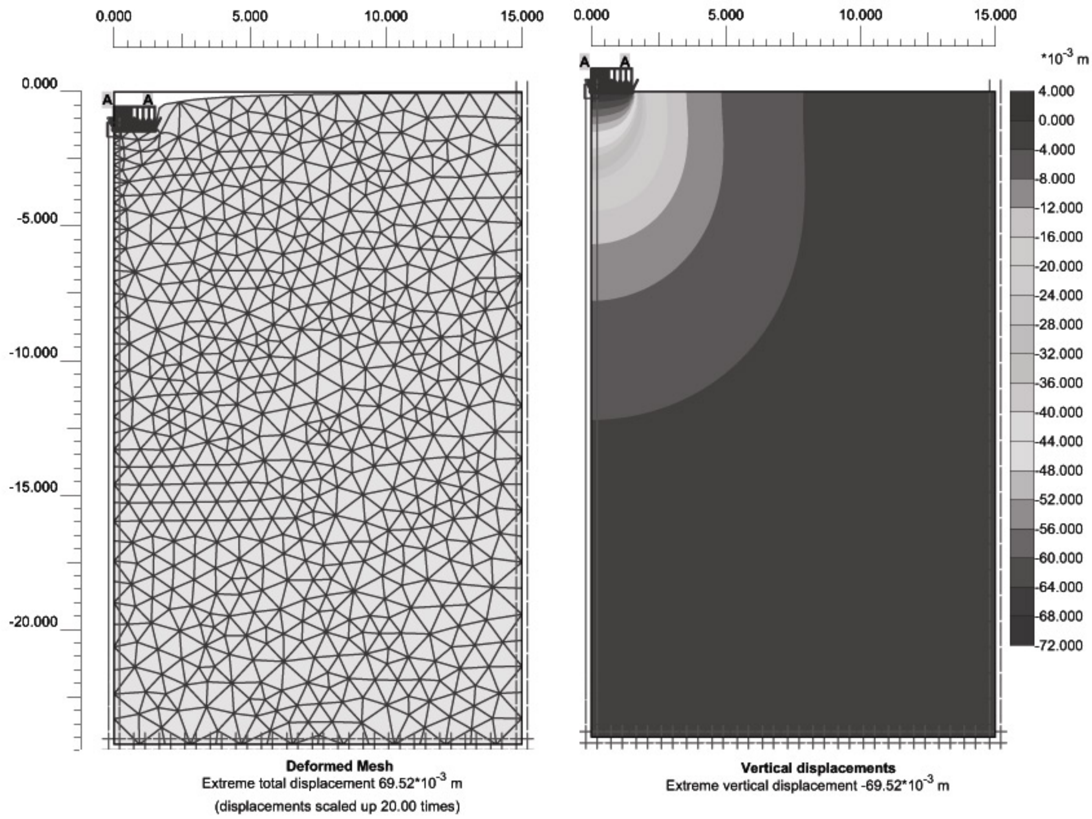

Figure 5.4 : Deformed mesh and vertical displacements for rigid footing

Results of the finite element analysis are summarized below in Table 5.1.

Table 5.1 : Outcome of finite element analysis

Foundation Type / Point	**Settlement**
Flexible, center	81.15 mm
Flexible, corner	56.46 mm
Rigid	69.52 mm

5.1.3. Solutions of Numerical Procedure using Hyperbolic Model

A spreadsheet has been prepared to evaluate the strains under the center and the corner of the circular foundation using HM, where the increments of normal stress and principles stresses – calculated with a separate spreadsheet using the all stress increments – are inputted for each soil segment of 0.05 meter thickness until a depth of 50 meters at where the strains caused by the surcharge were about $4x10^{-5}$, thus their effect on total settlement were less then $2x10^{-3}$ mm. This calculation is exemplified in Table 5.2 only up to 1 meters of depth for the point under the center of foundation.

Table 5.2 : Calculation of Stresses for HM

z	σ_3	σ_1	$\sigma_{1,\,Limit}$	$\sigma_{1,\,sel.}$	$\Delta\sigma_{,limit}$	$\Delta\sigma z$	$\Delta\sigma z_{,sel.}$	$\Delta\sigma y$	$\Delta\sigma y_{,sel.}$	$\Delta\sigma x$	$\Delta\sigma x_{,sel.}$
0.05	89.77	565.20	303.95	303.95	214.18	250.00	214.18	243.74	214.18	243.74	214.18
0.10	87.93	558.72	298.43	298.43	210.50	249.96	210.50	231.30	210.50	231.30	210.50
0.15	86.68	551.66	294.69	294.69	208.01	249.84	208.01	218.94	208.01	218.95	208.01
0.20	86.03	544.07	292.72	292.72	206.69	249.59	206.69	206.75	206.69	206.77	206.69
0.25	85.93	536.00	292.43	292.43	206.50	249.16	206.50	194.80	194.80	194.81	194.81
0.30	86.37	527.50	293.74	293.74	207.37	248.50	207.37	183.13	183.13	183.15	183.15
0.35	87.30	518.61	296.54	296.54	209.24	247.59	209.24	171.80	171.80	171.83	171.83
0.40	88.69	509.41	300.72	300.72	212.03	246.39	212.03	160.86	160.86	160.88	160.88
0.45	90.50	499.95	306.13	306.13	215.64	244.89	215.64	150.33	150.33	150.36	150.36
0.50	92.67	490.30	312.64	312.64	219.97	243.08	219.97	140.26	140.26	140.29	140.29
0.55	95.15	480.52	320.09	320.09	224.94	240.94	224.94	130.65	130.65	130.68	130.68
0.60	97.90	470.67	328.34	328.34	230.44	238.49	230.44	121.53	121.53	121.56	121.56
0.65	100.87	460.83	337.24	337.24	236.37	235.73	235.73	112.91	112.91	112.94	112.94
0.70	104.00	451.03	346.63	346.63	242.63	232.68	232.68	104.78	104.78	104.81	104.81
0.75	107.25	441.35	356.38	356.38	249.13	229.36	229.36	97.14	97.14	97.17	97.17
0.80	110.57	431.83	366.35	366.35	255.78	225.78	225.78	89.98	89.98	90.01	90.01
0.85	113.92	422.52	376.41	376.41	262.49	221.98	221.98	83.29	83.29	83.32	83.32
0.90	117.27	413.46	386.44	386.44	269.17	217.98	217.98	77.06	77.06	77.09	77.09
0.95	120.56	404.70	396.32	396.32	275.76	213.81	213.81	71.26	71.26	71.29	71.29
1.00	123.77	396.27	405.96	396.27	272.49	209.50	209.50	65.88	65.88	65.91	65.91

z is depth in meters, the stresses are in kPa and $_{sel.}$ stands for selected.

Here the major principles stress is checked whether it stands within the limit designated by the Mohr-Coulomb failure criteria (Figure 2.4), if not it is replaced by the limiting value. Therefore a limiting value of deviatoric stress is obtained as the difference of major and minor principles stresses. All normal stress increments are checked whether or not they excess this limiting value.

Secondly, the spreadsheet uses the given stresses to obtain the strains at each level of 0.05 meters internal as previously explained via Table 4.1 and Figure 4.7. This calculation is exemplified in Table 5.3 for the first two and the final steps where logarithmically incrementing the major principle stress and the constant minor principle stress at the relevant depth is used to produce the tangent modulus, with which the normal stress increments are utilized together in (2.7) to obtain strains. The calculation process is shown again only up to 1 meters of depth for the point under the center of foundation.

Table 5.3 : Calculation of strain and settlement using HM

σ_3	$\sigma_{1,1}$	E_{t1}	ε_1	$\sigma_{1,2}$	E_{t2}	ε_2	$\sigma_{1,9}$	E_{t9}	ε_9	ε_{total}	ΔS	ΣS
89.8	115.6	7,862	3.E-03	130.6	6,975	2.E-03	175.4	4,655	8.E-04	1.E-02	0.68	92.08
87.9	113.3	7,862	3.E-03	128.1	6,975	2.E-03	172.1	4,655	8.E-04	1.E-02	0.67	91.40
86.7	111.7	7,862	3.E-03	126.4	6,975	2.E-03	169.9	4,655	8.E-04	1.E-02	0.66	90.74
86.0	110.9	7,862	3.E-03	125.5	6,975	2.E-03	168.7	4,655	8.E-04	1.E-02	0.65	90.08
85.9	112.9	7,730	3.E-03	128.7	6,779	2.E-03	175.5	4,322	9.E-04	1.E-02	0.74	89.43
86.4	115.7	7,590	4.E-03	132.9	6,573	3.E-03	183.9	3,982	1.E-03	2.E-02	0.84	88.69
87.3	119.3	7,448	4.E-03	138.0	6,364	3.E-03	193.5	3,646	1.E-03	2.E-02	0.96	87.84
88.7	123.5	7,307	5.E-03	143.8	6,157	3.E-03	204.2	3,323	2.E-03	2.E-02	1.10	86.88
90.5	128.3	7,169	5.E-03	150.3	5,957	4.E-03	215.9	3,019	2.E-03	3.E-02	1.26	85.78
92.7	133.5	7,036	6.E-03	157.5	5,766	4.E-03	228.5	2,739	2.E-03	3.E-02	1.44	84.52
95.2	139.3	6,911	6.E-03	165.1	5,587	5.E-03	241.7	2,485	3.E-03	3.E-02	1.64	83.08
97.9	145.3	6,794	7.E-03	173.1	5,421	5.E-03	255.4	2,256	3.E-03	4.E-02	1.86	81.44
100.9	151.4	6,696	8.E-03	181.0	5,283	6.E-03	268.8	2,072	4.E-03	4.E-02	2.08	79.58
104.0	155.1	6,735	8.E-03	185.0	5,338	6.E-03	273.8	2,144	4.E-03	4.E-02	2.06	77.50
107.2	158.7	6,783	8.E-03	188.9	5,405	6.E-03	278.3	2,235	4.E-03	4.E-02	2.03	75.44
110.6	162.3	6,837	8.E-03	192.5	5,482	6.E-03	282.4	2,340	3.E-03	4.E-02	1.99	73.40
113.9	165.7	6,897	8.E-03	196.0	5,567	5.E-03	285.9	2,457	3.E-03	4.E-02	1.94	71.42
117.3	169.0	6,960	7.E-03	199.2	5,657	5.E-03	289.0	2,583	3.E-03	4.E-02	1.88	69.48
120.6	172.1	7,026	7.E-03	202.2	5,751	5.E-03	291.6	2,717	3.E-03	4.E-02	1.82	67.60
123.8	174.9	7,092	7.E-03	204.9	5,846	5.E-03	293.7	2,856	3.E-03	4.E-02	1.76	65.77

σ_3 , σ_1 are in kPa. E_{ti} is tangent modulus in kPa. ΔS and ΣS are incremental and total settlements (mm)

Results of the numerical procedure using HM and the settlement of a rigid foundation which can be derived from these results using (3.30) are summarized below in Table 5.4.

Table 5.4 : Outcome of numerical procedure using HM

Foundation Type / Point	Settlement
Flexible, center	92.08 mm
Flexible, corner	52.77 mm
Rigid	72.43 mm

Another way to obtain the settlement for a rigid circular foundation is to try mimicking the distribution of contact pressure as depicted in Figure 5.5 instead of a calculation using uniform load distribution.

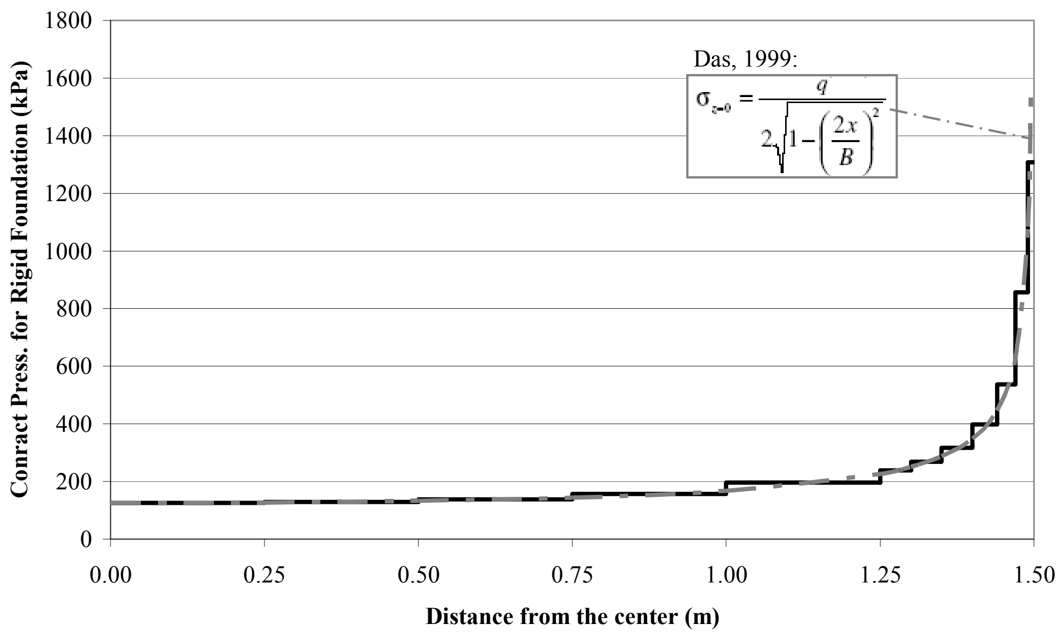

Figure 5.5 : Approximation for contact pressure under rigid foundation

This calculation involving superposition of uniformly loaded circular areas with varying values in loads and radiuses for approximation, tends to be far compelling than feasible. It does not give a uniform settlement profile as the results are stated in Table 5.5, even though it agrees with the settlement (72.43 mm) derived before.

Table 5.5 : Outcome of analysis of rigidity with contact pressure approximation

Foundation Type / Point	Settlement
Rigid, center	72.63 mm
Rigid, corner	64.39 mm

5.1.4. Results and Comparison of Solutions

The amount of immediate settlement of a circular footing calculated using different methods are summarized in Table 5.6. It can be recognized easily that the theory of elasticity estimates smaller degrees of settlement in contrast to the finite element method and the numerical procedure using HM.

Table 5.6 : Outcomes of settlement analysis

Foundation Type / Point	Analysis Method	Settlement
Flexible, center	Theory of Elasticity	71.84 mm
	Finite Element Method (PLAXIS)	81.15 mm
	Numerical Procedure using HM	92.08 mm
Flexible, corner	Theory of Elasticity	45.98 mm
	Finite Element Method (PLAXIS)	56.46 mm
	Numerical Procedure using HM	52.77 mm
Rigid	Theory of Elasticity	56.75 mm
	Finite Element Method (PLAXIS)	69.52 mm
	Numerical Procedure using HM	72.43 mm

To illustrate the linear and the nonlinear calculation procedures, refer to Figure 5.6 and Figure 5.7 where the agreement between the finite element method and the numerical procedure using HM is depicted better.

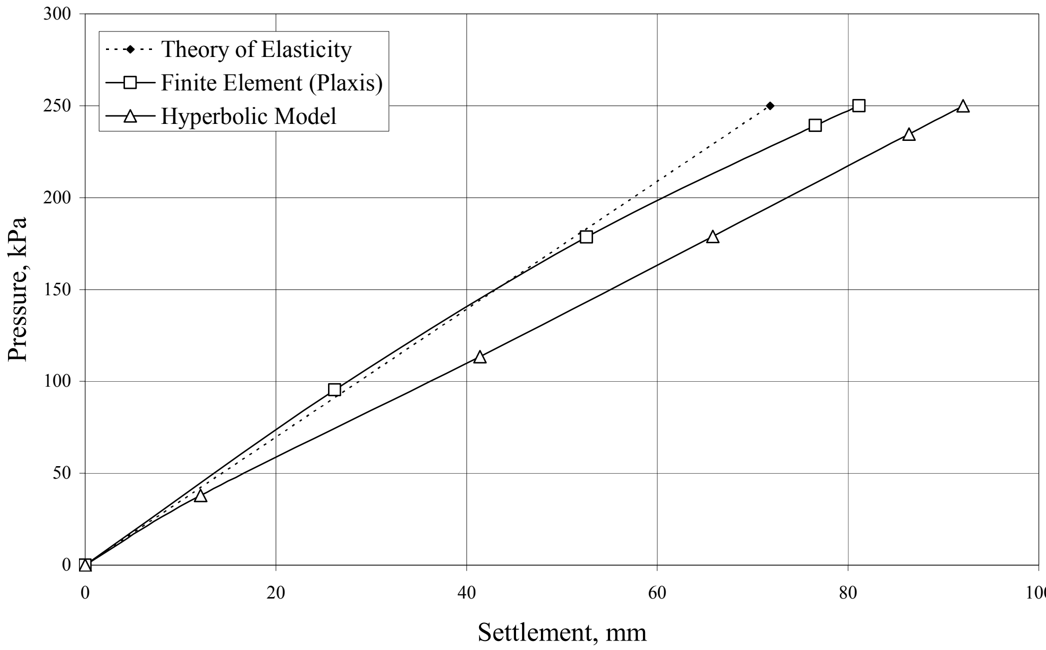

Figure 5.6 : Foundation pressures vs. settlement under center

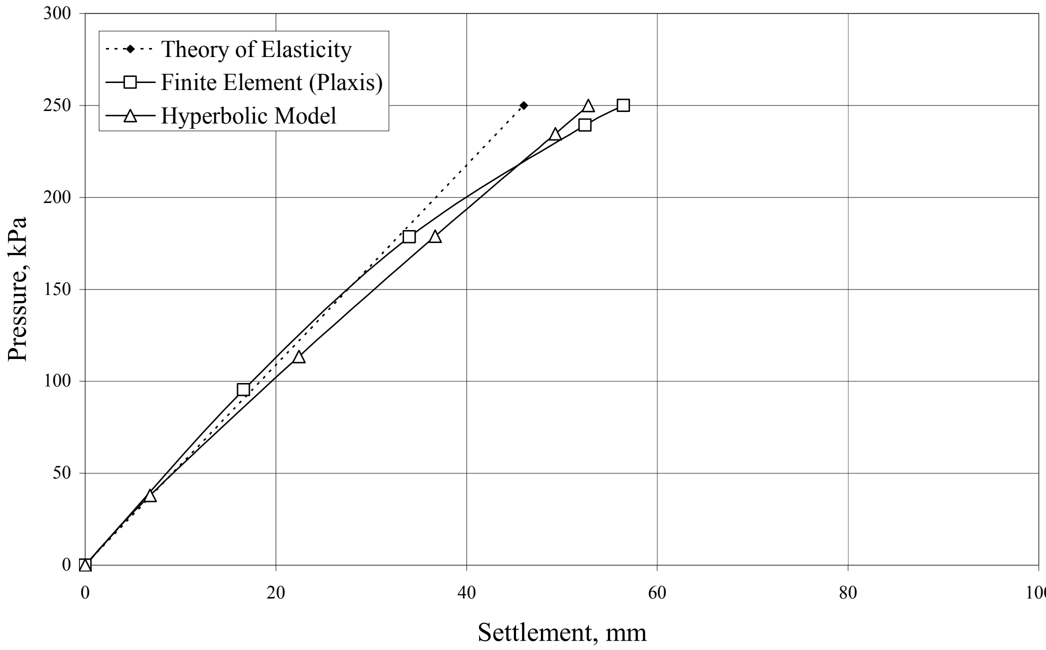

Figure 5.7 : Foundation pressures vs. settlement under corner

Yet in the analysis with HM, the elastic modulus is taken 9500 kPa even in depths of 50 meters, in contrast to a real situation in which the elasticity modulus increases with depth. Indeed the hyperbolic model originally implies the change in elasticity modulus with confining pressure as stated in (4.2). Therefore it has become more obvious after this solution that this phenomenon has to be recognized for more precise calculation conducted with HM, since the model tends to decrease the magnitude of the modulus of elasticity under high soil pressures, which, in the lack of the consideration for (4.2), results in the estimation of higher settlement values.

For the next example, where the settlement of an actual structure with a boring log of Standard Penetration Test will be analyzed, the increase in the modulus of elasticity with depth (both for the method of theory of elasticity and the hyperbolic model) is to be considered during calculations.

5.2. Observed and Computed Settlement of a Shallow Foundation on Sand

A study of a shallow foundation resting on medium dense sand – with a relative density D_R = 42 %, total unit weight γ=17.85 kN/m^3, friction angle ϕ=26° and cohesion c=0 as determined by laboratory tests – is presented by Maugeri *et al.* (1998). The observed settlements of the building, which is located in Mascali

(Catania, Italy) as a residential block encoded Block E1 (Figure 5.8), has been given together with a SPT profile at the bore-hole number 8 (Figure 5.9).

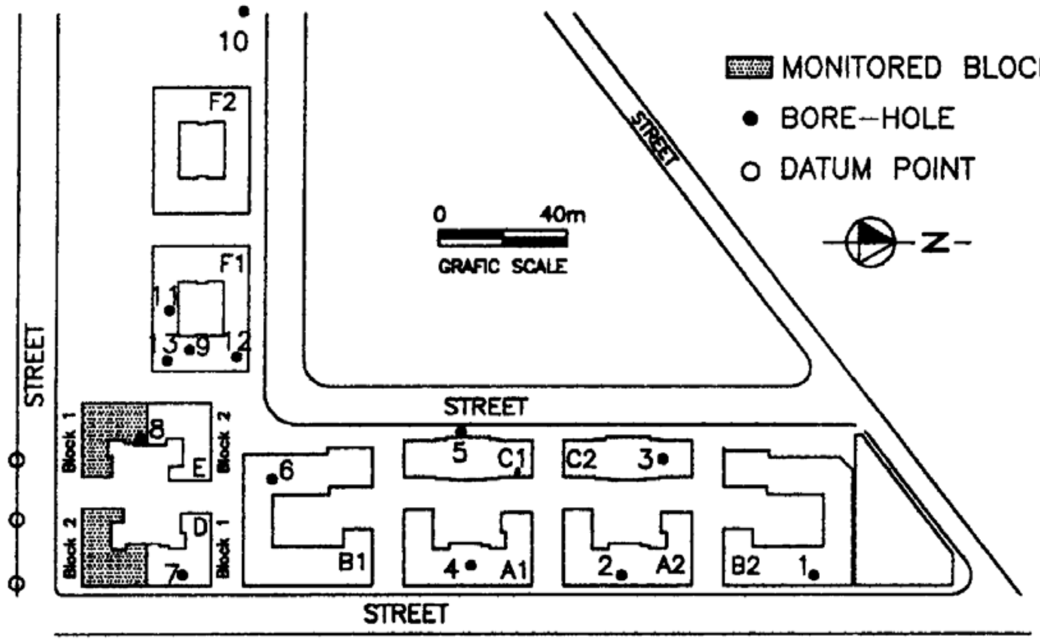

Figure 5.8 : Plan view of the location for investigated site (Maugeri et al., 1998)

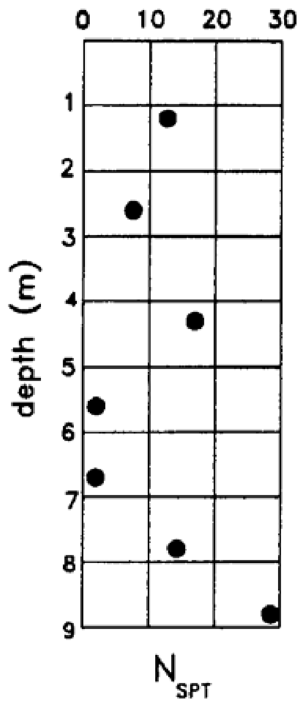

Figure 5.9 : Standard penetration test results for bore-hole 8 (Maugeri et al., 1998)

5.2.1. Observed Values and Calculation Results of Settlement

The authors suggests that the L-shaped building E1 having a raft foundation – with an embedment depth of 2.5 m – can be considered as an equivalent rectangular area with *L*=22.60 m and *B*=14.00 m.

Applied loads due to construction are measured as shown in Table 5.7.

Table 5.7 : Load surveys for Block E1 (Maugeri et al., 1998)

Stage	**Date**	***q*** (kPa)	**Δ*q*** (kPa)
1	8 December 1993	0	0
2	6 January 1994	6.30	6.30
3	28 May 1994	18.32	12.02

In the paper, a prediction of settlements using theory of elasticity is presented, where different correlations are used to estimate the modulus of elasticity. These correlations and the calculated settlements using them are summarized together with the actual settlement of building is presented below in Table 5.8.

Table 5.8 : Predicted and measured settlements of Block E1 (Maugeri et al., 1998)

q (kPa)	**Predicted Settlements using given correlations** (mm)			**Measured Settlements** (mm)
	E_s=500(N+15) E_s =13.53 MPa Bowles (1968)	E_s=0.478N+7.17 E_s =12.93 MPa Webb (1970)	E_s=2.6q_c [q_c=4N] E_s =12.52 MPa Schmertmann *et al.* (1968)	
6.30	3.7	3.9	4.0	0.8
18.32	10.7	11.3	11.6	4.2

The correlation between the prediction and the actual building performance is quite poor. Therefore we should question the reliability of such a simple analysis and perform more advanced yet relatively feasible – in contrast to complex numerical methods – calculation procedures in order to refine our judgment in this regular geotechnical problem.

5.2.2. Reconsidering the Method of Elasticity Theory

Using the recent advancements given in Section 3.1.7 for the theory of elasticity, the problem can be analyzed in a more detailed manner focusing on the SPT profile. As it can be regarded from Figure 5.9, the increase in the blow count can be defined via a linear regression where $E_s = E_0 + kz$. The change in the modulus of elasticity, which is calculated with E_s= 500(N+15) – the most conventional correlation as stated in Table 3.1 –, is approximated by two different regression are established; one being the best fit mathematically with E_0=10158 kPa and k=955 kPa/m and the other based on engineering judgment with E_0=4500 kPa and k=2500 kPa/m. The effect of disturbance due to construction in the upper parts of the sand is taken into account in the second regression as visualized in Figure 5.10.

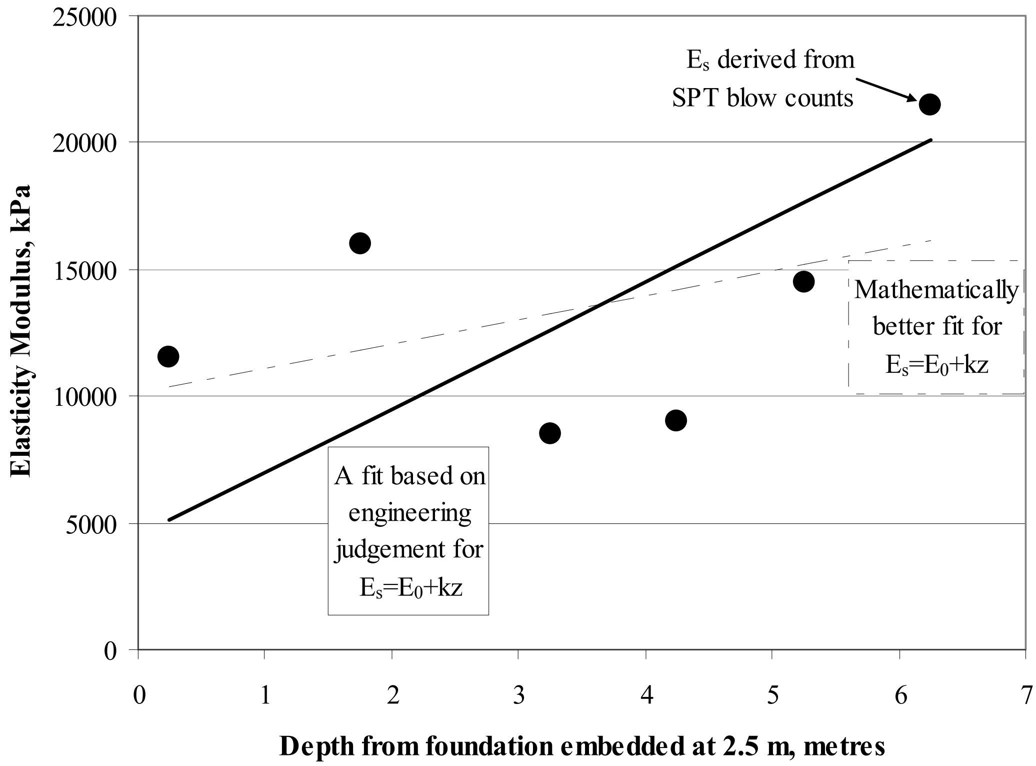

Figure 5.10 : Approximation for modulus of elasticity

The calculations executed according to (3.18) are tabulated below in Table 5.9. Note that the Poisson ratio is taken as 0.3 for medium dense sand from Table 2.1.

Table 5.9 : Calculations using improved relationship for immediate settlement

Estimation	E_0	k	I_G	I_F	I_E	q	S_e
#	(kPa)	(kPa/m)	(Figure 3.6)	(Figure 3.7)	(Figure 3.8)	(kPa)	(mm)
I	10158	955	0.06	0.79	0.97	6.30	0.52
						18.32	1.52
II	4500	2500	0.07	0.80	0.97	6.30	1.32
						18.32	3.83

Foundation thickness is taken as 2 meters and $E_{concrete}$=30000 MPa

5.2.3. Analysis by Numerical Procedure using Hyperbolic Model

For the utilization of HM, the change in elasticity modulus with confining pressure as stated before in (4.2) as $E_i = KP_a\left(\sigma_3/P_a\right)^n$ will be considered based on the SPT profile. Two different assumptions will be made. Firstly the soil will be separated into two layers where the parameters involving the initial modulus of elasticity differs after a depth of 5.75 meters, and secondly a general modeling of all the strata with the decease in the elasticity modulus caused by construction activity will be taken into account. Complementary to the first assumption, K=300 and n= 0.75 are selected for the determination of initial modulus until 5.75 meters where as K=350 and n= 3 are chosen for the depth beyond. For the second one, K=300 and n=1.25 are issued for the analysis. The approximations are given in Table 5.10 and Figure 5.11.

Table 5.10 : Calculations for initial modulus of elasticity

Depth (m)	σ_3 (kPa)	N	E_s=500(N+15) (kPa)	$E_{i,Ia}$ (kPa)	$E_{i,Ib}$ (kPa)	$E_{i,II}$ (kPa)
2.75	28	8	11500	11452	-	5973
4.25	43	17	16000	15873	-	10293
5.75	58	2	8500	-	6530	15019
6.75	68	3	9000	-	10564	18352
7.75	78	14	14500	-	15988	21811
8.75	88	28	21500	-	23010	25384

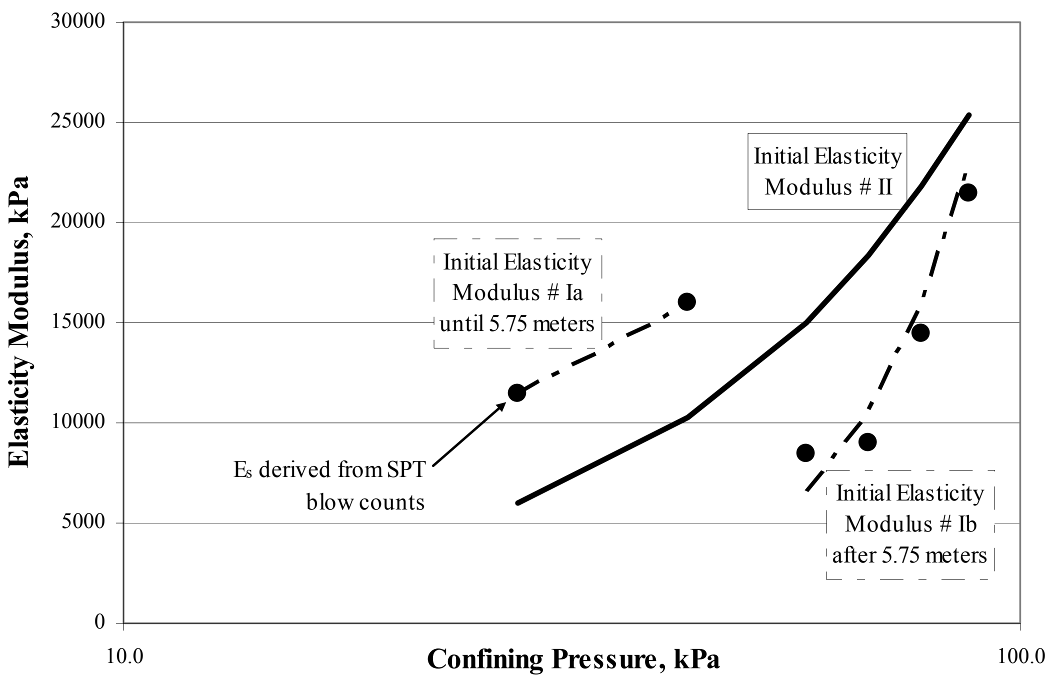

Figure 5.11 : Illustration of approximations for initial modulus of elasticity

Again spreadsheets are used together with the stress increments for a uniformly loaded (q_1=6.30 kPa and q_2=18.32 kPa) rectangular area (with L=22.60 m and B=14.00 m) to obtain the strains at each level of 0.05 meters internal as previously explained via Table 4.1 and Figure 4.7. This calculation is exemplified in Table 5.11 for the first and the final steps where logarithmically incrementing the major principle stress and the constant minor principle stress at the relevant depth is used to produce the tangent modulus which incorporates the initial modulus sensitive to confining pressure, with which the normal stress increments are utilized together in (2.7) to obtain strains. The calculation process is shown only up to 1 meters of depth for the point under the center of foundation for the loading of q_1=6.30 kPa using the first approximation for the initial elasticity modulus.

Table 5.11 : Calculation of strain and settlement using HM

σ_3	$E_{i,1}$	$\sigma_{1,1}$	E_{t1}	ε_1	$\sigma_{1,9}$	$E_{t,9}$	ε_9	ε_{total}	ΔS	ΣS
27.6	11,450	28.3	11,148	7.E-05	30.1	10,461	1.E-05	2.E-04	0.01	2.70
28.0	11,582	28.8	11,277	7.E-05	30.6	10,585	1.E-05	2.E-04	0.01	2.69
28.4	11,714	29.2	11,406	7.E-05	31.0	10,708	1.E-05	2.E-04	0.01	2.68
28.8	11,845	29.6	11,535	7.E-05	31.5	10,831	1.E-05	2.E-04	0.01	2.67
29.3	11,975	30.1	11,663	7.E-05	31.9	10,954	1.E-05	2.E-04	0.01	2.65
29.7	12,106	30.5	11,791	7.E-05	32.4	11,076	1.E-05	2.E-04	0.01	2.64
30.1	12,235	30.9	11,918	7.E-05	32.8	11,198	1.E-05	2.E-04	0.01	2.63
30.5	12,365	31.4	12,045	7.E-05	33.3	11,319	1.E-05	2.E-04	0.01	2.62
31.0	12,493	31.8	12,171	7.E-05	33.7	11,440	1.E-05	2.E-04	0.01	2.61
31.4	12,622	32.2	12,297	7.E-05	34.2	11,561	1.E-05	2.E-04	0.01	2.60
31.8	12,750	32.7	12,423	7.E-05	34.6	11,681	1.E-05	2.E-04	0.01	2.58
32.2	12,877	33.1	12,548	7.E-05	35.1	11,801	1.E-05	2.E-04	0.01	2.57
32.7	13,005	33.5	12,673	7.E-05	35.6	11,921	1.E-05	2.E-04	0.01	2.56
33.1	13,132	34.0	12,798	7.E-05	36.0	12,040	1.E-05	2.E-04	0.01	2.55
33.5	13,258	34.4	12,922	7.E-05	36.5	12,159	1.E-05	2.E-04	0.01	2.54
33.9	13,384	34.8	13,046	7.E-05	36.9	12,278	1.E-05	2.E-04	0.01	2.52
34.4	13,510	35.3	13,170	7.E-05	37.4	12,396	1.E-05	2.E-04	0.01	2.51
34.8	13,636	35.7	13,293	7.E-05	37.8	12,515	1.E-05	2.E-04	0.01	2.50
35.2	13,761	36.1	13,416	7.E-05	38.3	12,633	1.E-05	2.E-04	0.01	2.49
35.6	13,886	36.6	13,539	7.E-05	38.7	12,750	1.E-05	2.E-04	0.01	2.48

σ_3 , σ_1 are in kPa. E_i,E_{ti} are initial and tangent modulus are in kPa.
ΔS and ΣS are incremental and total settlements (mm)

Results of the numerical procedure using HM with two different approximations on initial elasticity modulus and the settlement of a rigid foundation – being the actual case – which can be derived from these results using (3.31) are summarized below in Table 5.12.

Table 5.12 : Outcome of numerical procedure using HM

Foundation Type / Point / Approximation #	Settlement for q_1=6.30 kPa	Settlement for q_2=18.32 kPa
Flexible, center, I	2.7 mm	10.7 mm
Flexible, corner, I	0.6 mm	1.7 mm
Rigid, I	**1.3 mm**	**4.7 mm**
Flexible, center, II	2.9 mm	10.3 mm
Flexible, corner, II	0.8 mm	2.4 mm
Rigid, II	**1.5 mm**	**5.0 mm**

5.2.4. Results and Comparison of Solutions

The amount of immediate settlement for the residential block, calculated using different methods are shown in Table 5.13, as well as the field measurements. A basic analysis disregarding the increase in the modulus of elasticity with depth lacks proper assessment of settlement magnitudes, which may lead to an over-design or worse to a structural damage due to extensive settlement afterwards. Fortunately there is no record of such incident in this case study, yet it signifies the fact that the quality of prediction for foundation displacement relies both on the extent of the in-situ investigations and the refinement of the computation methodology based on this extent.

Table 5.13 : Outcomes of settlement analysis

Analysis Method	Settlement for q_1=6.30 kPa	Settlement for q_2=18.32 kPa
Theory of Elasticity by Maugeri et al., 1998	3.7 mm	10.8 mm
Theory of Elasticity I	0.5 mm	1.5 mm
Theory of Elasticity II	**1.3 mm**	**3.8 mm**
Numerical Procedure using HM I	1.3 mm	4.7 mm
Numerical Procedure using HM II	**1.5 mm**	**5.0 mm**
Measured Values	0.8 mm	4.2 mm

The calculation by theory of elasticity is significantly refined by the engineering judgment involved in, which did not greatly affect the results for HM. Both of the methods agree with the measured values better than the original estimations.

5.3. Settlement of a Grain Silo Complex on Chalk

Burland and Davidson (1976) gave a case history of damage of a group of four silos (Figure 5.12) due to extensive foundation movements. The silos have independent circular raft foundations with 23 meters diameter resting on a soft chalk at an embedment depth of 2 meters. The chalk has a modulus of elasticity 120 MPa and a Poisson ratio of 0.3. Mohr Coulomb strength parameters are as the internal friction angle ϕ=16° and cohesion c=250 kPa.

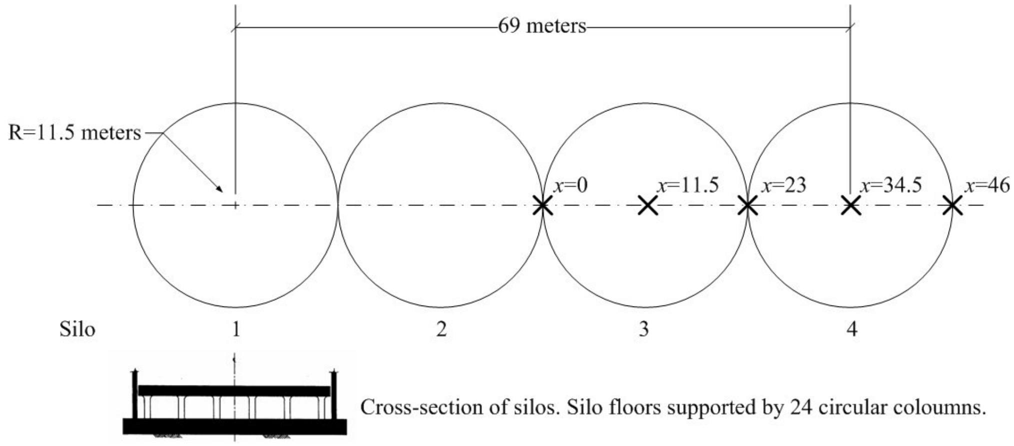

Figure 5.12 : Plan view of silo complex (produced from Hemsley, 2000)

5.3.1. Conducted Analysis and Measured Performance

Majid and Rahman (1982) have conducted a non-linear three-dimensional finite element analysis (Figure 5.13) on this structure. The computed settlements are due to live load only, which are disturbed between the floor and the walls in the proportion of 5000 t and 7000 t respectively.

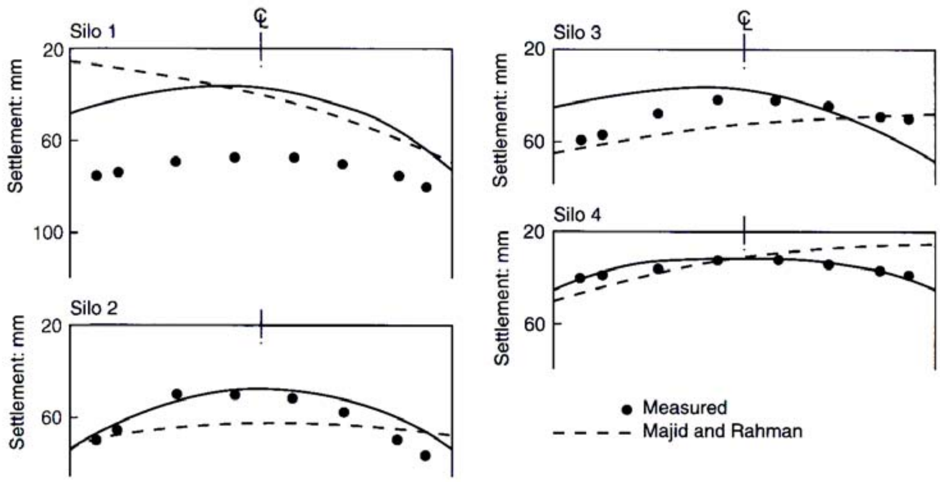

Figure 5.13 : 3D finite element analysis vs. field measurements (Hemsley, 2000)

The hogging mode of deformation is a result of this structural fact (the cross-section of a silo is given in Figure 5.12, where the distinction in load transferring between the wall and the floor can be clearly seen) and yet the measured and computed settlements by means of three-dimensional analysis, which are in a reasonable agreement.

5.3.2. Analysis by Numerical Procedure using Hyperbolic Model

It is not easy task to estimate the contact pressure distribution beneath silos, since the walls and the floor which is supported by columns tend to create unique hogging behavior in the raft foundation; a uniform load distribution is assumed. Its magnitude is estimated by dividing total live load (12000 t) by the area of a foundation ($\pi 11.5^2 = 415.5$ m^2) as 28.9 t/m^2 = 283.3 kPa.

The resulting stress increments of the silo complex are depicted below in Figure 5.14, where the stresses develop to higher pressures as a result of the interaction between adjacent silos, which cannot be illustrated with an analysis nor by the theory of elasticity, neither by a two dimensional finite element model.

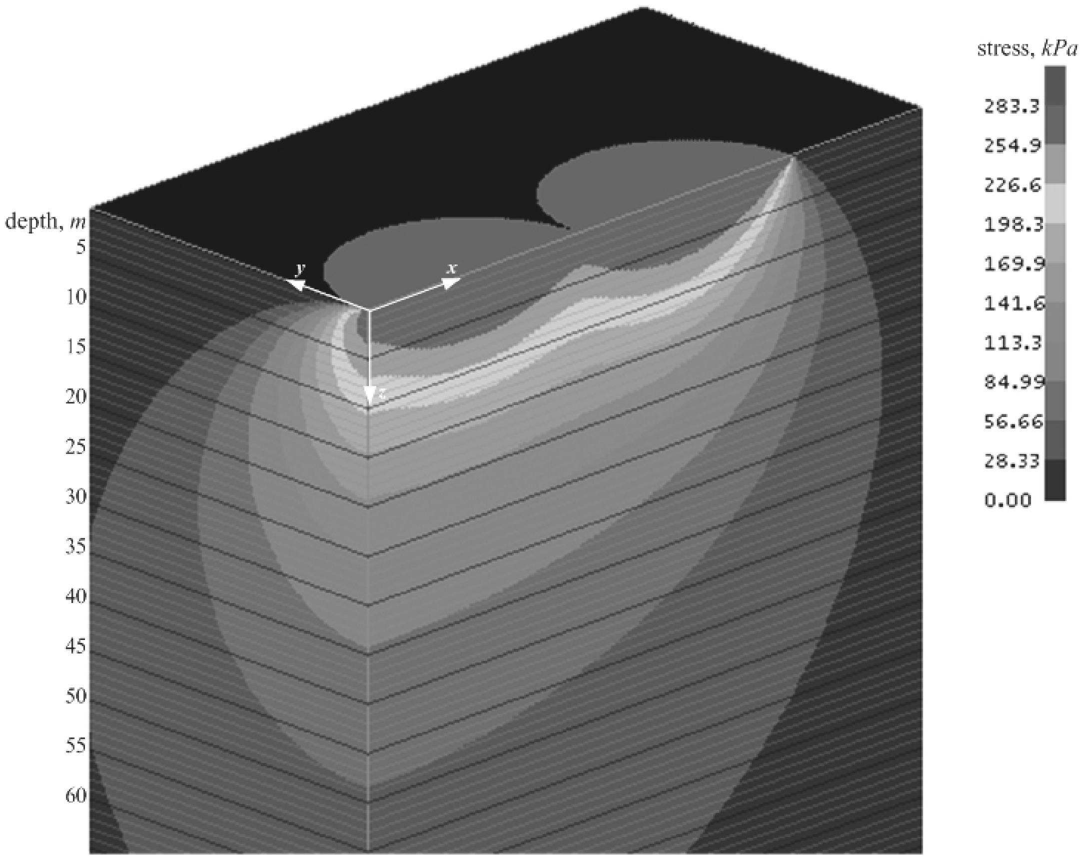

Figure 5.14 : Computed vertical stress increments for HM analysis

The results of HM analysis at the direction of lengthwise axis are given in Table 5.14 together with the results of non-linear three-dimensional finite element analysis and field measurements. While it cannot generate the hogging mode in deformation, HM analysis still gives reasonable values for the amount of total settlement of the silos.

Table 5.14 : Comparison of computed and observed settlements

x (meters)	**HM** (mm)	**3D FEM** (mm)	**Measured** (mm)
0.0	66.5	60.0	64.0
11.5	69.2	55.0	42.0
23.0	63.7	50.0	60.0
34.5	61.6	30.0	30.0
46.0	32.6	22.5	40.0

5.3.3. Structural Damage in Silos

The total settlement limit of 50 mm – as defined in Table 3.21 – has been exceeded as both measured in-situ and calculated by all methods. The further investigations showed that cracks developed in many of the columns supporting the floor of the silo. At a deflection ratio $\Delta/L = 0.6x10^{-3}$, it is reported that the cracking was severe enough for engineers to install temporary props. Figure 5.15 shows a sketch of one of the columns corresponding to the maximum measured deflection ratio of $1.07x10^{-3}$. The damage was considered severe enough to take expensive remedial measures.

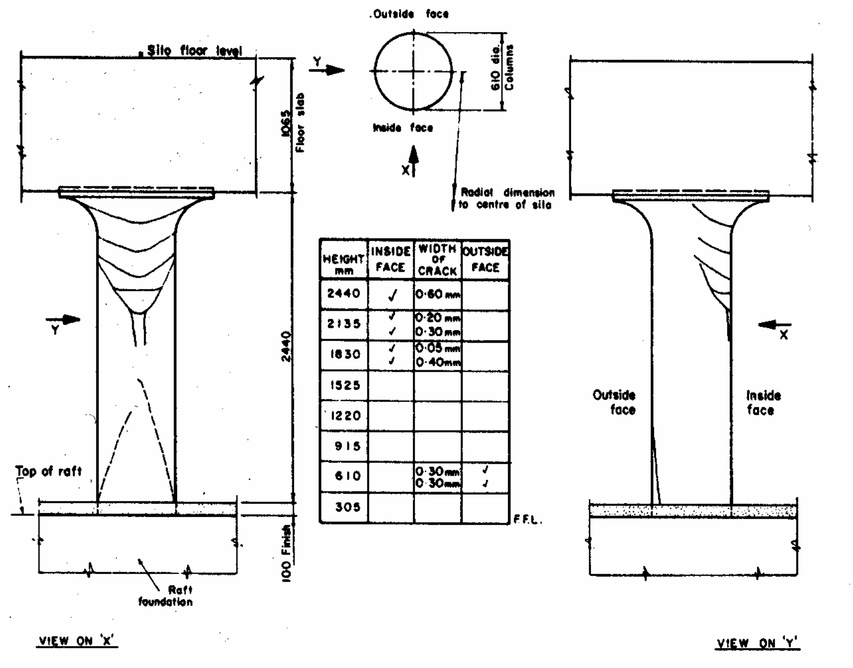

Figure 5.15 : Damage on a floor column of a silo (Burland and Davidson 1976)

6.CONCLUSIONS

The determination of settlement is one of the crucial steps in the design of civil engineering structures, of which the short-term behavior – being the elasto plastic or the immediate settlement – can be studied by many different methods.

In this study, the stress distribution (both geostatic and incremental due to a structural load) and the elasto plastic settlement as its resultant are investigated especially for shallow foundations (with varying shapes and loading situations) where linear – equations based on theory of elasticity and methods using Winkler springs – and nonlinear calculation methods – by means of finite element programs and a special numerical procedure using the hyperbolic model – are documented in detail, contrasted via illustrative examples and validated with actual measurements from case studies.

Applicable only for simple problems such as a single footing or a strip foundation, the theory of elasticity lacks to model the hardening behavior, thus underestimating the settlements. Yet its ease of use together with the recent improvements enables the engineer to conduct a fast check for the total settlement amount of a structure, whether or not it exceeds the tolerable limits defined by previous case histories and legitimate standards.

It is suggested for Winkler springs, which are rather useful to estimate moments and forces acting on structural elements for the design and selection of reinforcements or sections, that it is a better practice to obtain the modulus of subgrade reaction, as a ratio of contact pressure and amount of settlement, which is calculated with another method modeling the soil in a more decent way or by means of a proper field testing.

The finite element programs, which today are in a widespread use yet comprehended in the way they operate by a minority of experts, has to be approached with delicate care by trying to basically understand the produce beneath the code by consulting their scientific manual as well as the user guide for the sake of accuracy in the analysis. Once obtained such a package and becoming relative to it, analysis of complex structure-soil interaction by using advanced constitutive models may be conducted even in a three-dimensional manner.

The numerical procedure with hyperbolic model presented in this study, has proved to agree with the results of a finite element program in an illustrative example as well as correlating well with the measurement of actual settlements in two different case studies.

Consequently, it become a clear fact that an engineer today, who has some computer skills in using electronic spreadsheets, may conduct three-dimensional analysis of settlement by using a soil model, which competently emulates the problem at hand, where he/she can also include the engineering judgment, rather than using an old fashioned method or a prepaid expertise stocked in close coded, and complex structured program.

REFERENCES

Azizi, F., 2000. Applied analyses in geotechnics. E&FN Spon. New York.

Borowicka, H., 1936. Influence of rigidity of a circular foundation slab over the contact surface. Proceedings of the 1th ICSMFE. Cambridge, Vol. 2.

Boussinesq, J., 1878. Équilibre d'élasticité d'un solide isotrope sans pesanteur, supportant différents poids, in French. C. Rendus Acad. Sci. Paris, Vol. 86, pp. 1280-1263.

Bowles, J.E., 1974. Analytical and Computer Methods in Foundation Engineering. McGraw-Hill. New York.

Bowles, J.E., 1996. Foundation analysis and design, 5th edition. McGraw-Hill. New York.

Briaud, J.L., Gibbens R., 1999. Behavior of five large spread footings in sand, Journal of Geotechnical and Geoenvironmental Engineering, ASCE, Vol. 125, pp. 787-796.

Brooker, E.W., Ireland H.O., 1965. Earth pressure at rest related to stress history, Canadian Geotechnical Journal, 2, 1, pp. 1-15.

Burland, J.B., Broms B., De Molle, V.F.B., 1977. Behaviour of foundations and structures. State-of-the-art review. Proceedings of the 9th ICSMFE. Tokyo Vol. 2 pp. 495-546.

Burland, J.B., and Davidson, W., 1976. A case study of cracking of columns supporting a silo due to differential foundation settlement. Proc. Conf. On Performance of Building Structures, Glasgow, Pentech Press, London, 249 – 267.

Burmister, D.M., 1958. Evaluation of pavement systems of WASHO road testing layered systems method, Highway Research Board, Bulletin 177.

Cerruti, V., 1884. Sulla deformazione di uno strato isotropo indefinito limitato da due piani paralleli, in Italian. Atti Acad. Nazl. Lincei. Rend., Serie 4, Vol. 1, pp. 521-522.

Committee on Modeling Techniques in Geomechanics of Transportation Research Board, 2000. Modeling techniques in geomechanics. TRB, National Research Council, Washington.

Das, B.M., 1985. Advanced soil mechanics. McGraw-Hill. New York.

Das, B.M., 1999. Shallow foundations: bearing capacity and settlement. CRC Press. Boca Raton, Florida.

Das, B.M., 2001. Principles of geotechnical engineering, 5th edition. Brooks/Cole. California.

Davis, R.O., Selvadurai A.P.S., 1996. Elasticity and geomechanics. Cambridge University Press. Cambridge.

Dempsey, J.P., Li H., 1989. A rigid rectangular footing on an elastic layer. Géotechnique, Vol. 39, No. 1, 147-152.

Duncan, J.M., Chang, C.Y., 1970. Nonlinear analysis of stress and strain in soils, Journal of Soil Mechanics and Foundations Division, ASCE, SM 5, pp 1629-1653.

Egorov, K.E., 1958. Concerning the question of calculations for base under foundations with footings in the form of rings, Mekhanika Gruntov, Sb. Tr. no. 34, Gosstroiizdat, Moscow.

Eurocode 1, 1994. Basis of design and actions on structures. Brussels.

Eurocode 7, 1994. Geotechnical design – Part 1 : Geotechnical design, general rules. Brussels.

Eurocode 7, 2000. Geotechnical design – Part 3 : Design assisted by field testing, Brussels.

Foster, C.R., Ahlvin R.G., 1954. Stresses and deflections induced by a uniform circular load, Proceedings of Highway Research Board, Vol. 33., pp. 467-470.

Fadum, R.E., 1948. Influence values for estimating stresses in elastic foundations. Proceedings of the 2nd ICSMFE, Rotterdam, Vol. 2, pp. 77-84.

Feda, J., 1978. Stress in subsoil and methods of final settlement calculation. Elsevier. Prague.

FHWA, 2002. Geotechnical Engineering Circular No. 6 Shallow Foundations, Federal Highway Administration, Washington.

Florin, V.A., 1959. Fundamentals of soil mechanics, in Russian. Vol. i. Gosstroiizdat, Moscow.

Fox, L., 1948. Computations of trafic stresses in a simple road structure. Proceedings of the 2nd ICSMFE, Rotterdam, pp. 236-246.

Grant, R., Christian, J.T., Vanmarcke, E.H., 1974. Differential settlement of buildings. Journal of Geotechnical Engineering Division, ASCE, Vol. 100, No. GT 9, pp 973-992.

Harr, M.E., 1962.Groundwater and seepage. McGraw-Hill. New York.

Harr, M.E., 1966. Foundation of theoretical soil mechanics. McGraw-Hill. New York.

Hemsley, J.A., 2000. Design applications of raft foundations. Thomas Telford. London.

Holl, D.L., 1940. Stress transmission in earths. Proc. High. Res. Board, Vol. 20, pp. 709-721.

Ishihara, K., 1996. Soil behaviour in earthquake geotechnics. Oxford Engineering Science Series, No: 46, Clarendon Press, London.

Iyisan, R., 1994. Geoteknik özelliklerin belirlenmesinde sismik ve penetrasyon deneylerinin karşılaştırılması, in Turkish with English summary, Ph.D. Thesis, Istanbul Technical University.

Janbu, N., Bjerrum, L., Kjaernsli, B., 1956. Veiledning ved losing av fandamenteringsoppgaver (Soil mechanics applied to some engineering problems), in Norwegian with English summary. Norwegian Geotechnical Institute Publication No. 16, Oslo.

Koerner, R.M., 1985. Construction and geotechnical methods in foundation engineering. McGraw-Hill. New York.

Majid, K. I., Rahman, M.A., 1982. Non-linear analysis of structure-soil systems. Proceedings of Institution of Civil Engineers, Part 2, 73, March, pp. 53-84.

Marivoet, L., 1948. A simplified method for computing the bearing capacity of the soil supporting footings or piers. Proceedings of the 2nd ICSMFE, Rotterdam, Vol. 1, pp. 78-86.

Maugeri, M., Castelli, F., Massimino, M.R., Verona G., 1998. Observerd and computed settlements of two shallow foundations on sand. Journal of Geotechnical and Geoenvironmental Engineering, Vol. 124, No. 7.

Mayne, P.W., Poulos, H.G.,1999. Approximate displacement influence factors for elastic shallow foundations. Journal of Geotechnical and Geoenvironmental Engineering, ASCE, Vol. 125, No. 6, pp. 453-460.

Newmark, N. M., 1935. Simplified computation of vertical pressure in elastic foundations, University of Illinois Engineering Experiment Station Cir. No. 24, Urbana, IL, pp. 5-19.

Newmark, N. M., 1942. Influence charts for computation of stresses in elastic foundations, University of Illinois Engineering Experiment Station Cir. No. 338, Urbana, IL.

Osterberg, J.O., 1957. Influence values for vertical stresses in semi-infinite mass due to embankment loading, Proceedings of the 4th ICSMFE, London , Vol. 1.

Potts, D., Zdravkovic, L., 2001a. Finite element analysis in geotechnical engineering v. 1 theory. Thomas Telford, London.

Potts, D., Zdravkovic, L., 2001b. Finite element analysis in geotechnical engineering v. 2 application. Thomas Telford, London.

Poulos, H.G., Davis, E.H., 1974. Elastic solutions for soil land rock mechanics. John Wiley & Sons, New York.

Saglamer, A., 1973. Kohezyonsuz zeminlerde sükunetteki toprak basıncı katsayısının zemin parametreleri cinsinden ifadesi, in Turkish. Ph.D. Thesis, Istanbul Technical University.

Skempton, A.W., MacDonald, D.H., 1956. The allowable settlement of buildings. Proceedings of Institute of Civil Engineers, Vol. 5, Pt. 3, pp. 727-784.

Skempton, A.W., Bjerrum, L.A., 1957. A contribution to the settlement analysis of foundation on clay, Géotechnique Vol. 7, No. 4.

Sower, G.B., Sower, G.F., 1970. Introductory soil mechanics and foundations, 3rd edition. Macmillan, New York.

Terzaghi, K., 1924. Die theorie der hydrodynamischen spannungserscheinungen und ihr erdbautechnisches anwendungsgebeit, in German. Procedings of the 1^{st} International Congress on Applied Mechanics, Delft.

Terzaghi, K., 1955. Evaluation of coefficient of subgrade reaction. Géotechnique, Vol. 5, No. 4, pp. 297-326.

Terzaghi, K., Peck, R.B., 1967. Soil mechanics in engineering practice. Wiley. New York.

U.S. Army Corps of Engineers, 1992. Engineering and Design, Bearing Capacity of Soils, Washington.

Vesic, A.S., 1961. Beams on elastic subgrade and the Winkler's Hypothesis. Proceedings of the 5^{th} ICSMFE, Paris, Vol.1 pp. 845-850.

Winkler, E., 1867, Die lehre von der elastizitat und festigkeit, in German. Dominicus, Prague.

Wyllie, D.C., 1992. Foundations on rock. E&FN Spoon, New York.

Yılmaz, E., Saglamer, A., 2001. Secondary and tertiary compression behavior of Samsun soft blue clay. Proceedings of the 15th ICSMGE, Istanbul, pp. 329-332.

APPENDIX A – Tables for the Calculation of Stress Coefficients of Giroud's Solution from Feda, 1978

Coefficient K_0

Depth (z/L for the corner, $2z/L$ for the centre)	B/L = 0	0.1	0.2	1/3	0.4	0.5	2/3	1	1.5	2	2.5	3	5	10	∞
0	0.000	0.250	0.250	0.250	0.250	0.250	0.250	0.250	0.250	0.250	0.250	0.250	0.250	0.250	0.250
0.2	0.000	0.137	0.204	0.234	0.240	0.244	0.247	0.249	0.249	0.249	0.249	0.249	0.249	0.249	0.249
0.4	0.000	0.076	0.136	0.187	0.202	0.218	0.231	0.240	0.243	0.244	0.244	0.244	0.244	0.244	0.244
0.5	0.000	0.061	0.113	0.164	0.181	0.200	0.218	0.232	0.238	0.239	0.240	0.240	0.240	0.240	0.240
0.6	0.000	0.051	0.096	0.143	0.161	0.182	0.204	0.223	0.231	0.233	0.234	0.234	0.234	0.234	0.234
0.8	0.000	0.037	0.071	0.111	0.127	0.148	0.173	0.200	0.214	0.218	0.219	0.220	0.220	0.220	0.220
1	0.000	0.028	0.055	0.087	0.101	0.120	0.145	0.175	0.194	0.200	0.202	0.203	0.204	0.205	0.205
1.2	0.000	0.022	0.043	0.069	0.081	0.098	0.121	0.152	0.173	0.182	0.185	0.187	0.189	0.189	0.189
1.4	0.000	0.018	0.035	0.056	0.066	0.080	0.101	0.131	0.154	0.164	0.169	0.171	0.174	0.174	0.174
1.5	0.000	0.016	0.031	0.051	0.060	0.073	0.092	0.121	0.145	0.156	0.161	0.164	0.166	0.167	0.167
1.6	0.000	0.014	0.028	0.046	0.055	0.067	0.085	0.112	0.136	0.148	0.154	0.157	0.160	0.160	0.160
1.8	0.000	0.012	0.024	0.039	0.046	0.056	0.072	0.097	0.121	0.133	0.140	0.143	0.147	0.148	0.148
2	0.000	0.010	0.020	0.033	0.039	0.048	0.061	0.084	0.107	0.120	0.127	0.131	0.136	0.137	0.137
2.5	0.000	0.007	0.013	0.022	0.027	0.033	0.043	0.060	0.080	0.093	0.101	0.106	0.113	0.115	0.115
3	0.000	0.005	0.010	0.016	0.019	0.024	0.031	0.045	0.061	0.073	0.081	0.087	0.096	0.099	0.099
4	.0000	0.003	0.006	0.009	0.011	0.014	0.019	0.027	0.038	0.048	0.055	0.060	0.071	0.076	0.076
5	0.000	0.002	0.004	0.006	0.007	0.009	0.012	0.018	0.026	0.033	0.039	0.043	0.055	0.061	0.062
10	0.000	0.000	0.001	0.002	0.002	0.002	0.003	0.005	0.007	0.009	0.011	0.013	0.020	0.028	0.032
15	0.000	0.000	0.000	0.001	0.001	0.001	0.001	0.002	0.003	0.004	0.005	0.006	0.010	0.016	0.021
20	0.000	0.000	0.000	0.000	0.000	0.001	0.001	0.001	0.002	0.002	0.003	0.004	0.006	0.010	0.016
50	0.000	0.000	0.000	0.000	0.000	0.000	0.000	0.000	0.000	0.000	0.000	0.001	0.001	0.002	0.006

Coefficient K_1

Depth (z/L for the corner, $2z/L$ for the centre)	B/L = 0	0.1	0.2	1/3	0.4	0.5	2/3	1	1.5	2	2.5	3	5	10	∞
0	0.000	0.159	0.159	0.159	0.159	0.159	0.159	0.159	0.159	0.159	0.159	0.159	0.159	0.159	0.159
0.2	0.000	0.071	0.111	0.135	0.140	0.145	0.149	0.152	0.153	0.153	0.153	0.153	0.153	0.153	0.153
0.4	0.000	0.037	0.067	0.095	0.105	0.115	0.125	0.133	0.136	0.137	0.137	0.137	0.137	0.137	0.137
0.5	0.000	0.028	0.054	0.079	0.089	0.100	0.111	0.121	0.125	0.127	0.127	0.127	0.127	0.127	0.127
0.6	0.000	0.023	0.043	0.066	0.075	0.085	0.097	0.109	0.115	0.116	0.117	0.117	0.117	0.117	0.117
0.8	0.000	0.015	0.029	0.046	0.053	0.062	0.073	0.086	0.093	0.095	0.096	0.097	0.097	0.097	0.097
1	0.000	0.010	0.020	0.032	0.037	0.045	0.054	0.067	0.075	0.077	0.079	0.079	0.079	0.080	0.080
1.2	0.000	0.007	0.014	0.023	0.027	0.033	0.040	0.051	0.059	0.062	0.064	0.064	0.065	0.065	0.065
1.4	0.000	0.005	0.010	0.017	0.020	0.024	0.030	0.040	0.047	0.050	0.052	0.053	0.054	0.054	0.054
1.5	0.000	0.004	0.009	0.014	0.017	0.021	0.026	0.035	0.042	0.045	0.047	0.048	0.049	0.049	0.049
1.6	0.000	0.004	0.008	0.013	0.015	0.018	0.023	0.031	0.038	0.041	0.043	0.044	0.045	0.045	0.045
1.8	0.000	0.003	0.006	0.010	0.011	0.014	0.018	0.024	0.030	0.034	0.035	0.036	0.037	0.038	0.038
2	0.000	0.002	0.004	0.007	0.009	0.011	0.014	0.019	0.025	0.028	0.029	0.030	0.032	0.032	0.032
2.5	0.000	0.001	0.003	0.004	0.005	0.006	0.008	0.011	0.015	0.018	0.019	0.020	0.022	0.022	0.022
3	0.000	0.001	0.002	0.003	0.003	0.004	0.005	0.007	0.010	0.012	0.013	0.014	0.015	0.016	0.016
4	0.000	0.000	0.001	0.001	0.001	0.002	0.002	0.003	0.005	0.006	0.007	0.007	0.009	0.009	0.009
5	0.000	0.000	0.000	0.001	0.001	0.001	0.001	0.002	0.003	0.003	0.004	0.004	0.005	0.006	0.006
10	0.000	0.000	0.000	0.000	0.000	0.000	0.000	0.000	0.000	0.000	0.001	0.001	0.001	0.001	0.002
15	0.000	0.000	0.000	0.000	0.000	0.000	0.000	0.000	0.000	0.000	0.000	0.000	0.000	0.001	0.001
20	0.000	0.000	0.000	0.000	0.000	0.000	0.000	0.000	0.000	0.000	0.000	0.000	0.000	0.000	0.000
50	0.000	0.000	0.000	0.000	0.000	0.000	0.000	0.000	0.000	0.000	0.000	0.000	0.000	0.000	0.000

(After Giroud)

Coefficient K_2

	B/L														
Depth: z/L for the corner, $2z/L$ for the centre	0	0.1	0.2	1/3	0.4	0.5	2/3	1	1.5	2	2.5	3	5	10	∞
0	0.000	0.250	0.250	0.250	0.250	0.250	0.250	0.250	0.250	0.250	0.250	0.250	0.250	0.250	0.250
0.2	0.000	0.069	0.116	0.149	0.159	0.169	0.177	0.184	0.187	0.188	0.188	0.188	0.188	0.188	0.188
0.4	0.000	0.031	0.058	0.085	0.095	0.106	0.118	0.128	0.133	0.134	0.134	0.134	0.135	0.135	0.135
0.5	0.000	0.022	0.043	0.064	0.073	0.083	0.094	0.105	0.110	0.112	0.112	0.112	0.113	0.113	0.113
0.6	0.000	0.017	0.032	0.049	0.056	0.065	0.075	0.086	0.091	0.093	0.093	0.094	0.094	0.094	0.094
0.8	0.000	0.009	0.018	0.029	0.034	0.040	0.047	0.057	0.062	0.064	0.064	0.065	0.065	0.065	0.065
1	0.000	0.006	0.011	0.018	0.021	0.025	0.030	0.037	0.042	0.044	0.045	0.045	0.045	0.045	0.045
1.2	0.000	0.003	0.007	0.011	0.013	0.016	0.020	0.025	0.029	0.031	0.032	0.032	0.032	0.032	0.032
1.4	0.000	0.002	0.004	0.007	0.008	0.010	0.013	0.017	0.020	0.022	0.023	0.023	0.023	0.023	0.023
1.5	0.000	0.002	0.004	0.006	0.007	0.008	0.011	0.014	0.017	0.019	0.020	0.020	0.020	0.020	0.020
1.6	0.000	0.001	0.003	0.005	0.006	0.007	0.009	0.012	0.015	0.016	0.017	0.017	0.017	0.017	0.017
1.8	0.000	0.001	0.002	0.003	0.004	0.005	0.006	0.008	0.011	0.012	0.012	0.013	0.013	0.013	0.013
2	0.000	0.001	0.001	0.002	0.003	0.003	0.004	0.006	0.008	0.009	0.009	0.010	0.010	0.010	0.010
2.5	0.000	0.000	0.001	0.001	0.001	0.002	0.002	0.003	0.004	0.005	0.005	0.005	0.006	0.006	0.006
3	0.000	0.000	0.000	0.001	0.001	0.001	0.001	0.002	0.002	0.003	0.003	0.003	0.003	0.003	0.003
4	0.000	0.000	0.000	0.000	0.000	0.000	0.000	0.001	0.001	0.001	0.001	0.001	0.001	0.002	0.002
5	0.000	0.000	0.000	0.000	0.000	0.000	0.000	0.000	0.000	0.000	0.001	0.001	0.001	0.001	0.001
10	0.000	0.000	0.000	0.000	0.000	0.000	0.000	0.000	0.000	0.000	0.000	0.000	0.000	0.000	0.000
15	0.000	0.000	0.000	0.000	0.000	0.000	0.000	0.000	0.000	0.000	0.000	0.000	0.000	0.000	0.000
20	0.000	0.000	0.000	0.000	0.000	0.000	0.000	0.000	0.000	0.000	0.000	0.000	0.000	0.000	0.000
50	0.000	0.000	0.000	0.000	0.000	0.000	0.000	0.000	0.000	0.000	0.000	0.000	0.000	0.000	0.000

(After Giroud)

Coefficient K_3

	B/L														
Depth: z/L for the corner, $2z/L$ for the centre	0	0.1	0.2	1/3	0.4	0.5	2/3	1	1.5	2	2.5	3	5	10	∞
0	0.000	∞	∞	∞	∞	∞	∞	∞	∞	∞	∞	∞	∞	∞	∞
0.2	0.000	0.107	0.189	0.259	0.282	0.307	0.332	0.353	0.362	0.364	0.365	0.365	0.365	0.366	0.366
0.4	0.000	0.037	0.069	0.104	0.177	0.133	0.150	0.167	0.175	0.177	0.177	0.178	0.178	0.178	0.178
0.5	0.000	0.023	0.045	0.069	0.079	0.091	0.104	0.118	0.125	0.127	0.128	0.129	0.129	0.129	0.129
0.6	0.000	0.016	0.030	0.047	0.054	0.063	0.074	0.085	0.091	0.093	0.094	0.094	0.094	0.095	0.095
0.8	0.000	0.007	0.014	0.023	0.026	0.031	0.038	0.045	0.050	0.052	0.052	0.052	0.053	0.053	0.053
1	0.000	0.004	0.007	0.012	0.014	0.016	0.020	0.025	0.028	0.030	0.030	0.030	0.031	0.031	0.031
1.2	0.000	0.002	0.004	0.006	0.007	0.009	0.011	0.014	0.017	0.018	0.018	0.018	0.019	0.019	0.019
1.4	0.000	0.001	0.002	0.004	0.004	0.005	0.006	0.009	0.010	0.011	0.011	0.012	0.012	0.012	0.012
1.5	0.000	0.001	0.002	0.003	0.003	0.004	0.005	0.007	0.008	0.009	0.009	0.009	0.010	0.010	0.010
1.6	0.000	0.001	0.001	0.002	0.003	0.003	0.004	0.005	0.006	0.007	0.007	0.008	0.008	0.008	0.008
1.8	0.000	0.000	0.001	0.001	0.002	0.002	0.002	0.003	0.004	0.005	0.005	0.005	0.005	0.005	0.005
2	0.000	0.000	0.001	0.001	0.001	0.001	0.002	0.002	0.003	0.003	0.003	0.004	0.004	0.004	0.004
5.2	0.000	0.000	0.000	0.000	0.000	0.000	0.001	0.001	0.001	0.001	0.001	0.002	0.002	0.002	0.002
3	0.000	0.000	0.000	0.000	0.000	0.000	0.000	0.000	0.001	0.001	0.001	0.001	0.001	0.001	0.001
4	0.000	0.000	0.000	0.000	0.000	0.000	0.000	0.000	0.000	0.000	0.000	0.000	0.000	0.000	0.000
5	0.000	0.000	0.000	0.000	0.000	0.000	0.000	0.000	0.000	0.000	0.000	0.000	0.000	0.000	0.000
10	0.000	0.000	0.000	0.000	0.000	0.000	0.000	0.000	0.000	0.000	0.000	0.000	0.000	0.000	0.000
15	0.000	0.000	0.000	0.000	0.000	0.000	0.000	0.000	0.000	0.000	0.000	0.000	0.000	0.000	0.000
20	0.000	0.000	0.000	0.000	0.000	0.000	0.000	0.000	0.000	0.000	0.000	0.000	0.000	0.000	0.000
50	0.000	−0.000	−0.000	−0.000	−0.000	−0.000	0.000	−0.000	−0.000	0.000	0.000	−0.000	0.000	0.000	0.000

(After Giroud)

Coefficient K_5

Depth (z/L for the corner, $2z/L$ for the centre)	B/L = 0	0.1	0.2	1/3	0.4	0.5	2/3	1	1.5	2	2.5	3	5	10	∞
0	0.000	∞	∞	∞	∞	∞	∞	∞	∞	∞	∞	∞	∞	∞	∞
0.2	0.000	0.005	0.027	0.066	0.085	0.109	0.142	0.185	0.218	0.234	0.242	0.247	0.255	0.258	0.259
0.4	0.000	0.001	0.005	0.017	0.025	0.038	0.059	0.091	0.118	0.133	0.141	0.145	0.153	0.156	0.158
0.5	0.000	0.000	0.003	0.010	0.015	0.024	0.039	0.065	0.090	0.104	0.111	0.116	0.123	0.127	0.128
0.6	0.000	0.000	0.002	0.006	0.009	0.015	0.026	0.048	0.070	0.082	0.089	0.094	0.101	0.105	0.106
0.8	0.000	0.000	0.001	0.002	0.004	0.007	0.013	0.026	0.042	0.053	0.059	0.063	0.070	0.074	0.075
1	0.000	0.000	0.000	0.001	0.002	0.003	0.007	0.015	0.027	0.035	0.040	0.044	0.051	0.054	0.055
1.2	0.000	0.000	0.000	0.001	0.001	0.002	0.004	0.009	0.017	0.024	0.028	0.032	0.038	0.041	0.042
1.4	0.000	0.000	0.000	0.000	0.001	0.001	0.002	0.005	0.011	0.016	0.020	0.023	0.029	0.032	0.033
1.5	0.000	0.000	0.000	0.000	0.000	0.001	0.002	0.004	0.009	0.013	0.017	0.020	0.025	0.028	0.029
1.6	0.000	0.000	0.000	0.000	0.000	0.001	0.001	0.003	0.007	0.011	0.015	0.017	0.022	0.025	0.026
1.8	0.000	0.000	0.000	0.000	0.000	0.000	0.001	0.002	0.005	0.008	0.011	0.013	0.017	0.020	0.021
2	0.000	0.000	0.000	0.000	0.000	0.000	0.000	0.001	0.003	0.006	0.008	0.010	0.014	0.017	0.018
2.5	0.000	0.000	0.000	0.000	0.000	0.000	0.000	0.001	0.001	0.003	0.004	0.005	0.008	0.011	0.012
3	0.000	0.000	0.000	0.000	0.000	0.000	0.000	0.000	0.001	0.001	0.002	0.003	0.005	0.007	0.008
4	0.000	0.000	0.000	0.000	0.000	0.000	0.000	0.000	0.000	0.000	0.001	0.001	0.002	0.004	0.005
5	0.000	0.000	0.000	0.000	0.000	0.000	0.000	0.000	0.000	0.000	0.000	0.000	0.001	0.002	0.003
10	0.000	−0.000	0.000	0.000	0.000	0.000	0.000	0.000	0.000	0.000	0.000	0.000	0.000	0.000	0.001
15	0.000	−0.000	−0.000	0.000	0.000	0.000	0.000	0.000	0.000	0.000	0.000	0.000	0.000	0.000	0.000
20	0.000	−0.000	−0.000	−0.000	−0.000	0.000	0.000	0.000	0.000	0.000	0.000	0.000	0.000	0.000	0.000
50	0.000	−0.000	−0.000	−0.000	−0.000	−0.000	0.000	−0.000	−0.000	0.000	0.000	0.000	0.000	0.000	0.000

(After Giroud)

Coefficient K_2'

Depth (z/L for the corner, $2z/L$ for the centre)	B/L = 0	0.1	0.2	1/3	0.4	0.5	2/3	1	1.5	2	2.5	3	5	10	∞
0	0.000	0.234	0.219	0.199	0.189	0.176	0.156	0.125	0.094	0.074	0.061	0.051	0.031	0.016	0.000
0.2	0.000	0.059	0.097	0.118	0.121	0.122	0.118	0.103	0.082	0.067	0.056	0.048	0.030	0.016	0.000
0.4	0.000	0.026	0.048	0.069	0.075	0.082	0.086	0.083	0.071	0.060	0.051	0.045	0.029	0.015	0.000
0.5	0.000	0.019	0.036	0.054	0.060	0.067	0.073	0.074	0.066	0.056	0.049	0.043	0.028	0.015	0.000
0.6	0.000	0.015	0.028	0.043	0.049	0.056	0.062	0.066	0.061	0.053	0.047	0.041	0.028	0.015	0.000
0.8	0.000	0.009	0.018	0.029	0.033	0.039	0.046	0.052	0.052	0.047	0.043	0.038	0.026	0.015	0.000
1	0.000	0.007	0.013	0.021	0.024	0.029	0.035	0.042	0.044	0.042	0.039	0.035	0.025	0.014	0.000
1.2	0.000	0.005	0.009	0.015	0.018	0.022	0.027	0.034	0.037	0.037	0.035	0.032	0.024	0.014	0.000
1.4	0.000	0.004	0.007	0.012	0.014	0.017	0.021	0.027	0.032	0.033	0.032	0.030	0.023	0.014	0.000
1.5	0.000	0.003	0.006	0.010	0.012	0.015	0.019	0.025	0.029	0.031	0.030	0.029	0.022	0.014	0.000
1.6	0.000	0.003	0.006	0.009	0.011	0.013	0.017	0.023	0.027	0.029	0.028	0.027	0.022	0.013	0.000
1.8	0.000	0.002	0.005	0.007	0.009	0.011	0.014	0.019	0.024	0.025	0.026	0.025	0.021	0.013	0.000
2	0.000	0.002	0.004	0.006	0.007	0.009	0.012	0.016	0.020	0.023	0.023	0.023	0.020	0.013	0.000
2.5	0.000	0.001	0.002	0.004	0.005	0.006	0.008	0.011	0.015	0.017	0.018	0.019	0.017	0.012	0.000
3	0.000	0.001	0.002	0.003	0.003	0.004	0.006	0.008	0.011	0.013	0.015	0.015	0.015	0.011	0.000
4	0.000	0.000	0.001	0.002	0.002	0.002	0.003	0.005	0.007	0.008	0.010	0.011	0.012	0.010	0.000
5	0.000	0.000	0.001	0.001	0.001	0.002	0.002	0.003	0.004	0.006	0.007	0.008	0.009	0.009	0.000
10	0.000	0.000	0.000	0.000	0.000	0.000	0.001	0.001	0.001	0.002	0.002	0.002	0.003	0.005	0.000
15	0.000	0.000	0.000	0.000	0.000	0.000	0.000	0.000	0.001	0.001	0.001	0.001	0.002	0.003	0.000
20	0.000	0.000	0.000	0.000	0.000	0.000	0.000	0.000	0.000	0.000	0.000	0.001	0.001	0.002	0.000
50	0.000	0.000	0.000	0.000	0.000	0.000	0.000	0.000	0.000	0.000	0.000	0.000	0.000	0.000	0.000

(After Giroud)

Coefficient K'_3

Depth (z/L for the corner; $2z/L$ for the centre)	B/L														
	0	0.1	0.2	1/3	0.4	0.5	2/3	1	1.5	2	2.5	3	5	10	∞
0	0.000	0.143	0.128	0.109	0.100	0.088	0.071	0.047	0.027	0.017	0.011	0.008	0.003	0.001	0.000
0.2	0.000	0.025	0.040	0.048	0.049	0.048	0.044	0.033	0.021	0.014	0.010	0.007	0.003	0.001	0.000
0.4	0.000	0.009	0.016	0.023	0.025	0.026	0.026	0.023	0.016	0.011	0.008	0.006	0.003	0.001	0.000
0.5	0.000	0.006	0.011	0.016	0.018	0.020	0.021	0.019	0.014	0.010	0.008	0.006	0.003	0.001	0.000
0.6	0.000	0.004	0.008	0.012	0.013	0.015	0.016	0.016	0.012	0.009	0.007	0.005	0.002	0.001	0.000
0.8	0.000	0.002	0.004	0.007	0.008	0.009	0.010	0.011	0.009	0.007	0.006	0.005	0.002	0.001	0.000
1	0.000	0.001	0.003	0.004	0.005	0.006	0.007	0.008	0.007	0.006	0.005	0.004	0.002	0.001	0.000
1.2	0.000	0.001	0.002	0.003	0.003	0.004	0.005	0.006	0.006	0.005	0.004	0.004	0.002	0.001	0.000
1.4	0.000	0.001	0.001	0.002	0.002	0.003	0.003	0.004	0.004	0.004	0.004	0.003	0.002	0.001	0.000
1.5	0.000	0.000	0.001	0.002	0.002	0.002	0.003	0.004	0.004	0.004	0.003	0.003	0.002	0.001	0.000
1.6	0.000	0.000	0.001	0.001	0.002	0.002	0.002	0.003	0.003	0.003	0.003	0.003	0.002	0.001	0.000
1.8	0.000	0.000	0.001	0.001	0.001	0.001	0.002	0.002	0.003	0.003	0.003	0.002	0.001	0.001	0.000
2	0.000	0.000	0.000	0.001	0.001	0.001	0.001	0.002	0.002	0.002	0.002	0.002	0.001	0.001	0.000
2.5	0.000	0.000	0.000	0.000	0.000	0.001	0.001	0.001	0.001	0.001	0.001	0.001	0.001	0.000	0.000
3	0.000	0.000	0.000	0.000	0.000	0.000	0.000	0.001	0.001	0.001	0.001	0.001	0.001	0.000	0.000
4	0.000	0.000	0.000	0.000	0.000	0.000	0.000	0.000	0.000	0.000	0.001	0.001	0.001	0.000	0.000
5	0.000	0.000	0.000	0.000	0.000	0.000	0.000	0.000	0.000	0.000	0.000	0.000	0.000	0.000	0.000
10	0.000	0.000	0.000	0.000	0.000	0.000	0.000	0.000	0.000	0.000	0.000	0.000	0.000	0.000	0.000
15	0.000	0.000	0.000	0.000	0.000	0.000	0.000	0.000	0.000	0.000	0.000	0.000	0.000	0.000	0.000
20	0.000	0.000	0.000	0.000	0.000	0.000	0.000	0.000	0.000	0.000	0.000	0.000	0.000	0.000	0.000
50	0.000	−0.000	0.000	0.000	−0.000	0.000	0.000	0.000	0.000	0.000	0.000	0.000	0.000	0.000	0.000

(After Giroud)

Coefficient K'_5

Depth (z/L for the corner; $2z/L$ for the centre)	B/L														
	0	0.1	0.2	1/3	0.4	0.5	2/3	1	1.5	2	2.5	3	5	10	∞
0	0.000	∞	∞	∞	∞	∞	∞	∞	∞	∞	∞	∞	∞	∞	∞
0.2	0.000	0.036	0.069	0.105	0.120	0.139	0.164	0.197	0.223	0.236	0.244	0.248	0.255	0.258	0.259
0.4	0.000	0.016	0.031	0.049	0.058	0.069	0.085	0.107	0.127	0.137	0.143	0.147	0.153	0.157	0.158
0.5	0.000	0.011	0.023	0.036	0.043	0.051	0.064	0.083	0.100	0.109	0.115	0.118	0.124	0.127	0.128
0.6	0.000	0.009	0.017	0.028	0.032	0.039	0.050	0.065	0.080	0.088	0.093	0.096	0.102	0.105	0.106
0.8	0.000	0.005	0.010	0.017	0.020	0.024	0.031	0.042	0.053	0.059	0.063	0.066	0.071	0.074	0.075
1	0.000	0.003	0.007	0.011	0.013	0.016	0.020	0.028	0.036	0.041	0.045	0.047	0.052	0.054	0.055
1.2	0.000	0.002	0.004	0.007	0.009	0.011	0.014	0.019	0.025	0.030	0.033	0.035	0.039	0.041	0.042
1.4	0.000	0.002	0.003	0.005	0.006	0.007	0.010	0.014	0.018	0.022	0.024	0.026	0.030	0.032	0.033
1.5	0.000	0.001	0.003	0.004	0.005	0.006	0.008	0.012	0.016	0.019	0.021	0.023	0.026	0.028	0.029
1.6	0.000	0.001	0.002	0.004	0.004	0.005	0.007	0.010	00.14	0.016	0.019	0.020	0.023	0.025	0.026
1.8	0.000	0.001	0.002	0.003	0.003	0.004	0.005	0.008	0.010	0.013	0.014	0.016	0.019	0.020	0.021
2	0.000	0.001	0.001	0.002	0.002	0.003	0.004	0.006	0.008	0.010	0.011	0.012	0.015	0.017	0.018
2.5	0.000	0.000	0.001	0.001	0.001	0.002	0.002	0.003	0.005	0.006	0.007	0.007	0.009	0.011	0.012
3	0.000	0.000	0.000	0.001	0.001	0.001	0.001	0.002	0.003	0.004	0.004	0.005	0.006	0.008	0.008
4	0.000	0.000	0.000	0.000	0.000	0.000	0.001	0.001	0.001	0.002	0.002	0.002	0.003	0.004	0.005
5	0.000	0.000	0.000	0.000	0.000	0.000	0.000	0.000	0.001	0.001	0.001	0.001	0.002	0.003	0.003
10	0.000	0.000	0.000	0.000	0.000	0.000	0.000	0.000	0.000	0.000	0.000	0.000	0.000	0.000	0.001
15	0.000	0.000	0.000	0.000	0.000	0.000	0.000	0.000	0.000	0.000	0.000	0.000	0.000	0.000	0.000
20	0.000	0.000	0.000	0.000	0.000	0.000	0.000	0.000	0.000	0.000	0.000	0.000	0.000	0.000	0.000
50	0.000	0.000	0.000	0.000	0.000	0.000	0.000	0.000	0.000	0.000	0.000	0.000	0.000	0.000	0.000

(After Giroud)

Coefficient L_2

Depth: z/L for the corner, $2z/L$ for the centre	B/L = 0	0.1	0.2	1/3	0.4	0.5	2/3	1	1.5	2	2.5	3	5	10	∞
0	0.000	0.250	0.250	0.250	0.250	0.250	0.250	0.250	0.250	0.250	0.250	0.250	0.250	0.250	0.250
0.2	0.000	0.010	0.045	0.094	0.112	0.134	0.158	0.184	0.201	0.208	0.211	0.214	0.217	0.218	0.219
0.4	0.000	0.002	0.010	0.032	0.045	0.064	0.091	0.128	0.156	0.169	0.176	0.179	0.186	0.188	0.189
0.5	0.000	0.001	0.006	0.020	0.029	0.044	0.068	0.105	0.136	0.151	0.159	0.164	0.172	0.175	0.176
0.6	0.000	0.000	0.003	0.013	0.019	0.031	0.051	0.086	0.118	0.134	0.144	0.144	0.158	0.163	0.164
0.8	0.000	0.000	0.001	0.006	0.009	0.016	0.029	0.057	0.087	0.106	0.117	0.124	0.135	0.141	0.143
1	0.000	0.000	0.001	0.003	0.005	0.009	0.017	0.037	0.064	0.083	0.095	0.103	0.116	0.123	0.125
1.2	0.000	0.000	0.000	0.002	0.003	0.005	0.011	0.025	0.047	0.065	0.077	0.085	0.100	0.108	0.111
1.4	0.000	0.000	0.000	0.001	0.002	0.003	0.007	0.017	0.035	0.051	0.062	0.071	0.087	0.095	0.099
1.5	0.000	0.000	0.000	0.001	0.001	0.003	0.005	0.014	0.030	0.045	0.056	0.064	0.081	0.090	0.094
1.6	0.000	0.000	0.000	0.001	0.001	0.002	0.004	0.012	0.026	0.040	0.051	0.059	0.076	0.085	0.089
1.8	0.000	0.000	0.000	0.000	0.001	0.001	0.003	0.008	0.020	0.031	0.041	0.049	0.066	0.077	0.081
2	0.000	0.000	0.000	0.000	0.001	0.001	0.002	0.006	0.015	0.025	0.034	0.041	0.058	0.069	0.074
2.5	0.000	0.000	0.000	0.000	0.000	0.000	0.001	0.003	0.008	0.014	0.021	0.027	0.043	0.055	0.061
3	0.000	0.000	0.000	0.000	0.000	0.000	0.000	0.002	0.004	0.008	0.013	0.018	0.032	0.045	0.051
4	0.000	0.000	0.000	0.000	0.000	0.000	0.000	0.001	0.002	0.003	0.006	0.008	0.018	0.031	0.039
5	0.000	0.000	0.000	0.000	0.000	0.000	0.000	0.000	0.001	0.002	0.003	0.004	0.011	0.022	0.031
10	0.000	0.000	0.000	0.000	0.000	0.000	0.000	0.000	0.000	0.000	0.000	0.000	0.001	0.006	0.016
15	0.000	0.000	0.000	0.000	0.000	0.000	0.000	0.000	0.000	0.000	0.000	0.000	0.000	0.002	0.011
20	0.000	0.000	0.000	0.000	0.000	0.000	0.000	0.000	0.000	0.000	0.000	0.000	0.000	0.001	0.008
50	0.000	0.000	0.000	0.000	0.000	0.000	0.000	0.000	0.000	0.000	0.000	0.000	0.000	0.000	0.003

(After Giroud)

Coefficient L'_2

Depth: z/L for the corner, $2z/L$ for the centre	B/L = 0	0.1	0.2	1/3	0.4	0.5	2/3	1	1.5	2	2.5	3	5	10	∞
0	0.000	0.016	0.031	0.051	0.061	0.074	0.094	0.125	0.156	0.176	0.189	0.199	0.219	0.234	0.250
0.2	0.000	0.013	0.025	0.041	0.049	0.060	0.076	0.103	0.130	0.148	0.160	0.169	0.188	0.203	0.219
0.4	0.000	0.010	0.020	0.032	0.039	0.047	0.061	0.083	0.106	0.122	0.133	0.141	0.159	0.174	0.189
0.5	0.000	0.009	0.017	0.029	0.034	0.042	0.054	0.074	0.096	0.111	0.121	0.129	0.146	0.161	0.176
0.6	0.000	0.008	0.015	0.025	0.030	0.037	0.048	0.066	0.086	0.100	0.110	0.118	0.134	0.149	0.164
0.8	0.000	0.006	0.012	0.020	0.023	0.029	0.037	0.052	0.069	0.082	0.091	0.098	0.114	0.127	0.143
1	0.000	0.005	0.009	0.015	0.018	0.023	0.029	0.042	0.056	0.067	0.075	0.082	0.097	0.110	0.125
1.2	0.000	0.004	0.007	0.012	0.015	0.018	0.024	0.034	0.046	0.056	0.063	0.069	0.083	0.096	0.111
1.4	0.000	0.003	0.006	0.010	0.012	0.015	0.019	0.027	0.038	0.046	0.053	0.058	0.072	0.084	0.099
1.5	0.000	0.003	0.005	0.009	0.011	0.013	0.017	0.025	0.035	0.043	0.049	0.054	0.067	0.079	0.094
1.6	0.000	0.002	0.005	0.008	0.010	0.012	0.016	0.023	0.032	0.039	0.045	0.050	0.062	0.074	0.089
1.8	0.000	0.002	0.004	0.007	0.008	0.010	0.013	0.019	0.027	0.033	0.039	0.043	0.055	0.066	0.081
2	0.000	0.002	0.003	0.006	0.007	0.008	0.011	0.016	0.023	0.029	0.033	0.038	0.048	0.059	0.074
2.5	0.000	0.001	0.002	0.004	0.005	0.006	0.007	0.011	0.016	0.020	0.024	0.027	0.036	0.047	0.061
3	0.000	0.001	0.002	0.003	0.003	0.004	0.005	0.008	0.012	0.015	0.018	0.021	0.028	0.038	0.051
4	0.000	0.000	0.001	0.002	0.002	0.002	0.003	0.005	0.007	0.009	0.011	0.013	0.018	0.026	0.039
5	0.000	0.000	0.001	0.001	0.001	0.002	0.002	0.003	0.005	0.006	0.007	0.009	0.013	0.019	0.031
10	0.000	0.000	0.000	0.000	0.000	0.000	0.001	0.001	0.001	0.002	0.002	0.002	0.004	0.007	0.016
15	0.000	0.000	0.000	0.000	0.000	0.000	0.000	0.000	0.001	0.001	0.001	0.001	0.002	0.003	0.011
20	0.000	0.000	0.000	0.000	0.000	0.000	0.000	0.000	0.000	0.000	0.000	0.001	0.001	0.002	0.008
50	0.000	0.000	0.000	0.000	0.000	0.000	0.000	0.000	0.000	0.000	0.000	0.000	0.000	0.000	0.003

(After Giroud)

Coefficient M_0

Depth z/L \ B/L	0	0.1	0.2	1/3	0.4	0.5	2/3	1	1.5	2	2.5	3	5	10	∞
0	0.000	0.250	0.250	0.250	0.250	0.250	0.250	0.250	0.250	0.250	0.250	0.250	0.250	0.250	0.250
0.2	0.000	0.109	0.160	0.180	0.183	0.186	0.187	0.188	0.188	0.188	0.188	0.188	0.188	0.188	0.188
0.4	0.000	0.047	0.083	0.111	0.118	0.126	0.131	0.134	0.134	0.135	0.135	0.135	0.135	0.135	0.135
0.5	0.000	0.033	0.060	0.085	0.092	0.100	0.107	0.111	0.112	0.113	0.113	0.113	0.113	0.113	0.113
0.6	0.000	0.023	0.044	0.065	0.072	0.079	0.087	0.092	0.093	0.094	0.094	0.094	0.094	0.094	0.094
0.8	0.000	0.013	0.025	0.038	0.043	0.049	0.056	0.062	0.064	0.065	0.065	0.065	0.065	0.065	0.065
1	0.000	0.007	0.015	0.023	0.026	0.031	0.036	0.042	0.045	0.045	0.045	0.045	0.045	0.045	0.045
1.2	0.000	0.005	0.009	0.014	0.017	0.020	0.024	0.029	0.031	0.032	0.032	0.032	0.032	0.032	0.032
1.4	0.000	0.003	0.006	0.009	0.011	0.013	0.016	0.020	0.022	0.023	0.023	0.023	0.023	0.023	0.023
1.5	0.000	0.002	0.005	0.007	0.009	0.011	0.013	0.017	0.019	0.020	0.020	0.020	0.020	0.020	0.020
1.6	0.000	0.002	0.004	0.006	0.007	0.008	0.011	0.014	0.016	0.017	0.017	0.017	0.017	0.017	0.017
1.8	0.000	0.001	0.003	0.004	0.005	0.006	0.008	0.010	0.012	0.013	0.013	0.013	0.013	0.013	0.013
2	0.000	0.001	0.002	0.003	0.003	0.004	0.005	0.007	0.009	0.010	0.010	0.010	0.010	0.010	0.010
2.5	0.000	0.000	0.001	0.001	0.002	0.002	0.003	0.004	0.005	0.005	0.005	0.006	0.006	0.006	0.006
3	0.000	0.000	0.000	0.001	0.001	0.001	0.001	0.002	0.003	0.003	0.003	0.003	0.003	0.003	0.003
4	0.000	0.000	0.000	0.000	0.000	0.000	0.000	0.001	0.001	0.001	0.001	0.001	0.002	0.002	0.002
5	0.000	0.000	0.000	0.000	0.000	0.000	0.000	0.000	0.000	0.001	0.001	0.001	0.001	0.001	0.001
10	0.000	0.000	0.000	0.000	0.000	0.000	0.000	0.000	0.000	0.000	0.000	0.000	0.000	0.000	0.000
15	0.000	0.000	0.000	0.000	0.000	0.000	0.000	0.000	0.000	0.000	0.000	0.000	0.000	0.000	0.000
20	0.000	0.000	0.000	0.000	0.000	0.000	0.000	0.000	0.000	0.000	0.000	0.000	0.000	0.000	0.000
50	0.000	0.000	0.000	0.000	0.000	0.000	0.000	0.000	0.000	0.000	0.000	0.000	0.000	0.000	0.000

(After Giroud)

Coefficient M_1

Depth z/L for the corner, $2z/L$ for the centre \ B/L	0	0.1	0.2	1/3	0.4	0.5	2/3	1	1.5	2	2.5	3	5	10	∞
0	0.000	0.159	0.159	0.159	0.159	0.159	0.159	0.159	0.159	0.159	0.159	0.159	0.159	0.159	0.159
0.2	0.000	0.043	0.065	0.075	0.076	0.078	0.078	0.078	0.078	0.078	0.078	0.078	0.078	0.078	0.078
0.4	0.000	0.012	0.021	0.027	0.029	0.030	0.031	0.030	0.030	0.030	0.030	0.030	0.030	0.030	0.030
0.5	0.000	0.006	0.011	0.015	0.016	0.017	0.017	0.016	0.015	0.015	0.015	0.015	0.015	0.015	0.015
0.6	0.000	0.003	0.005	0.007	0.007	0.008	0.007	0.006	0.005	0.005	0.005	0.005	0.005	0.004	0.004
0.8	0.000	−0.000	−0.000	−0.001	−0.001	−0.002	−0.003	−0.004	−0.006	−0.006	−0.007	−0.007	−0.007	−0.007	−0.007
1	0.000	−0.001	−0.002	−0.003	−0.004	−0.005	−0.006	−0.008	−0.010	−0.011	−0.011	−0.011	−0.011	−0.011	−0.011
1.2	0.000	−0.001	−0.002	−0.004	−0.004	−0.005	−0.007	−0.009	−0.011	−0.011	−0.012	−0.012	−00.12	−0.012	−0.012
1.4	0.000	−0.001	−0.002	−0.003	−0.004	−0.005	−0.006	−0.008	−0.011	−0.011	−0.011	−0.012	−0.012	−0.012	−0.012
1.5	0.000	−0.001	−0.002	−0.003	−0.004	−0.004	−0.006	−0.008	−0.009	−0.010	−0.011	−0.011	−0.011	−0.011	−0.011
1.6	0.000	−0.001	−0.002	−0.003	−0.003	−0.004	−0.005	−0.007	−0.009	−0.010	−0.010	−0.011	−0.011	−0.011	−0.011
1.8	0.000	−0.001	−0.001	−0.002	−0.003	−0.003	−0.004	−0.006	−0.008	−0.009	−0.009	−0.009	−0.010	−0.010	−0.010
2	0.000	−0.001	−0.001	−0.002	−0.002	−0.003	−0.004	−0.005	−0.007	−0.007	−0.008	−0.008	−0.009	−0.009	−0.009
2.5	0.000	−0.000	−0.001	−0.001	−0.001	−0.002	−0.002	−0.003	−0.004	−0.005	−0.006	−0.006	−0.006	−0.006	−0.006
3	0.000	−0.000	−0.000	−0.001	−0.001	−0.001	−0.001	−0.002	−0.003	−0.004	−0.004	−0.004	−0.005	−0.005	−0.005
4	0.000	−0.000	−0.000	−0.000	−0.000	−0.001	−0.001	−0.001	−0.001	−0.002	−0.002	−0.002	−0.003	−0.003	−0.003
5	0.000	−0.000	−0.000	−0.000	−0.000	−0.000	−0.000	−0.001	−0.001	−0.001	−0.001	−0.001	−0.002	−0.002	−0.002
10	0.000	−0.000	−0.000	−0.000	−0.000	−0.000	−0.000	−0.000	−0.000	−0.000	−0.000	−0.000	−0.000	−0.000	−0.001
15	0.000	−0.000	−0.000	−0.000	−0.000	−0.000	−0.000	−0.000	−0.000	−0.000	−0.000	−0.000	−0.000	−0.000	−0.000
20	0.000	−0.000	−0.000	−0.000	−0.000	−0.000	−0.000	−0.000	−0.000	−0.000	−0.000	−0.000	−0.000	−0.000	−0.000
50	0.000	−0.000	−0.000	−0.000	−0.000	−0.000	−0.000	−0.000	−0.000	−0.000	−0.000	−0.000	−0.000	−0.000	−0.000

(After Giroud)

Coefficient M_2

Depth z/L	B/L = 0	0.1	0.2	1/3	0.4	0.5	2/3	1	1.5	2	2.5	3	5	10	∞
0	0.000	0.250	0.250	0.250	0.250	0.250	0.250	0.250	0.250	0.250	0.250	0.250	0.250	0.250	0.250
0.2	0.000	0.026	0.040	0.046	0.046	0.046	0.045	0.043	0.042	0.042	0.042	0.042	0.042	0.042	0.042
0.4	0.000	0.002	0.003	0.002	−0.001	−0.000	−0.002	−0.005	−0.007	−0.008	−0.008	−0.008	−0.008	−0.008	−0.008
0.5	0.000	−0.001	−0.002	−0.005	−0.006	−0.008	−0.010	−0.013	−0.015	−0.016	−0.016	−0.016	−0.016	−0.016	−0.016
0.6	0.000	−0.002	−0.004	−0.007	−0.009	−0.010	−0.013	−0.016	−0.018	−0.019	−0.019	−0.020	−0.020	−0.020	−0.020
0.8	0.000	−0.002	−0.005	−0.007	−0.009	−0.010	−0.013	−0.016	−0.018	−0.019	−0.019	−0.019	−0.019	−0.019	−0.019
1	0.000	−0.002	−0.003	−0.006	−0.007	−0.008	−0.010	−0.013	−0.015	−0.015	−0.016	−0.016	−0.016	−0.016	−0.016
1.2	0.000	−0.001	−0.002	−0.004	−0.005	−0.006	−0.007	−0.009	−0.011	−0.012	−0.012	−0.012	−0.013	−0.013	−0.013
1.4	0.000	−0.001	−0.002	−0.003	−0.003	−0.004	−0.005	−0.007	−0.008	−0.009	−0.009	−0.009	−0.010	−0.010	−0.010
1.5	0.000	−0.001	−0.001	−0.002	−0.003	−0.003	−0.004	−0.006	−0.007	−0.008	−0.008	−0.008	−0.008	−0.009	−0.009
1.6	0.000	−0.001	−0.001	−0.002	−0.002	−0.003	−0.004	−0.005	−0.006	−0.007	−0.007	−0.007	−0.007	−0.008	−0.008
1.8	0.000	−0.000	−0.001	−0.001	−0.002	−0.002	−0.003	−0.004	−0.005	−0.005	−0.005	−0.006	−0.006	−0.006	−0.006
2	0.000	−0.000	−0.001	−0.001	−0.001	−0.002	−0.002	−0.003	−0.003	−0.004	−0.004	−0.004	−0.005	−0.005	−0.005
2.5	0.000	−0.000	−0.000	−0.000	−0.001	−0.001	−0.001	−0.001	−0.002	−0.002	−0.002	−0.002	−0.003	−0.003	−0.003
3	0.000	−0.000	−0.000	−0.000	−0.000	−0.000	−0.001	−0.001	−0.001	−0.001	−0.001	−0.001	−0.002	−0.002	−0.002
4	0.000	−0.000	−0.000	−0.000	−0.000	−0.000	−0.000	−0.000	−0.000	−0.000	−0.001	−0.001	−0.001	−0.001	−0.001
5	0.000	−0.000	−0.000	−0.000	−0.000	−0.000	−0.000	−0.000	−0.000	−0.000	−0.000	−0.000	−0.000	−0.000	−0.000
10	0.000	−0.000	−0.000	−0.000	−0.000	−0.000	−0.000	−0.000	−0.000	−0.000	−0.000	−0.000	−0.000	−0.000	−0.000
15	0.000	−0.000	−0.000	−0.000	−0.000	−0.000	−0.000	−0.000	−0.000	−0.000	−0.000	−0.000	−0.000	−0.000	−0.000
20	0.000	−0.000	−0.000	−0.000	−0.000	−0.000	−0.000	−0.000	−0.000	−0.000	−0.000	−0.000	−0.000	−0.000	−0.000
50	0.000	−0.000	−0.000	−0.000	−0.000	−0.000	−0.000	−0.000	−0.000	−0.000	−0.000	−0.000	−0.000	−0.000	−0.000

(After Giroud)

Coefficient M_3

Depth z/L for the corner, $2z/L$ for the centre	B/L = 0	0.1	0.2	1/3	0.4	0.5	2/3	1	1.5	2	2.5	3	5	10	∞
0	0.000	∞	∞	∞	∞	∞	∞	∞	∞	∞	∞	∞	∞	∞	∞
0.2	0.000	0.013	0.017	0.012	0.008	0.002	−0.006	−0.015	−0.019	−0.020	−0.021	−0.021	−0.021	−0.021	−0.021
0.4	0.000	−0.006	−0.012	−0.020	−0.024	−0.028	−0.035	−0.042	−0.046	−0.047	−0.047	−0.048	−0.048	−0.048	−0.048
0.5	0.000	−0.006	−0.012	−0.019	−0.022	−0.026	−0.031	−0.037	−0.041	−0.042	−0.042	−0.043	−0.043	−0.043	−0.043
0.6	0.000	−0.005	−0.010	−0.015	−0.018	−0.021	−0.026	−0.031	−0.034	−0.035	−0.036	−0.036	−0.036	−0.036	−0.036
0.8	0.000	−0.003	−0.006	−0.009	−0.011	−0.013	−0.016	−0.020	−0.022	−0.023	−0.023	−0.023	−0.024	−0.024	−0.024
1	0.000	−0.002	−0.003	−0.005	−0.006	−0.008	−0.009	−0.012	−0.014	−0.014	−0.015	−0.015	−0.015	−0.015	−0.015
1.2	0.000	−0.001	−0.002	−0.003	−0.004	−0.004	−0.006	−0.007	−0.009	−0.009	−0.009	−0.010	−0.010	−0.001	−0.010
1.4	0.000	−0.001	−0.001	−0.002	−0.002	−0.003	−0.003	−0.004	−0.005	−0.006	−0.006	−0.006	−0.006	−0.006	−0.006
1.5	0.000	−0.001	−0.001	−0.001	−0.002	−0.002	−0.003	−0.004	−0.004	−0.005	−0.005	−0.005	−0.005	−0.005	−0.005
1.6	0.000	−0.000	0.001	−0.001	−0.001	−0.002	−0.002	−0.003	−0.004	−0.004	−0.004	−0.004	−0.004	−0.004	−0.004
1.8	0.000	−0.000	0.000	−0.001	−0.001	−0.001	−0.001	−0.002	−0.002	−0.003	−0.003	−0.003	−0.003	−0.003	−0.003
2	0.000	−0.000	0.000	−0.000	−0.001	−0.001	−0.001	−0.001	−0.002	−0.002	−0.002	−0.002	−0.002	−0.002	−0.002
2.5	0.000	−0.000	0.000	−0.000	−0.000	−0.000	−0.000	−0.000	−0.001	−0.001	−0.001	−0.001	−0.001	−0.001	−0.001
3	0.000	−0.000	−0.000	−0.000	−0.000	−0.000	−0.000	−0.000	−0.000	−0.000	−0.000	−0.000	−0.000	−0.000	−0.000
4	0.000	−0.000	−0.000	−0.000	−0.000	−0.000	−0.000	−0.000	−0.000	−0.000	−0.000	−0.000	−0.000	−0.000	−0.000
5	0.000	−0.000	−0.000	−0.000	−0.000	−0.000	−0.000	−0.000	−0.000	−0.000	−0.000	−0.000	−0.000	−0.000	−0.000
10	0.000	−0.000	−0.000	−0.000	−0.000	−0.000	−0.000	−0.000	−0.000	−0.000	−0.000	−0.000	−0.000	−0.000	−0.000
15	0.000	−0.000	0.000	−0.000	−0.000	−0.000	−0.000	−0.000	−0.000	−0.000	−0.000	−0.000	−0.000	−0.000	−0.000
20	0.000	−0.000	−0.000	−0.000	−0.000	−0.000	−0.000	−0.000	−0.000	−0.000	−0.000	−0.000	−0.000	−0.000	−0.000
50	0.000	−0.000	−0.000	−0.000	−0.000	−0.000	−0.000	−0.000	−0.000	−0.000	−0.000	−0.000	−0.000	−0.000	−0.000

(After Giroud)

Coefficient M_5

Depth (z/L for the corner, $2z/L$ for the centre)	B/L = 0	0.1	0.2	1/3	0.4	0.5	2/3	1	1.5	2	2.5	3	5	10	∞
0	0.000	∞	∞	∞	∞	∞	∞	∞	∞	∞	∞	∞	∞	∞	∞
0.2	0.000	0.003	0.015	0.031	0.036	0.042	0.046	0.045	0.040	0.036	0.034	0.032	0.030	0.029	0.028
0.4	0.000	0.000	0.001	0.004	0.006	0.007	0.008	0.006	0.002	-0.002	-0.004	-0.005	-0.008	-0.009	-0.009
0.5	0.000	0.000	0.001	0.002	0.002	0.003	0.003	0.001	-0.004	-0.007	-0.009	-0.010	-0.013	-0.014	-0.014
0.6	0.000	0.000	0.000	0.001	0.001	0.001	0.000	-0.002	-0.006	-0.009	-0.011	-0.012	-0.014	-0.015	-0.016
0.8	0.000	-0.000	-0.000	-0.000	-0.000	-0.000	-0.001	-0.003	-0.006	-0.009	-0.010	-0.012	-0.014	-0.015	-0.015
1	0.000	-0.000	-0.000	-0.000	-0.000	-0.000	-0.001	-0.002	-0.005	-0.007	-0.009	-0.010	-0.012	-0.013	-0.013
1.2	0.000	-0.000	-0.000	-0.000	-0.000	-0.000	-0.001	-0.002	-0.004	-0.005	-0.007	-0.008	-0.010	-0.011	-0.011
1.4	0.000	-0.000	-0.000	-0.000	-0.000	-0.000	-0.000	-0.001	-0.003	-0.004	-0.005	-0.006	-0.008	-0.009	-0.009
1.5	0.000	-0.000	-0.000	-0.000	-0.000	-0.000	-0.000	-0.001	-0.002	-0.003	-0.004	-0.005	-0.007	-0.008	-0.008
1.6	0.000	-0.000	-0.000	-0.000	-0.000	-0.000	-0.000	-0.001	-0.002	-0.003	-0.004	-0.005	-0.006	-0.007	-0.008
1.8	0.000	-0.000	-0.000	-0.000	-0.000	-0.000	-0.000	-0.001	-0.001	-0.002	-0.003	-0.004	-0.005	-0.006	-0.006
2	0.000	-0.000	-0.000	-0.000	-0.000	-0.000	-0.000	-0.000	-0.001	-0.002	-0.002	-0.003	-0.004	-0.005	-0.005
2.5	0.000	-0.000	-0.000	-0.000	-0.000	-0.000	-0.000	-0.000	-0.000	-0.001	-0.001	-0.002	-0.003	-0.003	-0.004
3	0.000	-0.000	-0.000	-0.000	-0.000	-0.000	-0.000	-0.000	-0.000	-0.000	-0.001	-0.001	-0.002	-0.002	-0.003
4	0.000	-0.000	-0.000	-0.000	-0.000	-0.000	-0.000	-0.000	-0.000	-0.000	-0.000	-0.000	-0.001	-0.001	-0.002
5	0.000	-0.000	-0.000	-0.000	-0.000	-0.000	-0.000	-0.000	-0.000	-0.000	-0.000	-0.000	-0.000	-0.001	-0.001
10	0.000	-0.000	-0.000	-0.000	-0.000	-0.000	-0.000	-0.000	-0.000	-0.000	-0.000	-0.000	-0.000	-0.000	-0.000
15	0.000	-0.000	-0.000	-0.000	-0.000	-0.000	-0.000	-0.000	-0.000	-0.000	-0.000	-0.000	-0.000	-0.000	-0.000
20	0.000	-0.000	-0.000	-0.000	-0.000	-0.000	-0.000	-0.000	-0.000	-0.000	-0.000	-0.000	-0.000	-0.000	-0.000
50	0.000	-0.000	-0.000	-0.000	-0.000	-0.000	-0.000	-0.000	-0.000	0.000	-0.000	-0.000	-0.000	-0.000	-0.000

(After Giroud)

Coefficient M'_2

Depth z/L	B/L = 0	0.1	0.2	1/3	0.4	0.5	2/3	1	1.5	2	2.5	3	5	10	∞
0	0.000	0.161	0.115	0.077	0.063	0.048	0.031	0.015	0.006	0.003	0.002	0.001	0.000	0.000	0.000
0.2	0.000	0.026	0.037	0.036	0.033	0.028	0.021	0.011	0.005	0.002	0.001	0.001	0.000	0.000	0.000
0.4	0.000	0.007	0.012	0.015	0.015	0.015	0.012	0.008	0.004	0.002	0.001	0.001	0.000	0.000	0.000
0.5	0.000	0.004	0.008	0.010	0.010	0.010	0.009	0.006	0.003	0.002	0.001	0.001	0.000	0.000	0.000
0.6	0.000	0.003	0.005	0.007	0.007	0.008	0.007	0.005	0.003	0.002	0.001	0.001	0.000	0.000	0.000
0.8	0.000	0.001	0.002	0.003	0.004	0.004	0.004	0.003	0.002	0.001	0.001	0.001	0.000	0.000	0.000
1	0.000	0.001	0.001	0.002	0.002	0.002	0.002	0.002	0.002	0.001	0.001	0.000	0.000	0.000	0.000
1.2	0.000	0.000	0.001	0.001	0.001	0.001	0.002	0.002	0.001	0.001	0.001	0.000	0.000	0.000	0.000
1.4	0.000	0.000	0.000	0.001	0.001	0.001	0.001	0.001	0.001	0.001	0.001	0.000	0.000	0.000	0.000
1.5	0.000	0.000	0.000	0.000	0.001	0.001	0.001	0.001	0.001	0.001	0.000	0.000	0.000	0.000	0.000
1.6	0.000	0.000	0.000	0.000	0.000	0.001	0.001	0.001	0.001	0.001	0.000	0.000	0.000	0.000	0.000
1.8	0.000	0.000	0.000	0.000	0.000	0.000	0.000	0.001	0.001	0.000	0.000	0.000	0.000	0.000	0.000
2	0.000	0.000	0.000	0.000	0.000	0.000	0.000	0.000	0.000	0.000	0.000	0.000	0.000	0.000	0.000
2.5	0.000	0.000	0.000	0.000	0.000	0.000	0.000	0.000	0.000	0.000	0.000	0.000	0.000	0.000	0.000
3	0.000	0.000	0.000	0.000	0.000	0.000	0.000	0.000	0.000	0.000	0.000	0.000	0.000	0.000	0.000
4	0.000	0.000	0.000	0.000	0.000	0.000	0.000	0.000	0.000	0.000	0.000	0.000	0.000	0.000	0.000
5	0.000	0.000	0.000	0.000	0.000	0.000	0.000	0.000	0.000	0.000	0.000	0.000	0.000	0.000	0.000
10	0.000	0.000	0.000	0.000	0.000	0.000	0.000	0.000	0.000	0.000	0.000	0.000	0.000	0.000	0.000
15	0.000	0.000	0.000	0.000	0.000	0.000	0.000	0.000	0.000	0.000	0.000	0.000	0.000	0.000	0.000
20	0.000	0.000	0.000	0.000	0.000	0.000	0.000	0.000	0.000	0.000	0.000	0.000	0.000	0.000	0.000
50	0.000	0.000	0.000	0.000	-0.000	0.000	0.000	0.000	0.000	0.000	0.000	0.000	0.000	0.000	0.000

(After Giroud)

Coefficient M'_3

Depth (z/L for the corner, $2z/L$ for the centre)	B/L														
	0	0.1	0.2	1/3	0.4	0.5	2/3	1	1.5	2	2.5	3	5	10	∞
0	0.000	0.080	0.043	0.017	0.009	0.001	−0.006	−0.009	−0.007	−0.005	−0.003	−0.001	−0.001	−0.000	0.000
0.2	0.000	0.004	0.005	0.001	−0.001	−0.003	−0.006	−0.007	−0.006	−0.004	−0.003	−0.002	−0.001	−0.000	0.000
0.4	0.000	−0.000	−0.001	−0.002	−0.003	−0.003	−0.004	−0.005	−0.004	−0.003	−0.003	−0.002	−0.001	−0.000	0.000
0.5	0.000	−0.001	−0.001	−0.002	−0.003	−0.003	−0.004	−0.004	−0.004	−0.003	−0.002	−0.002	−0.001	−0.000	0.000
0.6	0.000	−0.001	−0.001	−0.002	−0.002	−0.003	−0.003	−0.004	−0.003	−0.003	−0.002	−0.002	−0.001	−0.000	0.000
0.8	0.000	−0.000	−0.001	−0.001	−0.002	−0.002	−0.002	−0.003	−0.003	−0.002	−0.002	−0.001	−0.001	−0.000	0.000
1	0.000	−0.000	−0.001	−0.001	−0.001	−0.001	−0.002	−0.002	−0.002	−0.002	−0.002	−0.001	−0.001	−0.000	0.000
1.2	0.000	−0.000	−0.000	−0.001	−0.001	−0.001	−0.001	−0.002	−0.002	−0.002	−0.001	−0.001	−0.001	−0.000	0.000
1.4	0.000	−0.000	−0.000	−0.001	−0.001	−0.001	−0.001	−0.001	−0.001	−0.001	−0.001	−0.001	−0.001	−0.000	0.000
1.5	0.000	−0.000	−0.000	−0.000	−0.001	−0.001	−0.001	−0.001	−0.001	−0.001	−0.001	−0.001	−0.001	−0.000	0.000
1.6	0.000	−0.000	−0.000	−0.000	−0.000	−0.001	−0.001	−0.001	−0.001	−0.001	−0.001	−0.001	−0.001	−0.000	0.000
1.8	0.000	−0.000	−0.000	−0.000	−0.000	−0.000	−0.001	−0.001	−0.001	−0.001	−0.001	−0.001	−0.000	−0.000	0.000
2	0.000	−0.000	−0.000	−0.000	−0.000	−0.000	−0.000	−0.001	−0.001	−0.001	−0.001	−0.001	−0.000	−0.000	0.000
2.5	0.000	−0.000	−0.000	−0.000	−0.000	−0.000	−0.000	−0.000	−0.000	−0.000	−0.000	−0.000	−0.000	−0.000	0.000
3	0.000	−0.000	−0.000	−0.000	−0.000	−0.000	−0.000	−0.000	−0.000	−0.000	−0.000	−0.000	−0.000	−0.000	0.000
4	0.000	−0.000	−0.000	−0.000	−0.000	−0.000	−0.000	−0.000	−0.000	−0.000	−0.000	−0.000	−0.000	−0.000	−0.000
5	0.000	−0.000	−0.000	−0.000	−0.000	−0.000	−0.000	−0.000	−0.000	−0.000	−0.000	−0.000	−0.000	−0.000	0.000
10	0.000	−0.000	−0.000	−0.000	−0.000	−0.000	−0.000	−0.000	−0.000	−0.000	−0.000	−0.000	−0.000	−0.000	0.000
15	0.000	−0.000	−0.000	−0.000	−0.000	−0.000	−0.000	−0.000	−0.000	−0.000	−0.000	−0.000	−0.000	−0.000	0.000
20	0.000	−0.000	−0.000	−0.000	−0.000	−0.000	−0.000	−0.000	−0.000	−0.000	−0.000	−0.000	−0.000	−0.000	0.000
50	0.000	−0.000	−0.000	−0.000	−0.000	−0.000	−0.000	−0.000	−0.000	−0.000	−0.000	−0.000	−0.000	−0.000	0.000

(After Giroud)

Coefficient M'_5

Depth (z/L for the corner, $2z/L$ for the centre)	B/L														
	0	0.1	0.2	1/3	0.4	0.5	2/3	1	1.5	2	2.5	3	5	10	∞
0	0.000	∞	∞	∞	∞	∞	∞	∞	∞	∞	∞	∞	∞	∞	∞
0.2	0.000	0.016	0.028	0.038	0.041	0.044	0.045	0.043	0.038	0.035	0.033	0.032	0.030	0.029	0.028
0.4	0.000	0.002	0.004	0.006	0.006	0.006	0.006	0.003	−0.000	−0.003	−0.005	−0.006	−0.008	−0.009	−0.009
0.5	0.000	0.001	0.001	0.001	0.001	0.001	0.000	−0.002	−0.006	−0.008	−0.010	−0.011	−0.013	−0.014	−0.014
0.6	0.000	−0.000	−0.000	−0.001	−0.001	−0.002	−0.003	−0.005	−0.008	−0.010	−0.012	−0.013	−0.014	−0.015	−0.016
0.8	0.000	−0.001	−0.001	−0.002	−0.002	−0.003	−0.004	−0.006	−0.009	−0.010	−0.012	−0.012	−0.014	−0.015	−0.015
1	0.000	−0.001	−0.001	−0.002	−0.002	−0.003	−0.004	−0.005	−0.007	−0.009	−0.010	−0.011	−0.012	−0.013	−0.013
1.2	0.000	−0.000	−0.001	−0.002	−0.002	−0.002	−0.003	−0.004	−0.006	−0.007	−0.008	−0.009	−0.010	−0.011	−0.011
1.4	0.000	−0.000	−0.001	−0.001	−0.001	−0.002	−0.002	−0.003	−0.005	−0.006	−0.006	−0.007	−0.008	−0.009	−0.009
1.5	0.000	−0.000	−0.001	−0.001	−0.001	−0.002	−0.002	−0.003	−0.004	−0.005	−0.006	−0.006	−0.007	−0.008	−0.008
1.6	0.000	−0.000	−0.001	−0.001	−0.001	−0.001	−0.002	−0.003	−0.004	−0.004	−0.005	−0.006	−0.007	−0.007	−0.008
1.8	0.000	−0.000	−0.000	−0.001	−0.001	−0.001	−0.001	−0.002	−0.003	−0.004	−0.004	−0.005	−0.005	−0.006	−0.006
2	0.000	−0.000	−0.000	−0.001	−0.001	−0.001	−0.001	−0.002	−0.002	−0.003	−0.003	−0.004	−0.004	−0.005	−0.005
2.5	0.000	−0.000	−0.000	−0.000	−0.000	−0.001	−0.001	−0.001	−0.001	−0.002	−0.002	−0.002	−0.003	−0.003	−0.004
3	0.000	−0.000	−0.000	−0.000	−0.000	−0.000	−0.000	−0.001	−0.001	−0.001	−0.001	−0.002	−0.002	−0.002	−0.003
4	0.000	−0.000	−0.000	−0.000	−0.000	−0.000	−0.000	−0.000	−0.000	−0.001	−0.001	−0.001	−0.001	−0.001	−0.002
5	0.000	−0.000	−0.000	−0.000	−0.000	−0.000	−0.000	−0.000	−0.000	−0.000	−0.000	−0.000	−0.001	−0.001	−0.001
10	0.000	−0.000	−0.000	−0.000	−0.000	−0.000	−0.000	−0.000	−0.000	−0.000	−0.000	−0.000	−0.000	−0.000	−0.000
15	0.000	−0.000	−0.000	−0.000	−0.000	−0.000	−0.000	−0.000	−0.000	−0.000	−0.000	−0.000	−0.000	−0.000	−0.000
20	0.000	−0.000	−0.000	−0.000	−0.000	−0.000	−0.000	−0.000	−0.000	−0.000	−0.000	−0.000	−0.000	−0.000	−0.000
50	0.000	−0.000	−0.000	−0.000	−0.000	−0.000	−0.000	−0.000	−0.000	−0.000	−0.000	−0.000	−0.000	−0.000	−0.000

(After Giroud)

Coefficient N_2

Depth z/L	B/L = 0	0.1	0.2	1/3	0.4	0.5	2/3	1	1.5	2	2.5	3	5	10	∞
0	0.000	0.250	0.250	0.250	0.250	0.250	0.250	0.250	0.250	0.250	0.250	0.250	0.250	0.250	0.250
0.2	0.000	0.008	0.034	0.067	0.078	0.090	0.101	0.110	0.114	0.114	0.115	0.115	0.115	0.115	0.115
0.4	0.000	0.001	0.006	0.018	0.024	0.033	0.044	0.056	0.062	0.063	0.063	0.063	0.063	0.063	0.062
0.5	0.000	0.000	0.003	0.010	0.014	0.020	0.029	0.040	0.045	0.047	0.048	0.048	0.048	0.048	0.048
0.6	0.000	0.000	0.002	0.006	0.008	0.013	0.019	0.028	0.034	0.036	0.036	0.037	0.037	0.037	0.037
0.8	0.000	0.000	0.000	0.002	0.003	0.005	0.009	0.015	0.019	0.021	0.022	0.022	0.023	0.023	0.023
1	0.000	0.000	0.000	0.001	0.001	0.002	0.004	0.008	0.011	0.013	0.014	0.014	0.015	0.015	0.015
1.2	0.000	0.000	0.000	0.000	0.001	0.001	0.002	0.004	0.007	0.008	0.009	0.009	0.010	0.010	0.010
1.4	0.000	0.000	0.000	0.000	0.000	0.000	0.001	0.002	0.004	0.005	0.006	0.006	0.007	0.007	0.007
1.5	0.000	0.000	0.000	0.000	0.000	0.000	0.001	0.002	0.003	0.004	0.005	0.005	0.006	0.006	0.006
1.6	0.000	0.000	0.000	0.000	0.000	0.000	0.001	0.001	0.003	0.004	0.004	0.004	0.005	0.005	0.005
1.8	0.000	0.000	0.000	0.000	0.000	0.000	0.000	0.001	0.002	0.002	0.003	0.003	0.004	0.004	0.004
2	0.000	0.000	0.000	0.000	0.000	0.000	0.000	0.001	0.001	0.002	0.002	0.002	0.003	0.003	0.003
2.5	0.000	0.000	0.000	0.000	0.000	0.000	0.000	0.000	0.000	0.001	0.001	0.001	0.001	0.001	0.002
3	0.000	0.000	0.000	0.000	0.000	0.000	0.000	0.000	0.000	0.000	0.000	0.001	0.001	0.001	0.001
4	0.000	0.000	0.000	0.000	0.000	0.000	0.000	0.000	0.000	0.000	0.000	0.000	0.000	0.000	0.000
5	0.000	0.000	0.000	0.000	0.000	0.000	0.000	0.000	0.000	0.000	0.000	0.000	0.000	0.000	0.000
10	0.000	0.000	0.000	0.000	−0.000	0.000	0.000	0.000	0.000	0.000	0.000	0.000	0.000	0.000	0.000
15	0.000	0.000	0.000	0.000	0.000	−0.000	0.000	−0.000	0.000	0.000	0.000	0.000	0.000	0.000	0.000
20	0.000	0.000	0.000	0.000	0.000	0.000	0.000	0.000	0.000	0.000	0.000	0.000	0.000	0.000	0.000
50	0.000	0.000	0.000	0.000	0.000	0.000	−0.000	0.000	0.000	−0.000	0.000	0.000	0.000	0.000	0.000

(After Giroud)

Coefficient N_2'

Depth z/L	B/L = 0	0.1	0.2	1/3	0.4	0.5	2/3	1	1.5	2	2.5	3	5	10	∞
0	0.000	0.039	0.135	0.173	0.187	0.202	0.219	0.235	0.244	0.247	0.248	0.249	0.250	0.250	0.250
0.2	0.000	0.022	0.042	0.062	0.070	0.079	0.091	0.103	0.110	0.112	0.113	0.114	0.115	0.115	0.115
0.4	0.000	0.009	0.018	0.028	0.033	0.038	0.045	0.054	0.059	0.061	0.062	0.063	0.063	0.063	0.063
0.5	0.000	0.006	0.013	0.020	0.023	0.027	0.033	0.040	0.044	0.046	0.047	0.047	0.048	0.048	0.048
0.6	0.000	0.005	0.009	0.014	0.017	0.020	0.024	0.029	0.033	0.035	0.036	0.036	0.037	0.037	0.037
0.8	0.000	0.002	0.005	0.008	0.009	0.011	0.013	0.017	0.020	0.021	0.022	0.022	0.023	0.023	0.023
1	0.000	0.001	0.003	0.004	0.005	0.006	0.008	0.010	0.012	0.013	0.014	0.014	0.015	0.015	0.015
1.2	0.000	0.001	0.002	0.003	0.003	0.004	0.005	0.006	0.008	0.009	0.009	0.009	0.010	0.010	0.010
1.4	0.000	0.000	0.001	0.002	0.002	0.002	0.003	0.004	0.005	0.006	0.006	0.006	0.007	0.007	0.007
1.5	0.000	0.000	0.001	0.001	0.002	0.002	0.002	0.003	0.004	0.005	0.005	0.005	0.006	0.006	0.006
1.6	0.000	0.000	0.001	0.001	0.001	0.001	0.002	0.003	0.003	0.004	0.004	0.004	0.005	0.005	0.005
1.8	0.000	0.000	0.000	0.001	0.001	0.001	0.001	0.002	0.002	0.003	0.003	0.003	0.004	0.004	0.004
2	0.000	0.000	0.000	0.000	0.001	0.001	0.001	0.001	0.002	0.002	0.002	0.002	0.003	0.003	0.003
2.5	0.000	0.000	0.000	0.000	0.000	0.000	0.000	0.001	0.001	0.001	0.001	0.001	0.001	0.001	0.002
3	0.000	0.000	0.000	0.000	0.000	0.000	0.000	0.000	0.000	0.001	0.001	0.001	0.001	0.001	0.001
4	0.000	0.000	0.000	0.000	0.000	0.000	0.000	0.000	0.000	0.000	0.000	0.000	0.000	0.000	0.000
5	0.000	0.000	0.000	0.000	0.000	0.000	0.000	0.000	0.000	0.000	0.000	0.000	0.000	0.000	0.000
10	0.000	0.000	0.000	0.000	0.000	0.000	0.000	0.000	0.000	0.000	0.000	0.000	0.000	0.000	0.000
15	0.000	0.000	0.000	0.000	0.000	0.000	0.000	0.000	0.000	0.000	0.000	0.000	0.000	0.000	−0.000
20	0.000	0.000	0.000	0.000	0.000	0.000	0.000	0.000	0.000	0.000	0.000	0.000	0.000	0.000	−0.000
50	0.000	0.000	0.000	0.000	0.000	0.000	−0.000	0.000	0.000	−0.000	0.000	0.000	0.000	0.000	−0.000

(After Giroud)

APPENDIX B – Charts for Uniformly Loaded Arc-Shaped Areas

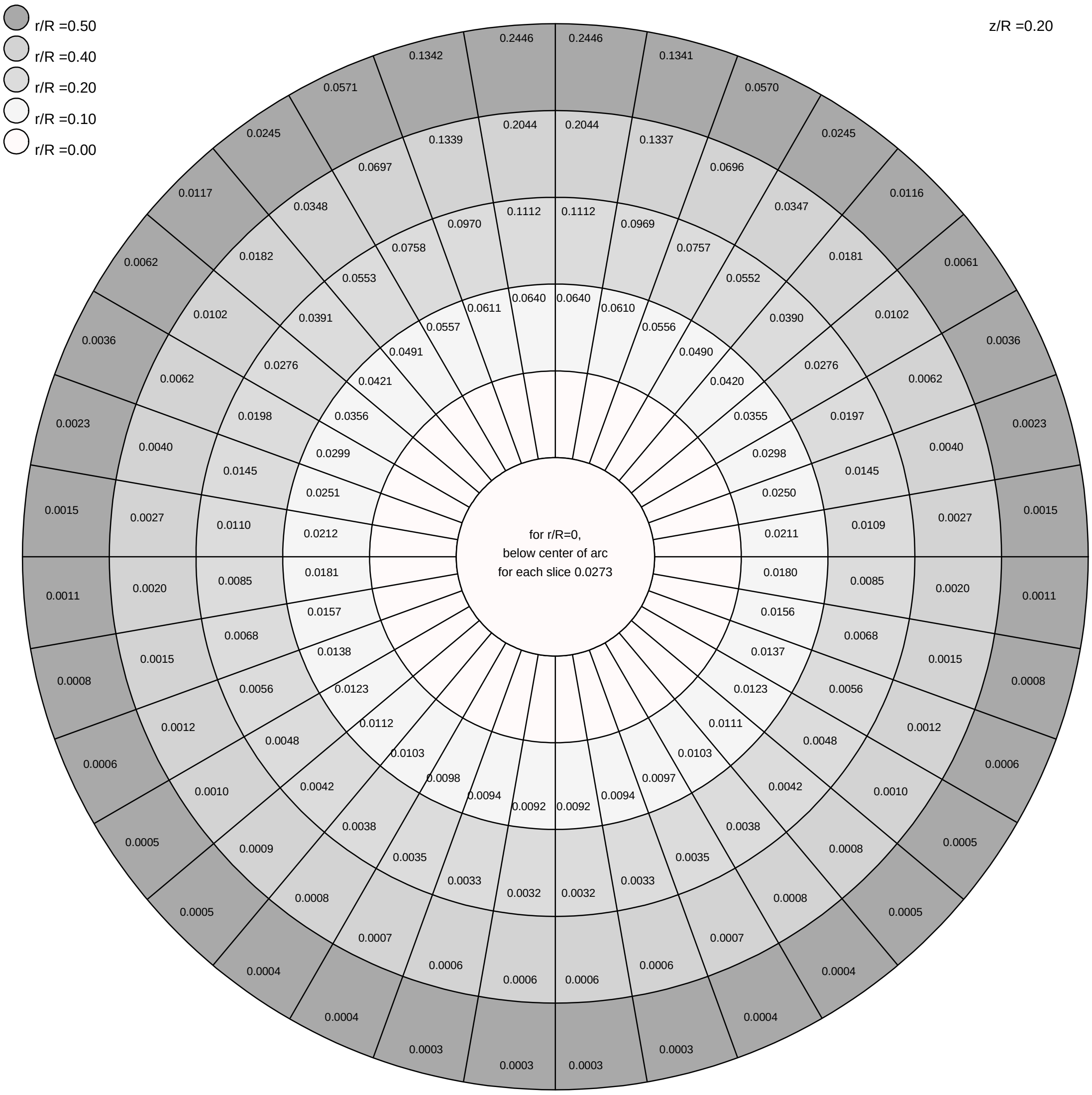

r/R =0.50
r/R =0.40
r/R =0.20
r/R =0.10
r/R =0.00
z/R =0.20
for r/R=0,
below center of arc
for each slice 0.0273
0.2446 0.1341 0.0570 0.0245 0.0116 0.0061 0.0036 0.0023 0.0015 0.0011 0.0008 0.0006 0.0005 0.0005 0.0004 0.0004 0.0003 0.0003
0.0003 0.0003 0.0004 0.0004 0.0005 0.0005 0.0006 0.0008 0.0011 0.0015 0.0023 0.0036 0.0062 0.0117 0.0245 0.0571 0.1342 0.2446
0.2044 0.1337 0.0696 0.0347 0.0181 0.0102 0.0062 0.0040 0.0027 0.0020 0.0015 0.0012 0.0010 0.0008 0.0008 0.0007 0.0006 0.0006
0.0006 0.0006 0.0007 0.0008 0.0009 0.0010 0.0012 0.0015 0.0020 0.0027 0.0040 0.0062 0.0102 0.0182 0.0348 0.0697 0.1339 0.2044
0.1112 0.0969 0.0757 0.0552 0.0390 0.0276 0.0197 0.0145 0.0109 0.0085 0.0068 0.0056 0.0048 0.0042 0.0038 0.0035 0.0033 0.0032
0.0032 0.0033 0.0035 0.0038 0.0042 0.0048 0.0056 0.0068 0.0085 0.0110 0.0145 0.0198 0.0276 0.0391 0.0553 0.0758 0.0970 0.1112
0.0640 0.0610 0.0556 0.0490 0.0420 0.0355 0.0298 0.0250 0.0211 0.0180 0.0156 0.0137 0.0123 0.0111 0.0103 0.0097 0.0094 0.0092
0.0092 0.0094 0.0098 0.0103 0.0112 0.0123 0.0138 0.0157 0.0181 0.0212 0.0251 0.0299 0.0356 0.0421 0.0491 0.0557 0.0611 0.0640

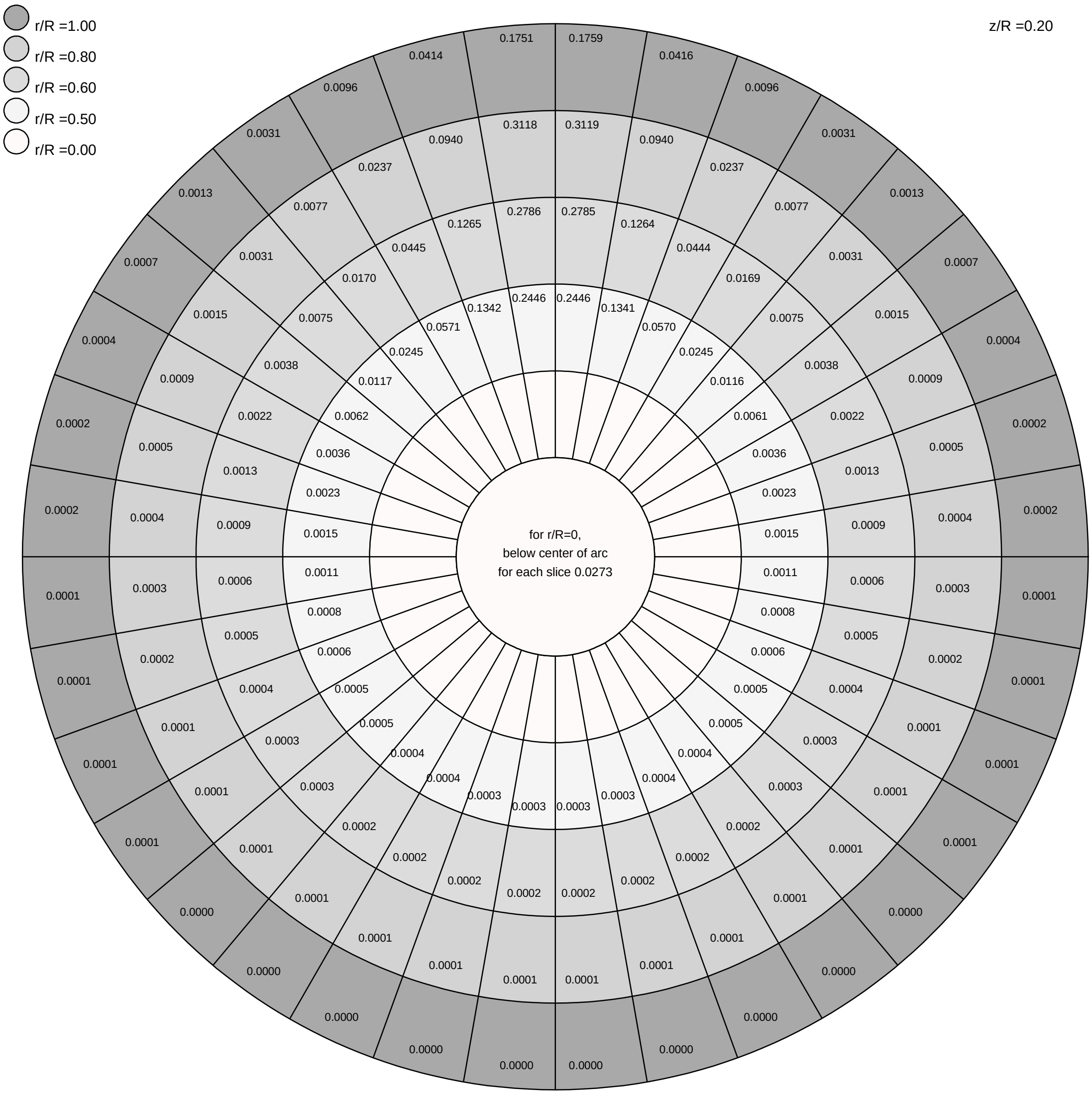

r/R =1.00
r/R =0.80
r/R =0.60
r/R =0.50
r/R =0.00
z/R =0.20
for r/R=0,
below center of arc
for each slice 0.0273
0.1751
0.1759
0.0414
0.0416
0.0096
0.0096
0.0031
0.0031
0.0013
0.0013
0.0007
0.0007
0.0004
0.0004
0.0002
0.0002
0.0002
0.0002
0.0001
0.0001
0.0001
0.0001
0.0001
0.0001
0.0001
0.0001
0.0001
0.0001
0.0000
0.0000
0.0000
0.0000
0.0000
0.0000
0.0000
0.0000
0.0000
0.0000
0.3118
0.3119
0.0940
0.0940
0.0237
0.0237
0.0077
0.0077
0.0031
0.0031
0.0015
0.0015
0.0009
0.0009
0.0005
0.0005
0.0004
0.0004
0.0003
0.0003
0.0002
0.0002
0.0001
0.0001
0.0001
0.0001
0.0001
0.0001
0.0001
0.0001
0.0001
0.0001
0.0001
0.0001
0.0001
0.0001
0.2786
0.2785
0.1265
0.1264
0.0445
0.0444
0.0170
0.0169
0.0075
0.0075
0.0038
0.0038
0.0022
0.0022
0.0013
0.0013
0.0009
0.0009
0.0006
0.0006
0.0005
0.0005
0.0004
0.0004
0.0003
0.0003
0.0003
0.0003
0.0002
0.0002
0.0002
0.0002
0.0002
0.0002
0.0002
0.0002
0.2446
0.2446
0.1342
0.1341
0.0571
0.0570
0.0245
0.0245
0.0117
0.0116
0.0062
0.0061
0.0036
0.0036
0.0023
0.0023
0.0015
0.0015
0.0011
0.0011
0.0008
0.0008
0.0006
0.0006
0.0005
0.0005
0.0005
0.0005
0.0004
0.0004
0.0004
0.0004
0.0003
0.0003
0.0003
0.0003

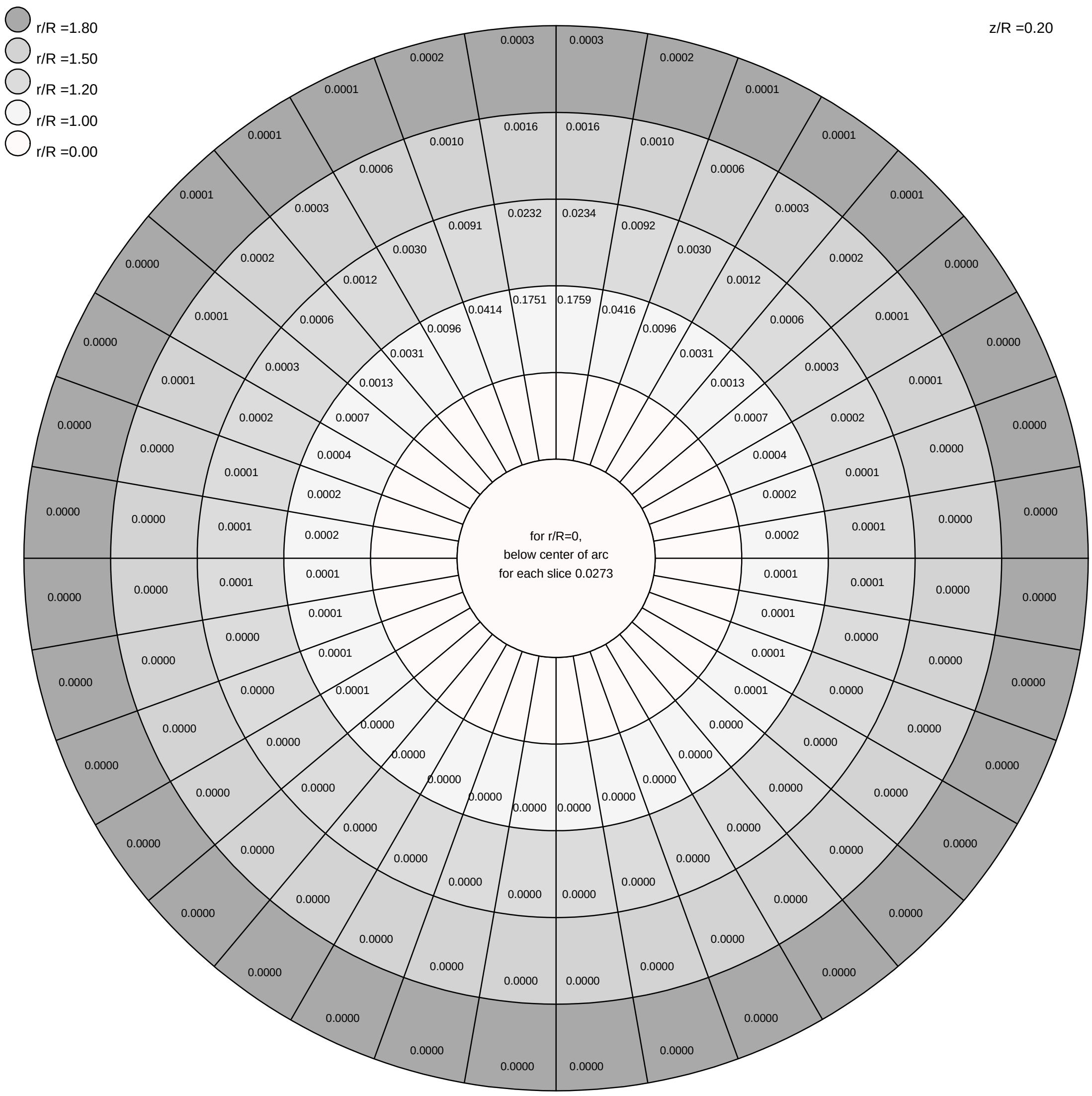
r/R =1.80
r/R =1.50
r/R =1.20
r/R =1.00
r/R =0.00
z/R =0.20
for r/R=0,
below center of arc
for each slice 0.0273

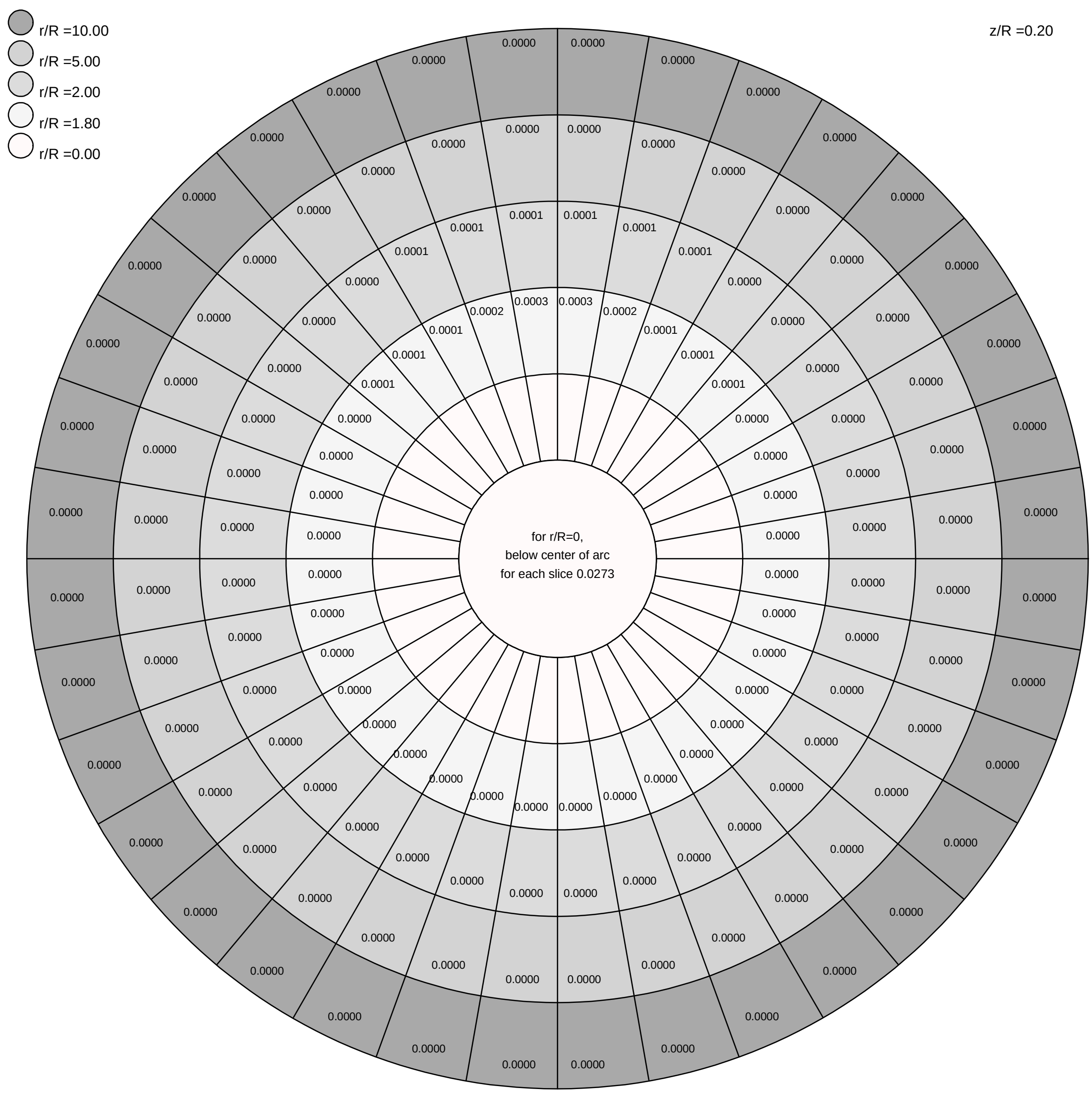
r/R =10.00
r/R =5.00
r/R =2.00
r/R =1.80
r/R =0.00
z/R =0.20
for r/R=0,
below center of arc
for each slice 0.0273

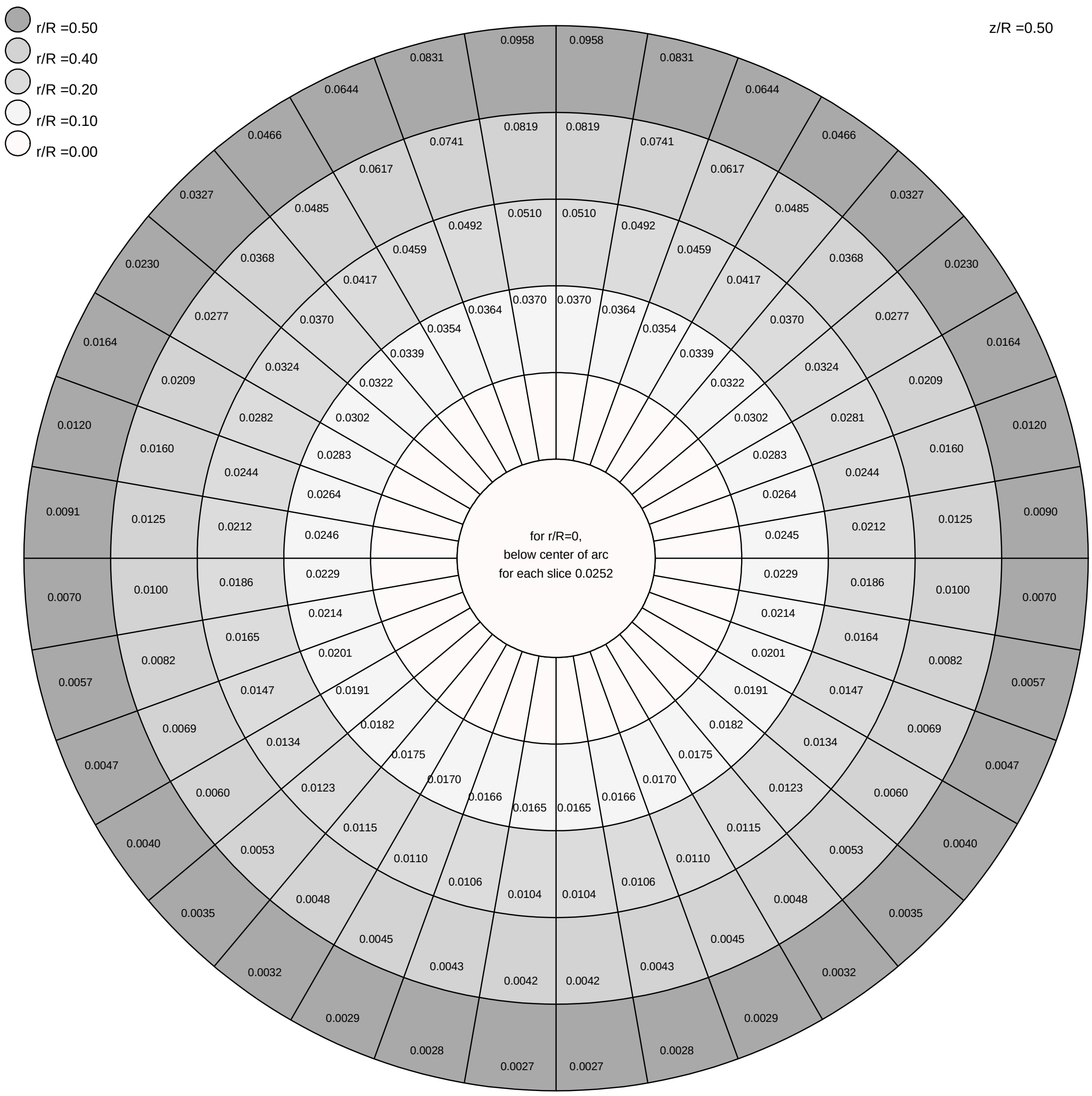

r/R =0.50
r/R =0.40
r/R =0.20
r/R =0.10
r/R =0.00
z/R =0.50
0.0958 0.0831 0.0644 0.0466 0.0327 0.0230 0.0164 0.0120 0.0090 0.0070 0.0057 0.0047 0.0040 0.0035 0.0032 0.0029 0.0028 0.0027
0.0958 0.0831 0.0644 0.0466 0.0327 0.0230 0.0164 0.0120 0.0091 0.0070 0.0057 0.0047 0.0040 0.0035 0.0032 0.0029 0.0028 0.0027
0.0819 0.0741 0.0617 0.0485 0.0368 0.0277 0.0209 0.0160 0.0125 0.0100 0.0082 0.0069 0.0060 0.0053 0.0048 0.0045 0.0043 0.0042
0.0819 0.0741 0.0617 0.0485 0.0368 0.0277 0.0209 0.0160 0.0125 0.0100 0.0082 0.0069 0.0060 0.0053 0.0048 0.0045 0.0043 0.0042
0.0510 0.0492 0.0459 0.0417 0.0370 0.0324 0.0281 0.0244 0.0212 0.0186 0.0164 0.0147 0.0134 0.0123 0.0115 0.0110 0.0106 0.0104
0.0510 0.0492 0.0459 0.0417 0.0370 0.0324 0.0282 0.0244 0.0212 0.0186 0.0165 0.0147 0.0134 0.0123 0.0115 0.0110 0.0106 0.0104
0.0370 0.0364 0.0354 0.0339 0.0322 0.0302 0.0283 0.0264 0.0245 0.0229 0.0214 0.0201 0.0191 0.0182 0.0175 0.0170 0.0166 0.0165
0.0370 0.0364 0.0354 0.0339 0.0322 0.0302 0.0283 0.0264 0.0246 0.0229 0.0214 0.0201 0.0191 0.0182 0.0175 0.0170 0.0166 0.0165
for r/R=0,
below center of arc
for each slice 0.0252

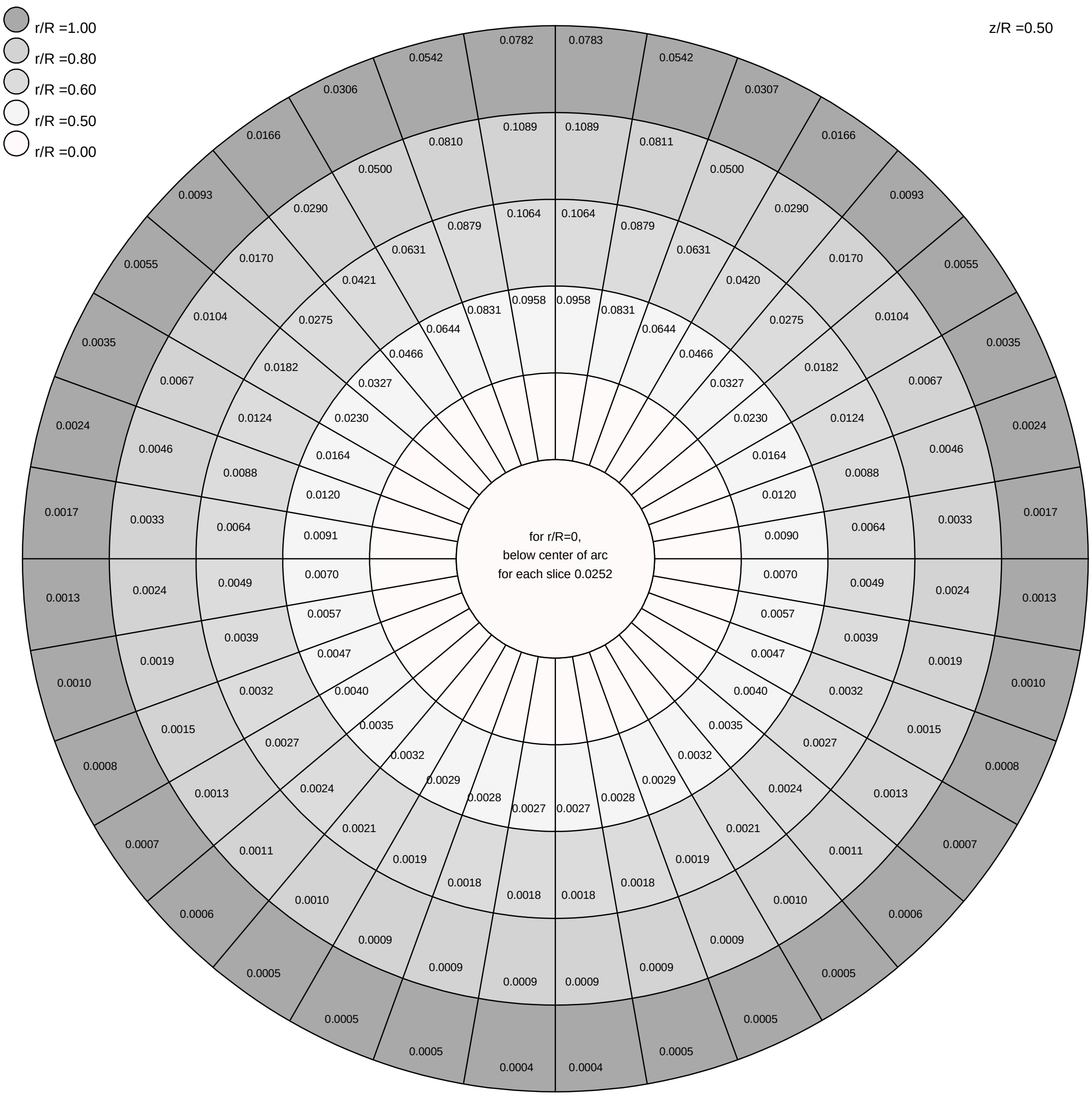
r/R =1.00
r/R =0.80
r/R =0.60
r/R =0.50
r/R =0.00
z/R =0.50
for r/R=0,
below center of arc
for each slice 0.0252
0.0017 0.0024 0.0035 0.0055 0.0093 0.0166 0.0306 0.0542 0.0782 0.0783 0.0542 0.0307 0.0166 0.0093 0.0055 0.0035 0.0024 0.0017
0.0013 0.0010 0.0008 0.0007 0.0006 0.0005 0.0005 0.0005 0.0004 0.0004 0.0005 0.0005 0.0005 0.0006 0.0007 0.0008 0.0010 0.0013
0.0033 0.0046 0.0067 0.0104 0.0170 0.0290 0.0500 0.0810 0.1089 0.1089 0.0811 0.0500 0.0290 0.0170 0.0104 0.0067 0.0046 0.0033
0.0024 0.0019 0.0015 0.0013 0.0011 0.0010 0.0009 0.0009 0.0009 0.0009 0.0009 0.0009 0.0010 0.0011 0.0013 0.0015 0.0019 0.0024
0.0064 0.0088 0.0124 0.0182 0.0275 0.0421 0.0631 0.0879 0.1064 0.1064 0.0879 0.0631 0.0420 0.0275 0.0182 0.0124 0.0088 0.0064
0.0049 0.0039 0.0032 0.0027 0.0024 0.0021 0.0019 0.0018 0.0018 0.0018 0.0018 0.0019 0.0021 0.0024 0.0027 0.0032 0.0039 0.0049
0.0091 0.0120 0.0164 0.0230 0.0327 0.0466 0.0644 0.0831 0.0958 0.0958 0.0831 0.0644 0.0466 0.0327 0.0230 0.0164 0.0120 0.0090
0.0070 0.0057 0.0047 0.0040 0.0035 0.0032 0.0029 0.0028 0.0027 0.0027 0.0028 0.0029 0.0032 0.0035 0.0040 0.0047 0.0057 0.0070

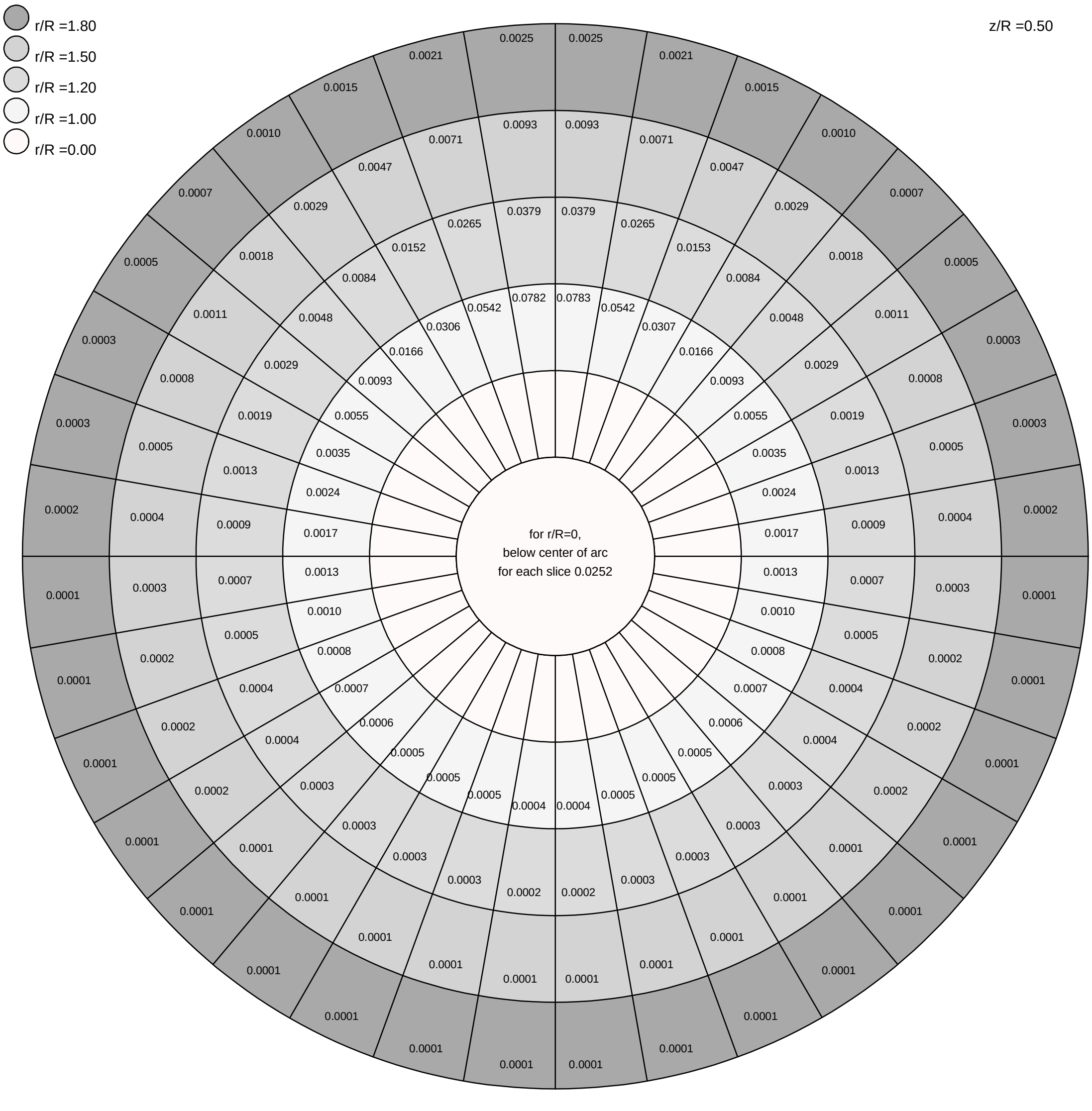
r/R =1.80
r/R =1.50
r/R =1.20
r/R =1.00
r/R =0.00
z/R =0.50
for r/R=0,
below center of arc
for each slice 0.0252
0.0025
0.0025
0.0021
0.0021
0.0015
0.0015
0.0010
0.0010
0.0007
0.0007
0.0005
0.0005
0.0003
0.0003
0.0003
0.0003
0.0002
0.0002
0.0093
0.0093
0.0071
0.0071
0.0047
0.0047
0.0029
0.0029
0.0018
0.0018
0.0011
0.0011
0.0008
0.0008
0.0005
0.0005
0.0004
0.0004
0.0379
0.0379
0.0265
0.0265
0.0152
0.0153
0.0084
0.0084
0.0048
0.0048
0.0029
0.0029
0.0019
0.0019
0.0013
0.0013
0.0009
0.0009
0.0782
0.0783
0.0542
0.0542
0.0306
0.0307
0.0166
0.0166
0.0093
0.0093
0.0055
0.0055
0.0035
0.0035
0.0024
0.0024
0.0017
0.0017

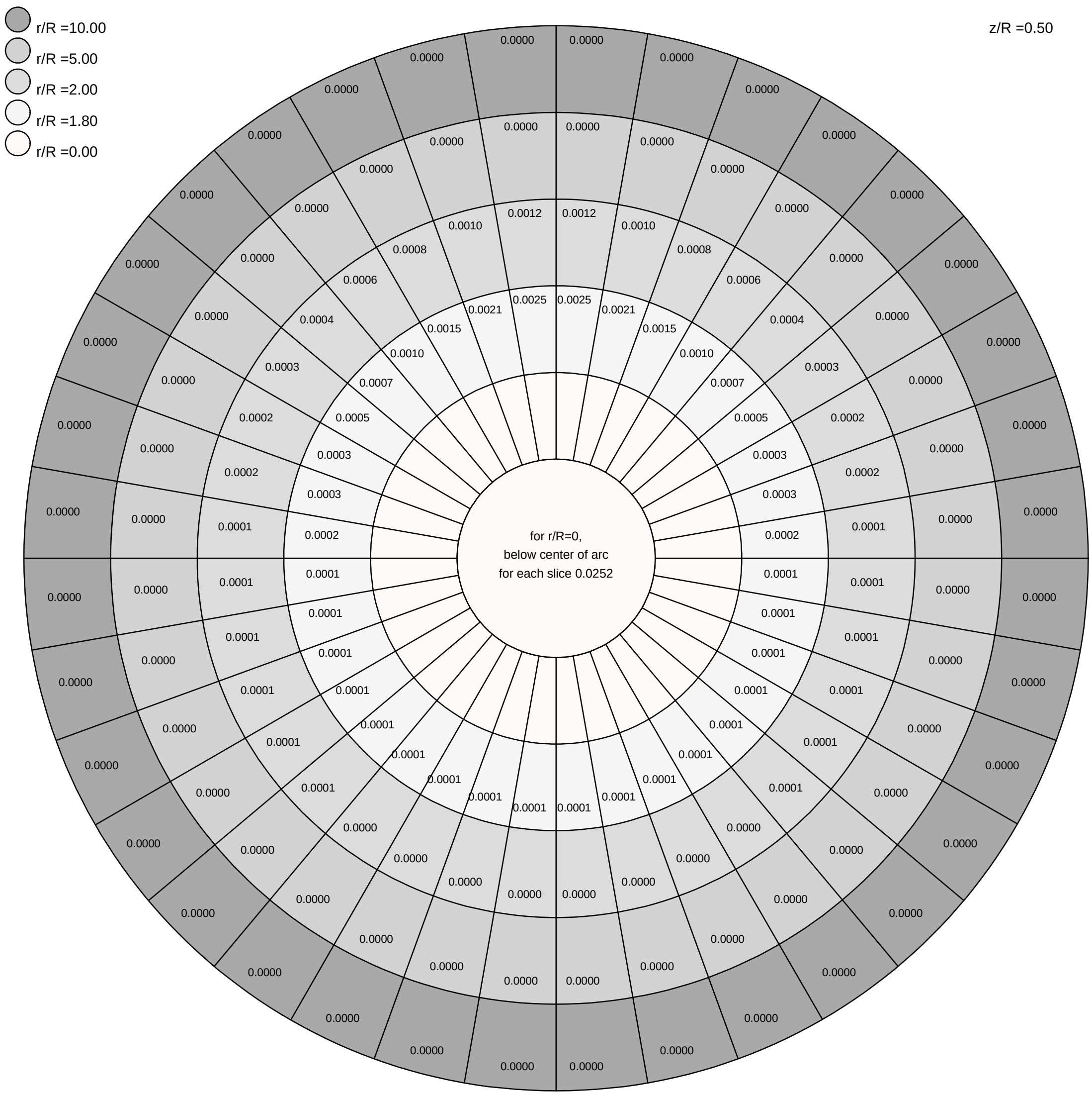
r/R =10.00
r/R =5.00
r/R =2.00
r/R =1.80
r/R =0.00
z/R =0.50
for r/R=0,
below center of arc
for each slice 0.0252

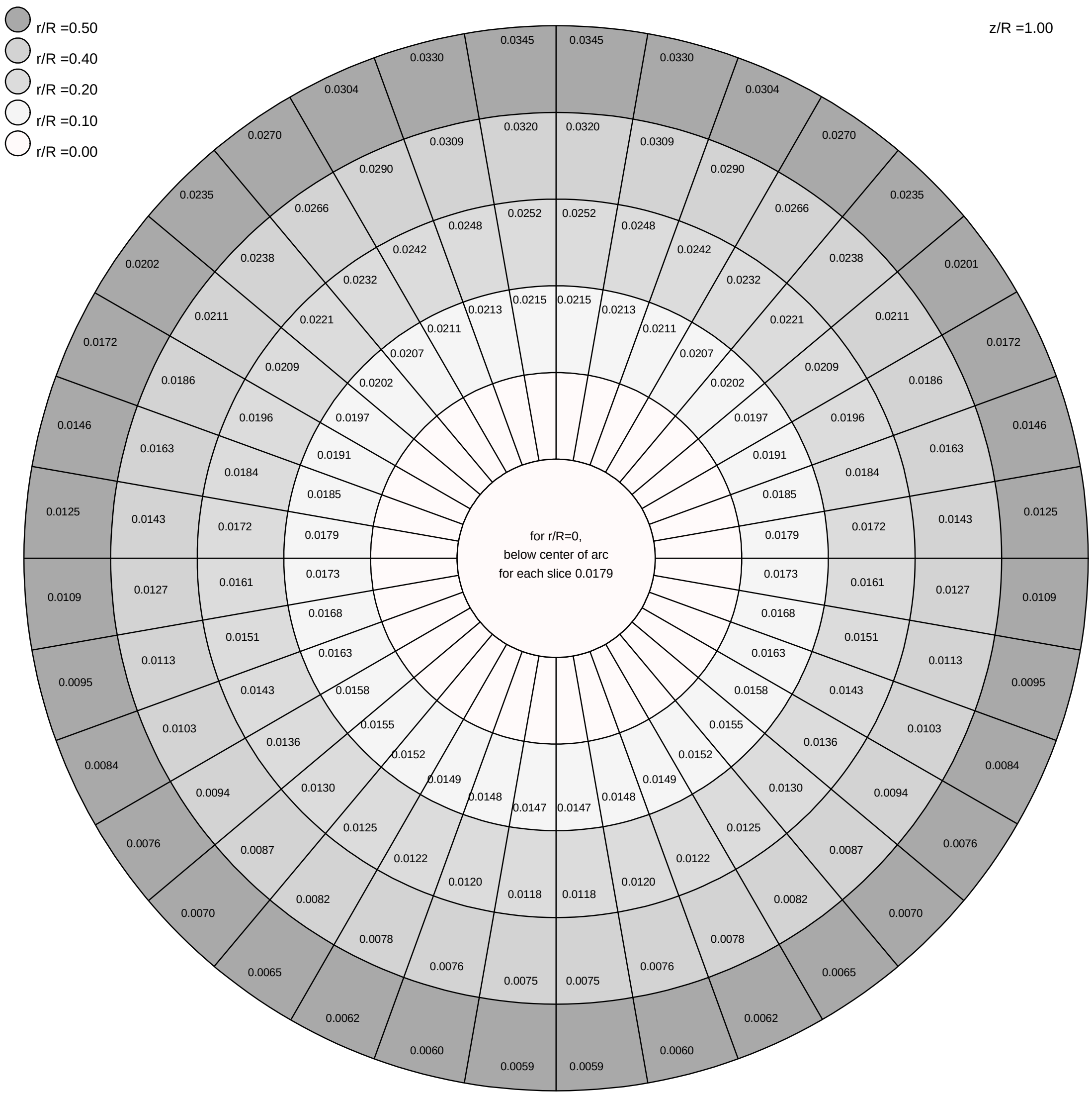
r/R =0.50
r/R =0.40
r/R =0.20
r/R =0.10
r/R =0.00
z/R =1.00
for r/R=0,
below center of arc
for each slice 0.0179
0.0345 0.0330 0.0304 0.0270 0.0235 0.0201 0.0172 0.0146 0.0125 0.0109 0.0095 0.0084 0.0076 0.0070 0.0065 0.0062 0.0060 0.0059
0.0345 0.0330 0.0304 0.0270 0.0235 0.0202 0.0172 0.0146 0.0125 0.0109 0.0095 0.0084 0.0076 0.0070 0.0065 0.0062 0.0060 0.0059
0.0320 0.0309 0.0290 0.0266 0.0238 0.0211 0.0186 0.0163 0.0143 0.0127 0.0113 0.0103 0.0094 0.0087 0.0082 0.0078 0.0076 0.0075
0.0320 0.0309 0.0290 0.0266 0.0238 0.0211 0.0186 0.0163 0.0143 0.0127 0.0113 0.0103 0.0094 0.0087 0.0082 0.0078 0.0076 0.0075
0.0252 0.0248 0.0242 0.0232 0.0221 0.0209 0.0196 0.0184 0.0172 0.0161 0.0151 0.0143 0.0136 0.0130 0.0125 0.0122 0.0120 0.0118
0.0252 0.0248 0.0242 0.0232 0.0221 0.0209 0.0196 0.0184 0.0172 0.0161 0.0151 0.0143 0.0136 0.0130 0.0125 0.0122 0.0120 0.0118
0.0215 0.0213 0.0211 0.0207 0.0202 0.0197 0.0191 0.0185 0.0179 0.0173 0.0168 0.0163 0.0158 0.0155 0.0152 0.0149 0.0148 0.0147
0.0215 0.0213 0.0211 0.0207 0.0202 0.0197 0.0191 0.0185 0.0179 0.0173 0.0168 0.0163 0.0158 0.0155 0.0152 0.0149 0.0148 0.0147

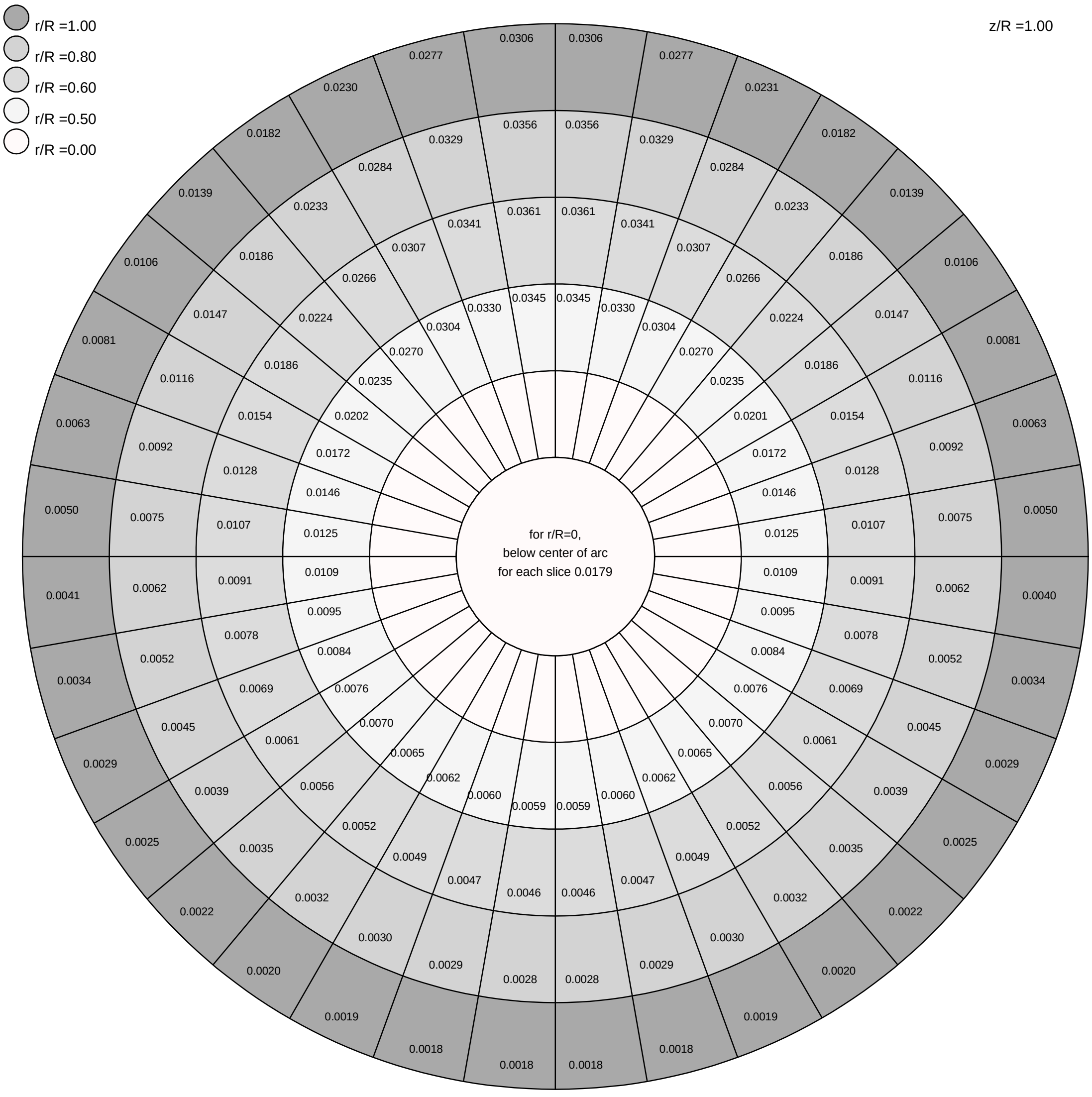
r/R =1.00
r/R =0.80
r/R =0.60
r/R =0.50
r/R =0.00
z/R =1.00
for r/R=0,
below center of arc
for each slice 0.0179

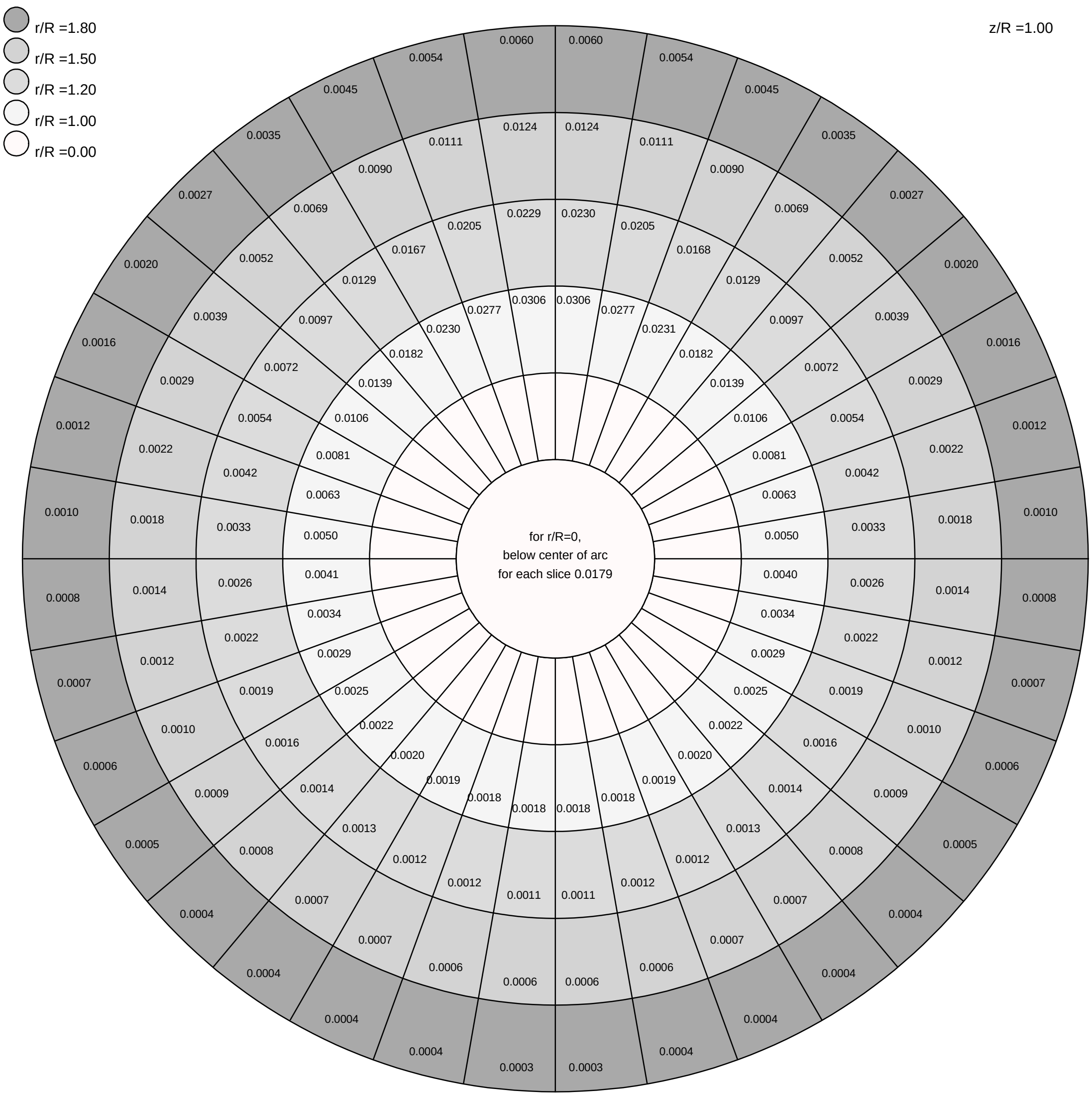
r/R =1.80
r/R =1.50
r/R =1.20
r/R =1.00
r/R =0.00
z/R =1.00
0.0060 0.0054 0.0045 0.0035 0.0027 0.0020 0.0016 0.0012 0.0010 0.0008 0.0007 0.0006 0.0005 0.0004 0.0004 0.0004 0.0004 0.0003
0.0060 0.0054 0.0045 0.0035 0.0027 0.0020 0.0016 0.0012 0.0010 0.0008 0.0007 0.0006 0.0005 0.0004 0.0004 0.0004 0.0004 0.0003
0.0124 0.0111 0.0090 0.0069 0.0052 0.0039 0.0029 0.0022 0.0018 0.0014 0.0012 0.0010 0.0009 0.0008 0.0007 0.0007 0.0006 0.0006
0.0124 0.0111 0.0090 0.0069 0.0052 0.0039 0.0029 0.0022 0.0018 0.0014 0.0012 0.0010 0.0009 0.0008 0.0007 0.0007 0.0006 0.0006
0.0230 0.0205 0.0168 0.0129 0.0097 0.0072 0.0054 0.0042 0.0033 0.0026 0.0022 0.0019 0.0016 0.0014 0.0013 0.0012 0.0012 0.0011
0.0229 0.0205 0.0167 0.0129 0.0097 0.0072 0.0054 0.0042 0.0033 0.0026 0.0022 0.0019 0.0016 0.0014 0.0013 0.0012 0.0012 0.0011
0.0306 0.0277 0.0231 0.0182 0.0139 0.0106 0.0081 0.0063 0.0050 0.0040 0.0034 0.0029 0.0025 0.0022 0.0020 0.0019 0.0018 0.0018
0.0306 0.0277 0.0230 0.0182 0.0139 0.0106 0.0081 0.0063 0.0050 0.0041 0.0034 0.0029 0.0025 0.0022 0.0020 0.0019 0.0018 0.0018
for r/R=0,
below center of arc
for each slice 0.0179

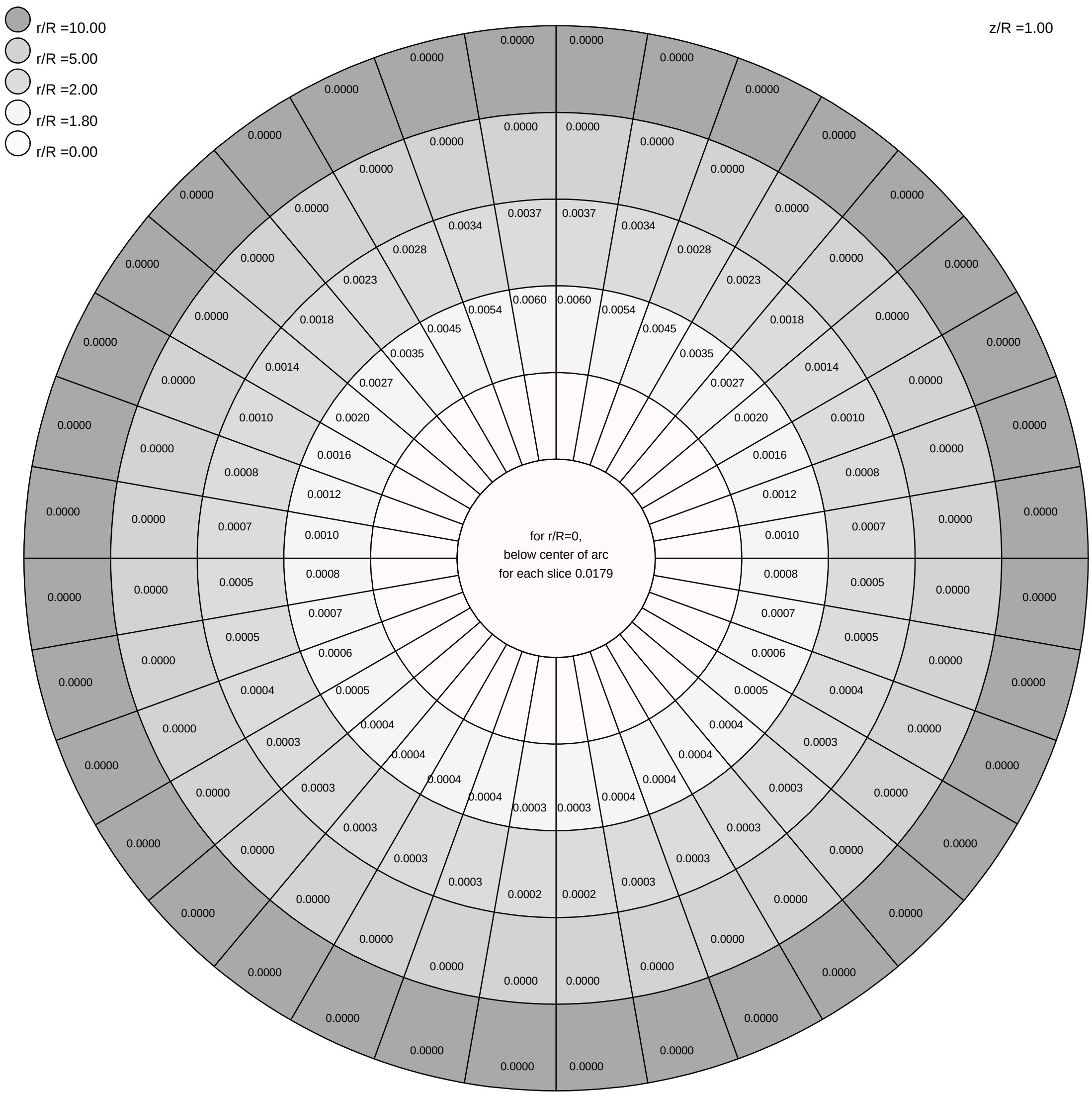
r/R =10.00
r/R =5.00
r/R =2.00
r/R =1.80
r/R =0.00
z/R =1.00
for r/R=0,
below center of arc
for each slice 0.0179

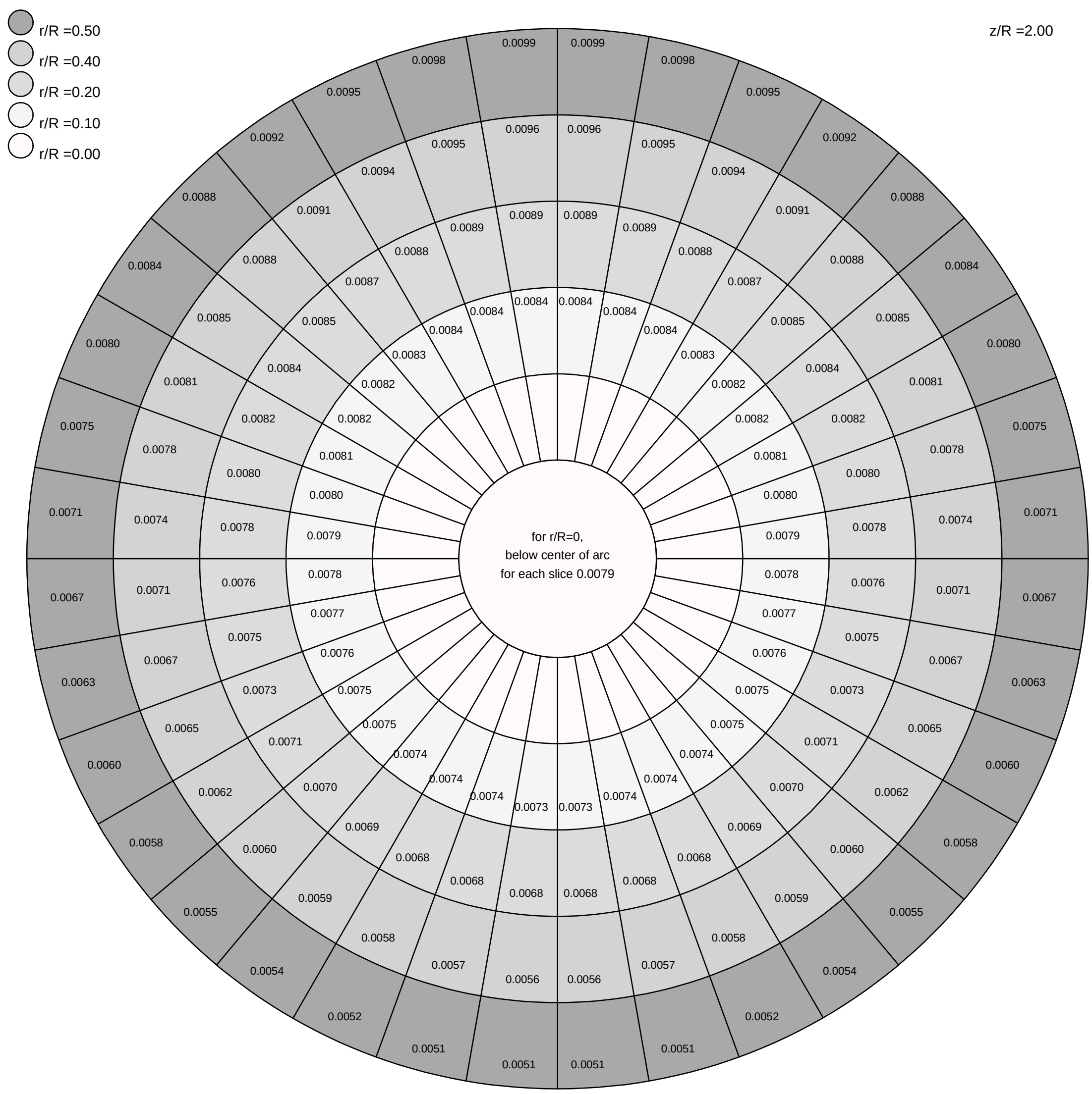
r/R =0.50
r/R =0.40
r/R =0.20
r/R =0.10
r/R =0.00
z/R =2.00
0.0099
0.0099
0.0098
0.0098
0.0095
0.0095
0.0096
0.0096
0.0092
0.0092
0.0095
0.0095
0.0094
0.0094
0.0088
0.0088
0.0091
0.0091
0.0089
0.0089
0.0089
0.0089
0.0088
0.0088
0.0084
0.0084
0.0088
0.0088
0.0087
0.0087
0.0084
0.0084
0.0084
0.0084
0.0085
0.0085
0.0085
0.0085
0.0084
0.0084
0.0080
0.0080
0.0083
0.0083
0.0084
0.0084
0.0081
0.0081
0.0082
0.0082
0.0082
0.0082
0.0082
0.0082
0.0075
0.0075
0.0078
0.0078
0.0081
0.0081
0.0080
0.0080
0.0080
0.0080
0.0071
0.0071
0.0074
0.0074
0.0078
0.0078
0.0079
0.0079
for r/R=0,
below center of arc
for each slice 0.0079
0.0078
0.0078
0.0067
0.0067
0.0071
0.0071
0.0076
0.0076
0.0077
0.0077
0.0075
0.0075
0.0067
0.0067
0.0076
0.0076
0.0063
0.0063
0.0073
0.0073
0.0075
0.0075
0.0065
0.0065
0.0075
0.0075
0.0071
0.0071
0.0060
0.0060
0.0074
0.0074
0.0074
0.0074
0.0070
0.0070
0.0062
0.0062
0.0074
0.0074
0.0073
0.0073
0.0069
0.0069
0.0058
0.0058
0.0060
0.0060
0.0068
0.0068
0.0068
0.0068
0.0068
0.0068
0.0059
0.0059
0.0055
0.0055
0.0058
0.0058
0.0057
0.0057
0.0054
0.0054
0.0056
0.0056
0.0052
0.0052
0.0051
0.0051
0.0051
0.0051

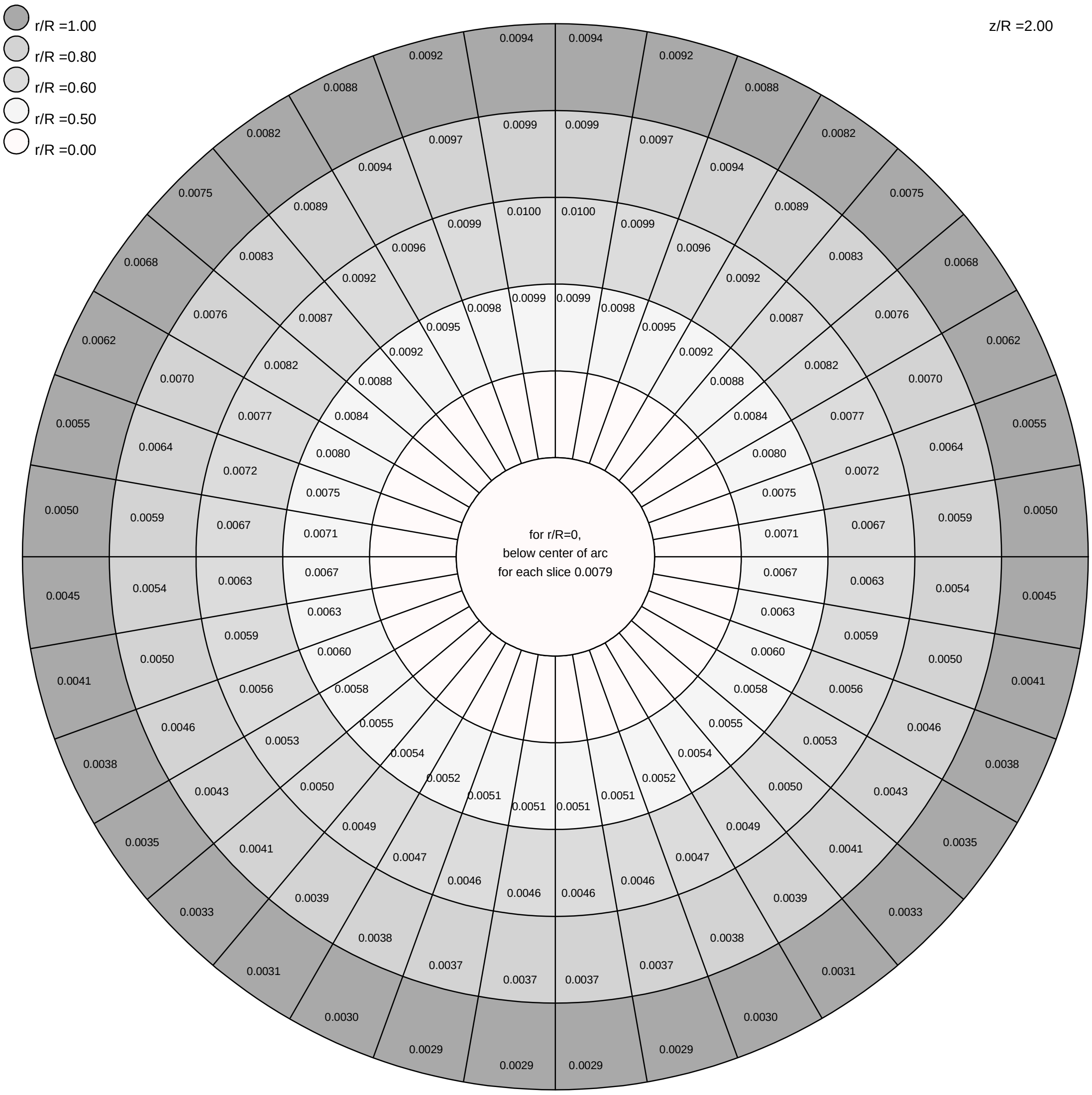

r/R =1.00
r/R =0.80
r/R =0.60
r/R =0.50
r/R =0.00
z/R =2.00
for r/R=0,
below center of arc
for each slice 0.0079

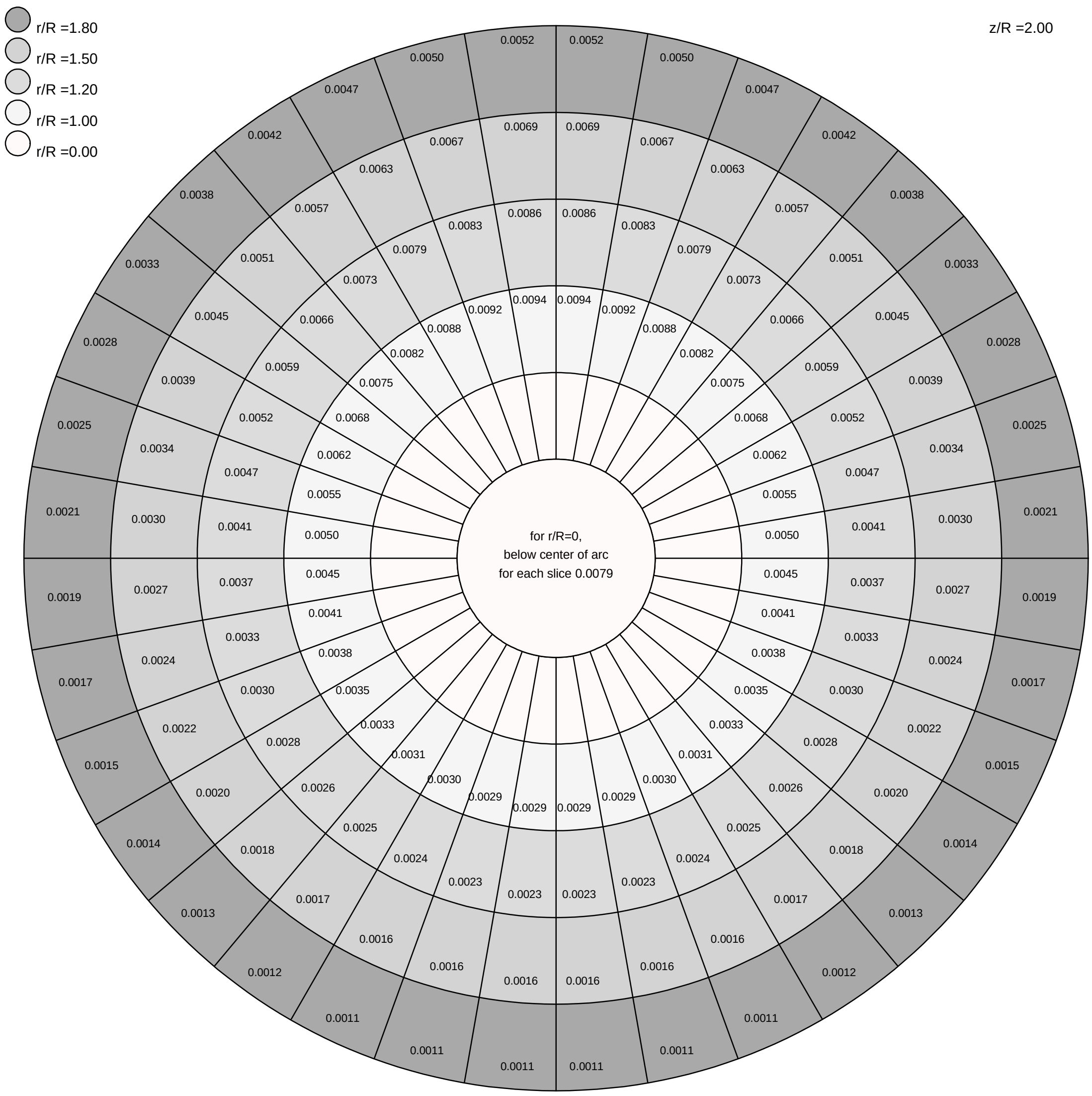
r/R =1.80
r/R =1.50
r/R =1.20
r/R =1.00
r/R =0.00
z/R =2.00
0.0052 0.0050 0.0047 0.0042 0.0038 0.0033 0.0028 0.0025 0.0021 0.0019 0.0017 0.0015 0.0014 0.0013 0.0012 0.0011 0.0011 0.0011
0.0052 0.0050 0.0047 0.0042 0.0038 0.0033 0.0028 0.0025 0.0021 0.0019 0.0017 0.0015 0.0014 0.0013 0.0012 0.0011 0.0011 0.0011
0.0069 0.0067 0.0063 0.0057 0.0051 0.0045 0.0039 0.0034 0.0030 0.0027 0.0024 0.0022 0.0020 0.0018 0.0017 0.0016 0.0016 0.0016
0.0069 0.0067 0.0063 0.0057 0.0051 0.0045 0.0039 0.0034 0.0030 0.0027 0.0024 0.0022 0.0020 0.0018 0.0017 0.0016 0.0016 0.0016
0.0086 0.0083 0.0079 0.0073 0.0066 0.0059 0.0052 0.0047 0.0041 0.0037 0.0033 0.0030 0.0028 0.0026 0.0025 0.0024 0.0023 0.0023
0.0086 0.0083 0.0079 0.0073 0.0066 0.0059 0.0052 0.0047 0.0041 0.0037 0.0033 0.0030 0.0028 0.0026 0.0025 0.0024 0.0023 0.0023
0.0094 0.0092 0.0088 0.0082 0.0075 0.0068 0.0062 0.0055 0.0050 0.0045 0.0041 0.0038 0.0035 0.0033 0.0031 0.0030 0.0029 0.0029
0.0094 0.0092 0.0088 0.0082 0.0075 0.0068 0.0062 0.0055 0.0050 0.0045 0.0041 0.0038 0.0035 0.0033 0.0031 0.0030 0.0029 0.0029
for r/R=0,
below center of arc
for each slice 0.0079

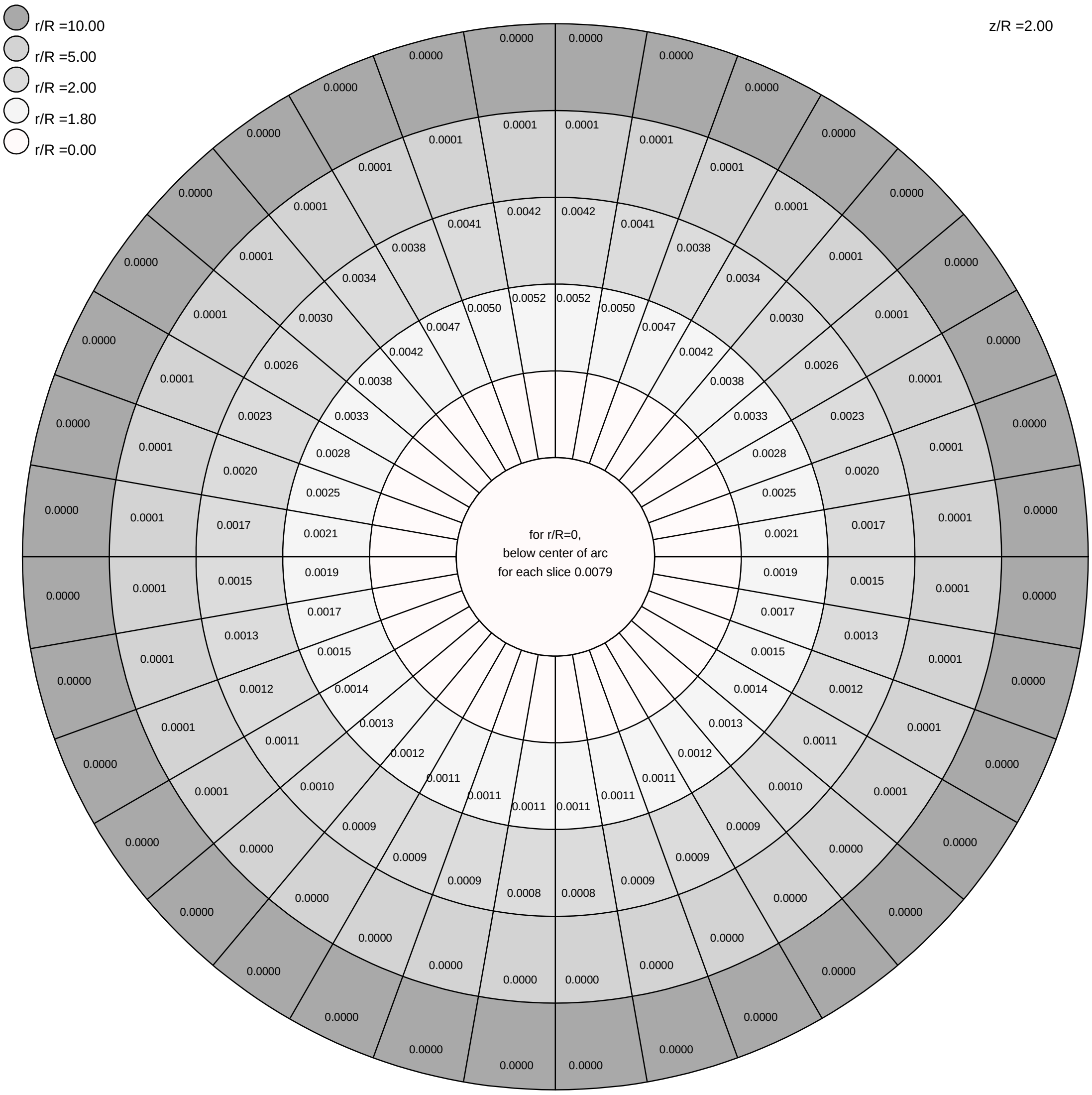
r/R =10.00
r/R =5.00
r/R =2.00
r/R =1.80
r/R =0.00
z/R =2.00
for r/R=0,
below center of arc
for each slice 0.0079
0.0000
0.0001
0.0042
0.0041
0.0038
0.0034
0.0030
0.0026
0.0023
0.0020
0.0017
0.0015
0.0013
0.0012
0.0011
0.0010
0.0009
0.0008
0.0052
0.0050
0.0047
0.0042
0.0038
0.0033
0.0028
0.0025
0.0021
0.0019
0.0017
0.0015
0.0014
0.0013
0.0012
0.0011

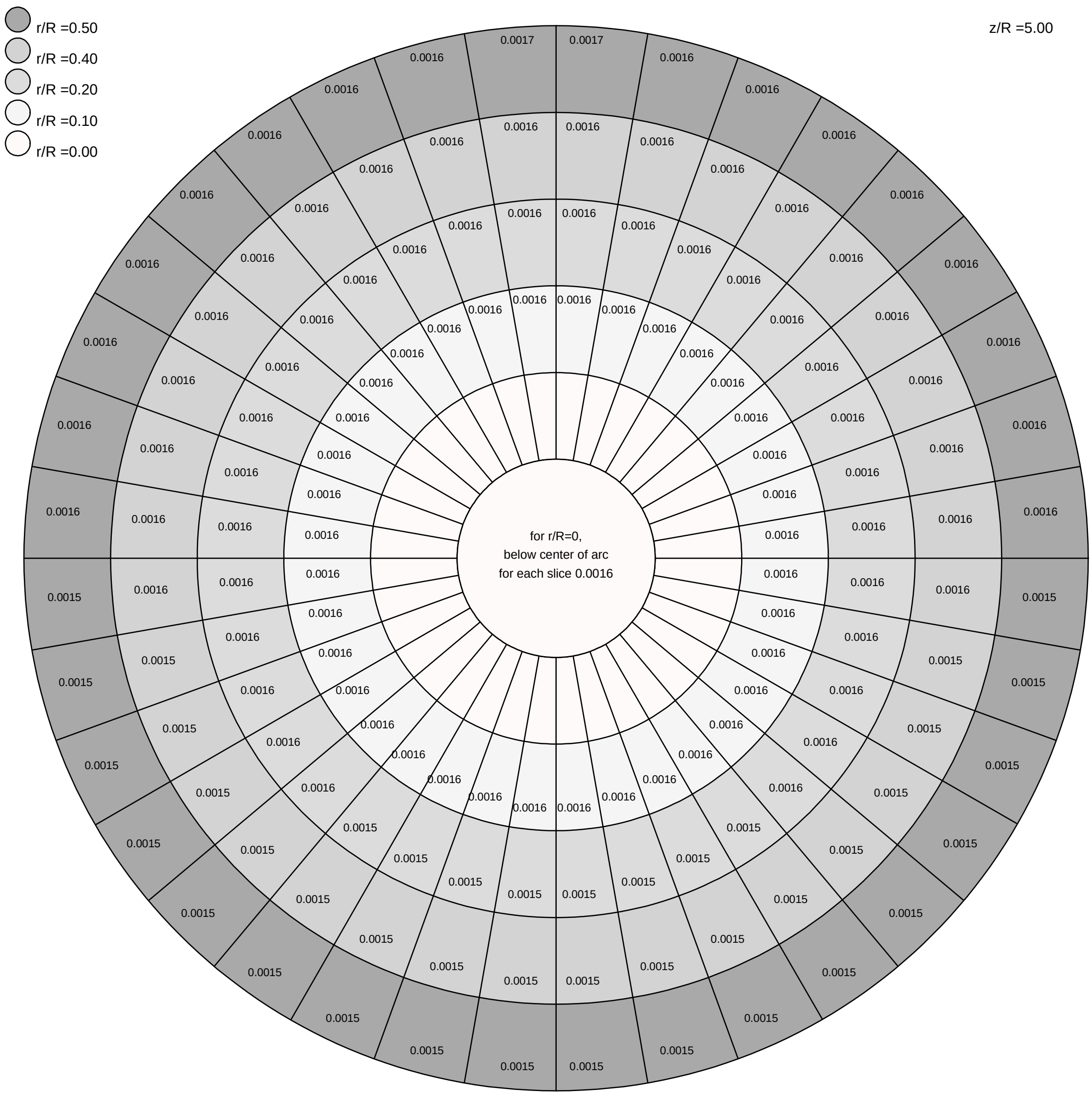
r/R =0.50
r/R =0.40
r/R =0.20
r/R =0.10
r/R =0.00
z/R =5.00
for r/R=0,
below center of arc
for each slice 0.0016

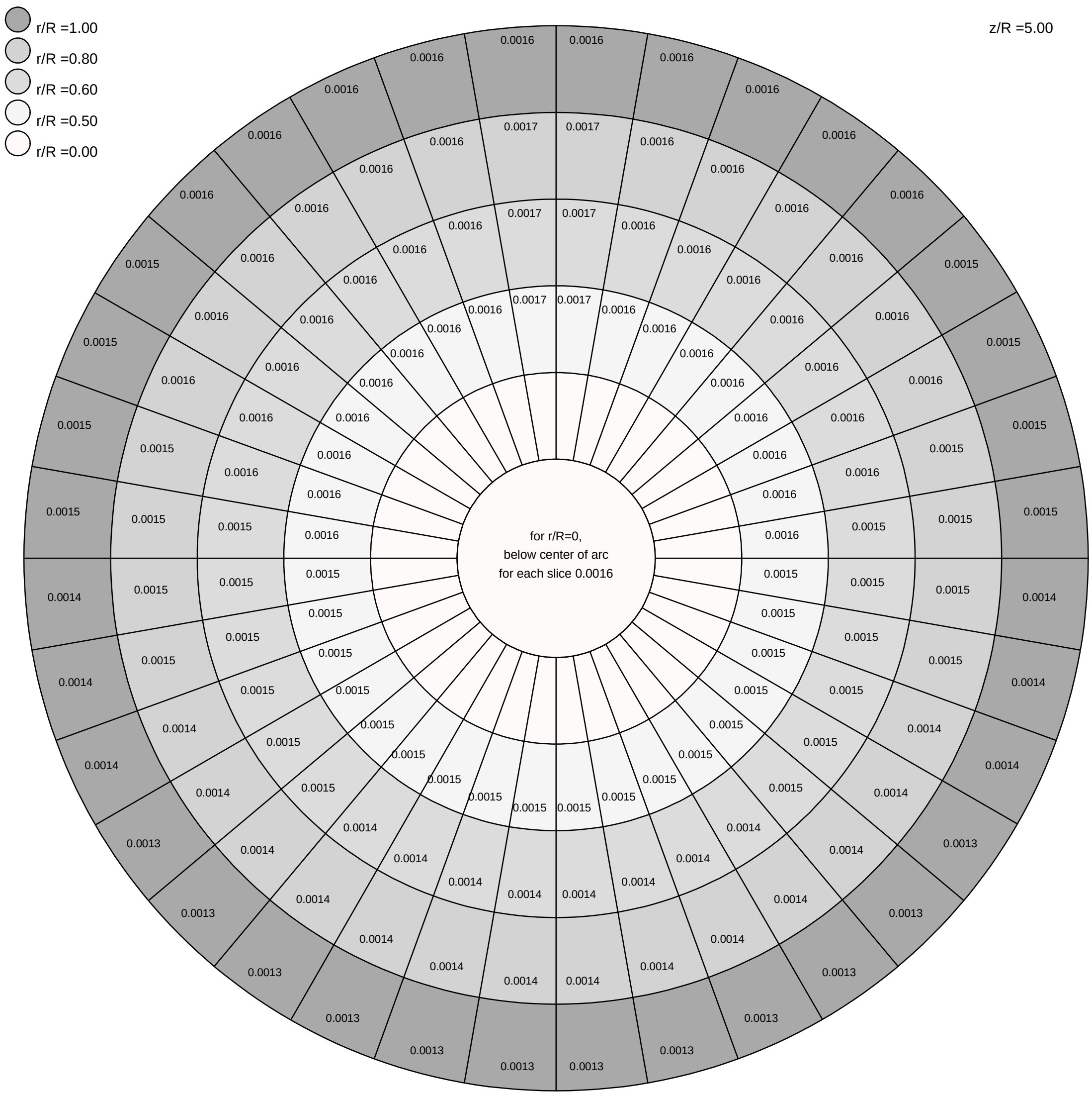
r/R =1.00
r/R =0.80
r/R =0.60
r/R =0.50
r/R =0.00
z/R =5.00
for r/R=0,
below center of arc
for each slice 0.0016

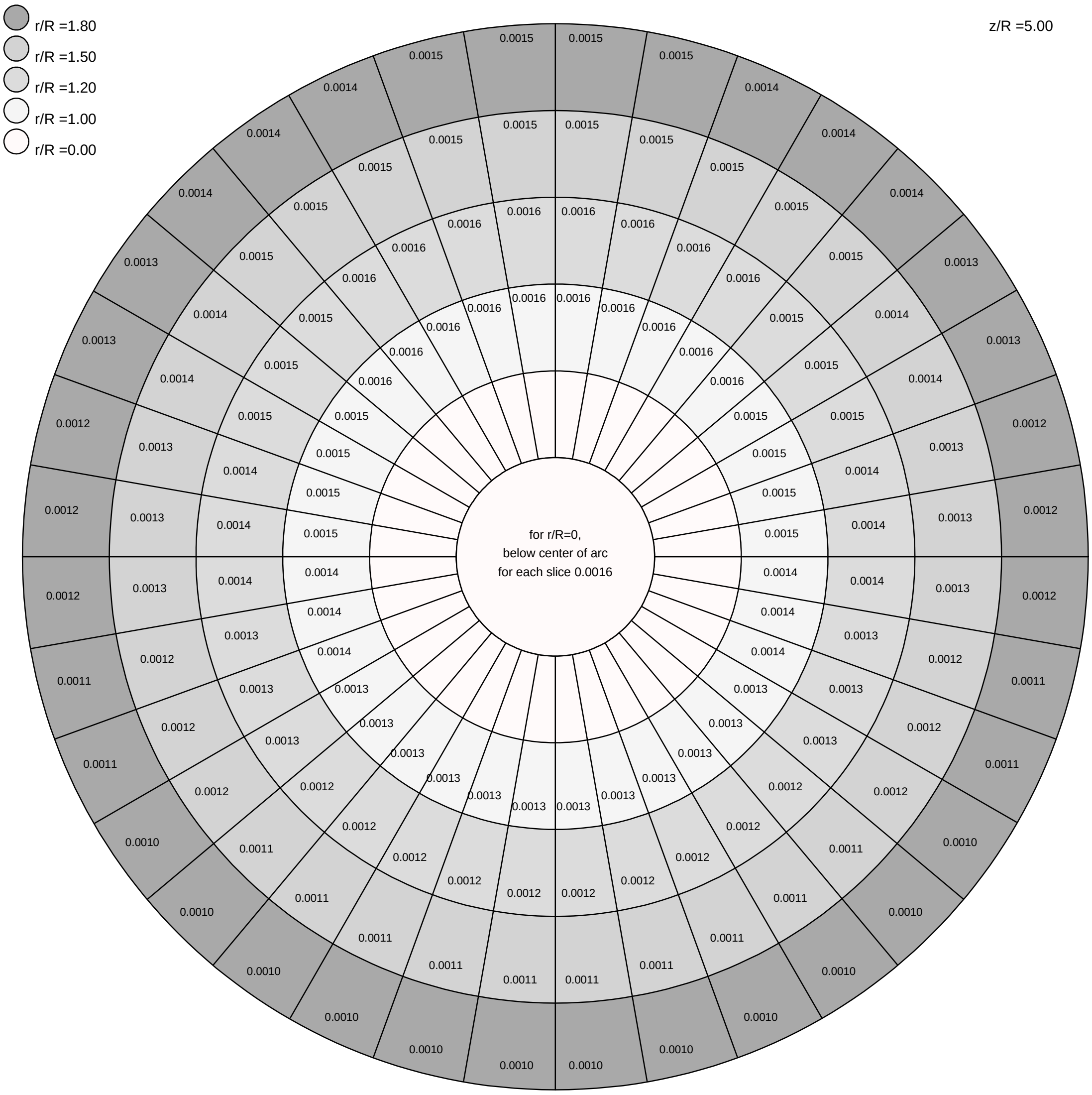
r/R =1.80
r/R =1.50
r/R =1.20
r/R =1.00
r/R =0.00
z/R =5.00
for r/R=0,
below center of arc
for each slice 0.0016

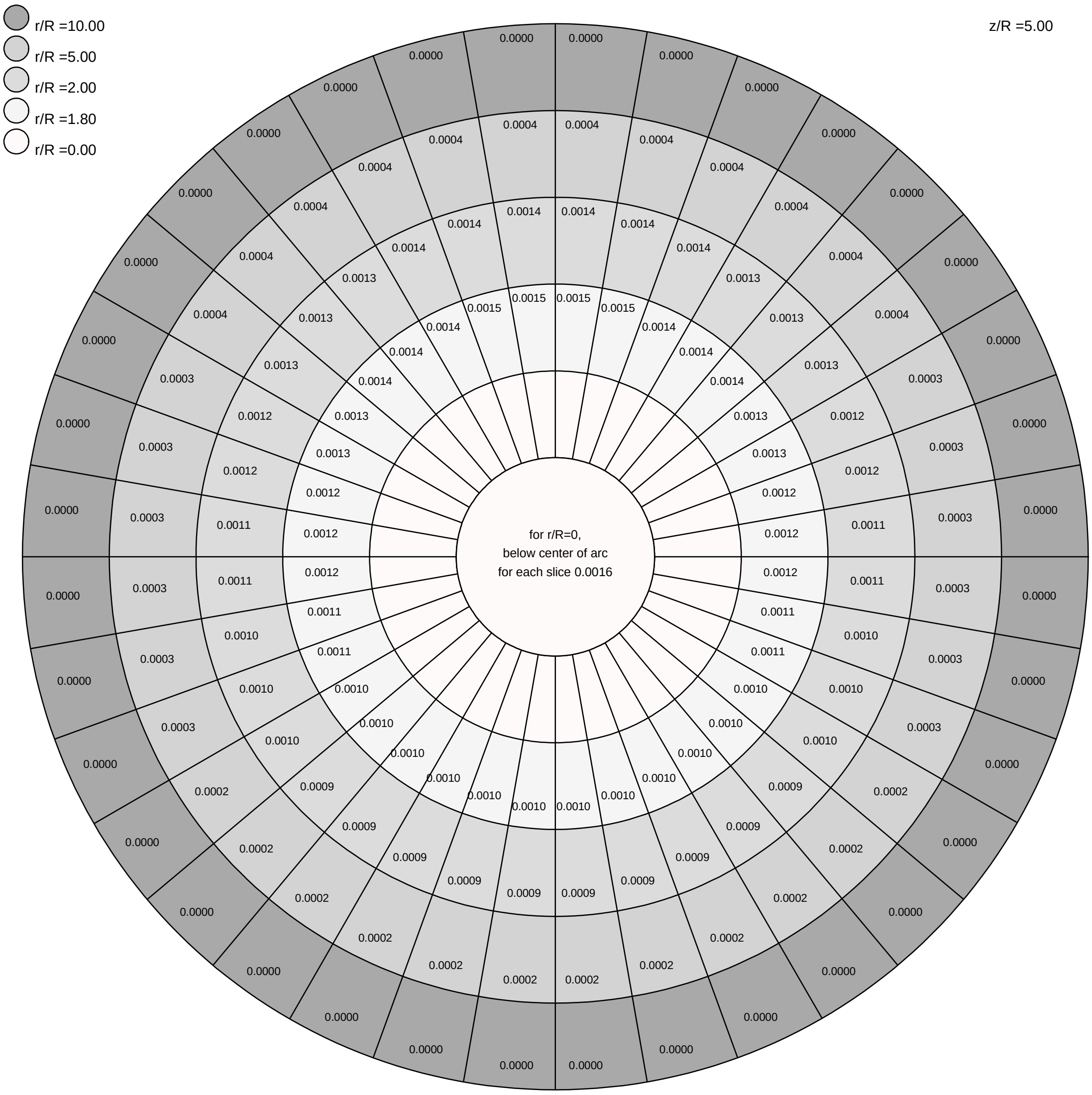
r/R =10.00
r/R =5.00
r/R =2.00
r/R =1.80
r/R =0.00
z/R =5.00
for r/R=0,
below center of arc
for each slice 0.0016

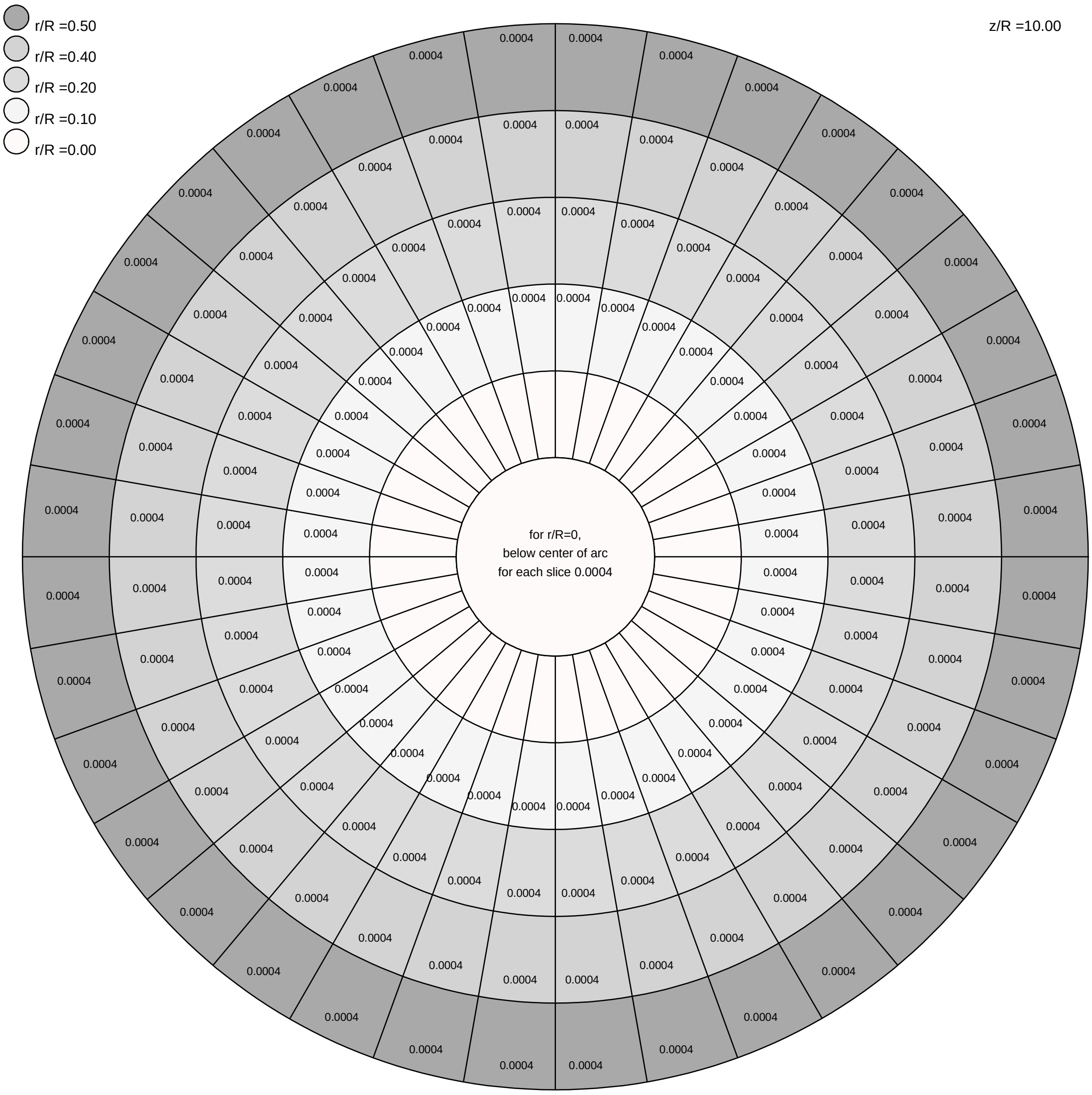
r/R =0.50
r/R =0.40
r/R =0.20
r/R =0.10
r/R =0.00
z/R =10.00
for r/R=0,
below center of arc
for each slice 0.0004
0.0004

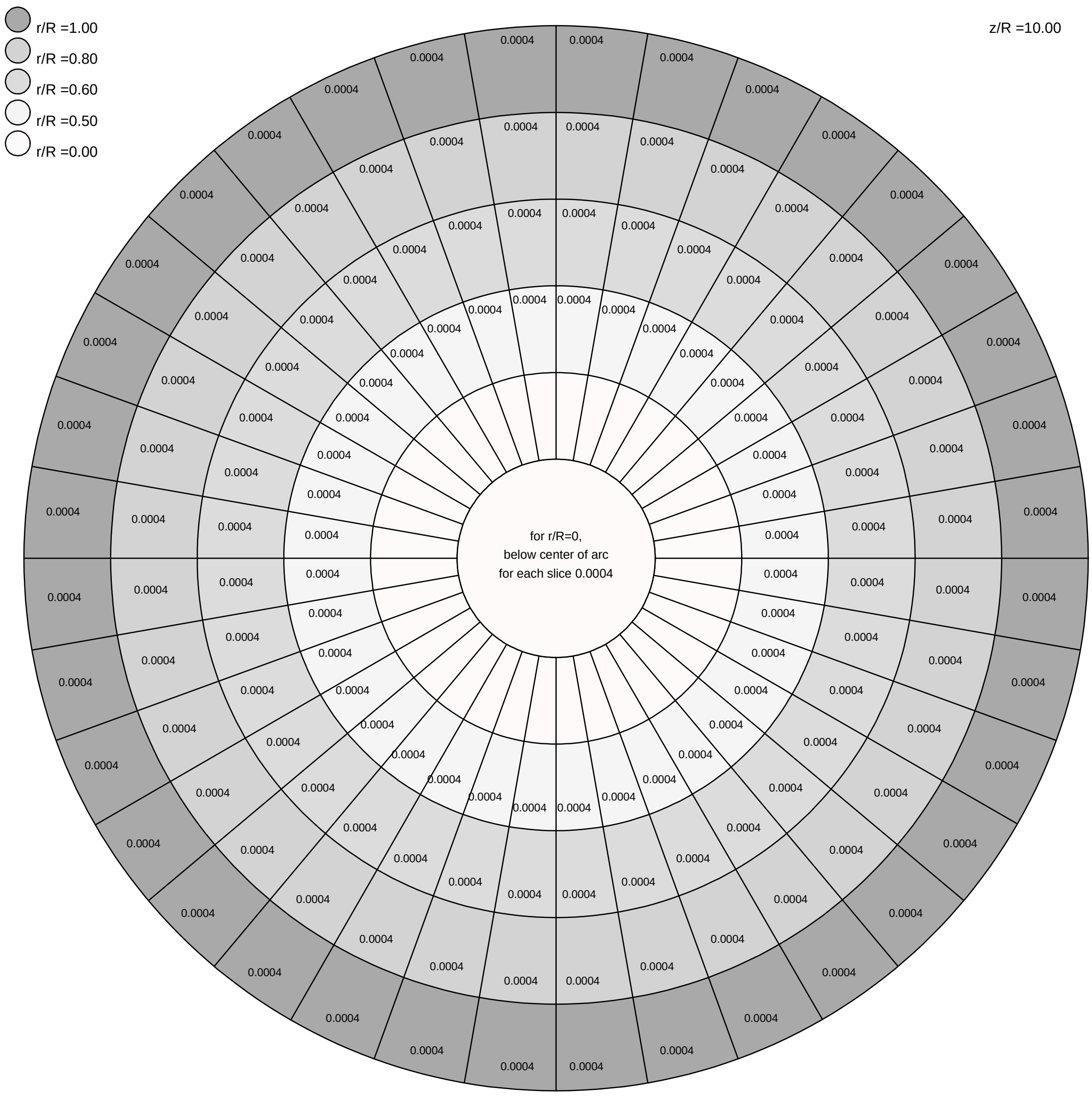
r/R =1.00
r/R =0.80
r/R =0.60
r/R =0.50
r/R =0.00
z/R =10.00
for r/R=0,
below center of arc
for each slice 0.0004

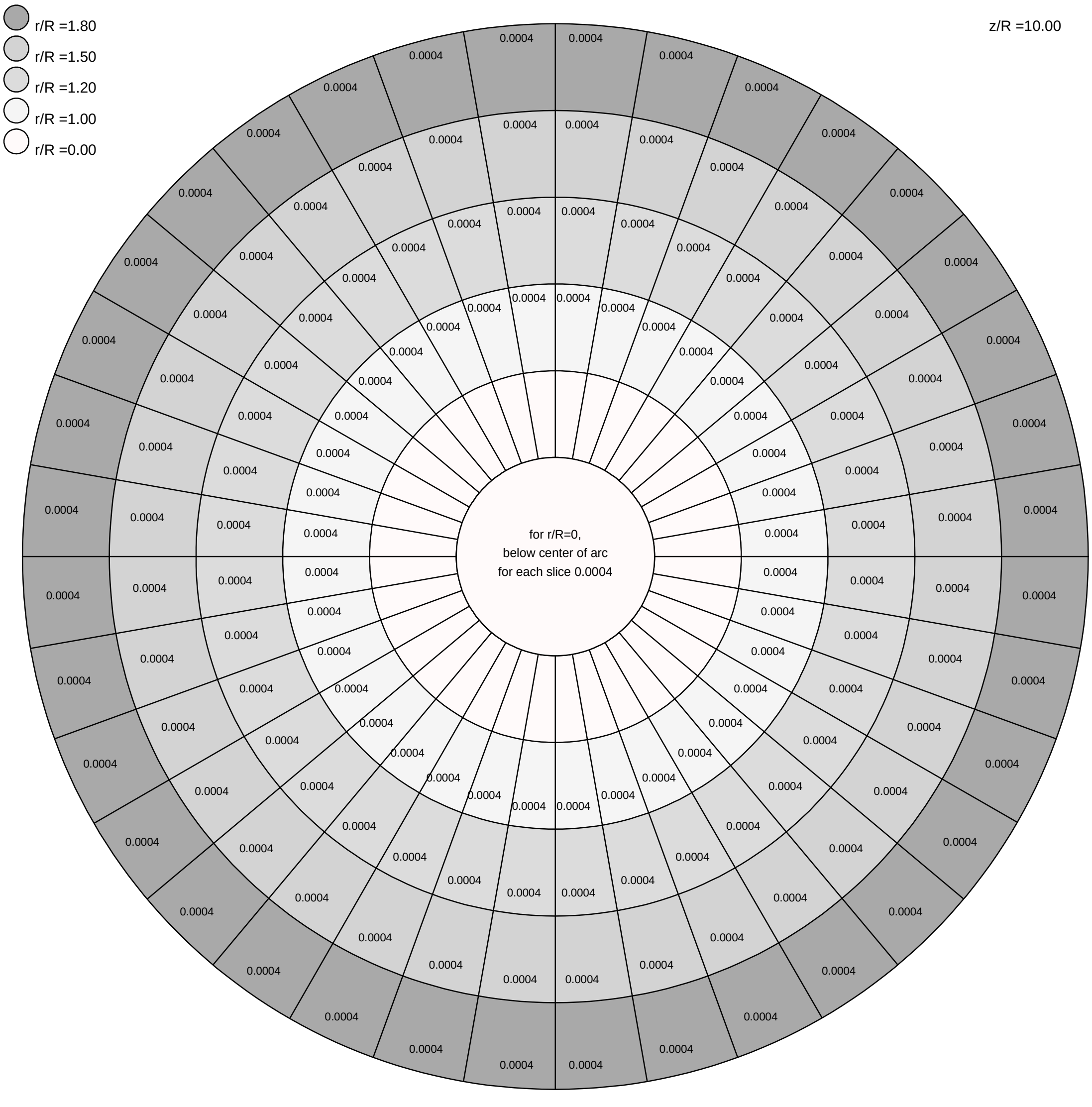
r/R =1.80
r/R =1.50
r/R =1.20
r/R =1.00
r/R =0.00
z/R =10.00
for r/R=0,
below center of arc
for each slice 0.0004

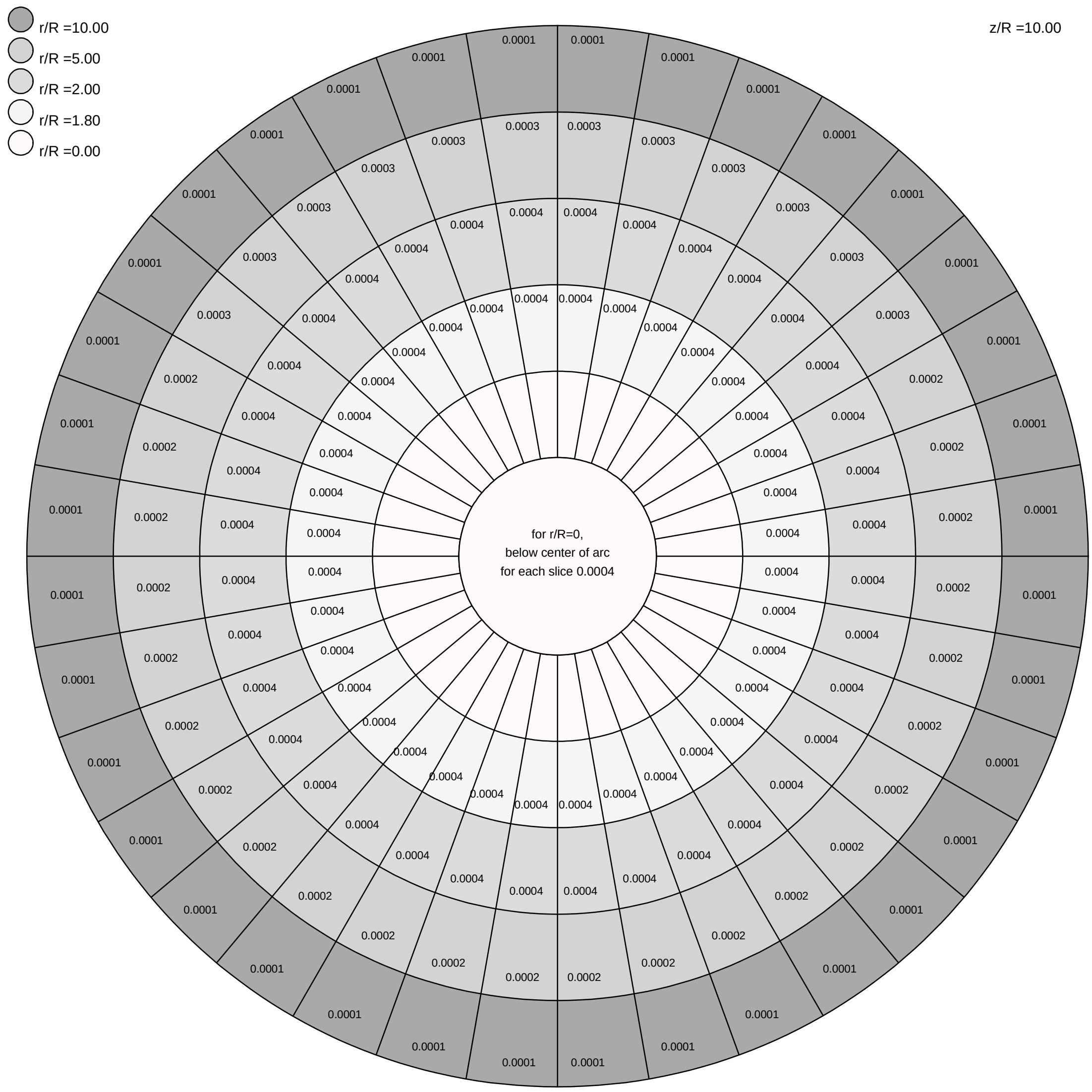
r/R =10.00
r/R =5.00
r/R =2.00
r/R =1.80
r/R =0.00
z/R =10.00
for r/R=0,
below center of arc
for each slice 0.0004

APPENDIX C – Newmark's Charts for Stress Increments for Uniform Loading over Any Area from Poulos and Davis, 1974

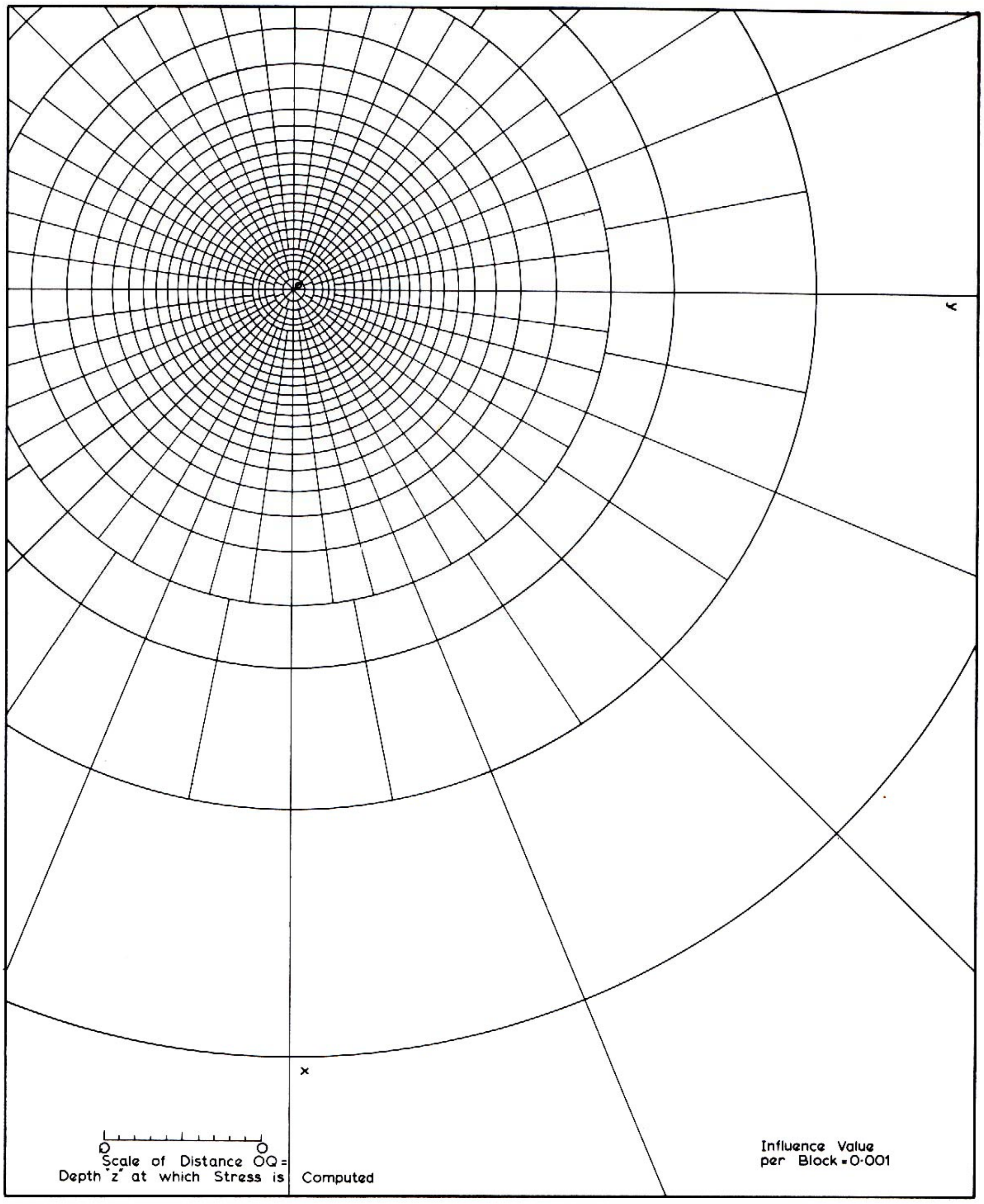

Influence chart for vertical stress σ_z (Newmark, 1942)
(All values of ν)

σ_z = .001Np
where N=no.of blocks.

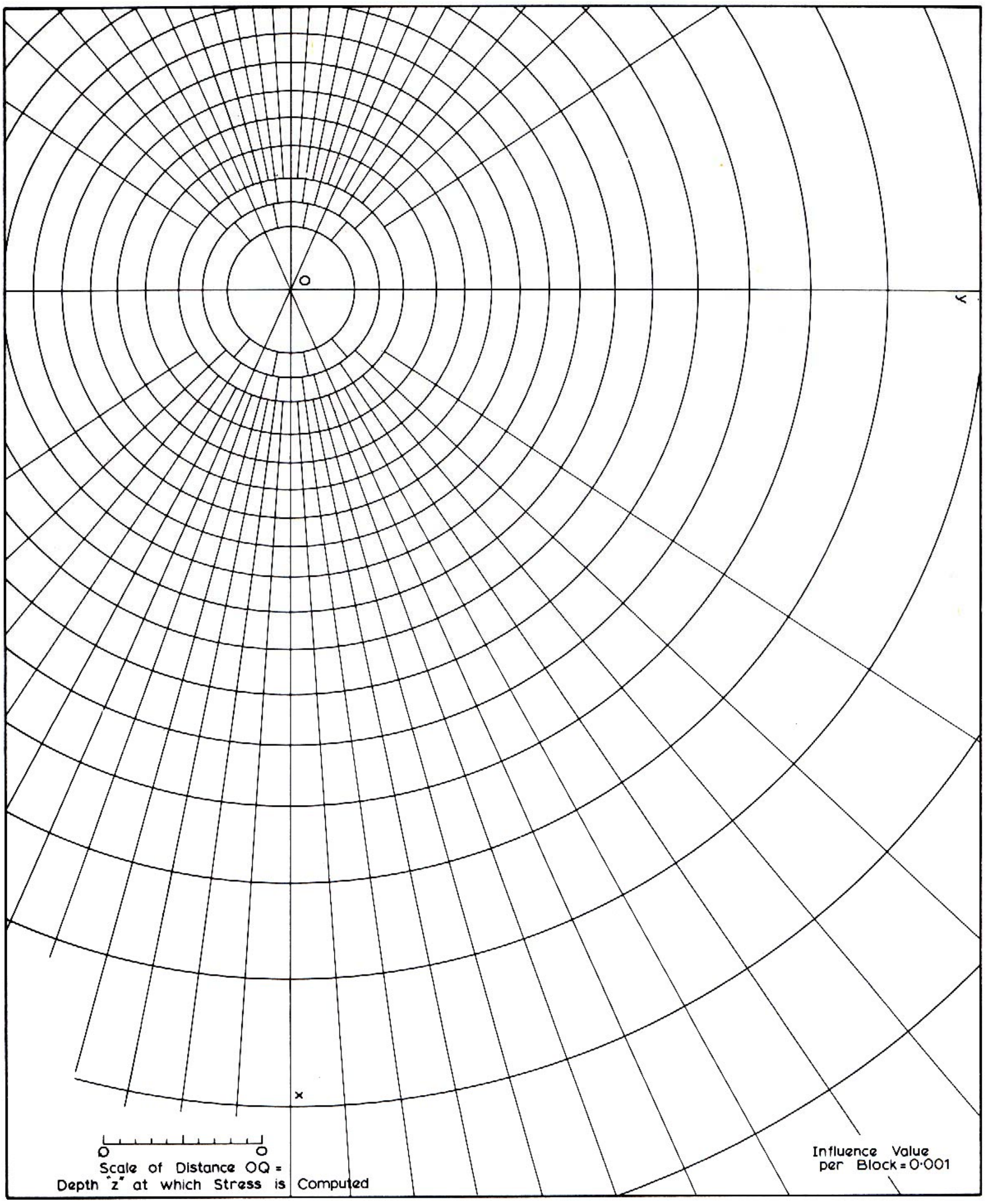

Influence chart for horizontal stress σ_x (Newmark, 1942).

ν=0.5

σ_x = .001Np

where N=no. of blocks.

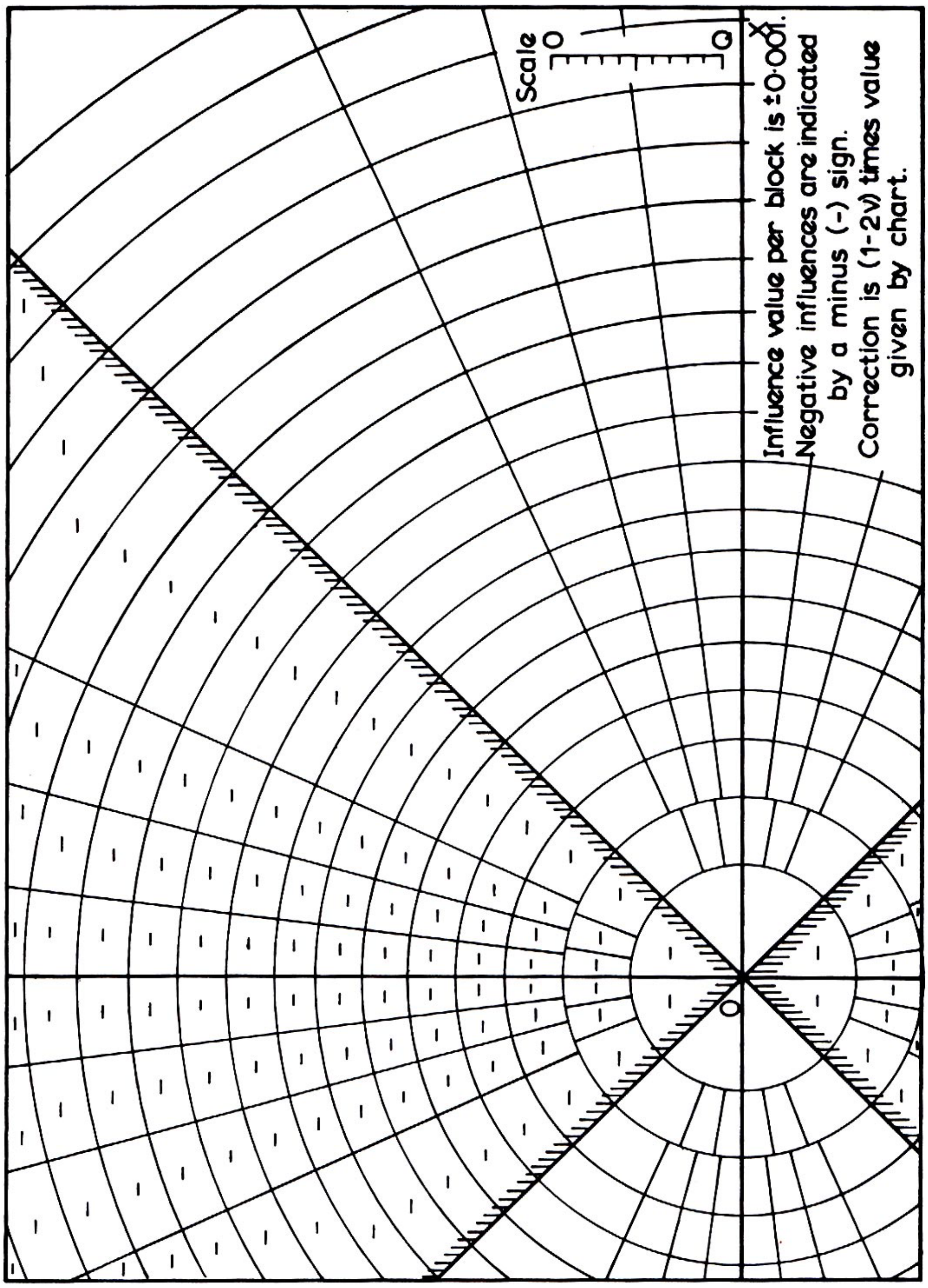

Influence chart for part of correction to σ_x for ν=0.5. (Newmark,1942).

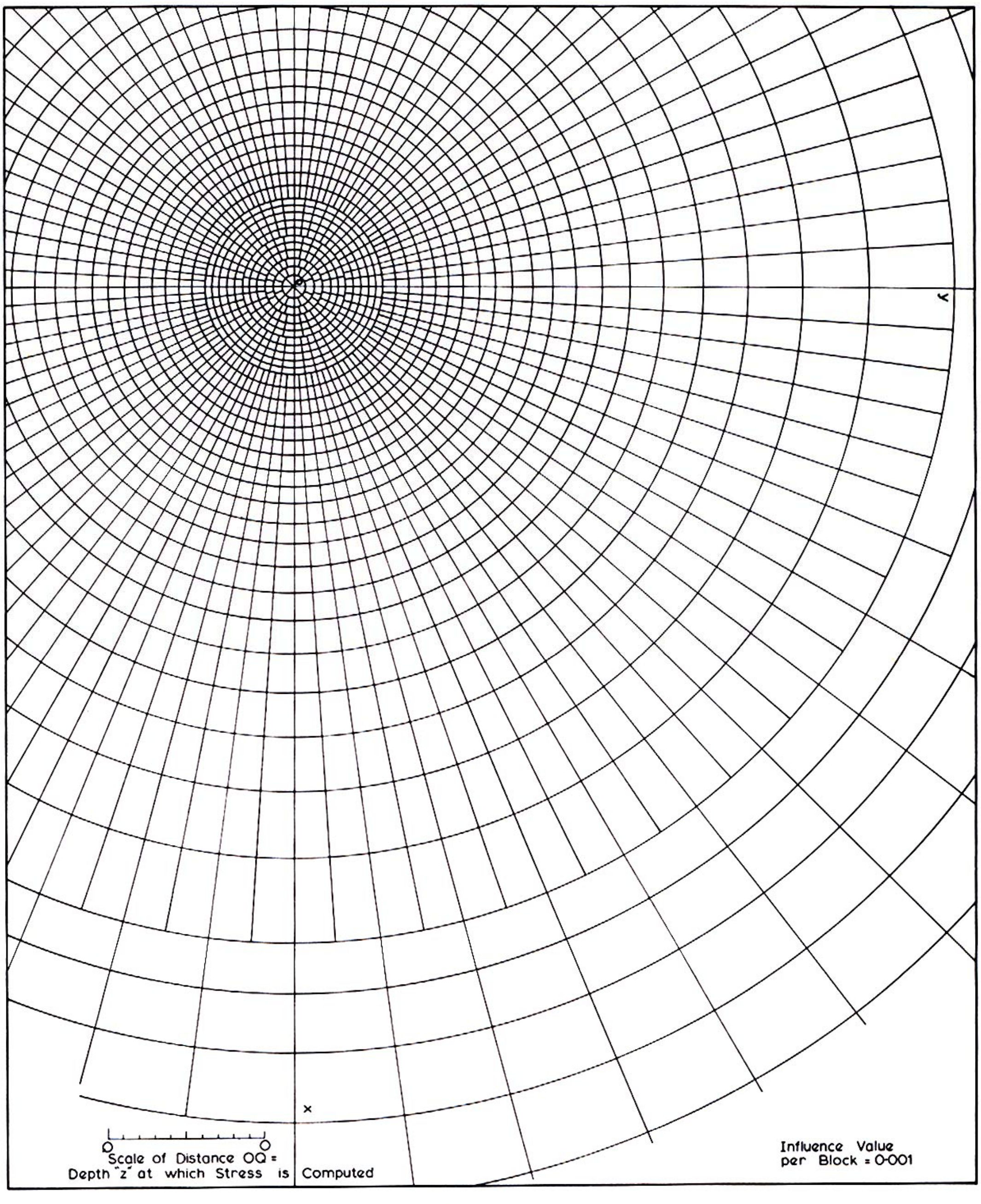

Influence chart for bulk stress Θ (Newmark, 1942)
(for all values of ν)

$$\sigma_x + \sigma_y + \sigma_z = \Theta = \frac{2(1+\nu)}{3} \,.001Np$$

where N=no.of blocks.

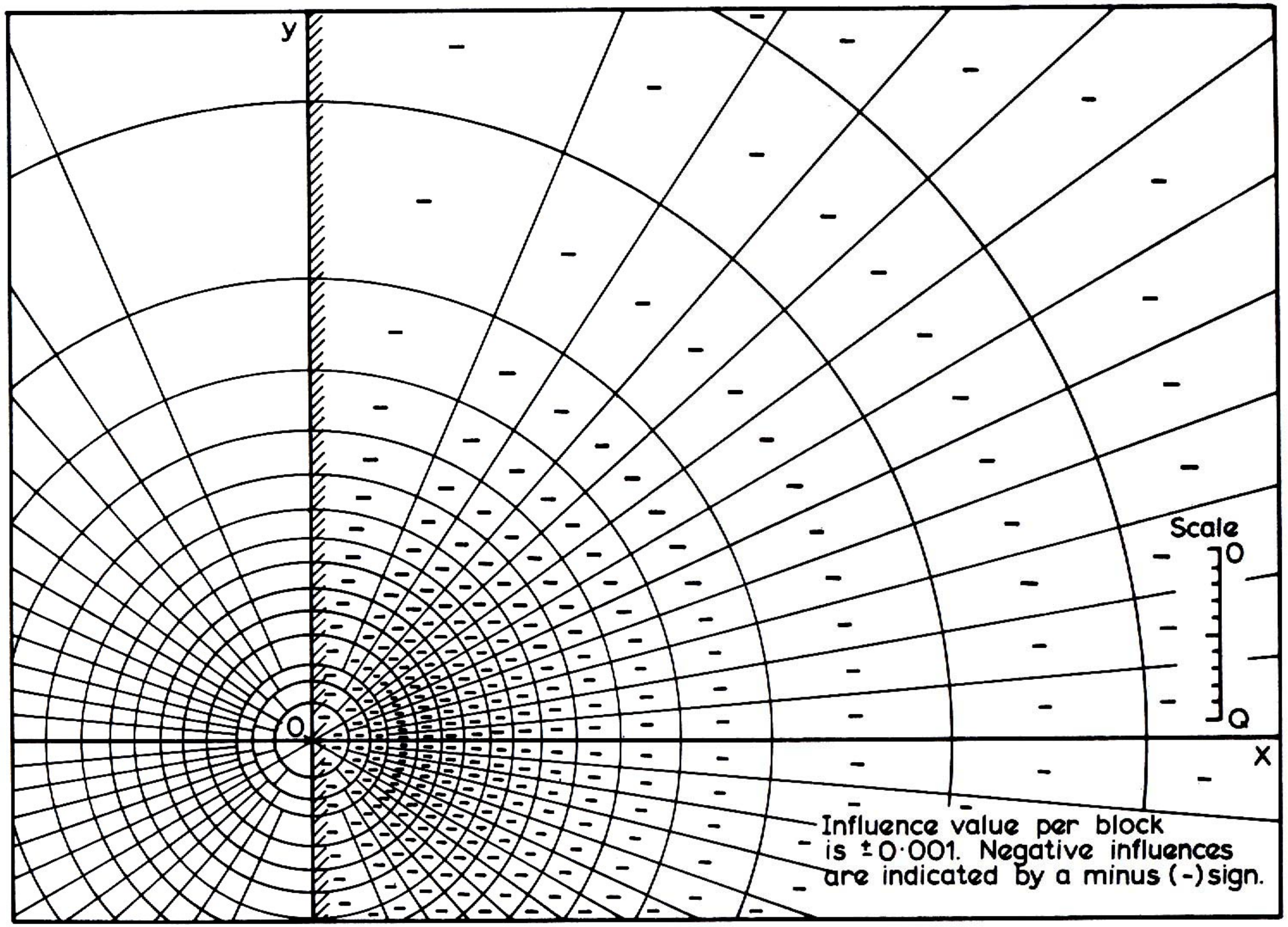

Influence chart for shear stress τ_{xz}. (Newmark, 1942).
(for all values of ν)

τ_{xz} = .001N p
where N=no.of blocks.

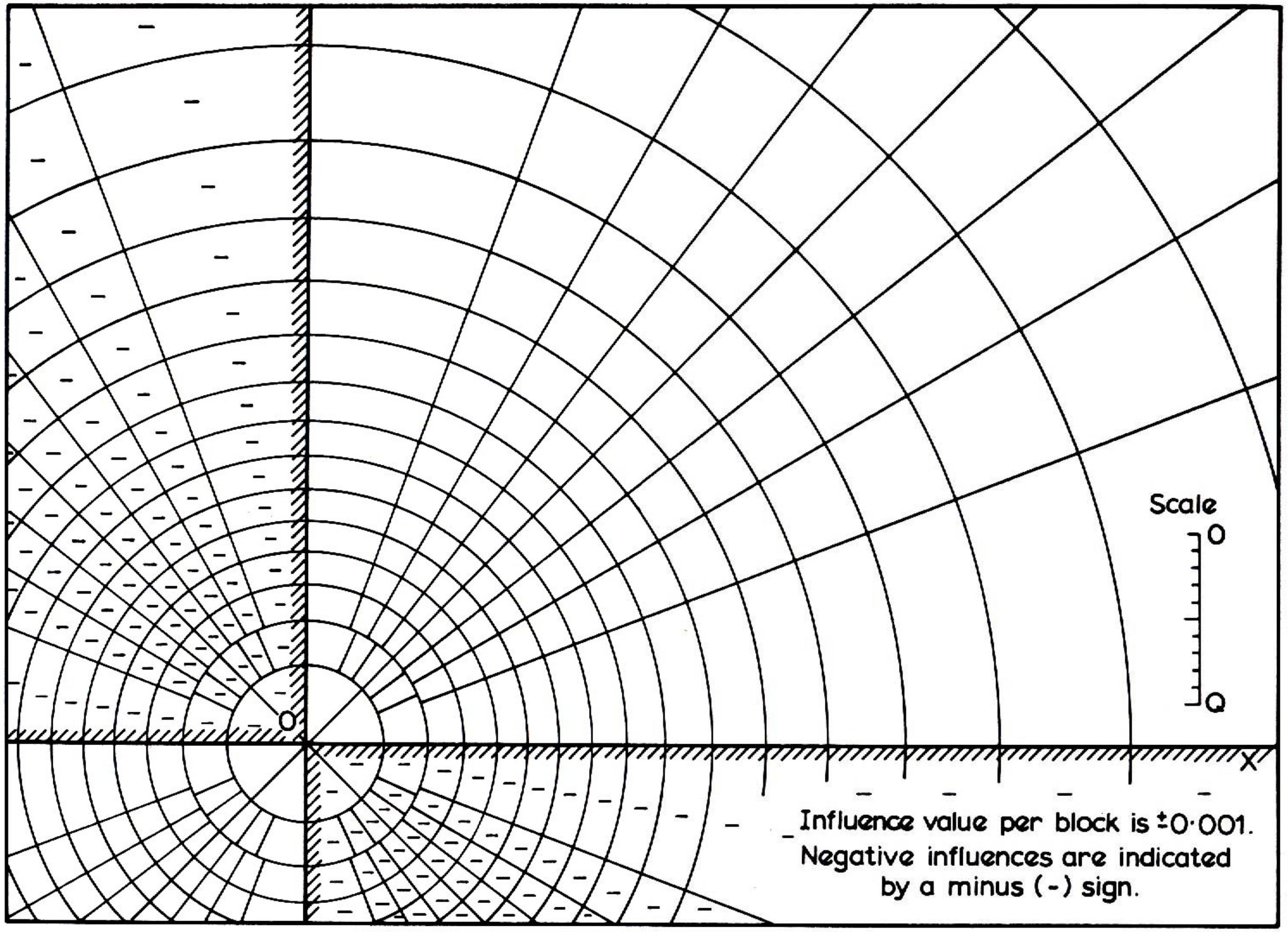

Influence chart for shear stress τ_{xy} for $\nu=0.5$ (Newmark, 1942).

$\tau_{xy} = .001 N p$

where N=no.of blocks.

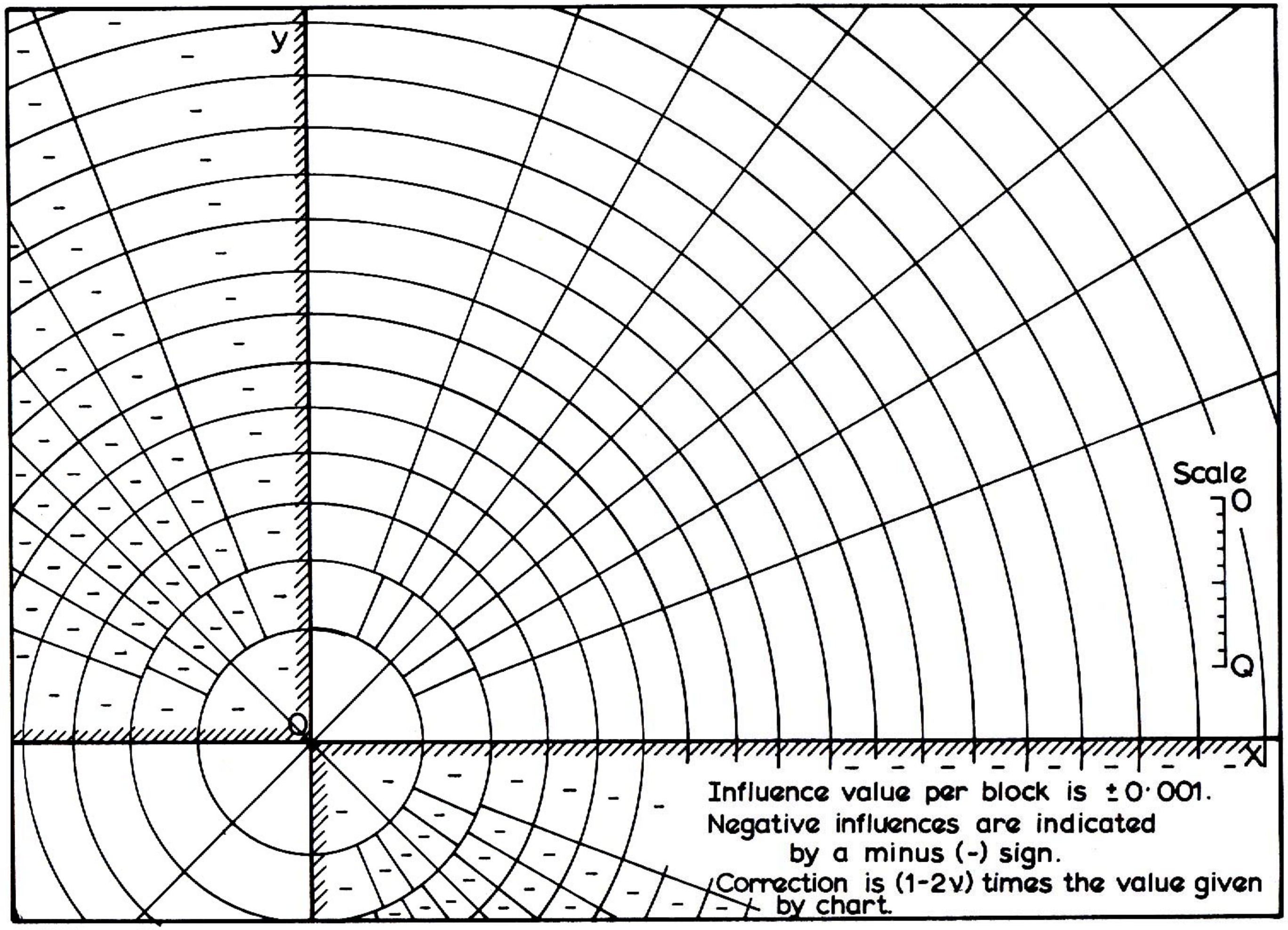

Influence chart for correction to τ_{xy} when $\nu \neq 0.5$. (Newmark, 1942).

APPENDIX D – Calculation of Bearing Capacity for Shallow Foundations

The ultimate bearing capacity is calculated using the following equation,

$$q_{ult} = cN_c s_c b_c + qN_q C_{Wq} s_q b_q d_q + 0.5\gamma B_f N_\gamma C_{W\gamma} s_\gamma b_\gamma$$

where,

c is the cohesion of foundation soil,

q is the soil pressure at foundation level which is created by embedment,

γ is the unit weight of foundation soil,

B_f is the width or the diameter of the foundation,

L_f is the length of the foundation,

N_c, N_q, N_γ are bearing capacity factors based on the internal friction angle of foundation soil as given in the following table by Das (1999):

ϕ	*Nc*	*Nq*	N_γ	ϕ	*Nc*	*Nq*	N_γ	ϕ	*Nc*	*Nq*	N_γ
0	5.70	1.00	0.00	17	14.60	5.45	2.18	34	52.64	36.50	38.04
1	6.00	1.1	0.01	18	15.12	6.04	2.59	35	57.75	41.44	45.41
2	6.30	1.22	0.04	19	16.57	6.70	3.07	36	63.53	47.16	54.36
3	6.62	1.35	0.06	20	17.69	7.44	3.64	37	70.01	53.80	65.27
4	6.97	1.49	0.10	21	18.92	8.26	4.31	38	77.50	61.55	78.61
5	7.34	1.64	0.14	22	20.27	9.19	5.09	39	85.97	70.61	95.03
6	7.73	1.81	0.20	23	21.75	10.23	6.00	40	95.66	81.27	115.31
7	8.15	2.00	0.27	24	23.36	11.40	7.08	41	106.81	93.85	140.51
8	8.60	2.21	0.35	25	25.13	12.72	8.34	42	119.67	108.75	171.99
9	9.09	2.44	0.44	26	27.09	14.21	9.84	43	134.58	126.50	211.56
10	9.61	2.69	0.56	27	29.24	15.90	11.60	44	151.95	147.74	261.60
11	10.16	2.98	0.69	28	31.61	17.81	13.70	45	172.28	173.28	325.34
12	10.76	3.29	0.85	29	34.24	19.98	16.18	46	196.22	204.19	407.11
13	11.41	3.63	1.04	30	37.16	22.46	19.13	47	224.55	241.80	512.84
14	12.11	4.02	1.26	31	40.41	25.28	22.65	48	258.28	287.85	650.87
15	12.86	4.45	1.52	32	44.04	28.52	26.87	49	298.71	344.63	831.99
16	13.68	4.92	1.82	33	48.09	32.23	31.94	50	347.50	415.14	1072.80

s_c, s_q, s_γ are shape correction factors as given in the following table by FHWA (2002):

Factor	Friction Angle	Cohesion Term (s_c)	Unit Weight Term (s_γ)	Surcharge Term (s_q)
Shape Factors, s_c, s_γ, s_q	$\phi = 0$	$1+\left(\frac{B_f}{5L_f}\right)$	1.0	1.0
	$\phi > 0$	$1+\left(\frac{B_f}{L_f}\right)\left(\frac{N_q}{N_c}\right)$	$1-0.4\left(\frac{B_f}{L_f}\right)$	$1+\left(\frac{B_f}{L_f}\tan\phi\right)$

b_c, b_q, b_γ are correction factors for the inclination of the base as given in the following table by FHWA (2002):

Factor	Friction Angle	Cohesion Term (c)	Unit Weight Term (γ)	Surcharge Term (q)
		b_c	b_γ	b_q
Base Inclination Factors, b_c, b_γ, b_q	$\phi = 0$	$1-\left(\frac{\alpha}{147.3}\right)$	1.0	1.0
	$\phi > 0$	$b_q - \left(\frac{1-b_q}{N_c \tan\phi}\right)$	$(1\text{-}0.017\alpha\tan\phi)^2$	$(1\text{-}0.017\alpha\tan\phi)^2$

α = footing inclination from horizontal, upward +, degrees

$C_{W\gamma}$, C_{Wq} are correction factors considering the location of the ground water table as given in the following table by FHWA (2002):

Depth of Ground Water Table, D_W	$C_{W\gamma}$	C_{Wq}
0	0.5	0.5
D_f	0.5	1.0
$> 1.5B_f + D_f$	1.0	1.0

d_q is a correction factor to account for the shearing resistance along the failure surface passing through cohesionless material above the bearing elevation as given in the following table by FHWA (2002):

Friction Angle, φ (degrees)	D_f/B_f	d_q
32	1	1.20
	2	1.30
	4	1.35
	8	1.40
37	1	1.20
	2	1.25
	4	1.30
	8	1.35
42	1	1.15
	2	1.20
	4	1.25
	8	1.30

The allowable bearing pressure is calculated using a safety factor, which is related with the type of the structure:

$$q_{allow} = q_{ult} / FS$$

The safety factor for shallow foundations of different structures is given in the following table by U.S. Army Corps of Engineers (1992):

Structure	Safety Factor, *FS*
Retaining	
Walls	3
Temporary braced excavations	> 2
Bridges	
Railway	4
Highway	3.5
Buildings	
Silos	2.5
Warehouses	2.5
Apartments, offices	3
Light industrial, public	3.5
Footings	3
Mats	> 3

CIRRICULAR VITAE

Born 5th May 1982, Istanbul. Had his primary and high education at Terakki Vakfı Özel Şişli Terakki Lisesi during 1988-2000, with full scholarship. Obtained B.Sc. in Civil Engineering at Istanbul Technical University in 2004.

Had internship on numerical analysis in Kumagai-Gumi Co. Ltd., Wakunami Tunnel Project Office, Ishikawa, Japan in 2003. Started his professional career in the field of geotechnical engineering in 2004. Attended 3rd International Congress of Young Geotechnical Engineers at Osaka, where presented preliminary results of this study, in 2005 as one of the official delegates of Turkish Society of Soil Mechanics and Foundation Engineering.

Interests in photography, music as a bass guitarist in a band playing ethnic and improvisational rock music and collecting Turkish science fiction objects.